

**REPORT ON THE MINERAL EXPLORATION  
IN  
THE MARRAKECH-TEKNA AREA  
THE KINGDOM OF MOROCCO  
PHASE I**

**MARCH 2003**

**METAL MINING AGENCY OF JAPAN**  
**JAPAN INTERNATIONAL COOPERATION AGENCY**

<b>MPN</b>
<b>CR(3)</b>
<b>03-059</b>

## Preface

In response to the request of the government of the Kingdom of Morocco, the Japanese Government decided to enforce various Survey on deposit exploration including geological and geophysical surveys to evaluate potential of mineral resources in the Marrakech-Tekna area located in the middle-west of Morocco and entrusted the Japan International Cooperation Agency (JICA) with the execution of such Survey. Since details of the Survey were concerned with specialized fields of geology and geological resources, JICA entrusted the Metal Mining Agency of Japan (MMAJ) to enforce them.

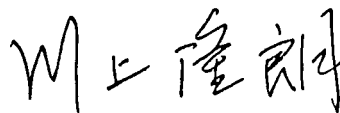
In 2002, the initial year of the Survey, JICA/MMAJ dispatched its survey teams to the site from September 10 to October 13, 2002 and from January 4 to March 7, 2003.

The field survey program in the area has completed as schedule in cooperation with Bureau de Recherches et de Participations Minières (BRPM).

This report summarizing the survey results obtained during the present fiscal year constitutes a part of our final report.

In conclusion, we would like to express our sincere gratitude to the government organizations concerned in the Kingdom of Morocco, the Ministries of Foreign Affairs and of Economy & Industry in Japan, the Japanese Embassy in the Kingdom of Morocco and other persons concerned for the cooperation and assistance rendered by them in the execution of our Survey.

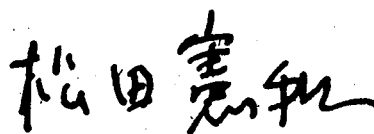
March, 2003



Takao Kawakami

President

Japan International Cooperation Agency



Norikazu Matsuda

Chairman of the Board of Directors

Metal Mining Agency of Japan

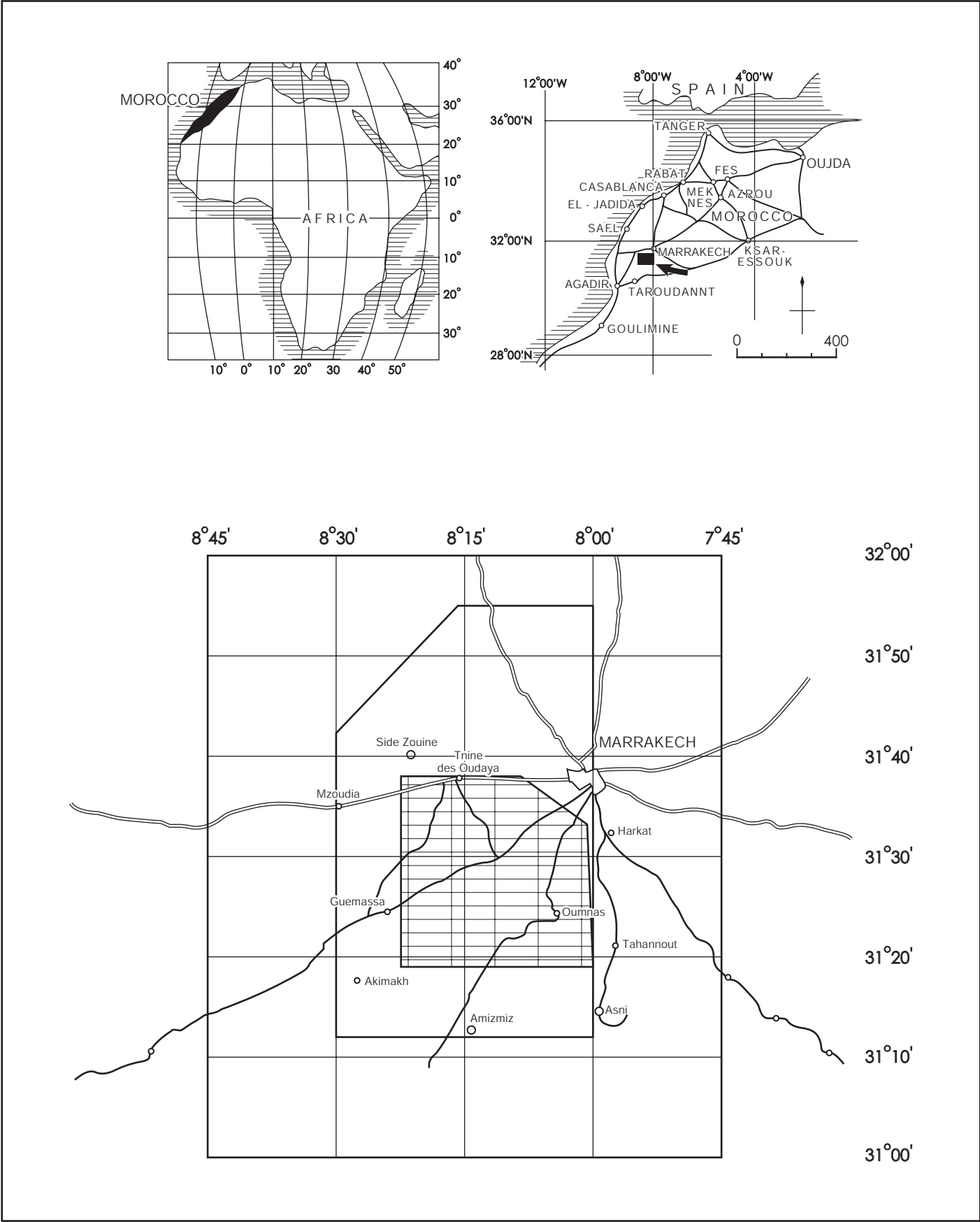


Fig I-1-1 Location Map of the Survey Area

## Summary

This survey was carried out in Marrakech-Tekna area, the Kingdom of Morocco. The purpose of this survey is to extract the prospective area of volcanic massive sulfide ore deposit of copper-lead-zinc by geological and geophysical survey and mineralization analysis. The technology transfer to the counterpart organization is also the major purpose of this survey.

As the phase I survey, the geological survey, drilling core observation and airborne geophysical survey were carried out to analyze the mineralization characteristics of massive sulfide ore deposit and to obtain the findings to analyze/interpret the results of the above airborne geophysical survey. As the result of the Survey is as followings.

The ore deposits distributed in Jubilet and Guemassa area are Cu – Pb – Zn – Fe massive sulfide ore deposits that occurred within the alternating beds of pelites and sandstones, the alternating beds of pelites and acid volcanic rocks. The shapes of these ore deposits are layered, massive, lenticular, and banded. The major combination of minerals is pyrrhotite, pyrite, galena, and chalcopyrite. Acid and/or basic volcanic rocks are distributed in the vicinity of the ore deposit. The volcanic rocks relates to the mineralization.

The mineralization repeatedly occurred in the massive sulfide ore deposit in the survey area. From the viewpoint of the combination of minerals, the mineralization stage is divided into “the early I sub-stage”, “the early II sub-stage” and “the late stage”. The early I sub-stage mineralization is represented by hexagonal pyrrhotite. The magnetism is comparatively weak. The early II sub-stage mineralization is represented by monoclinic pyrrhotite. The magnetism is strong. The late stage mineralization is represented by pyrite. The magnetism is weak. Furthermore massive sulfide deposits in the can be classified into following three types: “Early I sub-stage dominant type” (medium magnetic anomaly, representative deposit is Draa Sfar deposit), “Early I sub-stage + Late stage type” (medium + low magnetic anomaly, Frizen deposit and Kettara deposit) and “Early II sub-stage + the late stage” (high + low magnetic anomaly, Khwadra deposit and Hajar deposit).

According to the result mentioned above, because it is possible that there are not only the deposit that has high magnetic anomaly but also that has medium to low magnetic anomaly in the Survey area, following anomalies were selected as survey areas.

- 1) Low resistivity zone + high to medium magnetic anomaly: possibility of the existence of high magnetic massive sulfide ore deposit.
- 2) High magnetic anomaly zone: Possibility of the existence of high magnetic massive sulfide ore deposit.
- 3) Low resistivity zone: possibility of the existence of medium to low magnetic massive sulfide ore deposit.



## Content

Preface	
Location of the Survey Area	
Summary	
Part I The General .....	1
Chapter 1 Introduction .....	3
1-1 Purposes of the Survey.....	3
1-2 Outline of the Survey.....	3
1-2-1 The Survey Area .....	3
1-2-2 Contents and Quantities of the Survey .....	4
1-3 Organization of the Survey Team .....	4
1-4 The Survey Period.....	5
Chapter 2 Outline of the Survey Area .....	6
2-1 Location and Traffics .....	6
2-2 Geography and Climate .....	6
2-3 Infrastructure Preparation .....	7
Chapter 3 Survey Results and General Examination .....	8
3-1 Collection and Analysis of the Existing Data .....	8
3-2 Geology and Mineralization .....	15
3-3 Airborne Geophysical Survey.....	34
Chapter 4 Conclusion and Recommendation .....	41
4-1 Conclusion .....	41
4-2 Recommendation for the Second Year's Program .....	45

Part II	Details of the Survey.....	47
Chapter 1	Survey of the Existing Data.....	49
1-1	Method of the survey .....	49
1-2	Results of the survey.....	49
1-2-1	Outline of previous survey .....	49
1-2-2	Details of previous surveys.....	50
1-2-3	Conclusion.....	69
Chapter 2	Geological Survey .....	70
2-1	Method of the Geological Survey .....	70
2-2	Results of the survey.....	70
2-2-1	Outline of the survey area.....	70
2-2-2	Geological Stratigraphy in the Survey Area .....	73
Chapter 3	Existing Drilling Core Survey .....	107
3-1	Method of the survey .....	107
3-2	Results of the survey.....	107
Chapter 4	Laboratory Works .....	127
4-1	Sulfides ore minerals.....	127
4-1-1	Method.....	127
4-1-2	Results .....	127
4-1-2-1	Results of of the obserbation of thin section and polished thin section .....	127
4-1-2-2	Fluid inclusions .....	133
4-1-2-3	Sulfur isotope ratio measurements .....	137
4-1-2-4	X-ray diffraction (metallic minerals).....	139
4-2	Igneous Rocks.....	141
4-2-1	Method.....	141
4-2-2	Results .....	141
4-2-2-1	Whole rock chemical composition .....	141
4-2-2-2	Radioactive dating.....	148
4-3	Sedimentary rocks.....	153
4-3-1	Method.....	153
4-3-2	Results .....	153
4-3-2-1	Major components, main elements, and trace elements .....	153

4-3-2-2	Trace elements.....	158
4-3-2-3	Sulfur isotope .....	162
4-3-2-4	Fossil survey and others .....	167
Chapter 5	Airborne Geophysical Survey.....	168
5-1	Outline of the survey.....	168
5-2	Airborne electromagnetic/magnetic survey system .....	171
5-3	Results of the Airborne Gyophysical Survey .....	176
5-3-1	Outline .....	176
5-3-2	Digital topographical data .....	179
5-3-3	Airborne magnetic data .....	179
5-3-4	Airborne electromagnetic data.....	187
5-4	Interpretation and extraction of potential area .....	207
Chapter 6	Integrated Discussion .....	213
6-1	Characteristics of Sulfide ore deposits.....	213
6-2	Airborne Geophysical survey .....	235
Part III	Conclusion and Recommendation .....	239
Chapter 1	Conclusion.....	241
Chapter 2	Recommendation for the Second Year's Program .....	246

## List of Tables

Table I-1-1	Coordinate of the Survey area .....	3
Table I-1-2	Contents and Quantities of the Survey .....	4
Table I-1-3	Site Survey Schedule .....	5
Table I-2-1	Annual Temperatures and Precipitation in Marrakech .....	7
Table I-3-1	List of Summarized Survey History Already Performed.....	10
Table I-3-2	List of Major Airborne Geophysical Survey .....	13
Table I-3-3	The list of the characteristics of the mineral assemblage .....	28
Table I-3-4	The list of characteristics of mineralization .....	32
Table I-3-5	Specifications of the Airborne Geophysical Survey.....	34
Table II-1-1	List of Major Existing Geological Maps .....	52
Table II-1-2	List of previous Airborne Geophysical Surveys.....	55
Table II-1-3	List of Airborne Geophysical Anomaly.....	64
Table II-1-4	Geophysical data of rocks in the Survey Area (1).....	68
Table II-1-5	Geophysical data of rocks in the Survey Area (2).....	68
Table II-1-6	List of the Data Converted into GIS Data .....	69
Table II-1-7	Specifications of Lambert Conformal Projection.....	69
Table II-3-1	List of Observing Drilling Cores .....	108
Table II-4-1	List of Laboratory works (Sulfide ores) .....	127
Table II-4-1-1	List of key statistics of homogenization temperature and salinity of Quartz .....	134
Table II-4-2	List of Laboratory works (Igneous rocks).....	141
Table II-4-3	List of Laboratory works (Sedimentary rocks) .....	153
Table II-5-1	Schedule of the Airborne Geophysical Survey.....	168
Table II-5-2	Coordinate of Airborne Geophysical Survey .....	169
Table II-5-3	Airborne Electromagnetic system .....	171
Table II-5-4	GEOTEM system .....	173
Table II-5-5	Electromagnetic Sampling data.....	175
Table II-5-6	List of data acquisitioned in the survey .....	178
Table II-6-1	The list of the characteristics of the mineral assemblage .....	215
Table II-6-2	The list of the characteristics of mineralization .....	233

## List of Figures

Fig.I-1-1	Location map of the Survey Area	
Fig.I-2-1	Route to the Survey Area.....	6
Fig.I-3-1	Existing Geological Map map area .....	9
Fig.I-3-2	Area Map of the Previous Airborne Geophysical Survey .....	12
Fig.I-3-3	Interpretation map of existing Airborne Geophysical data.....	14
Fig.I-3-4	Geological Map of Marrakech-Tekna Area .....	17
Fig.I-3-5	Geological Column at Marrakech-Tekna area.....	19
Fig.I-3-6	Geological Cross Section of Marrakech-Tekna Area .....	21
Fig.I-3-7	Distribution of deposits at Marrakech-Tekna .....	23
Fig.I-3-8	Mineral Assemblage at each stage.....	27
Fig.I-3-9	Histogram of Homogenization Temperature about Mineralization Stage .....	29
Fig.I-3-10	The Histogram of Sulfur Isotope Ratio which Mineralization in each deposit .....	31
Fig.I-3-11	Airborne Magnetic Anomaly Map.....	36
Fig.I-3-12	Airborne Electromagnetic Anomaly Map .....	37
Fig.I-3-13	Interpretation Map of the Airborne Survey .....	40
Fig.I-4-1	Synthetic Map of the Survey .....	46
Fig.II-1-1	Exploration license around the Survey area .....	51
Fig.II-1-2	Existing Geological Map map area .....	53
Fig.II-1-3	Existing Airborne Magnetic Anomaly Map(Jebilet) .....	58
Fig.II-1-4	Existing Airborne Electromagnetic Anomaly Map (Jebilet) .....	59
Fig.II-1-5	Synthetic Map of Existing Geophysical Data (Jebilet) .....	60
Fig.II-1-6	Existing Airborne Magnetic Anomaly Map (Guemassa) .....	62
Fig.II-1-7	Synthetic Map of Existing Geophysical Data (Guemassa) .....	63
Fig.II-2-2-1	Location Map of the Survey Area .....	71
Fig.II-2-2-2	Location Map of Marrakech-Tekna Area .....	71
Fig.II-2-2-3	Geologica Map of Marrakech-Tekna Area.....	75
Fig.II-2-2-4	Geological Column at Marrakech-Tekna area.....	77
Fig.II-2-2-5	Geological Cross Section of Marrakech-Tekna.....	79
Fig.II-2-2-6	Geological Map of Jebilet Prospect.....	81
Fig.II-2-2-7	Geological Cross Section of Jebilet Prospect.....	83
Fig.II-2-2-8	Geological Column of Jebilet Prospect .....	88
Fig.II-2-2-9	Geological Map of Guemassa Prospect.....	91
Fig.II-2-2-10	Geological Cross Section of Guemassa Prospect.....	93

Fig.II-2-2-11	Geological Column of Guemassa Prospect .....	97
Fig.II-2-2-12	Distribution of deposits at Marrakech-Tekna area .....	99
Fig.II-3-1	The Location of Drilling Posit.....	109
Fig.II-3-2	Geological Column at Individual districts.....	113
Fig.II-4-1-1	Result of the Homogenization Temperature and Salinity of .....	135
	Fluid inclusion in Quartz at Guemassa Prospect	
Fig.II-4-1-2	Histogram of Sulfur Isotope of Deposits at Marrakech-Tekna Area .....	138
Fig.II-4-2	Plots of Major Elements against SiO <sub>2</sub> of Igneous Rocks of .....	142
	Tekna-Marakech Area	
Fig.II-4-3	Primitive mantle-normalized trace element abundances .....	144
Fig.II-4-4	LIL - HFS (Igneous rocks).....	146
Fig.II-4-5	LIL-HFS Spider diagram (Igneous rocks) .....	147
Fig.II-4-6	REE Spider diagram (Igneous rocks).....	147
Fig.II-4-7	K-Ar age of rocks of Tekna-Marakech area .....	151
Fig.II-4-8	Variation of Alkali Index and Metal contents (Cu+Pb+Zn) by Depth of Drilling... 155	
Fig.II-4-9	Relationship between Al <sub>2</sub> O <sub>3</sub> contents and various constituents of .....	156
	Sedimentary Rocks (1)	
Fig.II-4-10	Relationship between Al <sub>2</sub> O <sub>3</sub> contents and various constituents of .....	157
	Sedimentary Rocks (2)	
Fig.II-4-11	Spider Graph of REE (normalized Chondrite) .....	159
Fig.II-4-12	La-Sm diagram and La-Yb diagram.....	160
Fig.II-4-13	TREE, Ce/Ce* and Eu/Eu* of Mudstone (Depth).....	161
Fig.II-4-14	Histogram of Sulfide Isotope of sulfide in Mudstone (1).....	163
Fig.II-4-15	Histogram of Sulfide Isotope of sulfide in Mudstone (2).....	164
Fig.II-4-16	Variation of Sulfur Isotope of sedimentary rocks by depth of drilling.....	165
Fig.II-5-1	Area of Airborne Geophysical Survey .....	169
Fig.II-5-2	Geological Map of Marrakech - Tekna Area .....	170
Fig.II-5-3	GEOTEM Electromagnetic and Magnetic System.....	172
Fig.II-5-4	The Half-sinoidal Bipolar Current Wave from showing .....	172
	the On Time and Off Time	
Fig.II-5-5	Flight Path .....	177
Fig.II-5-6	Digital Terrain Model .....	181
Fig.II-5-7	Total Magnetic Intensity.....	183
Fig.II-5-8	Residual Magnetic Intensity .....	185
Fig.II-5-9	(dB/dt) <sub>x_early time</sub> .....	189
Fig.II-5-10	(dB/dt) <sub>x_late time</sub> .....	191

Fig.II-5-11	(dB/dt) $z_{early}$ time.....	193
Fig.II-5-12	(dB/dt) $z_{late}$ time.....	195
Fig.II-5-13	Apparent Conductivity .....	197
Fig.II-5-14	Total Energy Envelope .....	201
Fig.II-5-15	Decay Constant.....	203
Fig.II-5-16	Moment .....	205
Fig.II-5-17	Interpretation Map of Airborne Geophysical Survey .....	209
Fig.II-6-1	Mineral Assemblage at each Stage .....	215
Fig.II-6-2	The Flow Chart of Mineralization by the Mineral Classification .....	217
Fig.II-6-3	The Characteristic of the Early I mineralization Stage .....	220
Fig.II-6-4	The Characteristic of the Early II mineralization Stag .....	221
Fig.II-6-5	Histogram of Homogenization Temperature about Mineralization Stage .....	224
Fig.II-6-6	The Histogram of Sulfur Isotope Ratio which mineralisation in each Deposit.....	229
Fig.II-6-7	The average and standard deviation of Sulfur Isotope Ratio in each Deposit.....	230
Fig.II-6-8	Schematic geological model of Marrakech-Tekna Area.....	234
Fig.II-6-9	Synthetic Map of the Survey .....	237

## Appendices

Appendix 1.	Geologic Core Logs of Existed Drillings .....	A- 1
Appendix 2.	Sample List.....	A- 49
Appendix 3.	Photomicrographs of Thin Sections.....	A- 59
Appendix 4.	Microscopic Observation of Thin Sections .....	A-179
Appendix 5.	Results of X-ray Diffraction Analysis .....	A-197
Appendix 6.	Results of Chemical analysis.....	A-207



## **Part I The General**

## Part I: General Remarks

### Chapter 1: Introduction

#### 1-1 Purposes of the Survey

Marrakech-Tekna in the Kingdom of Morocco as the target area of our survey has a high potential of the massive sulfide deposit existence containing multiple metal elements similar to those in KUROKO in Japan or Iberian pyrite belt distributed in Spain and Portugal, where BRPM and private mining companies (including those abroad) have energetically enforced their deposit explorations. The government of the Kingdom of Morocco requested the Japanese Government in its official correspondence No. 293 dated November 21, 2001 to conduct the “The Mineral Exploration Survey” as cooperation with the development of mineral resources. In response to this request, the Japanese Government placed its signature on the Scope of Work (S/W) and Minutes of Meeting (M/M) on July 17, 2002 and thereby decided to find promising districts with the existence of massive sulfide deposits and to contrive technical transfer to the government officers of the country through fields work and analysis of the geological conditions and mineralization.

#### 1-2 Outline of the Survey

##### 1-2-1 The Survey Area

Out of 2,100 km<sup>2</sup> as the total survey area, 550 km<sup>2</sup> was the scope of our exploration where exploration claims are owned by BRPM alone. Airborne geophysical survey was performed on a rectangular area of approx. 1,100 km<sup>2</sup> (34 x 34 km) with Hajar mine and Kwadra deposit located at its southeast and northwest corners (Fig. I-1 and Table I-1-1 show the coordinate of the Survey area).

Table I-1-1: Coordinate of the Survey area

	Latitude	Longitude
Northeastern End	31° 55'00”	8° 00'00”
Southeastern End	31° 15'00”	8° 00'00”
Southwestern End	31° 15'00”	8° 30'00”
Northwestern End	31° 35'00”	8° 30'00”
Northern End	31° 55'00”	8° 15'00”

### 1-2-2 Contents and Quantities of the Survey

Compilation of existing data, geological survey, existing drilling core logging to identify ore horizon and airborne geophysical survey are applied as for the Phase I Survey in order to find survey area of massive sulfide ore deposits.

Table I-1-2 Contents and Quantities of the Survey

Items	Quantity
Geological survey	2,100km <sup>2</sup> (entire area),
Drilling core survey	3638.15 km (core length), 27 existing drilling cores
Airborne geophysical survey	6,853.5km (flight length), 1,110km <sup>2</sup> (survey area)

### 1-3 Organization of the Survey Team

The survey team consisted of the members below who participated in the survey planning, negotiation for conclusion of the agreement and the field survey.

#### (1) Survey planning and negotiation

Japanese side:

(Leader)

Ken Nakayama      Managing Director of Global Minerals Exploration Group., MMAJ

(Staff)

Munenori Kikuta      Mineral Resources Sect., Resources & Fuels Dept.,  
Agency of Resources & Energy, Ministry of Economy & Industry

Yoshiki Ebara      Resources Development & Investigation Sect.,  
Mineral Industry Development & Investigation Dept., JICA

Hiroshi Kubota      Exploration Team, Global Minerals Exploration Group., MMAJ

Hiroshi Shimotori      Overseas Researcher in London, MMAJ

Moroccan side:

(Leader)

El Bachir BARODI      Director of Exploration,  
Bureau de Recherches et de Participations Minières : BRPM

(Staff)

Hassan MAZNOUDI      BRPM

M'hamed ANNICH      BRPM

Ahmed KORCHI      BRPM

Mustapha CHAIB      BRPM

Said QUASRI      BRPM

Abderrahim QALBI      BRPM

(2) Site survey team (geological survey)

Japanese side:

(Leader)

Hiroshi Kubota Exploration Team, Global Minerals Exploration Group, MMAJ

(Staff)

Nobuaki Ishikawa Exploration Team, Global Minerals Exploration Group, MMAJ

Hiroshi Shimotori Overseas Researcher in London, MMAJ

Moroccan side:

Mustapha CHAIB BRPM

Abderrahim QALBI BRPM

(3) Site survey team (airborne geophysical survey)

Japanese side:

(Leader)

Mr. J.C. Radenac Fugro Airborne Survey Pty Ltd

(Staff)

Mr. Gerry Trepanier Fugro Airborne Survey Pty Ltd

Mr. Eric Picaud Fugro Airborne Survey Pty Ltd

Mr. Chris Karpowich Fugro Airborne Survey Pty Ltd

Mr. David Murrar Fugro Airborne Survey Pty Ltd

Mr. Jerzy Wojcicki Fugro Airborne Survey Pty Ltd

Mr. Mustafa Bakkal Fugro Airborne Survey Pty Ltd

Moroccan side:

Mustapha CHAIB BRPM

Muhamed NAJAH I BRPM

Supervisor at the site:

Hiroshi Kubota Exploration Team, Global Minerals Exploration Group, MMAJ

1-4 The Survey Period

The site survey was conducted in accordance with the schedule indicated in the table below.

Table I-1-3: Site Survey Schedule

Description of survey	Period
Preliminary survey	July 14 to 24, 2002
Geological survey	September 10 to October 13, 2002
Airborne geophysical survey	January 4 to March 7, 2003

## Chapter 2: Outline of the Survey Area

### 2-1 Location and Traffics

The Survey area is located in the south western of Marrakech, and in the north of the Anti-Atlas Mountains approximately 330km to the south of Rabat, the capital of the Kingdom of Morocco. Most of the roads running from the capital Rabat to the Survey area were paved and superhighways were constructed. It takes approximately an hour to drive on the highways from Rabat to Casablanca and approximately three hours to drive on the paved trunk road from Casablanca to Marrakech.

In addition to those in Rabat and Casablanca, there is also an international airport in Marrakech for flights directly to Europe (Paris, London, etc.)

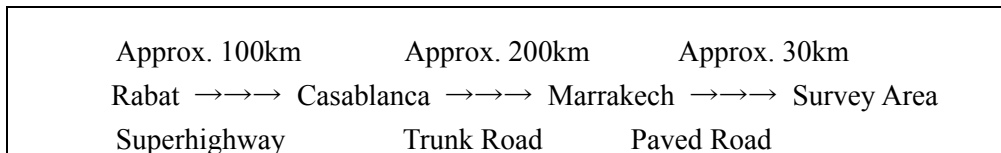


Fig. I-2-1: Route to the Survey Area

### 2-2 Geography and Climate

The Survey area consists of hilly land, 400 to 800m high from the sea level, which are smooth on the whole. The area is roughly divided into three parts in different topographies, i.e. Jebilet mountain area in the north, Haouz plain area in the center and Guemassa mountain area in the south. Jubilet and Guemassa area consist of regional metamorphosed sedimentary and volcanic rocks of Palaeozoic age. In Haouz plain, basement rocks of Palaeozoic age are overlain by sediments from Tertiary to Quaternary age in thickness of 80 to 120 mm, and little outcrops of rocks have exposed there.

The area is dry with inland climate, and much difference in temperatures is noted between daytime and night or among seasons; the temperatures rise to more than 40°C in summer and fall to almost 0°C in winter. With little plantation in general; only olives, citrus fruits, grapes and wheat suitable to dry land are grown and sheep are pastured. Rainy seasons are from April to May and from October to November, and the annual rainfall is approximately 300mm. However, floods sometimes occur resulting from local down pours in the rainy seasons.

Table I-2-1: Annual Temperatures and Precipitation in Marrakech

Month	Jan.	Feb.	Mar.	Apr.	May	Jun.	Jul.	Aug.	Sep.	Oct.	Nov.	Dec.
Highest Temperature(°C)	17	20	23	26	29	33	38	38	33	28	23	18
Lowest Temperature(°C)	3	6	10	11	14	17	20	20	18	14	10	6
Precipitation (mm)	29	31	31	33	20	8	2	3	10	17	27	34

The above highest and lowest temperatures represent monthly average temperatures, and the precipitation represents the average monthly figures. (Source: '94 Materials prepared by Tourism Bureau, the Government of Morocco)

### 2-3 Infrastructure Preparation

Marrakech City located on the east of the survey area is an international tourist city with a population of 350,000. It has a history of more than 1000 years and is designated officially as precious assets of world heritage. It's infrastructure including electricity, water supply, roads, medical treatment and communications is prepared very well. The roads in the survey area are sufficiently paved, and cellular phones are usable in most of the area.

## Chapter 3: Survey Results and General Examination

### 3-1 Collection and Analysis of the Existing Data

Exploration of the periphery of this area has been conducted by BRPM and its joint explorers on Jebilet, Guemassa and Haouz plain. The activities can be divided into three periods of time as follows;

Around 1930s: Surface survey was performed on gossan in the area of outcrops (Kettara deposit in Jebilet),

1960s onward: geophysical survey was performed on the ground concealed deposits and surface prospects and the underground extension of gossan (Draa Sfar deposit in the south of Jebilet),

The latter half of 1980s onward: airborne geophysical survey and the ground survey on concealed deposits (discovery of Hajar deposit in the east of Guemassa mountain mass and Khwadra deposit in Haouz plain - both of them are concealed deposits).

As a result, we confirmed high-magnetism anomaly in the airborne magnetic survey and known deposits, especially gossan ranging from Lachach in Jebilet, Kt. Aicha, Kechnet to Jbel Hedit and gossan ranging from Bensliman to Kerkoz and gossan distributed in the south and north of Kettara showed extremely good correspondence with each other. Basic volcanic rocks such as microgabbros, structural elements such as faults and contact metamorphic rocks such as granites and quartzites distributed in the eastern and western edges of the survey area are found to have caused the high-magnetism anomaly.

On the other hand, with respect to the anomaly of airborne electro-magnetism (resistivity), since most of gossan (deposits and mineral occurrences) show middle to low resistivities (~ several hundred  $\Omega/m$ ), and basic volcanic rocks show high resistivities (3000  $\Omega/m$  ~), we found that the resistivity is effective to identify the two matters similarly showing high anomalies in airborne magnetism.

As a result of the above examination of the existing data, it can be considered that deposit potential is high in the parts with high magnetism anomaly and low resistivity.

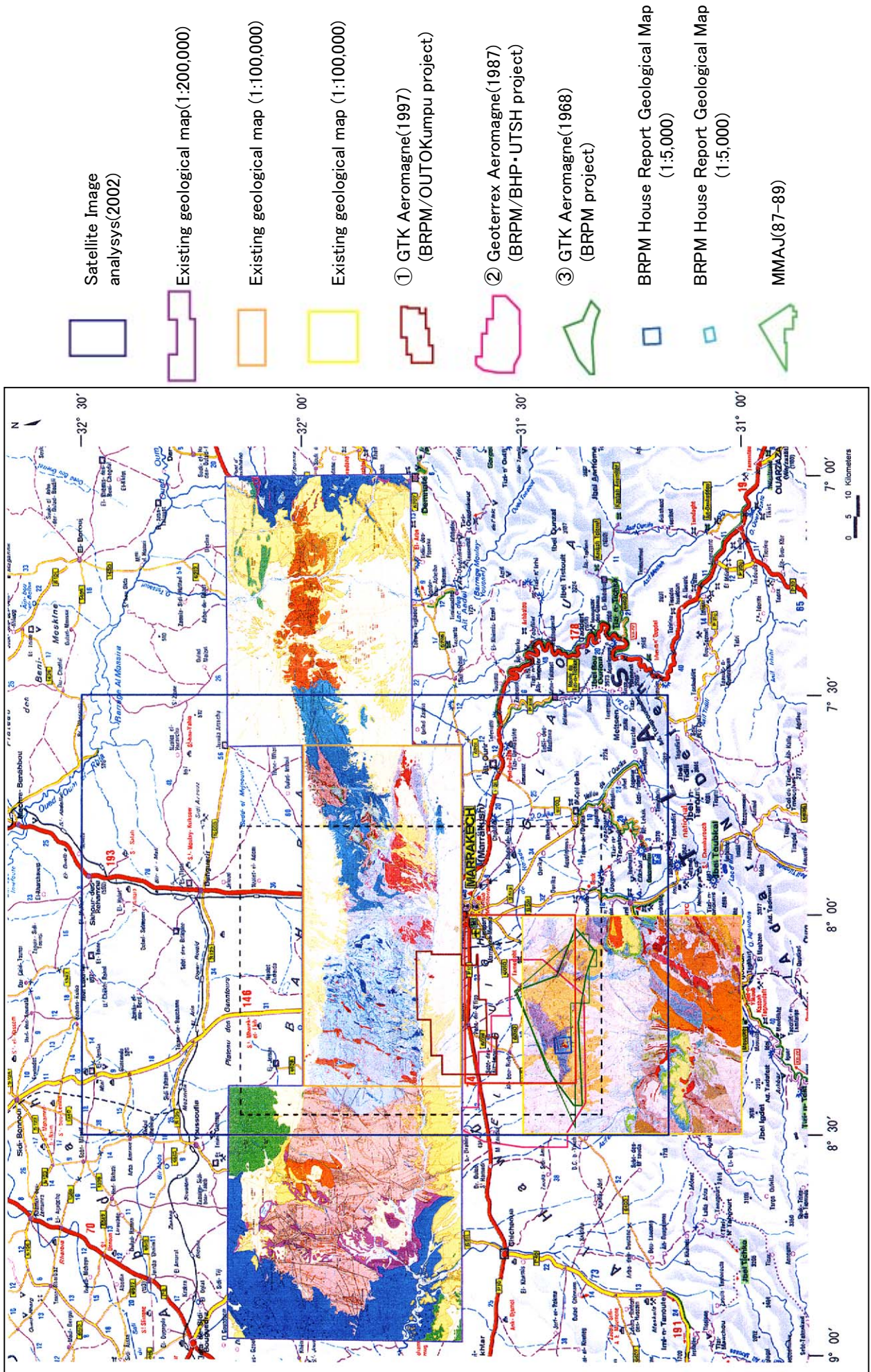


Fig.I-3-1 Existing Geological Map and Airborne Geophysics Map Area



Table I-3-1 List of Summerized Survey Survey HistoryAlready Performed (Jebilet Area)

No.	Area	BRPM(-84)			REMINEX1(84-88)			REMINEX2(88-94)			BRPM/some patners		
		Geol.	Geophy.	Drill.	Geol.	Geophy.	Drill.	Geol.	Geophy.	Drill.	Geol.	Geophy.	Drill.
1	DRAA SFAR	Carte	Mag, PS, EM, Res	48		Mag, Grav	5: 1998m	Carte	Mag, PPL, Melis	10c: 3915m, 3p: 476m			4,500m
2	KOUDIAT AICHA	Carte	Mag, PS, EM	4: 405m	Carte, GeoChem	Mag	9:2480m		PPL, Melis, Pulse	2c: 1576m, 2p: 495m			
3	LACHACH	Carte	Mag	4:415m	Carte		2: 343m	Carte	PPL, Mag, VLF, Melis	5: 925m			
4	DRA TRIFANI				Carte			Carte	Mag, PPL	3p: 612m			
5	KERKOZ	Carte	Mag, PS, EM, Res	6: 610m				Carte	Mag	3p: 585m			
6	EL_MNA							Carte	Mag, PPL				
7	J_HADID	Carte	Mag, PS, EM	2: 260m		Mag			Mag	1p: 156m			
8	Kt. HAMURA	Carte			Carte	Mag	1: 112m	Carte	PPL				
9	Kettara East		Mag		Carte	Mag	1: 211m	Carte, Geochem					
10	NZALET HAMEL		Mag			Grav	1: 253m		Mag				
11	BEN SLIMAN	Carte	Mag, PS, EM, Res	10 :1147m		Mag	1: 196m	Carte					
12	BOUHANE	Carte	Mag, PS, EM	3: 383m									
13	Dra SELGOUF /GOURSEFRA	Carte	Mag, PS, EM	3: 321m	Carte, Geochem								
14	J.SARHLEF		PS		Carte, Geochem								
15	Dr RHIRAT					Mag	1: 249m						
16	No.27 (north Bouhane)					Mag	1: 221m						
17	No.15 (east Si MBAREK)					Mag	1: 222m						
18	No.26 (DRAA EL KEBIR)					Mag							
19	No.29 (southwest)					Mag							
20	No.10				Carte	Mag							
21	No.4 (A'ZIB AI BACHA)					Mag							
22	SAFSAFA												
23	KHWADRA											Mag, Grav, EM	20: 11,126m
24	KETTARA												
25	KOUDIAT DELAA												
26	No.24												

(Data Source : BRPM)

Table I-3-1 List of Summerized Survey Survey HistoryAlready Performed (Guemassa Area)

No.	Area	BRPM(64-66)			BRGM(82-87)			BRPM(84-87)			BHP-UTAH(87-89)			JICA(87-90)			BRPM(90- )			
		Geol.	Geophy.	Drill.	Geol.	Geophy.	Drill.	Geol.	Geophy.	Drill.	Geol.	Geophy.	Drill.	Geol.	Geophy.	Drill.	Geol.	Geophy.	Drill.	
1	SALEM																			
2	TAGUENZA																1/5000	Mag		
3	TAMESLOHT					Mag														
4	AL MRAH																1/5000	Mag, Grav, Pulse	5: 2433m	
5	AMZOUGH				1/5000	Mag, PS		1/2000	Mag, Reses	2: 537m				1/10000	IP, Grav	4: 400m	1/2000	Mag, Grav, Pulse	3: 521m (+P)	
6	BEL AOUD								Mag, Grav, Reses				1: 100m							
7	LALLA ATTOUCH								Mag									Mag, Grav	1: ***m (+P)	
8	SOUKSOU																1/5000	Mag, Grav, Pulse	1: 371m	
9	GHOULA				1/5000	Mag, PS							1/5000	Mag, Max-Min, Pulse	1: 120m		1/5000	Mag, Grav, Pulse	2:835m	
10	ANABIA								Mag(T)								1/5000			
11	HALOUDI EAST																	Mag, Pulse	1: 404m (+P)	
12	HALOUDI WEST							1/10000	Mag, Grav									Pulse	1:365m (+P)	
13	MJED-NORTH							1/10000					1/5000	Mag, Max-						
14	MEJED							1/10000	Mag, Grav	1: 250m							1/5000	Pulse	3:949m (+P)	
15	MEJED-SOUTH																			
16	EL KARIA							1/5000	Mag, Pulse											
17	NZALA-SOUTH							1/5000	Mag, Max-											
18	NAZALA-EAST							1/5000	Mag, Pulse											
19	NAZALA-WEST							1/5000	Mag, Max-											
20	TAOUILILT							1/5000	Mag, Max-											
21	FRIZEM	1/1000	Mag	8: 1269m	1/2000 1/5000	PS, VLF, Grav, Max-Min, Elec		1/5000	Mag, PS, Turam, Misea la Mas	9: 2503m		1/5000	Mag, , VLV, Max-Min, Pulse	3: 388m	1/10000	IP	3: 1200m		Mag, Grav, Son, Elec	5: 2195m
22	ARISSA											1/5000	Max-Min, Mag, Pulse							
23	FRIZEM SOUTH								Mag, Max-											
24	SALEK											1/5000	Max-Min, Mag							
25	NSAFER												Mag, Pulse							
26	MOUKARA												Mag, Pulse						Mag, Grav	
27	EL HEDOUD												Mag, Pulse						Mag, Grav, Pulse, SE	1:255m
28	YASMIN																		Mag, Grav	

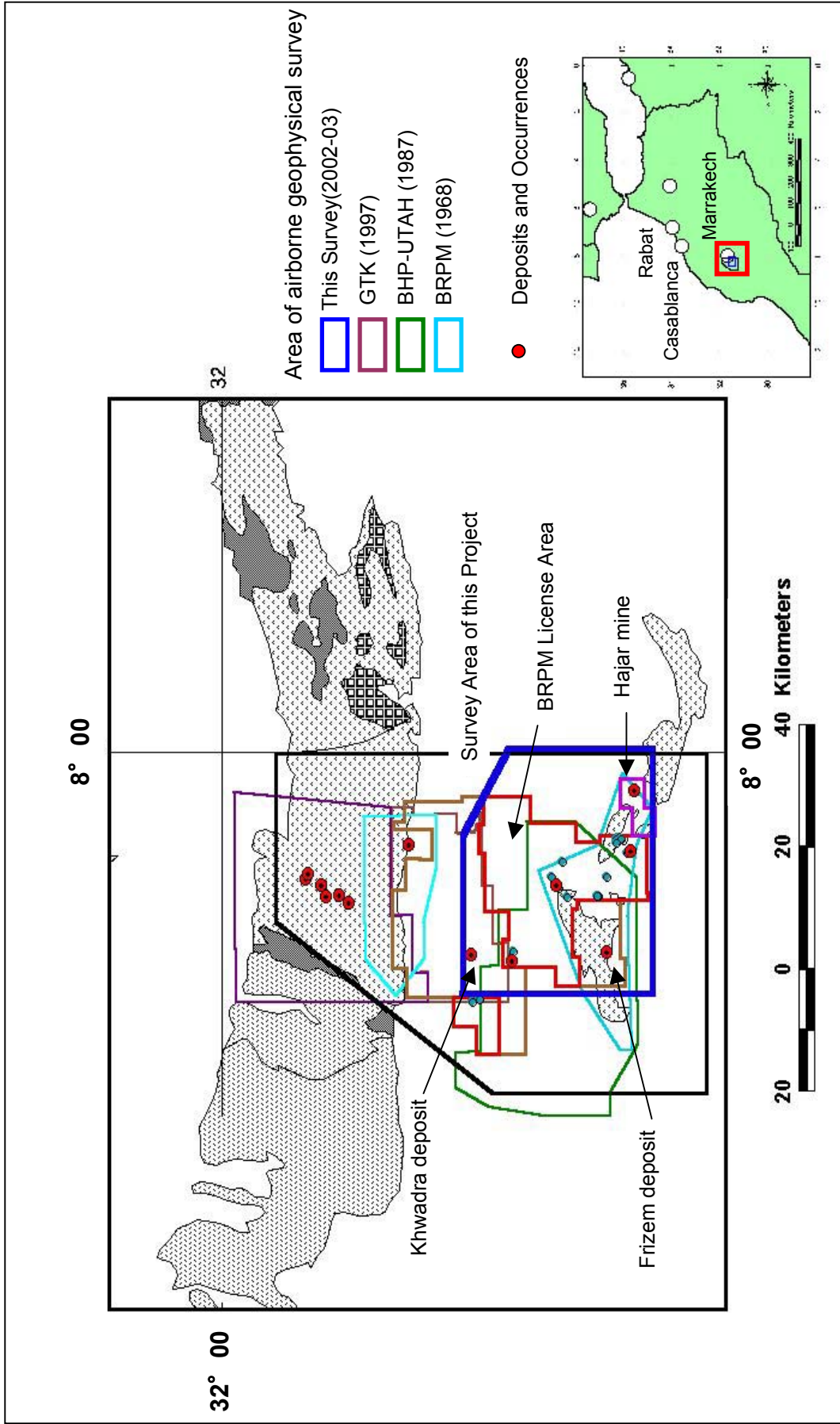


Fig 1-3-2. Area Map of the Existed Airborne Geophysical Survey

Table I-3-2: List of Major Airborne Geophysical Surveys

No.	Year	Area	Specification	Contractor
1	1964	Jebilet Central, Rehamma	Method : Mag Spacing of Line : 500m Direction of Line : Altitude : 100m Total Liniear	SAPA
2	1968	Guemassa, Jebilet Central	Method : Mag, Input Spacing of Line : 200m Direction of Line : E-W Altitude : 100-150m Total Liniear 2640km	Geoterrex
3	1971	Jebilet, Guemassa, Central Morocco	Method : EM Spacing of Line : 3000m Direction of Line : (U.K) Altitude : 600m Total Liniear : (U.K)	CGG
4	1985	Haut Atlas west, Haouz central (BRPM)	Method : Mag, VLF Spacing of Line : 3000m Direction of Line : (U.K) Altitude : 600m Total Liniear : (U.K)	ARMIC
5	1987	Guemassa (BRPM/BHP-UTAH)	Method : Mag, EM Geotem 12 ch Spacing of Line : 275m Direction of Line : E-W Altitude : 120m Total Liniear 3685km Travers spacing : 5km	Geoterrex
6	1997	Guemassa, Jebilet (BRPM-OUTOKUMP-CMG)	Method : Mag, Furequential EM Spacing of Line : (U.K) Direction of Line : E-W Altitude : 30-50m Total Liniear 3800km	GTK

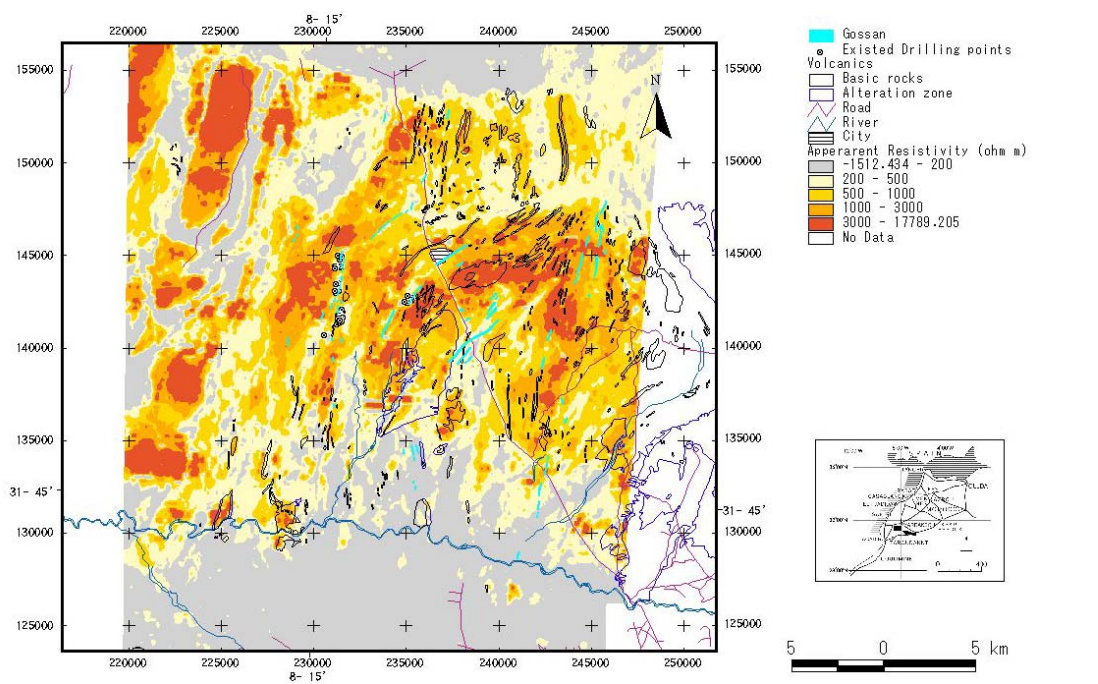
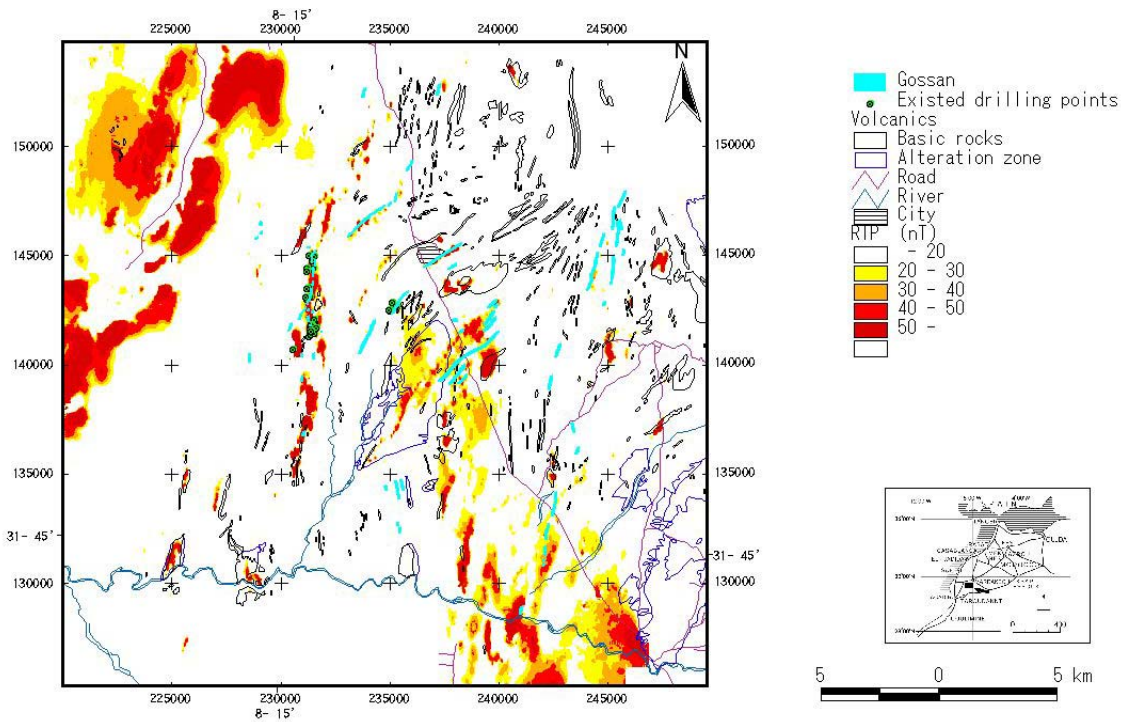


Fig.I-3-3 Interpretation map of existing Airborne Geophysical data

## 3-2 Geology and Mineralization

### (1) General Geology

The central Jubilet in the north of the Survey area consists of the basement rocks that were deposited with the strike of the direction approximate NS or NNE – SSW and the dip to the east. On the other hand, the geological structure of Guemassa in the south of the Survey area consists of the sediments with the strike of the direction NNW – SSE or NE – SW and the dip to the east. The basement rocks are mainly composed of pelite rocks of Devonian - Carboniferous - Permian that are interbedded with limestone, tuff and psammytic rock layers. Besides them, the basement rocks are interbedded with many acid or basic sills.

The geology of Visean, upper Carboniferous, in the central Jubilet and Guemassa, is composed of pelite rocks, acid volcanic rocks, basic volcanic rocks, rhythmic alternation, phyllite of the Sarhlef Formation, and carbonate rocks and pelite rocks of the Tequsim Formation that is the upper of the Sarhlef Formation (Fig.I-3-4, Fig.I-3-5)

### (2) Characteristics of sedimentary rocks

Sedimentary rocks consist of shale, slate and schist and include much sericite, chlorite etc. by microscopic observation and X-ray diffraction. They are highly affected by regional metamorphism and alteration of ore mineralization. Variation of alkaline alteration strength at hanging wall and footwall of massive sulfide ore deposit was studied by boring core and the result showed some high alteration strength at hanging wall side. This indicates the possibility that hydrothermal activity continued for some time after formation of the ore deposit or was overlapped by another hydrothermal activities. As for major elements, positive correlation with  $Al_2O_3$  and  $TiO_2$  which are said to inflect the origin of broken chips, and V,  $K_2O$  and  $P_2O_3$  and negative correlation with  $SiO_2$ ,  $CaO$  and  $Fe_2O_3$  exist and the trends of general sea floor sediments are recognized. The dispersion of  $SiO_2$  in Hajar, Draa Sfar, and Kettara deposits is due to the supply of detritus origin material by acid volcanic activity. The content of  $CaO$  has a tendency to be higher than others in Khwardra deposit because the supply of biogenic origin material is higher than others. As for rare earths pattern, LREE is rich and Eu anomaly is observed. This is due to island arc volcanic detritus origin material. The tendency that total rare earths (TREE) increases at the hanging wall side of the ore deposit is considered to be due to the move of rare earths from the hanging side to the floor side by hydrothermal solution. Sulfur isotope of sulfide in pelite varies from about -35 % to +25 % and has tendency to be lighter at hanging wall side than floor wall side. This tendency seems to indicate that the environment of sedimentation changes from Anoxic environment to oxidic environment according to Kajiwara (1989), Kajiwara and Kaiho (1992), Komuro (1999).





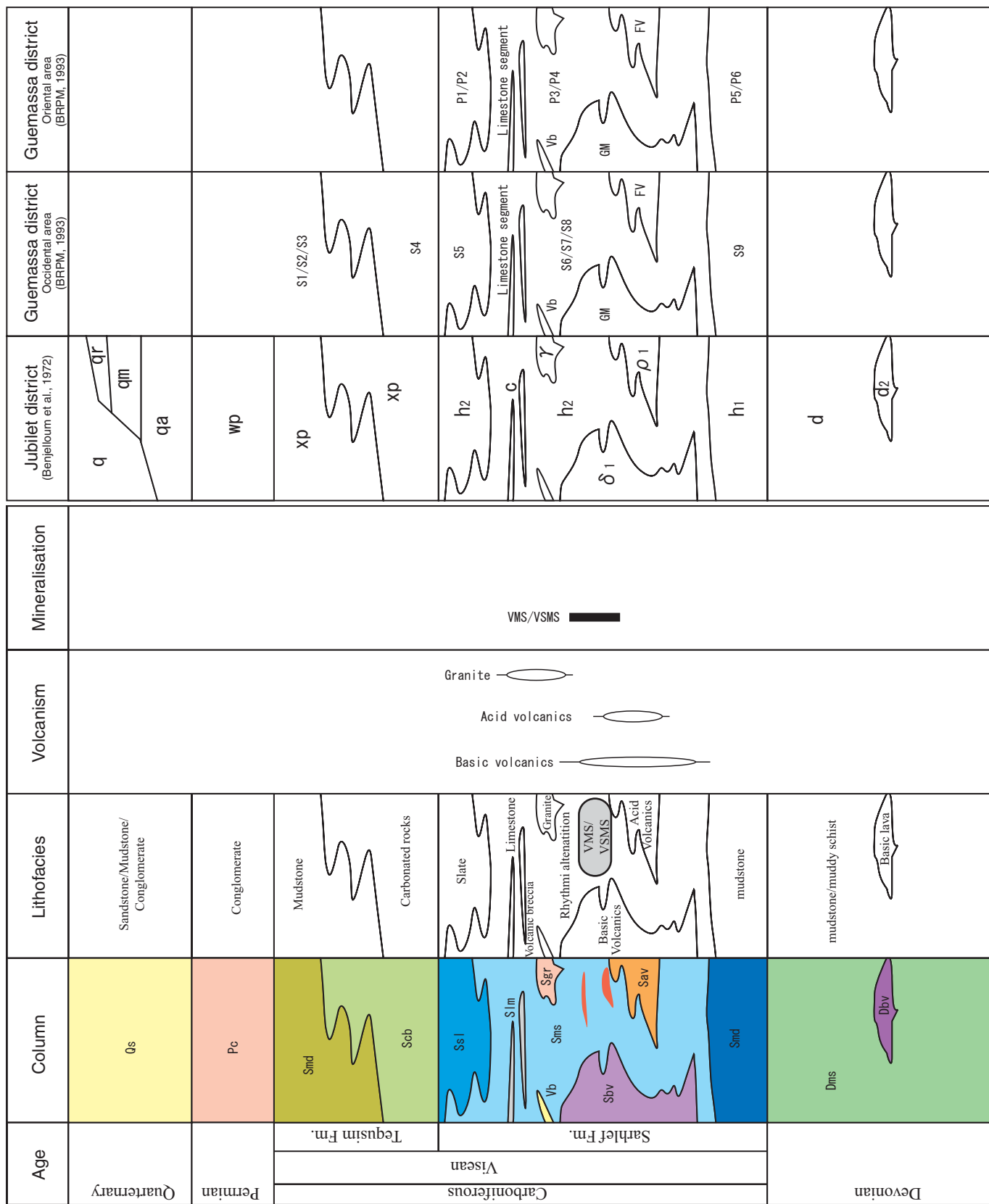


Fig. 1-3-5 Geological column at Marrakech-Tekna area



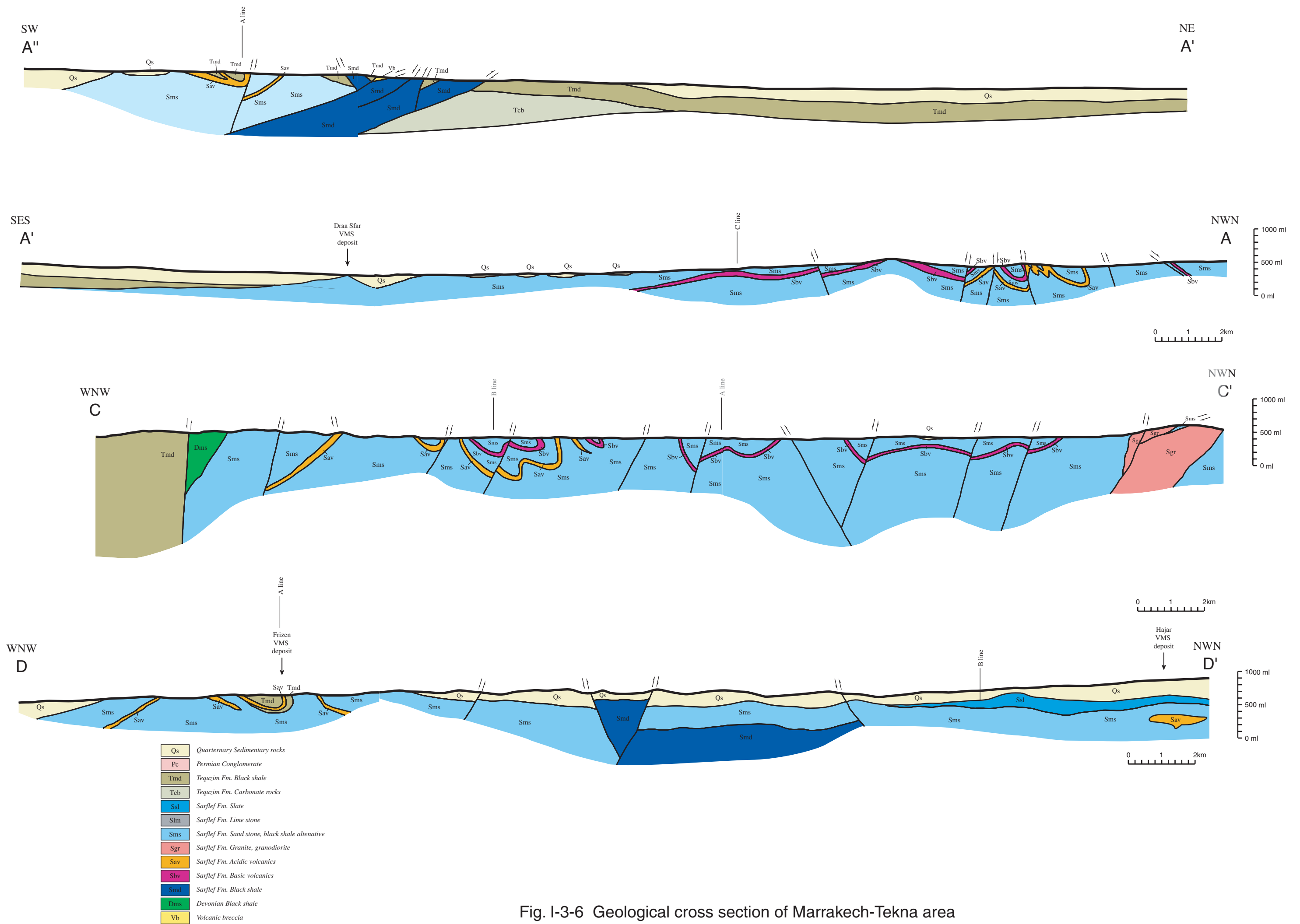


Fig. I-3-6 Geological cross section of Marrakech-Tekna area



### (3) Characteristics of igneous rocks

Chemical composition and radioactive dating were studied on the volcanic rocks distributing in the neighborhood of each ore deposit in this area. The result of the chemical composition analysis showed the rare earths pattern of acid volcanic rocks (rhyolite) in Hajar, Khwardra, and Draa Sfar deposits has light rare earths abundantly and flat pattern having Eu anomaly. As for major components, similar tendency indicating negative correlation with SiO<sub>2</sub>, K<sub>2</sub>O, Rb, Ba and Cs is seen so that these acid volcanic rocks are considered to have similar geochemical properties. However, the neighboring Safsafa deposit has different properties of the acid volcanic rocks (tonalitic mylonite) of. Also when comparing the basic volcanic rocks (dolerite) of this area with basalt, LIL element and HFS element of other area, it was found that the basic volcanic rocks of this area has features of island arc dolerite having much LIL element and differs from N-MORB which has poor LIL and HFS.

From the results of the measurement of K-Ar radioactive dating aiming at grasping mineralizing dating and igneous activity dating, volcanic rocks are classified to plutonic igneous activity, acid volcanic activity, mineralizing alteration (Guemassa) and mineralizing alteration (Jebilet). The datings of plutonic igneous activity and acid volcanic activity are 290 to 360 Ma, the dating of mineralizing alteration (Guemassa) is 260 to 320 Ma and are equivalent to the late stage of the activities of abyssal rock and volcanic rock, and the dating of mineralizing alteration (Jebilet) is equivalent to after the activities of plutonic rocks and volcanic rocks.

### (4) Characteristics of Mineralization

The ore deposits in Jubilet and Guemassa districts are the Cu-Pb-Zn-Fe massive sulfide ore deposits that were embedded in sedimentary rocks and volcanoclastic rocks of Sarhlef Formation, Viséan.

Kettara deposit in the central Jubilet, Draa Sfar and Khwadra deposits in the southern end of the Jubilet mountain massif forming the boundary area of the basement and Tertiary layer, Hajar deposit in the western end of the Guemassa, and Frizen deposit in the east are the main massive sulfide ore deposits in this area.

The shapes of these ore deposits are layered, massive, lenticular, and banded. The major combination of minerals is pyrrhite, pyrite, galena, and chalcopyrite. Acid and/or basic volcanic rocks are distributed in the vicinity of the ore deposit. The volcanic rocks relates to the mineralization.

### (5) Characteristics of Sulfide Ore deposits

The purpose of this Survey is to find the potential area of massive sulfide deposits by

examining the geology and mineral occurrences in Jubilet and Guemassa area, referring to the characteristics of the concealed massive sulfide ore deposit in the Marrakech district, For this purpose, the characteristics of the massive sulfide ore deposit that were obtained by the geological survey, study of past drilling cores and the laboratory works are shown below.

#### 1) Classification of Mineralization and the Mode of Occurrence of Pyrrhotite

Khwadra, Draa Sfar, Kettara, Hajar, and Frizen deposits are classified as the massive sulfide ore deposits by the deposit shape, the combination of minerals and related igneous rocks. It becomes obvious that these ore deposits were formed by repetition of mineralization in the early stage and the late stage, considering the mode of occurrence of these ore deposit, ore minerals and alteration of the host rocks. The classification of mineralization and the combination of minerals and gangue minerals are shown in Fig.I-3-8. The characteristics of the mineralization and the combination of ore and gangue are listed in Table I-3-3. There is no known paper that described the classification of mineralization and the repetition of mineralization about the massive sulfide ore deposits in Morocco.

The early stage and the late stage mineralization are represented by pyrrhotite and pyrite respectively from the viewpoint of Fe-S minerals. The early stage of mineralization is divided into the early I sub-stage and the early II sub-stage in the Khwadra ore deposit and the Hajar ore deposit. The former is represented by hexagonal pyrrhotite and the latter is represented by monoclinic pyrrhotite. Hexagonal pyrrhotite crystallized in the early I sub-stage was generally changed to monoclinic pyrrhotite in wide area by the mineralization of the later stage. On the other hand, monoclinic pyrrhotite crystallized in the early II sub-stage was changed to marcasite. The sulfide minerals that were crystallized in each stage of mineralization coexist with quartz. The accumulated histogram of the homogenized temperature of fluid inclusion within quartz is shown in Fig.I-3-9.

The homogenized temperature of fluid inclusion within quartz that coexists with hexagonal pyrrhotite of the early I sub-stage is 270 – 280 °C. Monoclinic pyrrhotite of the early II sub-stage was directly crystallized with quartz and sphalerite under the temperature 300 °C (230 – 250 °C). The homogenized temperature of fluid inclusion of quartz that coexists with pyrite and sphalerite is 200 – 250 °C.

The composition of the pyrrhotite crystallized in the different mineralization stage changed according to the different mineralization stage, and after the crystallization the component changed according to the  $fs_2$  change of the different mineralization in the massive sulfide ore deposit in this area.

Mineral	MINERALISATION									
	Early-I			Early-II	Latar			Stockwork		
	1	2	3	2	1	2	3	2	3	
Ore minerals	sphalerite	█	█	█	█	█	█	█	█	█
	galena	█	█		█	█	█	█	█	
	chalcopyrite	█	█	█	█	█	█	█	█	█
	pyrite (euhedral)		█	█	█	█	█	█	█	█
	pyrrhotite	█	█	█	█					
	arsenopyrite									
	marcasite (euhedral)		█	█	█	█				█
	marcasite (exfoliating lamellae)				█					
	magnetite		█	█	█		█	█	█	█
	ilmenite									
	hematite							█		█
	covellite						█	█		
	acanthite		█							
	stannite		█							
Primary minerals	quartz		█	█	█		█	█	█	█
	plagioclase		█		█		█	█	█	█
	augite		█	█			█	█	█	█
	hornblende									
Altered minerals	clay minerals		█	█	█		█	█	█	█
	carbonate minerals				█		█	█		

Fig. I-3-8 Mineral assemblage at each stage

Table I-3-3 The list of the characteristics of the mineral assemblage

Mineralisation	Stage	Ore mineral	Gungue mineral	Discription
Early mineralisation	Early-I	pyrrhotite(hexagonal)· sphalerite· chalcopyrite		hex.po→mono.po
	Early-II	pyrrhotite(monoclinic)· sphalerite· galena· (pyrite)	quartz, carbonate minerals	mono.po→marcasite
Later mineralisation	Later	pyrite· sphalerite· galena· chalcopyrite· marcasite	quartz, clay minerals, carbonate minerals	

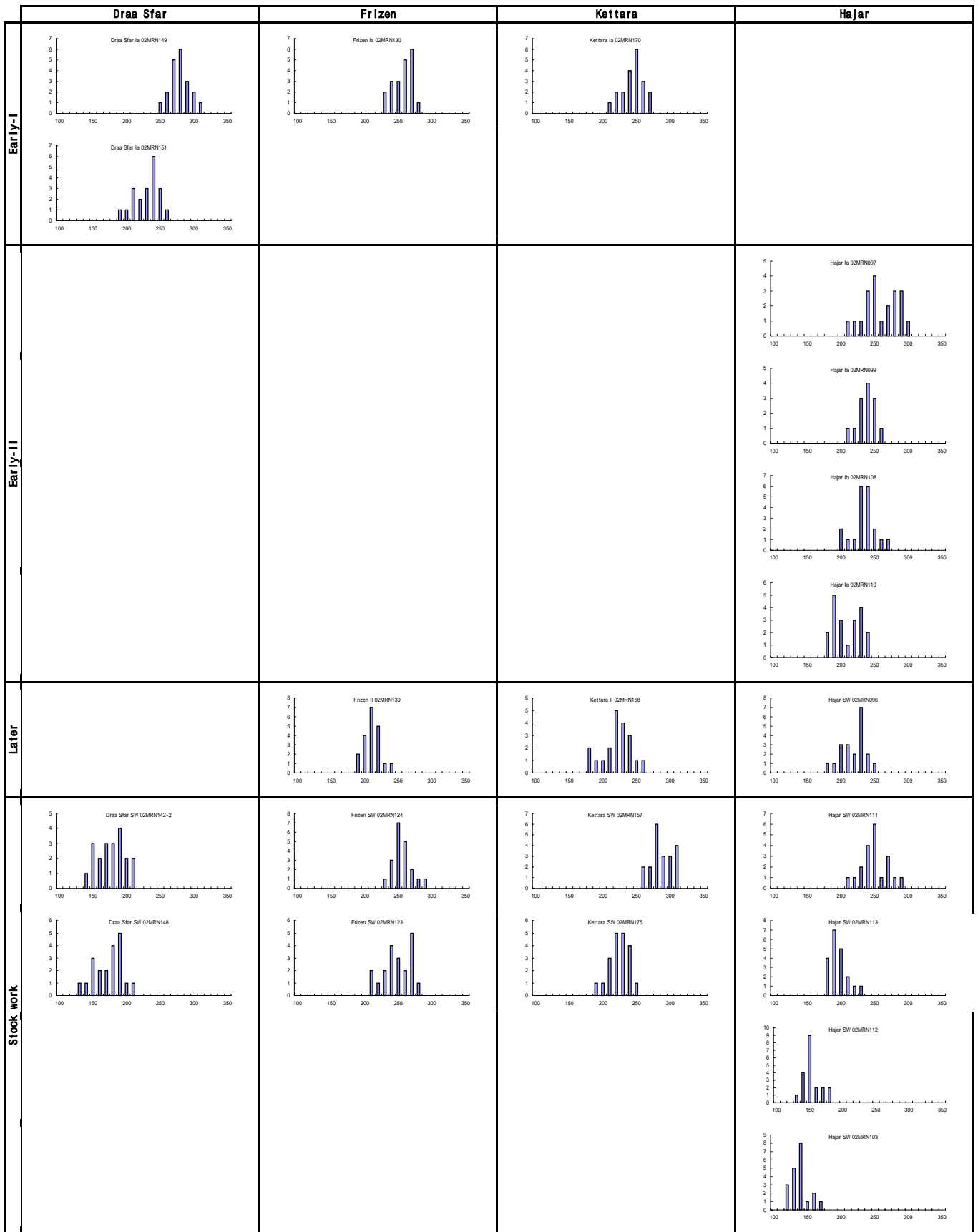


Fig. I-3-9 Histogram of Homogenization Temperature about Mineralization Stage

## 2) Characteristics of Sulfur Isotope Ratio

The characteristics of sulfur isotope ratio were studied to understand the difference of the mineralization environment of the early stage and the late stage in Khwadra, Draa Sfar, Kettara, Hajar and Frizen deposits. The accumulated histogram of sulfur isotope ratio of each mineralization stage in each ore deposit is shown in Fig.I-3-10. Referring to the Figure, the differences of the ratio in the early stage by the ore deposit are distinct. That is, the ratio, from lowest to highest, is in Khwadra deposit, Draa Sfar deposit, Kettara deposit, Hajar deposit, and Frizen deposit.

The marked variation of the sulfur isotope ratio within one ore deposit or within one ore-bearing area is in sharp contrast to the uniform sulfur isotope ratio of the KUROKO deposit in Japan. The following reasons are considered as the causes of the difference; the difference of the physical and the chemical conditions of mineralization, the mixing of sulfur of organic origin and the restriction of supply of seawater origin sulfur to the hydrothermal water in the mineralization. Based on the above consideration, it is considered that there is a relatively large effect of mixing of organic origin sulfur in Khwadra deposit, and the relatively large contribution of magma origin sulfur to mineralization in Hajar deposit.

## 3) Mineralization and Magnetism

It becomes obvious that the magnetism of the area around each ore deposit is related to the characteristic of the polymorphism of pyrrhotite of each ore deposit. That is, the high magnetic anomalies are detected in Khwadra and Hajar deposits where the monoclinic pyrrhotite characteristically occurs. On the other hand, a high magnetic anomaly area and a low magnetic anomaly area are adjacent in Draa Sfar deposit where hexagonal pyrrhotite and monoclinic pyrrhotite coexist. The low magnetic anomalies were only detected in Kettara deposit and Frizen deposit where hexagonal pyrrhotite and pyrite coexist.

Therefore, it is pointed out that the possibility of existence of a Pb–Zn massive ore deposit with low magnetism that consists of hexagonal pyrrhotite and pyrite in the medium to low magnetic anomaly area like Kettara deposit and Frizen deposit, and the possibility of existence of a Pb–Zn massive sulfide ore deposit with relatively low magnetism that consists of hexagonal pyrrhotite and monoclinic pyrrhotite in the area where a high magnetic anomaly area and a low magnetic anomaly area are adjacent.

## 4) Conclusion

The total review of sulfide ore is summarized in Table I-3-4. The following findings about the massive sulfide ore deposit of Morocco was obtained.

(1) The mineralization repeatedly occurred in the massive sulfide ore deposit in the survey area.



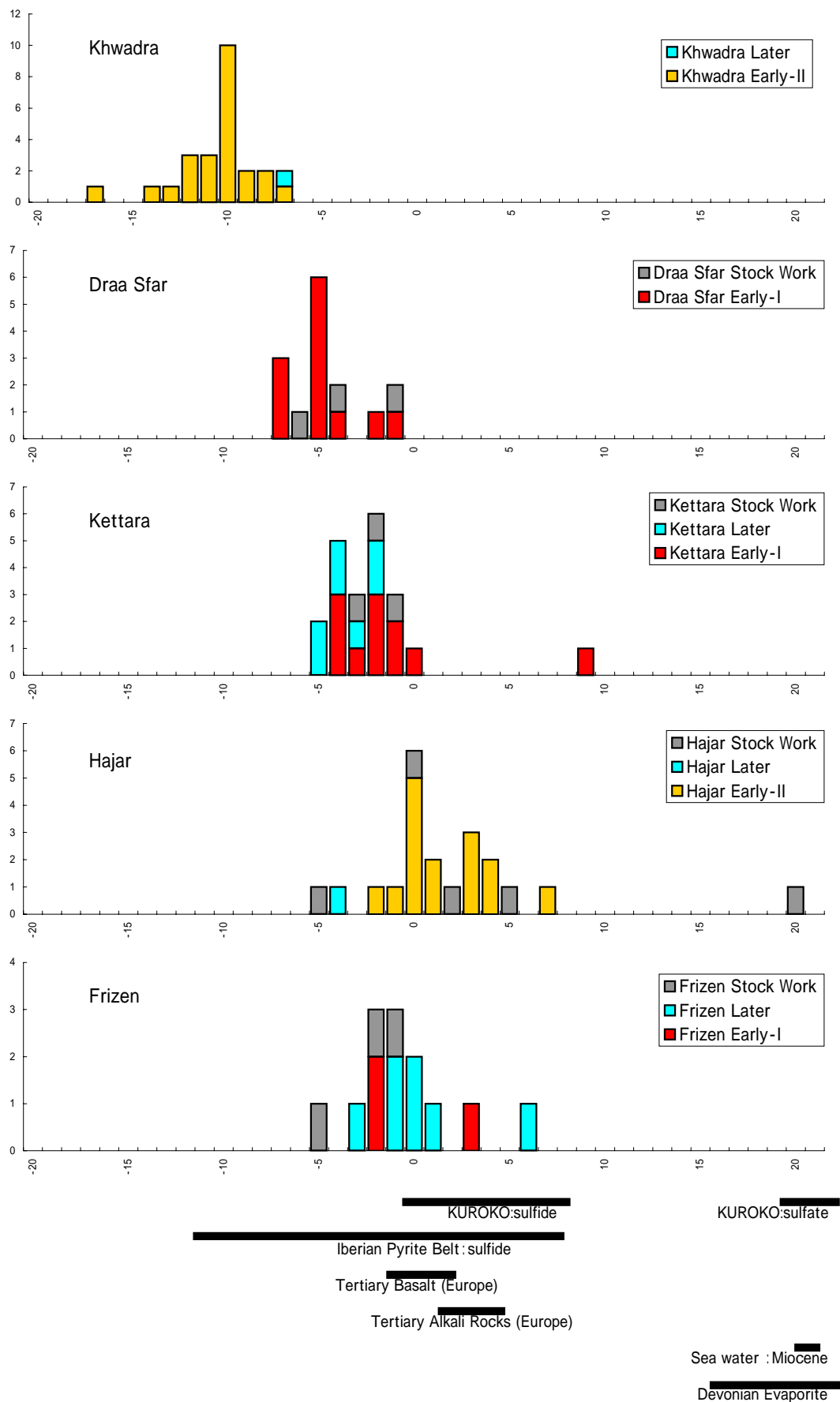


Fig . I-3-10 The histogram of sulfur isotope ratio which mineralisation in each deposit

Table I-3-4 The list of the characteristics of mineralisation

Deposit	Mineralisation type	Sulfide mineral	Homogenization Temperature	Magnetic Anomaly
Draa Sfar	Early I	<b>pyrrhotite(hex.)</b> pyrrhotite(mono) Sphalerite galena chalcopyrite	High-Temp.  ( 270-280°C concentrate )	Medium anomaly
Kettara Frizen	Early I + Later	<b>pyrrhotite(hex.)</b> pyrrhotite(euhedral) sphalerite galena chalcopyrite	High Temp. + Low Temp.  ( 270-280°C and 180-250°C concentrate )	Medium anomaly + Low anomaly
Khwadra Hajar	Early II + Later	<b>pyrrhotite(mono.)</b> marcasite (lamella) <b>pyrite(euhedral)</b> sphalerite galena chalcopyrite	Medium Temp. + Low Temp.  ( 230-250°C and 180-250°C concentrate )	High anomaly Low anomaly

From the viewpoint of the combination of minerals, the mineralization stage is divided into the early I sub-stage, the early II sub-stage and the late stage.

- (2) - The early I sub-stage mineralization is represented by hexagonal pyrrhotite and its magnetism is comparatively weak.
  - The early II sub-stage mineralization is represented by monoclinic pyrrhotite and its magnetism is strong.
  - The late stage mineralization is represented by pyrite. The magnetism is weak.
- (3) The mineralization temperature was 270–280 °C in the early I sub-stage, 230– 250 °C in the early II sub-stage and 200–250 °C in the late stage, judging from the homogenized temperature of fluid inclusion of quartz which coexists with sulfide ore minerals.
- (4) The marked variation of sulfur isotope ratio within the area is explained by the difference of the physical and chemical conditions, mixing of the sulfur of organic origin and limitation of providing sulfur of seawater origin to the hydrothermal water. It is considered that in Khwadra deposit, the contribution of the sulfur mixing of organic origin was effective, and in Hajar deposit and Frizen deposit, the contribution of the sulfur of magma origin was relatively effective.
- (5) According to the above fact, the classification of the ore deposit types is following three types of ore deposits seem to exist in this area:
  - (a) Early I sub-stage dominant type
    - Medium magnetic anomaly [Draa Sfar deposit]
  - (b) Repeated type of the early I sub-stage + the late stage
    - Medium + low magnetic anomaly [Frizen deposit, Kettara deposit]
  - (c) Repeated type of the early II sub-stage + the late stage
    - High + low magnetic anomaly [Khwadra deposit, Hajar deposit]

### 3-3 Airborne Geophysical Survey

#### (1) Outline of the airborne geophysical survey

The purposes of the airborne geophysical survey in the Phase I was to find potential of massive sulfide ore deposits in the Survey for consideration of the area of detail survey in Phase II. Airborne magnetic and electro-magnetic survey was carried out in the field and examined existing data of airborne geophysical survey in the Phase I.

The survey area (Tekna area) was an area of about 1,110km<sup>2</sup> between the Jebilet mountain massif and the Guemassa mountain massif, which lies southwest of Marakkech. We use the fixed wing aircraft for data acquisition. Out line of specification of the survey are summarized in Table.I-1-5.

Table I-3-5 Specifications of the Airborne Geophysical Survey

Item	Description
Traverse line length	6853.5km
Traverse line interval	200m (East-to-west direction) 1,000m (South-to-north direction)
Terrain clearance	120 ± 20m
Electromagnetic measurement system	Time domain measurement (GEOTEM)

#### (2) Result of the survey

The grid data that was acquired in this survey includes one kind of magnetic data (residual magnetic intensity) and four kinds of electromagnetic data (apparent conductivity, total energy envelope, decay constant, and moment).

##### 1) Airborne magnetic data

According to the data of Residual Magnetic Intensity (RMI) and Total Magnetic Intensity (TMI), the southern part of the area is a low magnetic zone and its northern part a high magnetic zone. The boundary between these two zones almost corresponds to that between the flat ground and the hill. Judging from this, the boundaries seemingly originate from its geological structure such as a fault (NE-SW).

A high magnetic anomaly zone in the northern magnetic zone is relatively large with its diameter of 2-4km. There is a high magnetic anomaly with its diameter of about 8km at the northeastern end of the area, which seems to be a stock of granites.

There are dotted slight magnetic anomalies with their diameter of 200m from the center of the high magnetic zone in the northern part of the area. On the eastern part, there is a repetition of

minor magnetic rolls extending in the NW-SW direction. Judging from their appearances, they may be related to the stratification or schistosity.

The low magnetic zone on the southern side has a NW-SE trend as a whole, and there is a wide low magnetic anomaly zone with the same trend extending especially on its central part. There are a high magnetic anomaly (almost corresponding to the Hajar deposit) at the eastern end of the zone and a high magnetic anomaly (a part of it almost corresponding to the Frizen ore deposit) at the western margin of the zone. The zone has a structure looking as if it has been cut in several sections by NE-SW faults.

There is a high magnetic anomaly with its diameter of 1-3 km confirmed in the western and eastern directions outside of the wide low magnetic anomaly zone.

## 2) Airborne electromagnetic data

Overviewing a drawing obtained from four kinds of electromagnetic data (apparent conductivity, total energy envelope, decay constant, and moment), all data indicate the same tendency in general, but there are differences in details. Culture noises due to power-transmission wires, etc. are almost removed in the total energy envelope, but remains remarkable in the moment and the decay constant. In the apparent conductivity, they are almost removed on the western side of the area and remains on its eastern side.

Resistivity structures on the northern and southern sides of a national highway running NE-SW in the middle of the area are different from each other, and the highway boundary seemingly corresponds to the boundary between its geological structures.

According to the Apparent conductivity map, on the southern side of the resistivity boundary dividing the area into two parts, a high resistivity zone with its large distribution area on the western part and some high resistivity zones on the eastern part almost correspond to the exposed part of bedrocks (Paleozoic carboniferous-series sedimentary rocks and pyroclastic rocks) on the existing geological map. And it is obvious that the bedrocks generally show a high resistivity. On the other hand, almost the entire part other than the bedrocks exposed is an area where the Neogene's sediments (mp) distribute and the area has a low resistivity. Also, most of the distribution area (q) of the Quaternary sediments on the eastern part shows its low resistivity. It seems that there is a clear boundary between the high resistivity part which seems to be bedrocks and the low resistivity part around the former part and that the outcrop of a stratum boundary with its sharp inclination is covered.

The northern side generally has low-to-mid resistivity, but there is an area nearing the resistivity boundary in the middle, in a part of which a high resistivity distributes. There is a remarkable low resistivity zone confirmed on the western part. Comparing the part with the

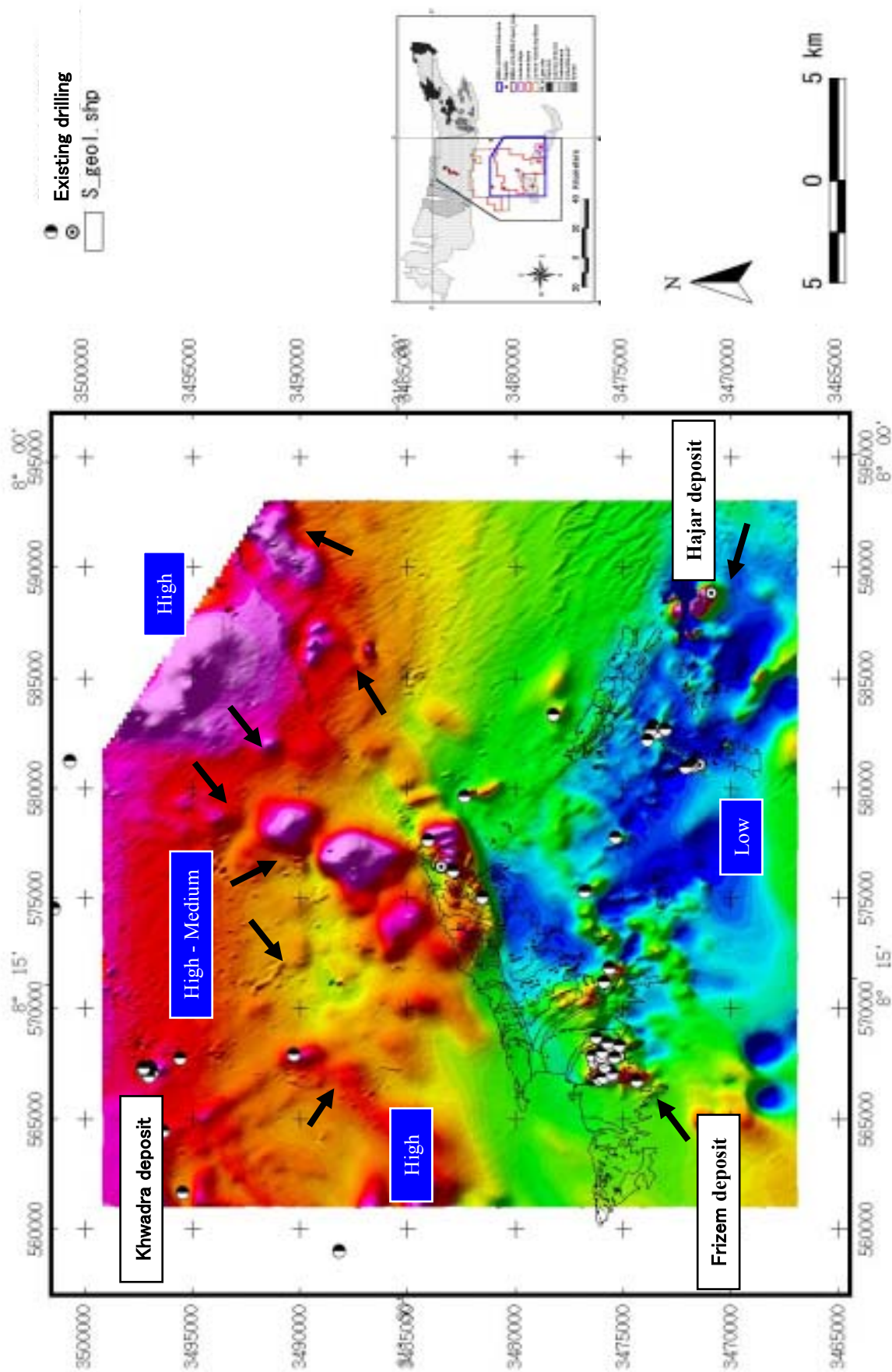


Fig.I-3-11 Airborne Magnetic Anomaly Map

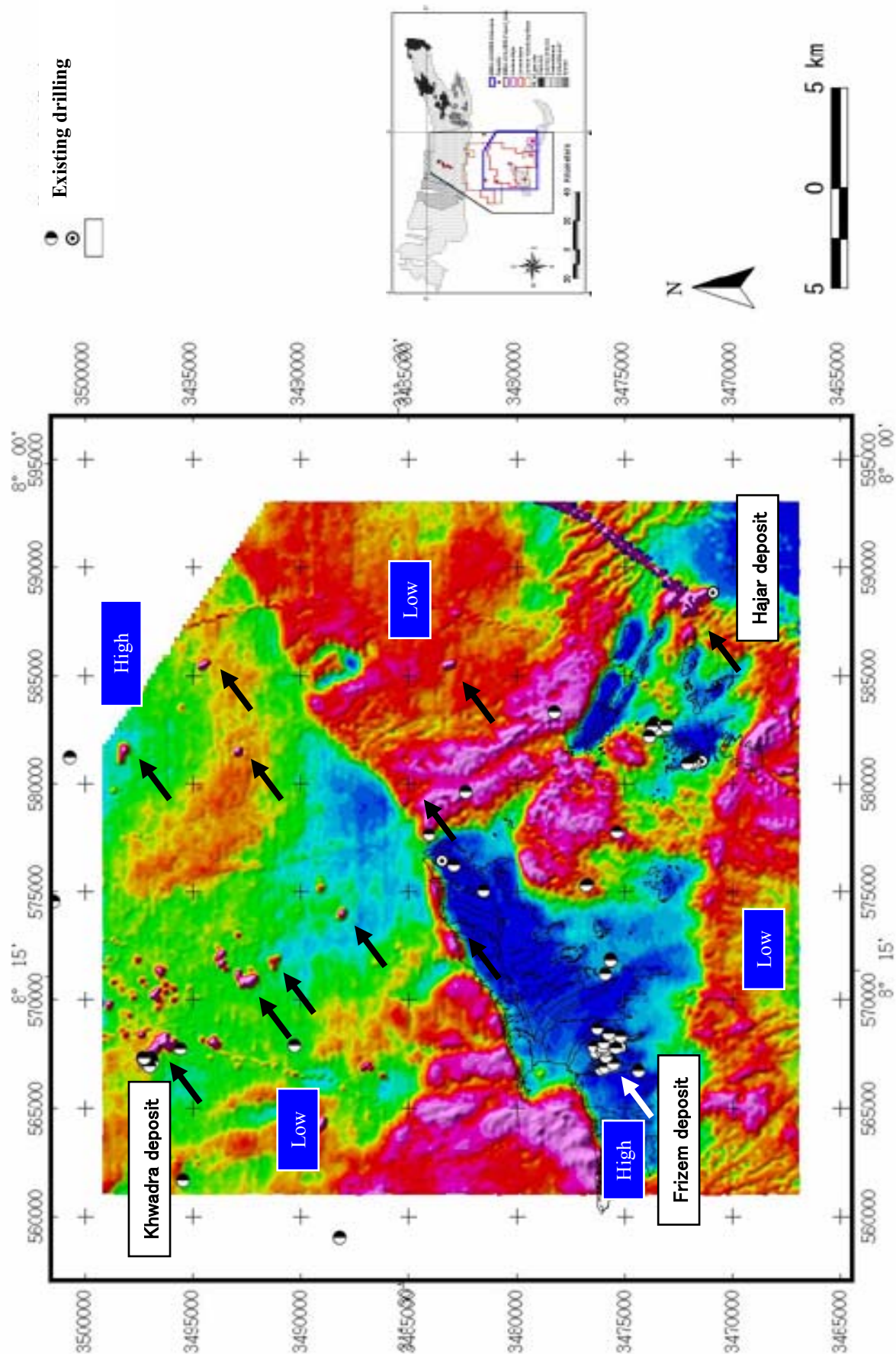


Fig.I-3-12 Airborne Electromagnetic Anomaly Map

existing geological map, the zone corresponds to the distribution area (mp, pV2) of the Neogene's sediments. Besides, in the regional low-to-middle resistivity zones, a large number of marked local low resistivity areas of 200 – 2000 m are seen. No particular regularity is observed in the distribution or arrangement.

### 3) Interpretation

Interpreting the geology of the survey area by combining airborne magnetic survey data with airborne electromagnetic survey data gives following results:

#### (1) South of the boundary of resistivity at the center of the survey area (NE-SW system)

The distribution area of basement rock (exposed and concealed outcrop) is a part extracted as a low magnetic zone by RMI and low resistivity zone by the decay constant. It is thought that the resistivity is high with a shallow outcrop of basement rock and middle with a deep one. All from igneous rocks through volcanic clastic rocks occur at 3 points: southeast (Hajar deposit), west (Frizen deposit) and north. In addition, magnetic indications suggestive of the occurrence of the said rocks in other area can be observed.

Given as promising sites are those where there is concurrence of local low resistivity and high magnetic anomaly or where these two are adjacent.

#### (2) North of the boundary of resistivity at the center of the survey area (NE-SW system)

As a result of studying the airborne magnetic survey data, it is estimated that physical properties (resistivity) of the basement rocks in this area is largely different from that of the south side. A comparison between the total energy envelope (resistivity structure at shallow part) and the decay constant (resistivity structure at a deep zone) make it possible to extract the following 3 areas:

- (a) Area at the west end: low resistivity from shallow through deep part
- (b) Central area extending from east to west: middle/high resistivity at shallow part - low resistivity at deep part
- (c) Northern area extending from east to west: low resistivity at shallow part-middle resistivity at deep part

If in the areas (b) and (c) there is a basement rock with concealed outcrop, the location containing igneous rock to volcanic clastic rock shows a high magnetic anomaly with a diameter of 2 to 4 km as verified by RMI.

Given as promising sites are the zones of overlapping local low resistivity and high magnetic anomaly locally or where these two are adjacent. Such a zone are obtained in the northwest area and around high magnetic anomalies that is considered granite stock in the



northeast area.

## 2) Potential of existing massive sulfide deposits

Areas where following airborne geophysical anomalies had been observed were selected as survey areas considering the probability of the existence of mineral deposit due to low resistivity and magnetic anomaly, and medium to low magnetic anomaly obtained by airborne geophysical survey.

### (1) Low resistivity zone + high to medium magnetic anomaly

- (a) The area where low resistivity zone overlaps medium magnetic anomaly which exist numerously from Khwadra deposit at northwest part of the airborne geophysical survey area to Choula district in Guemassa though marked high magnetic anomaly was not obtained by the survey at this time.
- (b) Low resistivity area existing in relatively large scale high magnetic anomaly in the northeast part, western part of Marrakech airport.

### (2) High magnetic anomaly part

- (a) Small scale medium to high magnetic anomaly zone dotted in relatively large scale high magnetic anomaly in the north east part, western part of Marrakech airport.
- (b) Small scale medium to high magnetic anomaly zone dotted in relatively large scale high magnetic anomaly at south west part of Khwadra ore deposit, Nasfar.

### (3) Low resistivity part

- (a) Low resistivity zone near Tamasloht, eastern direction of Ghoula. Magnetic anomaly is not seen.

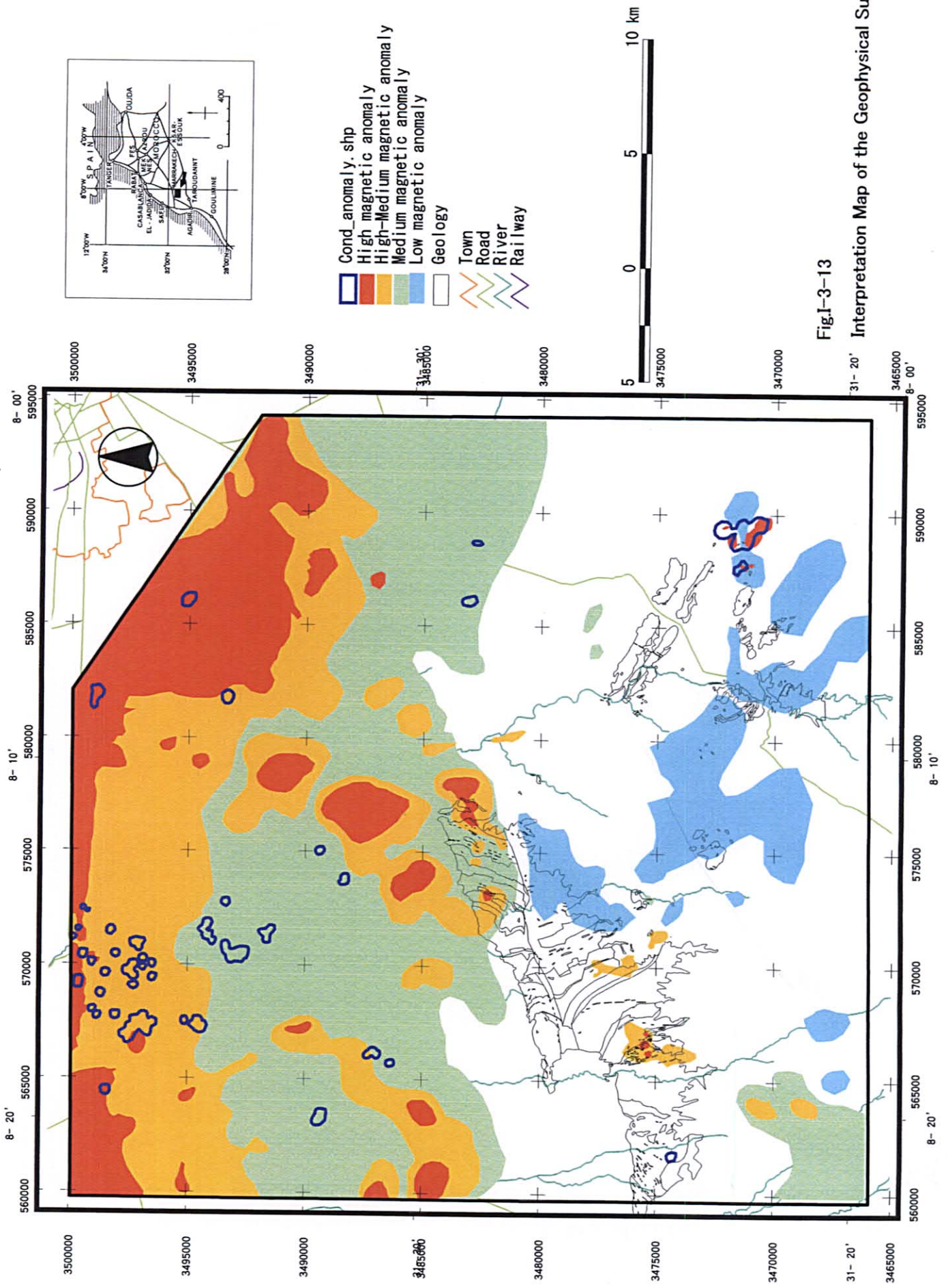


Fig.1-3-13

Interpretation Map of the Geophysical Survey

## Chapter 4: Conclusion and Recommendation

### 4-1 Conclusion

#### (1) Geology and Mineralization

##### (Geology and Ore Showing in Jubilet District and Guemassa District)

The central of the Jubilet in the north of the area consists of the basement rocks that were deposited with the strike of the direction approximate NS or NNE – SSW and the dip to the east. On the other hand, the geological structure of Guemassa in the south of the area consists of the sediments with the strike of the direction NNW – SSE or NE – SW and the dip to the east. The basement rocks are mainly composed of pelite rocks of Devonian - Carboniferous - Permian that are interbedded with limestone, tuff and psammytic rock layers. Besides them, the basement rocks are interbedded with many acid or basic sill. The geology of Visean, upper Carboniferous, in the central Jubilet mountain massif and Guemassa district, is composed of pelite rocks, acid volcanic rocks, basic volcanic rocks, rhythmic alternation, phyllite of the Sarhlef Formation, and carbonate rocks and pelite rocks of the Tequsim Formation that is the upper of the Sarhlef Formation.

The ore deposits in Jubilet and Guemassa districts are the Cu-Pb-Zn-Fe massive sulfide ore deposits that were embedded in sedimentary rocks of Visean and volcanoclastic rocks.

Kettara deposit in the central Jubilet, Draa Sfar and Khwadra deposits in the southern end of the Jubilet mountain massif forming the boundary area of the basement and Tertiary layer, Hajar deposit in the western end of the Guemassa and Frizen deposit in the east are the main massive sulfide ore deposits in this area.

The shapes of these ore deposits are layered, massive, lenticular, and banded. The major combination of minerals is pyrrhotite, pyrite, galena, and chalcopyrite. Acid and/or basic volcanic rocks are distributed in the vicinity of the ore deposit. The volcanic rocks relates to the mineralization.

##### (Characteristics of Sulfide Ore minerals)

Kettara deposit in the central Jubilet, Draa Sfar and Khwadra deposits in the southern end of the Jubilet mountain massif forming the boundary area of the basement and Tertiary layer, Hajar deposit in the western end of the Guemassa, and Frizen deposit in the east are the main massive sulfide ore deposits in this area. The shapes of these ore deposits are layered, massive, lenticular, and banded. The major combination of minerals is pyrrhotite, pyrite, galena, and chalcopyrite. Acid and/or basic volcanic rocks are distributed in the vicinity of the ore deposit. The volcanic rocks relates to the mineralization.

Khwadra, Draa Sfar, Kettara, Hajar, and Frizen deposits are classified as the massive

sulfide ore deposits by the deposit shape, the combination of minerals and related igneous rocks. It becomes obvious that these ore deposits were formed by repetition of mineralization in the early stage and the late stage, considering the mode of occurrence of these ore deposit, ore minerals and alteration of the host rocks.

The early stage and the late stage mineralization are represented by pyrrhotite and pyrite respectively from the viewpoint of Fe-S minerals. The early stage of mineralization is divided into the early I sub-stage and the early II sub-stage in the Khwadra ore deposit and the Hajar ore deposit. The former is represented by hexagonal pyrrhotite and the latter is represented by monoclinic pyrrhotite. Hexagonal pyrrhotite crystallized in the early I sub-stage was generally changed to monoclinic pyrrhotite in wide area by the mineralization of the later stage. On the other hand, monoclinic pyrrhotite crystallized in the early II sub-stage was changed to marcasite. The homogenized temperature of fluid inclusion within quartz that coexists with each stage of mineralization, the early I sub-stage mineralization is 270 – 280 °C, the early II sub-stage mineralization is 230 – 250 °C, the late-stage mineralization is 200 – 250 °C.

The marked variation of the sulfur isotope ratio within one ore deposit or within one ore-bearing area is in sharp contrast to the uniform sulfur isotope ratio of the KUROKO deposit in Japan. The following reasons are considered as the causes of the difference; the difference of the physical and the chemical conditions of mineralization, the mixing of sulfur of organic origin and the restriction of supply of seawater origin sulfur to the hydrothermal water in the mineralization. Based on the above consideration, it is considered that there is a relatively large effect of mixing of organic origin sulfur in Khwadra deposit, and the relatively large contribution of magma origin sulfur to mineralization in Hajar deposit.

#### (Mineralization and Magnetism)

That is, the high magnetic anomalies are detected in Khwadra and Hajar deposits where the monoclinic pyrrhotite characteristically occurs. On the other hand, a high magnetic anomaly area and a low magnetic anomaly area are adjacent in Draa Sfar deposit where hexagonal pyrrhotite and monoclinic pyrrhotite coexist. The low magnetic anomalies were only detected in Kettara deposit and Frizen deposit where hexagonal pyrrhotite and pyrite coexist.

Therefore, it is pointed out that the possibility of existence of a Pb–Zn massive ore deposit with low magnetism that consists of hexagonal pyrrhotite and pyrite in the medium to low magnetic anomaly area like Kettara deposit and Frizen deposit, and the possibility of existence of a Pb–Zn massive sulfide ore deposit with relatively low magnetism that consists of hexagonal pyrrhotite and monoclinic pyrrhotite in the area where a high magnetic anomaly area and a low magnetic anomaly area are adjacent.

According to the above fact, the classification of the ore deposit types is following three

types of ore deposits seem to exist in this area:

- (a) Early I sub-stage dominant type  
Medium magnetic anomaly [Draa Sfar deposit]
- (b) Repeated type of the early I sub-stage + the late stage  
Medium + low magnetic anomaly [Frizen deposit, Kettara deposit]
- (c) Repeated type of the early II sub-stage + the late stage  
High + low magnetic anomaly [Khwadra deposit, Hajar deposit]

(conclusion)

As the result of consideration of geology, existing drilling core and laboratory works, following exploration index are obtained.

- (a) Districts of expecting distribution of rhythmic alternation of Sarhlef formation under deeper surface.
- (b) Districts of expecting distribution of acidic volcanic rocks of Sarhlef formation under deeper surface.
- (c) Districts of expecting existing of massive sulfide ore deposits that has magnetic anomaly mentioned above under coverage of Tertiary or later.

(2) Airborne geophysical survey

(Geological structure)

Interpreting the geology of the survey area by combining airborne magnetic survey data with airborne electromagnetic survey data shows that magnetic and resistivity structure is different in north and south of the boundary of resistivity at the center of the survey area (NE-SW system) in this area.

In the south distribution area of basement rock is a part extracted as a low magnetic zone by RMI and low resistivity zone by the decay constant. It is thought that the resistivity is high with a shallow outcrop of basement rock and middle with a deep one. All from igneous rocks through volcanic clastic rocks occur at 3 points: southeast (Hajar deposit), west (Frizen deposit) and north. In addition, magnetic indications suggestive of the occurrence of the said rocks in other area can be observed. Given as promising sites are those where there is concurrence of local low resistivity and high magnetic anomaly or where these two are adjacent.

In the north resistivity structure make it possible to extract the following 3 areas:

- (a) Area at the west end: low resistivity from shallow through deep part
- (b) Central area extending from east to west: middle/high resistivity at shallow part - low resistivity at deep part
- (a) Northern area extending from east to west: low resistivity at shallow part-middle

resistivity at deep part

If in the areas (b) and (c) there is a basement rock with concealed outcrop, the location containing igneous rock to volcaniclastic rock shows a high magnetic anomaly with a diameter of 2 to 4 km as verified by RMI. Given as promising sites are the zones of overlapping local low resistivity and high magnetic anomaly locally or where these two are adjacent. Such a zone are obtained in the northwest area and around high magnetic anomalies that is considered granite stock in the northeast area.

(Potential of existing massive sulfide deposits)

Areas where following airborne geophysical anomalies had been observed were selected as survey areas considering the probability of the existence of mineral deposit due to low resistivity and magnetic anomaly, and medium to low magnetic anomaly obtained by airborne geophysical survey.

(1) Low resistivity zone + high to medium magnetic anomaly

- (a) The area where low resistivity zone overlaps medium magnetic anomaly which exist numerously from Khwadra deposit at northwest part of the airborne geophysical survey area to Choula district in Guemassa though marked high magnetic anomaly was not obtained by the survey at this time.
- (b) Low resistivity area existing in relatively large scale high magnetic anomaly in the northeast part, western part of Marrakech airport.

(2) High magnetic anomaly part

- (a) Small scale medium to high magnetic anomaly zone dotted in relatively large scale high magnetic anomaly in the north east part, western part of Marrakech airport.
- (b) Small scale medium to high magnetic anomaly zone dotted in relatively large scale high magnetic anomaly at south west part of Khwadra ore deposit, Nasfar.

(3) Low resistivity part

- (a) Low resistivity zone near Tamasloht, eastern direction of Ghoula. Magnetic anomaly is not seen

#### 4-2 Recommendation for the Second Year's Program

Khwadra, Draa Sfar, Kettara, Hajar, and Frizen deposits are classified as the massive sulfide ore deposits by the deposit shape, the combination of minerals and related igneous rocks. It becomes obvious that these ore deposits were formed by repetition of mineralization in the early stage and the late stage, considering the mode of occurrence of these ore deposit, ore minerals and alteration of the host rocks, and that each deposit has a different magnetic feature.

Areas where following airborne geophysical anomalies had been observed were selected as prospecting areas considering the probability of the existence of mineral deposit due to low resistivity and magnetic anomaly obtained by airborne geophysical prospecting, and medium to low magnetic anomaly obtained by geological survey.

- 1) Low resistivity zone + high to medium magnetic anomaly zone: possibility of the existence of high magnetic massive sulfide ore deposit.
- 2) High magnetic anomaly zone: possibility of the existence of high magnetic massive sulfide ore deposit.
- 3) Low resistivity zone: possibility of the existence of medium to low magnetic massive sulfide ore deposit.

We recommend followings as the second year survey:

- 1) Conducting gravitational survey, based on the property that the high density of massive sulfide ore deposit, as well as ground magnetic and electromagnetic survey to narrow the potential zone of existing massive sulfide ore deposit.
- 2) Conducting a drilling survey in the geophysical survey anomaly zone extracted by ground geophysical survey to confirm the underground geological structure and the condition of mineralization.







## **Part II Details of the Survey**

## Part II: **Details of the Survey**

### Chapter 1: Survey of the Existing Data

#### 1-1 Method of the survey

The existing data on geology and deposits were collected, converted into digital data to be compatible with GIS and compared with the existing data of airborne geophysical explorations.

#### 1-2 Results of the survey

##### 1-2-1 Outline of previous survey

The periphery of the area whose survey was requested includes Jebilet of north side and Guemassa/Haouz of south side which were surveyed by Bureau of Geology, Ministry of Mines and BRPM. From 1930s onward, gossan has been explored and developed focusing on the central part of Jebilet. In Kettara where gossan exploration was conducted to obtain data on copper and ochre, pyrrhotite was drilled as a reducer of phosphate ores in 1937 to 1982. Also in Draa Sfar where existence of gossan was recognized mineralized belts were discovered by SEGM (Deposit Study Sect.) in 1953, ground magnetism anomalies were identified by CPGNA (Geophysical Survey Co. in North Africa), and deposits were discovered in 1966. Although magnetic survey, drilling survey, 200m prospecting tunnel were conducted in 1960s to 1980s, no remarkable results were obtained. However, since concealed mineralized belts of zinc and copper were added as a result of the Drilling survey conducted by BRPM in the former half of 1990s, the data have been reviewed, and construction of 400m vertical shaft and exploration are now undertaken toward the development intended to take place in 2004.

In Guemassa and Haouz area, BRPM started its survey in 1964 and sporadic surveys were attempted up to 1980s, and the scale of the surveys has been on the increase from 1990 onward. Because of the existence of gossan, surveys were conducted centering on Frizem. No anomaly was extracted as a result of the airborne magnetic survey conducted by BRPM (enforced by Geotrex) in 1968. However, anomaly was extracted from Hajar deposit through reanalysis conducted by BRGM in France, and existence of mineralized belts of zinc, copper and lead was identified as a result of drilling conducted in 1984. In Guemassa, although geological and airborne magnetic surveys were conducted by BHP-UTAH and BRPM (Geotrex) and drilling was done in Ghoula and Belaoud in 1987, such activities were withdrawn in 1989. During the period of FYs 1987 to 1989, a geochemical survey, CSAMT method, IP method, a gravity survey and Drilling of 4 cores were conducted there by MMAJ/JICA and BRPM in Guemassa district as the “The Mineral Exploration in the the Haouz Plain” and mineralized portions of copper, lead, and zinc were discovered by Amzourh

anomaly.

It was about 1994 or 1995 when attention was paid to Haouz as BRPM discovered mineralized zones of zinc and lead in Draa Sfar. In 1995 BRPM, together with OUTOKUMP, established exploration license there, and anomaly was extracted as a result of the airborne magnetic survey conducted (enforced by GTK in Finland) in 1997, and mineralized zones of zinc, copper and lead were captured through the ground magnetic and gravity surveys, EM method done afterwards and the drilling conducted in 2000.

#### 1-2-2 Details of previous surveys

##### (1) Exploration license

The conditions of the mine license located in the periphery of the area surveyed are shown in the Fig.II-1-1. Out of approx. 2,100km<sup>2</sup> of the area investigated, the area of the part where BRPM alone possesses mineral claims is approx. 550 km<sup>2</sup>. Other parts are the mine claims jointly handled by BRPM and private companies including those abroad.

##### (2) Geological data

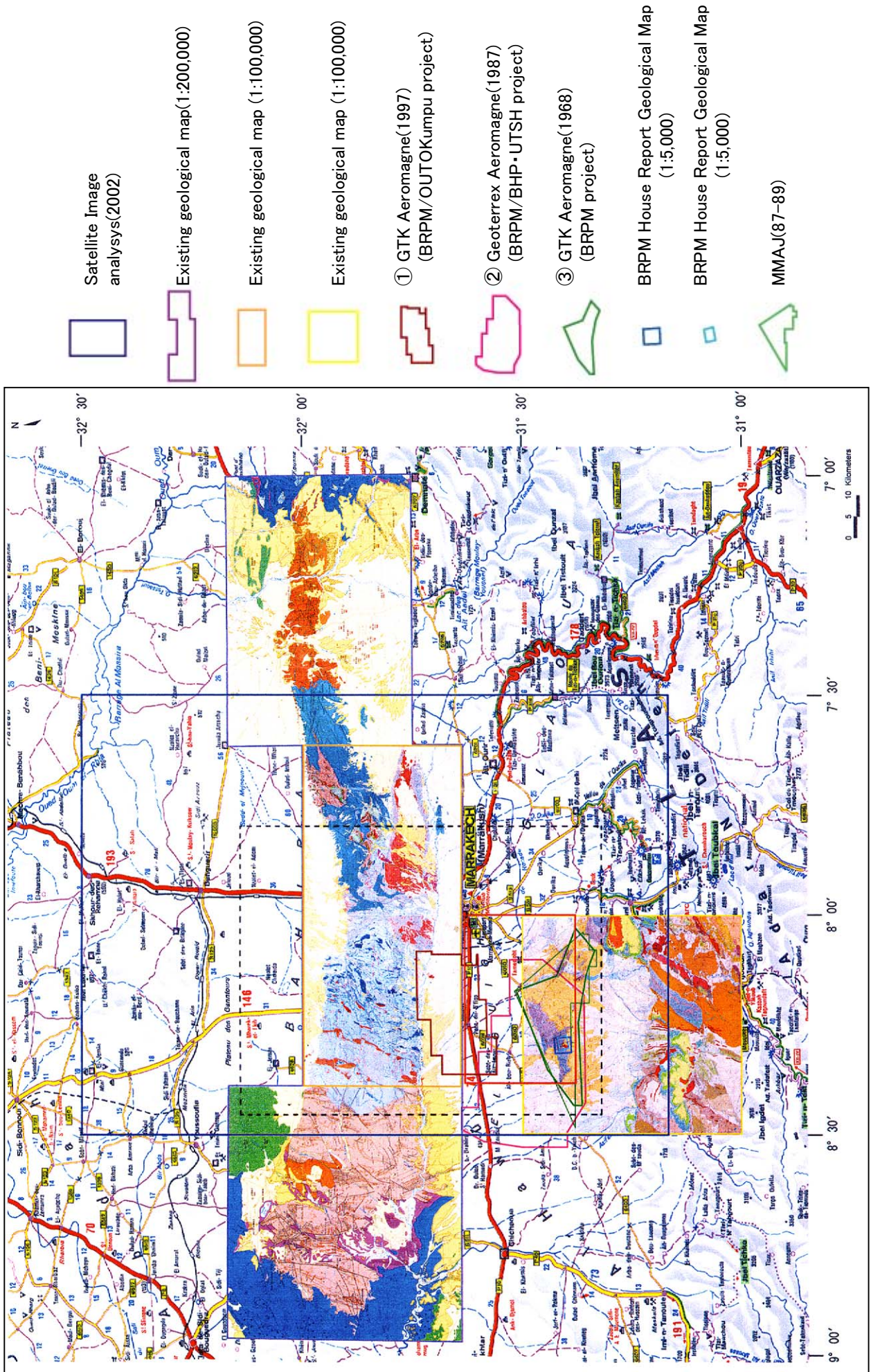
With regard to the geological features and deposits of the area covered by this survey, the Jebilet in the north and the Guemassa area in the south where have outcrops are compiled in 1/200000 and 1/100000 geological maps. In addition, BRPM and joint surveyors prepared more detailed geological maps and academic side surveyed in those areas. The maps that we acquired are listed in TableII-1-1 and shown on Fig.II-1-2 as their scope of covering area. Details of geology are described in Chapter 2 “Geological Survey”.



Table II-1-1: List of Major Existing Geological Maps

No.	Title	Scale	Coordinate		Remarks
1	CARTE GEOLOGIQUE DES JEBILET	1/100,000	7° 37' ~8° 23'W	31° 38' ~32° 00'N	DIRECTION DES MINES ET DE LA GEOLOGE 1972
2	CARTE GEOLOGIQUE DES JEBILET	1/200,000	7° 00' ~8° 58'	31° 45' ~32° 10'N	DIRECTION DES MINES ET DE LA GEOLOGE
3	CARTE GEOLOGIQUE DES GUEMASSA	1/100,000	8° 00' ~8° 30'W	31° 30' ~31° 00'N	DIRECTION DES MINES ET DE LA GEOLOGE 1992
4	Compilation map (Guemassa)	1/30,000	216~248	86~106	BRPM 1993 *1
5	Guemassa	1/100,000	8° 02' ~8° 28'W	31° 30' ~31° 20'N	JICA-MMAJ 1989
6	Geological Map of the Marrakrh-Guemassa- Tekna Area	1/50,000	185~253.75 (8° 00' ~8° 45'W)	80~131.25 (31° 17' ~31° 45'N)	BHP-UTAH 1987 *1
7	Frizen Carte de Synthese	1/5,000	223.6~226.3	92.5~95	BRPM(K. Benhida) 1991 *1
8	Carte Geologique des Jebilet et Guemassa	1/100,000	202~253	84~155	BRPM/DE/DRM *1
9	Carte Geologique, (Koudiat_Aicha, Lachach, Koudiat Chib)	1/10,000	231~234	147.5~137	BRPM-REMINEX-SACEM 1986 *1
10	Carete Geologique des Jebilet Centrales	1/50,000	8° 00' ~8° 18'W	31° 38' ~32° 00'N	M.Bordonaro 1983 *1
11	Jebilet Lachche Carte de synthese	1/4,000	231.0~231.9	142.4~145.5	REMINEX 2001 *1
12	CONVENTION-JEBILET KOUDIAT-AICHA CARTE-DE-SYNTHESE	1/2,000	231~232	141~142.4	REMINEX 1998 *1
13	JEBILET BEN SLIMANE CARTE-DE-SYNTHESE	1/2,500	234.8~236.0	142.1~143.6	REMINEX 2001 *1

\*1 : Lambert Conformal Conic (Morocco Zone I) (unit : km)



Satellite Image  
analysis(2002)

Existing geological map(1:200,000)

Existing geological map (1:100,000)

Existing geological map (1:100,000)

① GTK Aeromagne(1997)  
(BRPM/OUTOKumpu project)

② Geoterrex Aeromagne(1987)  
(BRPM/BHP-UTSH project)

③ GTK Aeromagne(1968)  
(BRPM project)

BRPM House Report Geological Map  
(1:5,000)

BRPM House Report Geological Map  
(1:5,000)

MMAJ(87-89)

Fig.II-1-2 Existing Geological Map and Airborne Geophysics Map Area



### (3) Existing Data of Airborne Geophysical Survey

The airborne geophysical prospecting on the periphery of the area surveyed began with the airborne magnetic survey on Guemassa area conducted by BRPM (Geotrex) in 1968. No magnetic anomaly was extracted from the analysis result obtained at that time. Through reanalysis conducted by BRGM in France in 1983, however, magnetic anomaly was extracted from the concealed deposit of Hajar, and this led to the discovery of mineralized zone of zinc, copper and lead through the drilling conducted in 1984. In the days of 1968, it appeared impossible to capture any high magnetic anomaly arising from the deposit since thickness of veneer layer of Tertiary or later was assumed as thinner than the actual thickness (the depth of Palaeozoic basement containing deposits was assumed as shallower). This case of exploration and analysis showed that an airborne magnetic survey was effective for the survey of concealed deposits and that assumption of the basement depth was one of the extremely important points to extract magnetic anomaly derived from deposits.

In 1987, a geological survey and airborne magnetic prospecting were conducted by BRPM and BHP-UTAH (Geotrex) in Guemassa and a belt of magnetic anomaly was revealed in the outcrop and veneer rocks area. Drilling was performed in Frizem, Ghoula and Belaoud, but withdrawn in 1989.

In the beginning of 1990s, when BRPM discovered mineralized zone of zinc and lead, interests of explorers were focused on Haouz zone extending between Guemassa and Jebillet. In 1997, BRPM and OUTOKUMP Co. conducted a survey (Geological Survey of Finland ; GTK) and extracted magnetic anomalies. Through the ground magnetic prospecting, gravity survey and EM method done later and the Drilling conducted in 2000, mineralized belts of zinc, copper and lead were discovered.

In this survey, the obtained data were examined for correspondence with the existing deposits and geology of outcrops zones converted into digital data out of the existing data. The above data include those obtained from the airborne magnetic survey (total magnetism) conducted by BRPM and BHP-UTAH in Guemassa in 1987, the data of the airborne magnetic survey, (total magnetism and polar magnetism), airborne electromagnetic survey (resistivity), radioactivity (Radiometric K.) in 1997 by BRPM and OUTOKUMP Co. and the data of the airborne electromagnetic survey (resistivity) and airborne magnetic survey (total magnetism) conducted by BRGM in 1968 for contour map reanalyzed by BRGM in 1984.

As a result, high magnetic anomaly of the airborne magnetic survey and known deposits, (especially on the gossan ranging from Lachach, Kt. Aicha, Kechnet to Jbel Hedit in Jebillet district the gossan ranging from Bensliman to Kerkoz, the gossan distributed from the north to the south of Kettara) were found in extremely good correspondence with one another. On the other hand, in the eastern part of the central Jebillet, high magnetic anomalies of the airborne

Table II -1-2 List of previous Airborne Geophysical Survsys

No.	Deposit	Anomaly	Survey
1	Kettara	100nT dipole magnetic anomaly on the ore body Max 400nT anomaly -300mV anomaly 20 Ω/m resistivity	1968 Geoterrex airborne Surface magnetic survey SP method IP method
2	Draa Sfar (south)  Tazakourt	Input anomaly not match occasions  NNE-SSW axis, two 50-60nT anomaly; south anomaly = outline of ore body, north anomaly = Sidi M'barek gossan -150mV anomaly  Max 1,000nT magnetic anomaly	1964 SAPA airborne  1968 Geoterrex airborne  Self-potential (SP) method  Surface magnetic survey
3	Hajar	No anomaly (caused by Plio-Quaternary sediment)  E-W axis 1.4km dipole anomaly south anomaly = 42,300nT, north anomaly = 3,900nT distance from pole to pole=570m Max 1,000nT anomaly (spreading 800m)  Three ESE-WNW axis, on e is on the ore body, Not identify the topography of the basement and thickness of ore body	1968 Geoterrex (INPUT)  1968 Geoterrex (Mag.)  Surface magnetic survey  Surface gravity survey
4	Khwadra		
5	Frizen 1  Frizen 2	75nT anomaly, 5ch input anomaly SP anomaly (-80mV), 400nT anomaly = gossan 60nT anomaly, SP anomaly (-100nT), MT anomaly = vein, network ominerlization  No anomaly	1968 Geoterrex (INPUT) 1984 Surface magnetic survey
6	Amzourh (Imarine)	50nT magnetic anomaly, 3ch input anomaly -60mV SP anomaly, 300nT magnetic anomaly	1968 Geoterrex airborne Surface magnetic survey



magnetism ranged for a fairly wide area from outcrops to the district overlain by sediments of Tertiary age onward, and this makes it difficult to capture magnetic anomalies existing in Draa Sfar Deposit in this area. The high magnetic anomalies extending to the east is caused by granites exposed in the north of Marrakech city. This may be caused in part by similar rocks extending the district overlain by sediments of Tertiary age or later.

A lot of rocks are distributed in the central Jebilet intruded by acidic volcanic rocks and basic volcanic rocks. High magnetic anomalies are also distributed in the basic volcanic rocks, and high magnetic anomalies are also noted in some structural lines (faults) - Maserati fault in the north of Kettara. Therefore, in extracting the deposit potential, it is necessary to exclude those caused by structural factors such as basic volcanic rocks and faults from such high magnetic anomalies.

With regard to its relations with airborne electromagnetic anomalies(resistivity), while most of the gossan (deposits and mineral occurrences) shows medium or low resistivities (several hundred  $\Omega$  m and below), volcanic rocks especially the basic volcanic rocks show high resistivities (3000  $\Omega$ /m or higher). In Draa Sfar deposit in the east where it was difficult to discriminate anomalies in the airborne magnetism, the resistivity of the acidic volcanic rocks (dacite/rhyolite) is higher than that of the surrounding sediments of Tertiary age or later (acidic volcanic rocks: about 340  $\Omega$  m; Sediments of the Tertiary age or later: about 70  $\Omega$  m). Therefore, it is clearly distinguished as the body with high resistivity. However, the airborne electromagnetic anomalies in Haouz plain overlain by sediments of Tertiary age or later extracted only from the acidic volcanic rocks of the vicinity of Draa Sfar deposit. In case such anomalies reflect geological features there, in case the layers where exploration is available are not sufficiently deep, or in case such anomalies are attributable to the fact that the strength of obtainable data is different between the district covered by outcrops and the district covered by sediments of Tertiary age or later (the data of the latter is weaker), it may be necessary to make a separate analysis for each zone.

Interpretation of the airborne electromagnetism shows us that different anomalies appear depending on the distribution of rocks and topography. In other words, in extracting anomalous values, metal ore bodies with high conductivity (low resistivity) should be extracted. It should be noted, however, that even the rocks with relatively high resistivity (acidic volcanic and pelites) may appear as the rocks with low resistivity if they are distributed in the rocks with extremely high resistivity (quartzites and granites). To avoid this misunderstanding, it is effective to make interpretation in consideration of the magnetic anomalies. Further, the basic rocks such as microgabros show high magnetic anomalies similar to those of volcanic massive sulfides as mentioned above, sometimes they are distributed together with gossan ore bodies, and sometimes they exist alone. The former can be considered as an target of our

exploration, but the latter cannot be the object of our exploration and should be excluded from the results of electromagnetic survey as a part with high resistivity (low conductivity). Further, the resistivities of rocks and ore bodies differ depending on the conditions of weathering (oxidization), and this should be noted in their interpretation. (The gossan that we collected from the ground surface of Kettara deposit is considered that rocks containing much massive sulfides (pyrrhotite and others) , but it was strongly weathered and its resistivity (about hundreds of  $\Omega/m$ ) and charging rate (10mV/V) are different from those of sulfides. On the other hand, the graphite distributed in the zone adjacent to the granitic area in the east of the central Jebilet shows low resistivity (about tens of  $\Omega/m$ ) and high charging rate (hundreds of mV/V) which are almost the same as those of iron pyrite. It is distinguishable from the graphite if examination is made taking magnetism and gravity anomalies into consideration. (Anomalies of graphite are low magnetism and low gravity.)

From the above examination of the existing data, the part with high magnetic anomaly and low resistivity can be considered as having high deposit potential.

Fig. II-1-3 to II-1-7 show the anomalous belts extracted from the result of airborne geophysical surveys, Table II-1-3 was compiled the geological/metallogenetic factors as the causes of such anomalies, Table II-1-4 were compiled geophysical data from JICA/MMAJ 1989 and BRPM house report and Geophysical data obtained this survey were shown in Table II-1-5.

#### (4) Drilling data (BRPM, REMINEX)

The locations of the previous drilling conducted by BRPM, REMINEX and JICA-MMAJ were listed in Table II-3-1 and Fig. II-3-1. Details of existing drilling core are described in Chapter 3 “ Existing drilling core survey”.

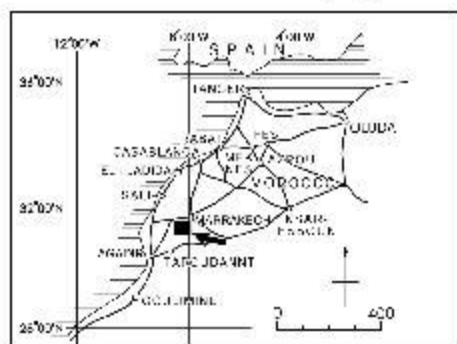
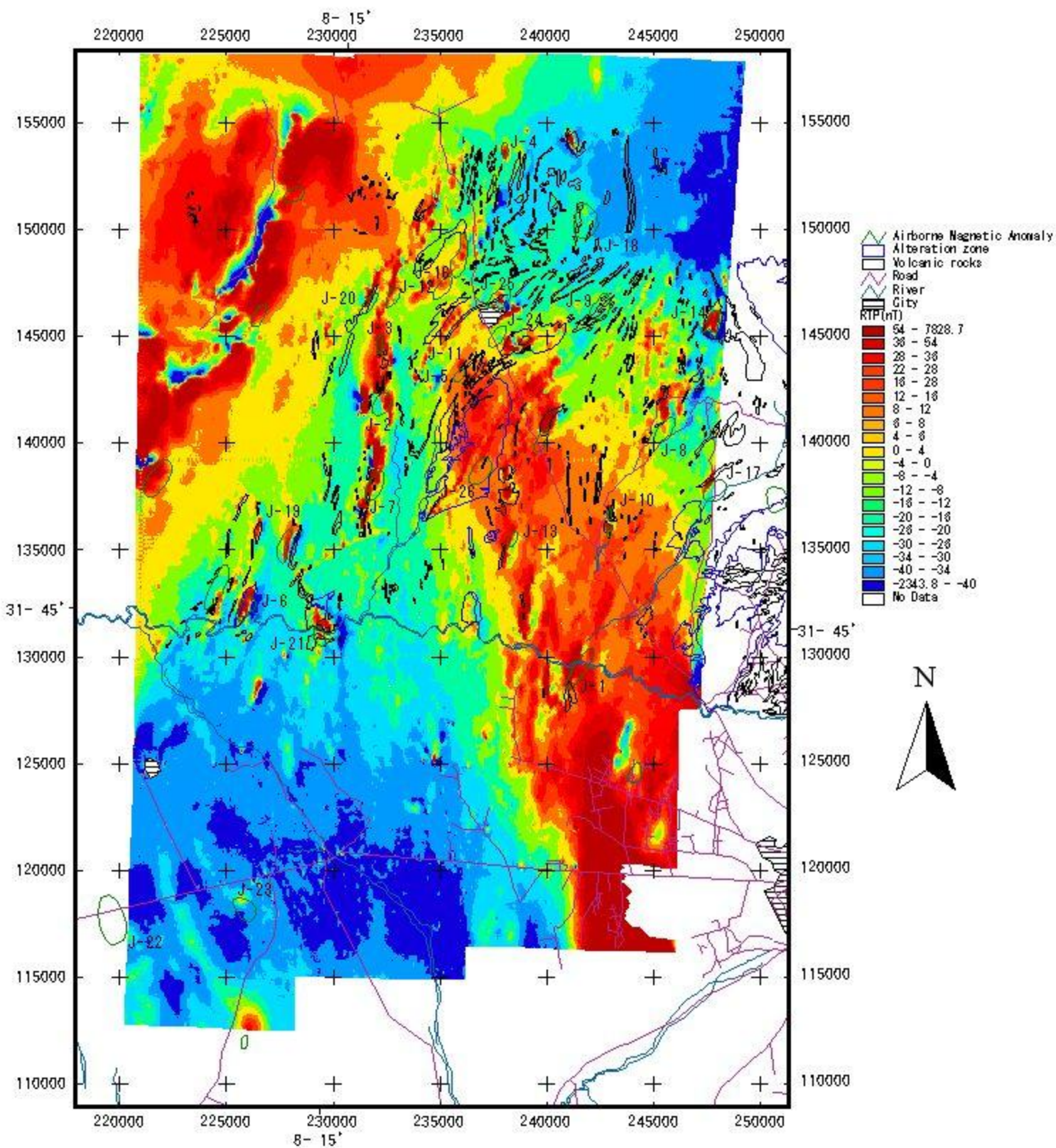


Fig.II-1-3 Existing Airborne Magnetic Anomaly (Jebilet; RTP)



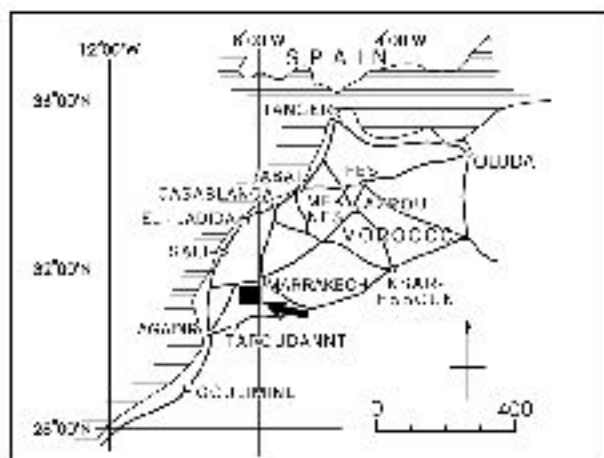
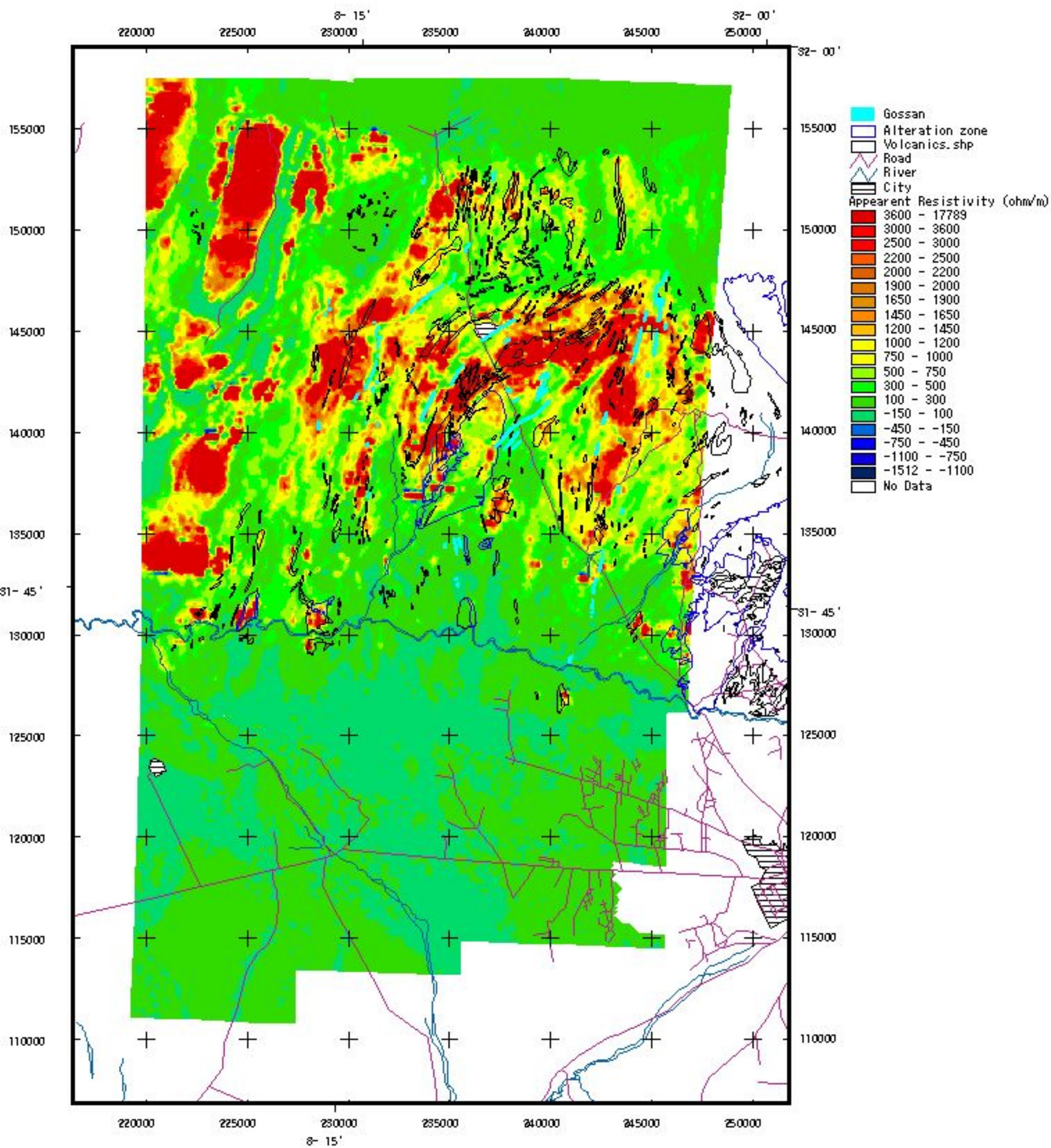


Fig.II-1-4 Existing Airborne Electromagnetic Anomaly (Jebilet)



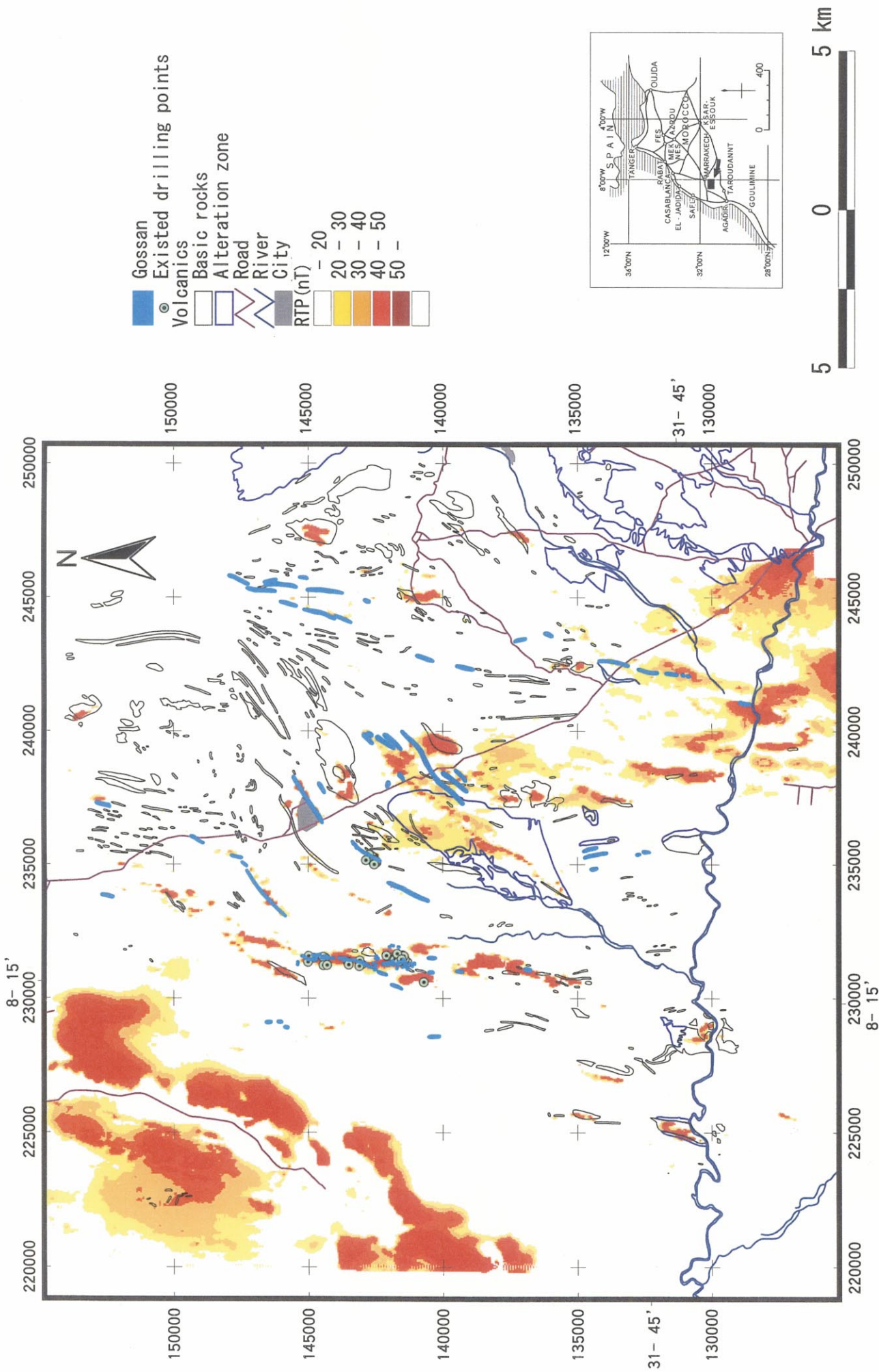


Fig.II-1-5 Synthetic Map of Existing Geophysical Data (Jebilet Area, RTP)



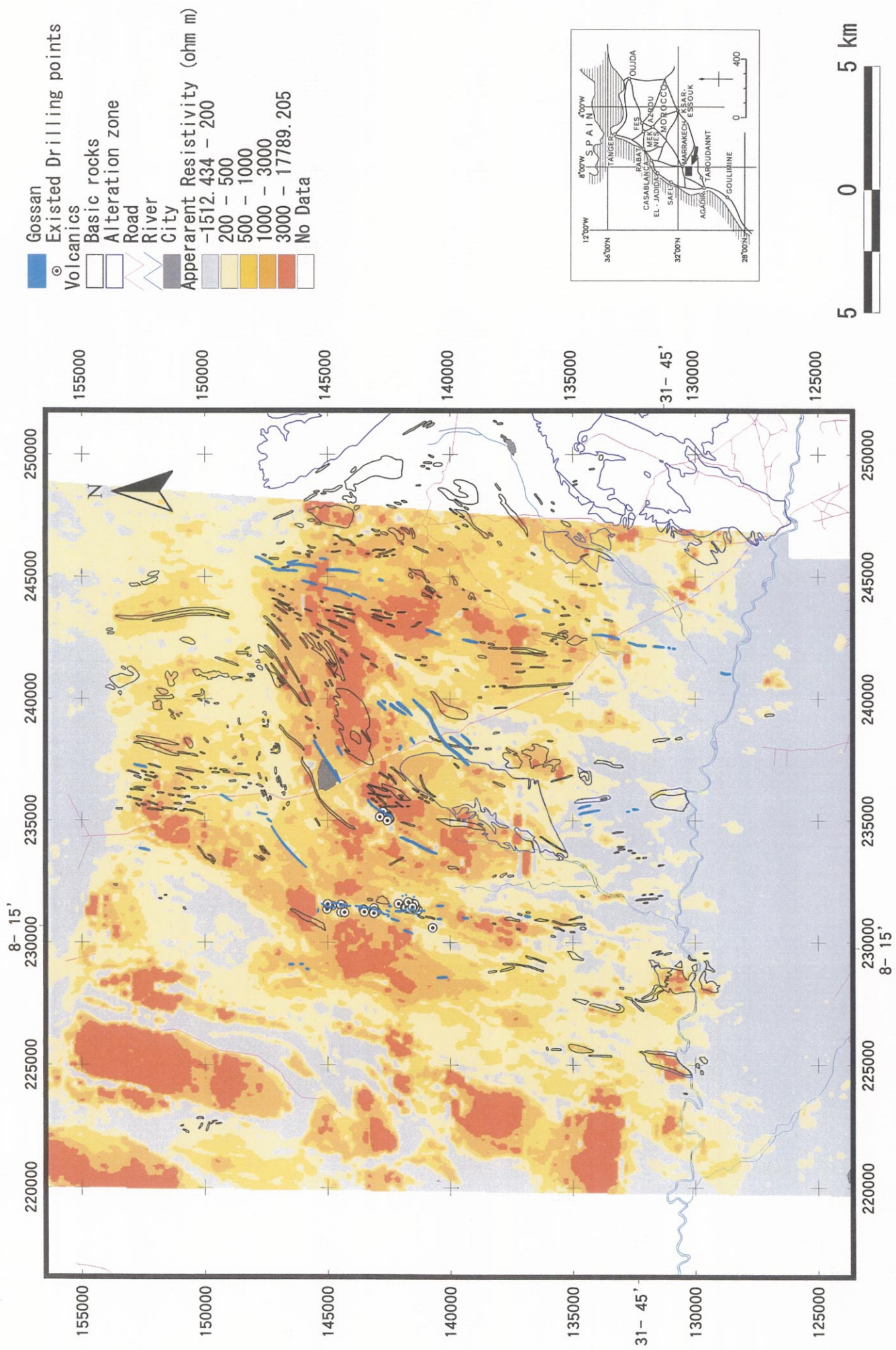


Fig.II-1-5 Synthetic Map of Existing Geophysical Data (Jebilet Area, Apparent Resistivity)



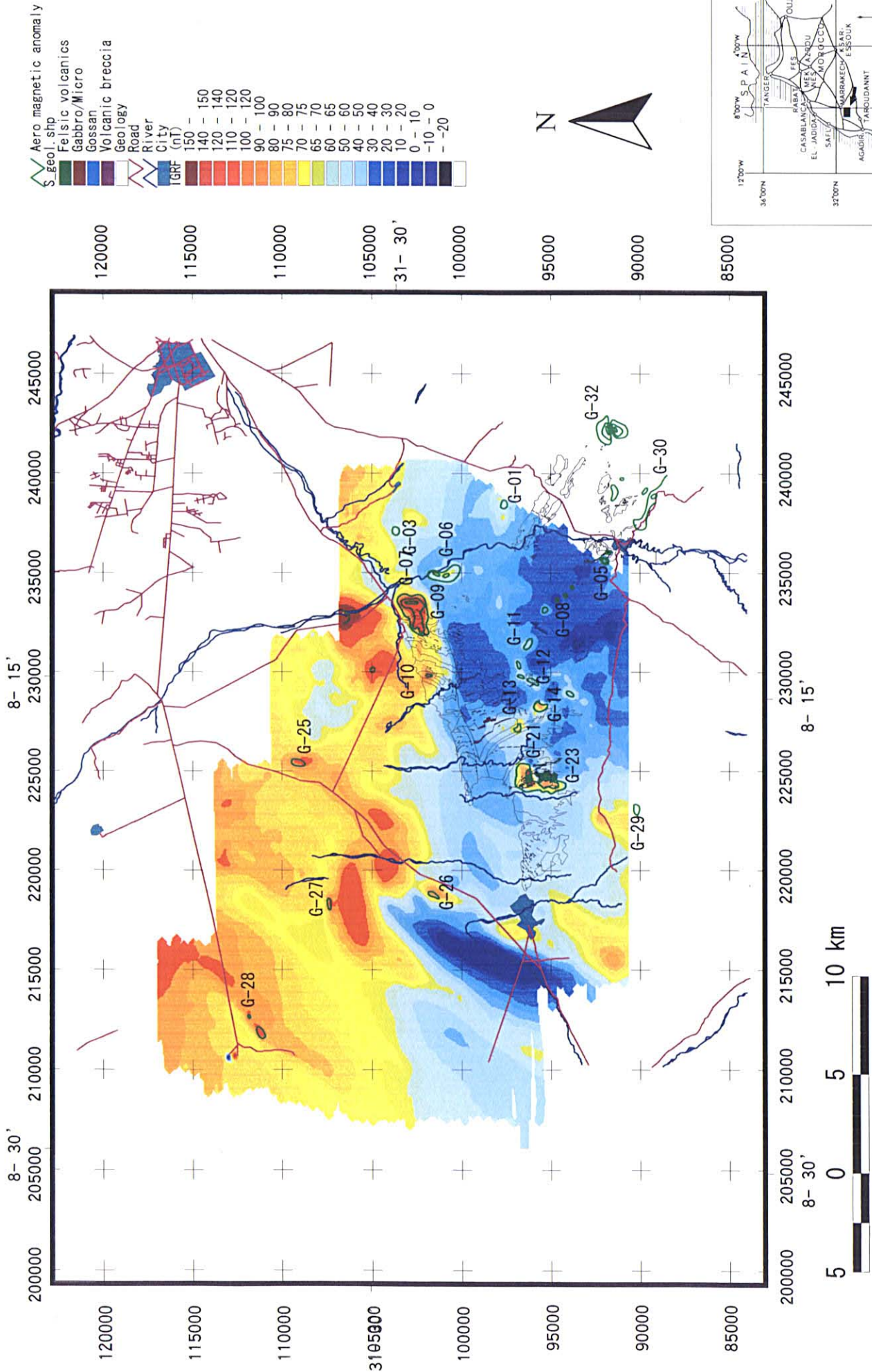


Fig.II-1-6 Existing Airborne Magnetic Anomaly Map (Guemassa Area, IGRF)

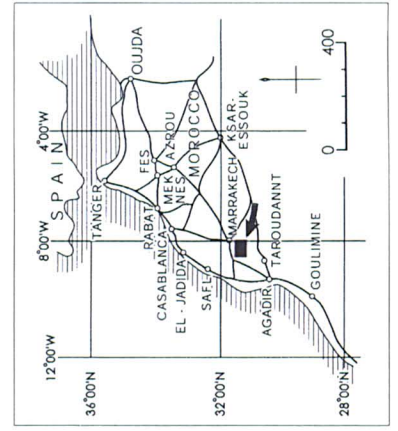
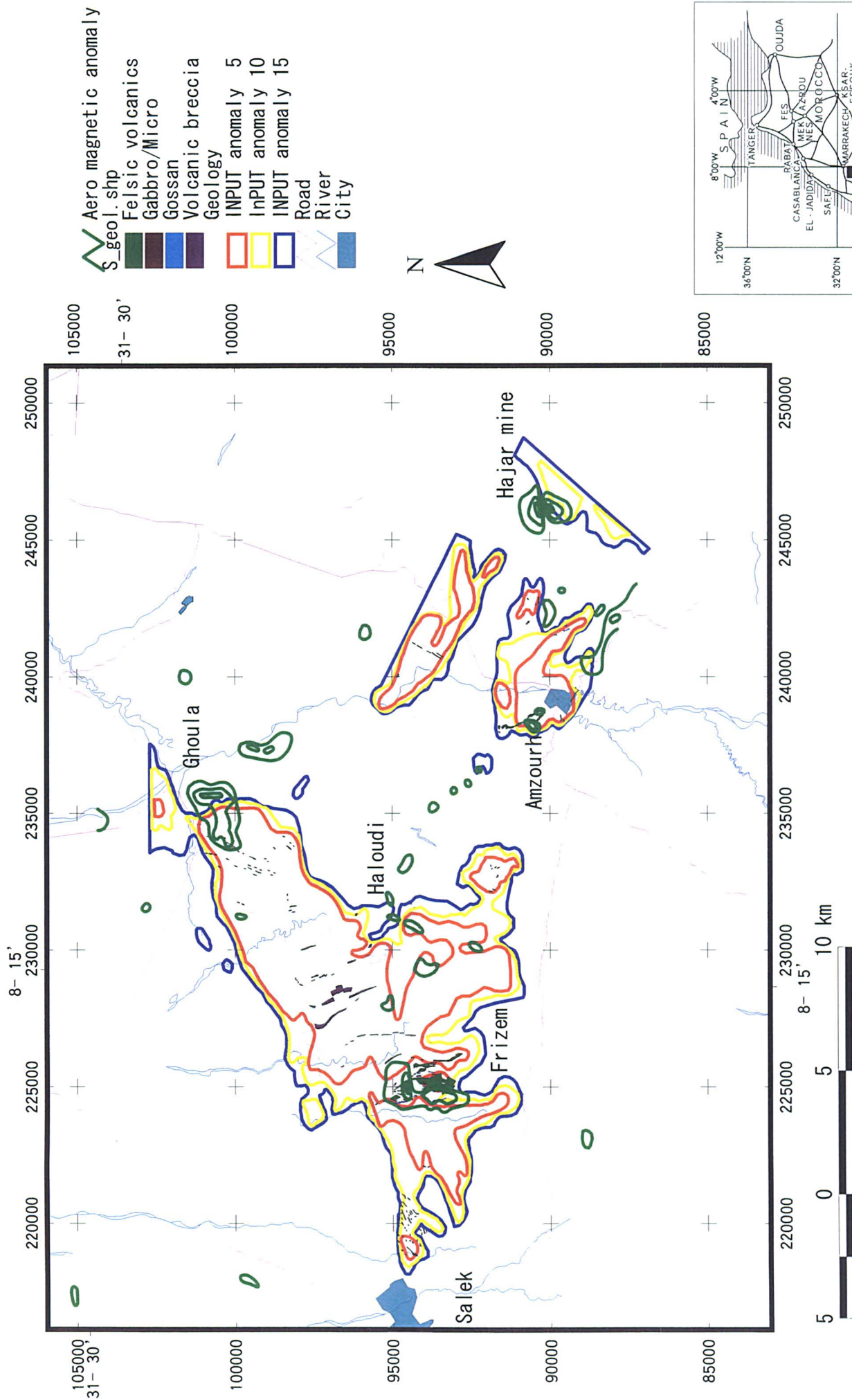


Fig.II-1-7 Synthetic Map of Existing Geophysical Data (Guemassa)



Table II-1-3 List of Airborne Geophysical Anomaly (Jebilet Area)

Code	Area	Geophysical Anomaly			BRPM(-84)			REMINEX1(84-88)			REMINEX2(85-94)			BRPM/some paths			UTM-X	UTM-Y	
		Type of Airborne Anomaly	Anomaly Size (Airborne Magn)	Type of Surface Anomaly	Cause of Anomaly	Geol.	Geophy.	Drill.	Geol.	Geophy.	Drill.	Geol.	Geophy.	Drill.	Geol.	Geophy.			Drill.
J-1	DRAA SFAR	Magn High, EM Low	2200x600m	Mag: Strongly Positive, PS: Positive, EM: Positive, Res	Mag High, EM Low: Deposit (North), Gossan, EM High, Basic Rock	Carte	Mag, PS, EM, Res	48	Carte	Mag, Grav	5: 1988m	Carte	Mag, PPL, Melis	10c: 3915m, 3p: 476m			4,500m	582,189	3,509,276
J-2	KOUDIAT AICHA	Magn High, EM Low	1100x750m	Mag: Positive, PS: Positive, EM: Positive, Res	Mag High, EM Low: Gossan, EM High, Basic Rock	Carte	Mag, PS, EM	4: 405m	Carte, GeoChem	Mag	9: 2480m	Carte	PPL, Melis, Pulse	2c: 1576m, 2p: 495m, 5: 925m				572,546	3,522,133
J-3	LACHACH	Magn High, EM Low	850x300m	Mag: Positive	Mag High, EM High: Basic Rock	Carte	Mag	4: 415m	Carte		2: 343m	Carte	PPL, Mag, VLF, Melis				572,000	3,524,741	
J-4	DRA TRIFANI	Magn High	600x300m, 800x100m		Mag High, EM Low: Gossan, EM High, Basic Rock				Carte			Carte	Mag, PPL	3p: 612m				577,519	3,532,807
J-5	KERKOZ	Magn High, EM Low	400x700m	Mag: Positive, PS: Positive, EM: Positive, Res: Weak	Mag High, EM Low: Gossan, EM High, Basic Rock	Carte	Mag, PS, EM, Res	6: 610m	Carte			Carte	Mag	3p: 585m				576,003	3,523,346
J-6	EL_MNA	Magn High, EM Low/High	600x1200m		Mag High, EM Low: Gossan, Acidic Rock? EM High, Basic Rock							Carte	Mag, PPL					566,118	3,511,702
J-7	J_HADID	Magn High, EM Low	650x1500m	Magn: Negative	Mag High, EM Low: Gossan, EM High, Basic Rock	Carte	Mag, PS, EM	2: 260m	Carte	Mag		Carte	Mag	1p: 156m				572,304	3,517,585
J-8	KI_HAMJURA	Magn High, EM Low	630x1450m		Mag High, EM Low: Vein dep?	Carte	Mag		Carte	Mag	1: 112m	Carte	PPL					585,949	3,521,163
J-9	Kettara East	Magn High, EM High	800x1300m	Magn: Negative	Mag High, EM High: Basic Rock		Mag		Carte	Mag	1: 211m	Carte, Geochem						582,614	3,526,864
J-10	NZALET HAMEL	Magn High, EM Low	250x450m, 100x480m	Magn: Positive	Mag High, EM Low: Gossan		Mag			Grav	1: 253m		Mag					583,463	3,516,978
J-11	BEN SLIMAN	Magn High, EM Low	220x300m	Mag: Strongly Positive, PS: Positive, EM: Weak, Res: Positive	Mag High, EM Low: Gossan, (Gossan zone: W5-40XL450XD250m over), (Hematite zone: W2-40XL1300m), Host rock: Shale	Carte	Mag, PS, EM, Res	10: 1147m	Carte	Mag	1: 196m	Carte						575,215	3,525,045
J-12	BOUHANE	Magn High, EM High?	550x1300m, 500x1000m	Mag: Positive, PS: Positive, EM: Positive	Fault?, gossan	Carte	Mag, PS, EM	3: 383m										572,789	3,526,985
J-13	Dra SELGOUF /GOURSEFRA	Magn High	350x730m	Mag: Negative, PS: Positive, EM: Positive	?	Carte	Mag, PS, EM	3: 321m	Carte, Geochem									578,793	3,515,766
J-14	J.SARHLEF	Magn High	700x1200m	Mag: Negative	Magn: Basic rocks?		PS		Carte, Geochem			Carte, Geochem						588,133	3,526,379
J-15	Dr. RHIRAT	Magn High	700x2100m		Mag High, EM Low: Gossan					Mag	1: 249m							575,821	3,529,047
J-16	No.27 (north Bouhane)	Magn High, EM Low	870x1250m		Mag High, EM High: Basic Rock?					Mag	1: 221m							588,193	3,518,191
J-17	No.15 (east Si MBAREK)	Magn High, EM High	1100x1650m		Mag High, EM High: Basic Rock					Mag	1: 222m							581,704	3,530,806
J-18	No.26 (DRAA EL KEBIR)	Magn High, EM Low	370x1500m	Magn: Negative	Mag High, EM High: Basic Rock					Mag								567,816	3,515,098
J-19	No.29 (southwest JHADIT)	Magn High, EM Low/High	420x1150m		Mag High, EM High: Basic Rock					Mag		Carte						571,515	3,526,682
J-20	No.10	Magn High								Mag									

Table II-1-3 List of Airborne Geophysical Anomaly (Jebilet Area)

Code	Area	Geophysical Anomaly			Cause of Anomaly	BRPM(-84)			REMINEX(184-88)			REMINEX(285-94)			BRPM/some paths			UTM-X	UTM-Y
		Type of Airborne Anomaly	Anomaly Size (Airborne Magn)	Type of Surface Anomaly		Geol.	Geophy.	Drill.	Geol.	Geophy.	Drill.	Geol.	Geophy.	Drill.	Geol.	Geophy.	Drill.		
J-21	No.4 (AZIB ALBACHA)	Magn High, EM High	500x950m		Mag High, EM High: Basic Rock												569,589	3,510,779	
J-22	SAFSAFA	Magn High		Magn: Negative	?				Mag								560,224	346,981	
J-23	KHWADRA	Magn High	700x1200m	Grav: Positive, Mgne: Positive	Deposit										Mag, Grav, EM	20: 11,126m	566,663	3,497,733	
J-24	KETTARA	Magn High, EM Low/High	550-1200m	Mag: Strongly Positive, PS: Positive, EM: Positive	Mag High, EM Low: Gossan?, EM High: Basic Rock?												577,617	3,525,412	
J-25	KOUDIAT DELAA	Magn High, EM Low	500-1200m		Mag High, EM Low: Gossan												577,910	3,527,210	
J-26	No.24	Magn High, EM Low/High	800-1450m		Mag High, EM Low: Gossan?, EM High: Basic Rock?												582,189	3,509,276	

(Data Source : BRPM)

Table II-1-3 List of Airborne Geophysical Anomaly (Guemassa Area)

Code Area	Geophysical Anomaly			BRPM(64-66)		BRGM(82-87)		BRPM(84-87)		BHP-UJAH(87-89)		JICA(87-90)		BRPM(90-)		UTM-X	UTM-Y	
	Type of Airborne Anomaly	Anomaly Size (Airborne)	Type of Surface Anomaly	Cause of Anomaly	Geol.	Drill.	Geol.	Drill.	Geol.	Drill.	Geol.	Drill.	Geol.	Drill.	Geophy			Drill.
G-1 SALEM	Magn High	600x500m													Mag		584,685	3,477,713
G-2 TAGUENZA	Magn High	600x800m		Fault?			Mag								Mag, Pulse		582,630	3,485,029
G-3 TAMESLOHT	Magn High	450x700m		Stockwork, diss. & submassive sulfide											Mag, Pulse			
G-4 AL MRAH	Magn High	700x750m		Remanance?											Mag, Pulse			
G-5 AMZOUGH	Magn High, INPUT	200-400x1150m		Magnetite - specularite of the gabbro											Mag, Pulse			
G-6 BEL AOUD	Magn High	450x800m		Thick Tertiary (200m over)											Mag, Pulse			
G-7 LALLA ATTOUCH	Magn High	500x500mX3 (2000m)		paleorelief? (hors)											Mag, Pulse			
G-8 SOUKSOU	Magn High	500x1050m		Lateral body? --> off hole pulse EM anomaly											Mag, Pulse			
G-9 GHOUILA	Magn High, INPUT	350x500m													Mag, Pulse			
G-10 ANABIA	Magn High	400x700m		Brechia with pyrrhotite											Mag, Pulse			
G-11 HALOUDI EAST	Magn High	450x800m		Remanance?											Mag, Pulse			
G-12 HALOUDI WEST	Magn High	650x800m													Mag, Pulse			
G-13 MJED-NORTH	Magn High	800x900m		Pyrrhotite-laminated slate, Tertiary contact zone, mafic intrusive											Mag, Pulse			
G-14 MEJED	Magn High	500x600m		Tertiary cover?											Mag, Pulse			
G-15 MEJED-SOUTH	Magn High, INPUT	500x100m		Fault (gossan),											Mag, Pulse			
G-16 EL KARIA	Magn, INPUT	300x150m		Fault (Tertiary/Paleozoic s), No gossans											Mag, Pulse			
G-17 NZALA-SOUTH	Magn, INPUT	500x400m		Fault (Tertiary/Paleozoic s), No gossans structural?											Mag, Pulse			
G-18 NAZALA-EAST	INPUT	1200x2000m		Semi-massive to massive pyrrhotite and/or pyritic sulphide											Mag, Pulse			
G-19 NAZALA-WEST	INPUT	300x100m		?											Mag, Pulse			
G-20 TAOUILIT	INPUT	850x2000m		Paleorelief? (channeling?)											Mag, Pulse			
G-21 FRIZEM	Magn High	300x100m		Mafic intrusives?											Mag, Pulse			
G-22 ARISSA	INPUT														Mag, Pulse			
G-23 FRIZEM SOUTH	INPUT														Mag, Pulse			
G-24 SALEK	INPUT														Mag, Pulse			

Table II-1-3 List of Airborne Geophysical Anomaly (Guemassa Area)

Code	Area	Geophysical Anomaly				BRPM(64-66)		BRGM(62-87)		BRPM(84-87)		BHP-JTAH(87-89)		JICA(87-90)		BRPM(80- )		UTM-X	UTM-Y
		Type of Airborne Anomaly	Anomaly Size (Airborne)	Type of Surface Anomaly	Cause of Anomaly	Geol.	Drill.	Geol.	Drill.	Geol.	Drill.	Geol.	Drill.	Geol.	Drill.	Geol.	Drill.		
G-25	NSAFER	Magn 60nT	1000-2400m	Magn Low, No-EM conductor	Thick Tertiary (200m over)													566,879	3,491,182
G-26	MOUKARA	Magn High	350x700m	Magne Low, No-EM conductor	Thick Tertiary (200m over)													557,940	3,486,999
G-27	EL HEDDOUD	Magn High	500x850m	Magne Low, No-EM conductor	Thick Tertiary (200m over)													557,608	3,486,884
G-28	YASMIN	Magn High																548,682	3,493,481
G-29	AZIB EL GUEIDA	Magn High	700-400m															564,580	3,468,273
G-30	TIFERWINE	Magn High	2000x500m															584,768	3,468,427
G-31	DOUOR AKHLJ	Magn High	500x200m		Faults?														
G-32	HAJAR	Magn High; +42300nT, -39000nT, +-Axis:570m.	1400x600m	High Magn 1000nT, High Grav	Deposit													589,558	3,470,572

(Data Source : BRPM)

Table II-1-4 Geophysical data of rocks in the Survey Area (1)

No.	Formation	Rock Name	Resistivity ( $\Omega$ m)	Density (g/cc)	Suceptibility ( $10^{-3}$ cgs/emu)	
1	Quaternary	Sandstone	57	2.28	2	*1
2	Permian-Carboniferous	Mudstone	330	2.71	2	*1
3		Siltstone	880			
4		Carbonatic Schist / Pelitic Schist	500			
5		Dacite	340			
6		Quartz vein	1100			
7	Hajar	Pb-Zn-Pyrr. Ore	15	4.27	530	*1
8	Jebilet Central	Mineralization, Ore	20~50			*2
9	Basic rocks	Micro Gabblo	500~1000			*2
10		Quartzite, Granit	3000~5000			*2

(\*1:JICA-MMAJ1989, 2:REMINEX Material for internal use)

Table II-1-5 Geophysical data of rocks in the Survey Area (2)

No.		Rock Name	Resistivity ( $\Omega$ m)	Chargability (mV/V)	Suceptibility ( $10^{-3}$ cgs/emu)	Loc.	
1	Permian -Carboniferous	Gabblo	1,841.63	3.10	0.37	Ketarra	03MR-K001
2		Rhyolite	2,545.74	5.26	0.53	Bouhane	03MR-K002
3		Limestone	4,739.56	13.09	0.11	Bouhane	03MR-K003
4		Gabblo(sill)	2,009.29	7.52	0.65	Ben Sliman	03MR-K004
5		Shist(mud)	182.75	5.36	0.2	Ben Sliman	03MR-K004
6	Ordovician	Limestone	5,099.90	47.97	0.1	Mardina	03MR-K006
7	Permian -Carboniferous	Gossan	598.68	6.71	0.15	Kettara	03MR-K007
8		Pyrite	18.72	491.79	15.6	Kettara	03MR-K008
9	Permian -Carboniferous	Graphyte	10.18	512.48	0.24	Marrakech E	02MR-K067
10		Quartzite	6,782.11	11.45	0.06	Mardina W	02MR-S048
11		Granite	2,216.34	8.21	0.14	Tabouchent	02MR-S040
12		Granite	1,267.44	6.19	0.27	Tabouchent	02MR-N152
13		Granite	2,781.51	9.18	0.33	Tabouchent	02MR-N153

### 1-2-3 Conclusion

We collected geological maps and the maps of geophysical prospecting anomalies as the existing data and compiled them by using Geographic Information System (GIS). The data collected include geographical information based on the topographical map drawn on a scale of 1/100000, the geological map of Jebilet area drawn on a scale of 1/100000, information on geology and geological structure based on Geological Maps of Guemassa area drawn on scales of 1/30000 and 1/10000, the list of deposits and prospects (gossan, etc.), information on the locations of deposits and drilling cores based on the existing list of drilling spots, information on airborne geophysical exploration based on the existing airborne geophysical prospecting data and the compiled chart of geophysical prospectings, as well as the locations of mine claims. These data were converted into the digital data compatible with ArcView 3.2 (ESRI).

Table II-1-6 List of the Data Converted into GIS Data

No.	Data	Data Type	Original Data
1	Geological Map (lithofacies, structure, etc.)	Polygon, line	1/100000 geological map of Jebilet, 1/30000 and 1/10000 geological maps of Guemassa
2	Deposits (mines, deposits, gossan)	Point	BRPM house report
3	Drilling Data	Point	BRPM house report
4	Geographical Information (rivers, main roads and cities)	Polygon, point, line	1/100,000 Topographical map
5	Anomalies Extracted from Airborne Geophysical Survey	Polygon	BRPM house report
6	Satellite Images (mainly false color, main component, rationing, geological unit)	Raster	Landsat 7
7	Topographical Map	Raster	1/100,000 Topographical map
8	Map of Geophysical Survey Anomalies (Airborne magnetism and resistivity)		BRPM house report

Table II-1-7 Specifications of Lambert Conformal Projection

Specification	Parameter	
	Zone I	Zone II
Zone		
1er standard parallele	34.8658333	31.725
2eme standard parallele	31.725	28.098
Parallele d' origine	33.3	29.7
False easting	500 000 m	500 000 m
False northing	300 000 m	300 000 m
Centaral meridian	-5.4	-5.4

## Chapter 2 Geological Survey

### 2-1 Method of the Geological Survey

We used existing data and satellite images of all survey area to locate survey points and routes. Our local surveys mainly focused on known deposits, prospects, and mine cavities to grasp the stratigraphy and mineralization. The geological structures were examined mainly with existing data.

We used a 1/50,000-scaled topography, which was enlarged from a 1/100,000-scale topography, in our surveys of known deposits and prospects. We also used GPS and a simplified navigation system (MIRIN: Mineral Resource Image Navigator) to confirm the locations of mineralization belts and outcrops. In addition, we took samples, and took photos of outcrops, and made sketches at especially important outcrops. A mine underground survey was conducted in the Hajar Mine, whose surroundings were undergoing the mining of massive sulfide ore deposits, and the Draa Sfar Mine, which was under construction.

### 2-2 Results of the survey

#### 2-2-1 Outline of the survey area

##### 1) Location and traffic

The Survey area is located in the south western of Marrakech, and in the north of the Anti-Atlas Mountains approximately 330km to the south of Rabat, the capital of the Kingdom of Morocco. Most of the roads running from the capital Rabat to the Survey area were paved and superhighways were constructed. It takes approximately an hour to drive on the highways from Rabat to Casablanca and approximately three hours to drive on the paved trunk road from Casablanca to Marrakech (Fig.II-2-2-1. and Fig.II-2-2-2).

In addition to those in Rabat and Casablanca, there is also an international airport in Marrakech for flights directly to Europe (Paris, London, etc.)

##### 2) Geography and Topography

The Survey area located north of Anti-Atlas mountain area and consists of hilly land, 400 to 800m high from the sea level.

Geology of this area composed Paleozoic basement rocks that were low to medium grade metamorphosed and Tertiary or later sediments that covers over basement rocks. Climate is dry and surface is rock and sand desert.

This survey area includes basement rocks in the north central Jebilet that are extending from east to west, Marrakech plain that covers over Paleozoic basement rocks in the south part of Jebilet, and Guemassa area that is Paleozoic window in the Tertiary sediments.

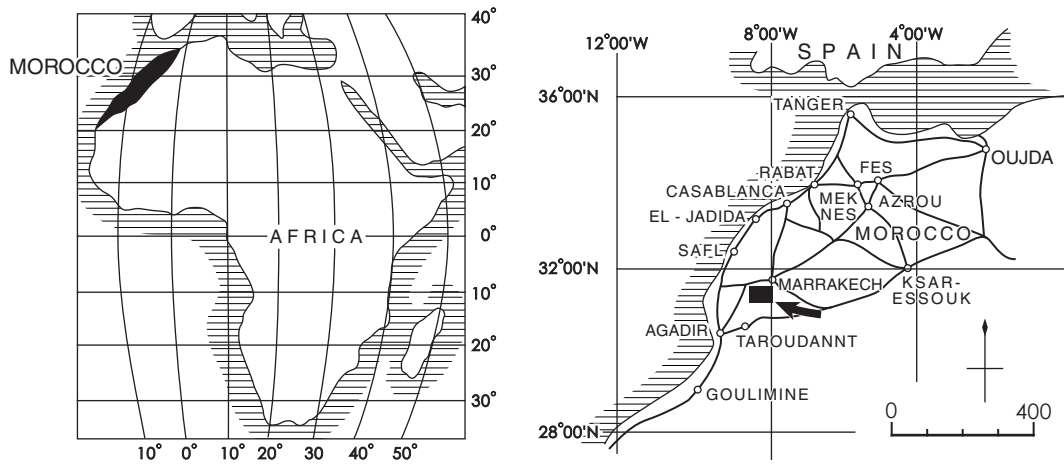


Fig. II-2-2-1 Location Map of the Survey Area

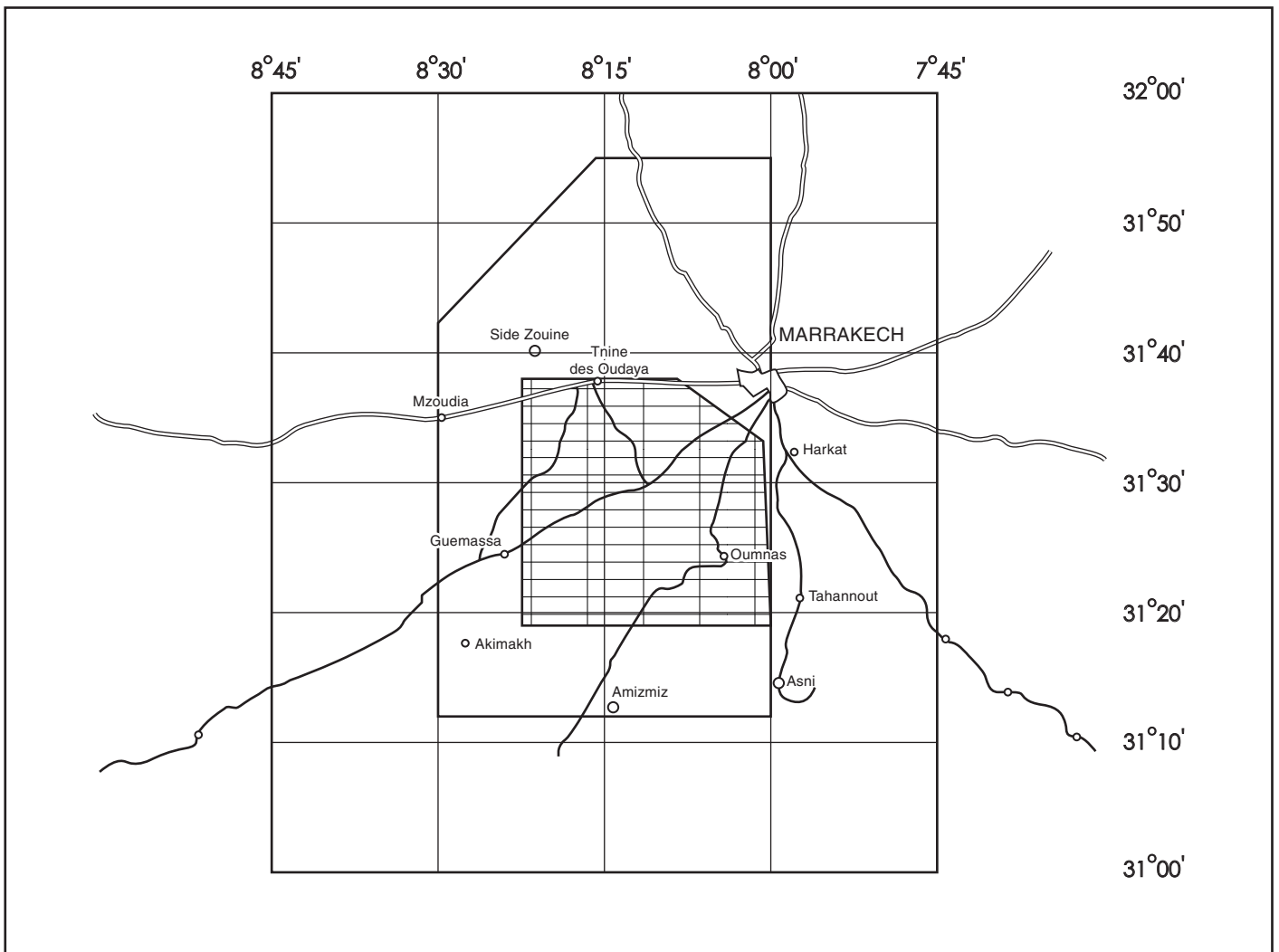


Fig. II-2-2-2 Location Map of Marrakech-Tekna Area



### 3) Geohistory and Ore Deposits

Geohistory and ore deposits of this area and surroundings are mentioned based on Michrd (1976), Viland (1998), Pique (1994), and Matsutoya (1999). Morocco went through an age of graben tectonism during 30 million years of the Palaeozoic Era (530-235Ma). After the Pan Africa tectonism, the areas that covered the Legiobad forebackbone through Anti Alas were continuously subsiding.

When entering the Infra-Cambrian period, the western to central Anti-Atlas areas began to undergo local and temporal subsidence along bi-modal volcanic activities being dominant. IAPRTUS Sea, which began to form in around 650Ma when mountain building in Anti-Atlas had its peak, began to settle down on the North America Continent. Eastern Anti-Atlas also began to subside along local and small-scale eruptions of alkaline basalt. When entering the Cambrian period, central Morocco was covered with the sea and continued to subside with interruptions of local sedimentation and developments of depression contours. Sedimentary hematite ore sedimented in Meseta in the Silurian period, and in the Legibad forebackbone in the Devonian period.

In the Carboniferous period, Hercynian mountain building began to take place, and Anti-Atlas turned into slow upheavals. In eastern Morocco to south-western Algeria, which were then under the sea, a coal bed began to form. Meanwhile, Visean stage and Namurian stage in central Morocco underwent foldings, low degree of low P/T alteration, and granite intrusion (337-319Ma) from the inland. Localization of sedimentary basins advanced in the central gorge. In the Visean stage, a local extension belt was formed from the Tanncharfi, located in the northeastern survey area in the central gorge, to Jebilet through Haouz in the southern areas, where basic rock-dominated bi-modal submarine volcanic activities began. In Jebilet a bedded magnetite sulfide deposit was formed. In Haouz, located in the south to Jebilet, a massive sulfide deposit was formed. In northeastern Tanncharfi, where basalt activity was observed, no kuroko-like mineral is observed but hematite is concentrated in this area.

When entering the Permian Period, granite intrusion (301-265Ma) occurred in many parts, and at the end of the Permian Period, the granite intrusions turned into lands completely. Existing deposits are described based on Michrd (1976), Viland (1988), Pique (1994), Matsutoya (1999), and others. Deposits in the Jebilet area are massive sulfide ore deposits of copper, lead, zinc, and iron, which were embedded in the Visean series of the Carboniferous period. These deposits include the Kettara deposit. The vicinity of the border area, where basement rock appears on the surface of the ground in the southern limit of the Jebilet mountain mass, has the Draa Sfar deposit. Deposits observed in the Guemassa area include the Hajar deposit and the Frizen deposit. The Mrrakech area in a semi-desert region is covered with sediments formed from the Miocene of the Neogene period. The lower part of the

area consists of the Carboniferous period layer, where the Khwadra deposit, a volcanic massive sulfide ore deposit, is distributed as a concealed deposit.

These deposits are similar to KUROKO type deposits in Japan or Iberian pyrite belt type deposits that are distributed in Spain and Portugal, when considering their deposit form (stratigraphy, lenticular, stripe), combination of minerals (dominance of magnetite, sphalerite, galena, pyrite, chalcopyrite, etc.), and mineralization with acid and basic volcanic rocks.

#### 2-2-2 Geological Stratigraphy in the Survey Area

This section explains the geology of the basement rocks being distributed in north and south of the survey area, namely the Jebilet and Guemassa areas. Geological map of those area, geological columnar section, geological section area shown in Fig II-2-2-3, Fig II-2-2-4 and Fig II-2-2-5. Because there is no drilling data of the basement rocks in the Marrakech area, this report could not describe the geology before Tertiary in the area.

##### (1) Geological stratigraphy in the Jebilet area

The Jebilet zone is located in northern Marrakech. The Jebilet area, extending to the east-west directions, belongs to the Hercynian orogenic mountain masses. The similar geological belts include the Rehamna mountain mass in the north of the Jebilet mountain mass and the Guemassa area in the south. The Jebilet mass extends some 170 km in the east-west directions. The mountain mass in the east-west directions can be classified into three geological belts as follows (Fig.II-2-2-6, Fig.II-2-2-7)

-Western Jebilet area: The area consists of the Cambrian to Ordovician systems, where folds and metamorphism are hardly or not at all observed.

-Eastern Jebilet area: The area consists of the Cambrian and Devonian systems in the west side while the eastern side consists of Viséan in the upper Carboniferous, parts of which are deformed.

-Central Jebilet area: The area consists of Viséan in the upper Carboniferous, and some parts of which are deformed and metamorphosed. The mass is characterized as having acid and basic intrusive rocks and granite magma. The central Jebilet, has almost SN or NNE-SSW strikes. It consists of baserocks sedimented with an east dip. These rocks were formed in the Devonian period, Carboniferous period, and to the Permian period in the Palaeozoic Era. The basement rocks mainly consist of lutite, partly limestone layer, tuff layer, and arenaceous rock layer. In addition, in the area acid or basic sills are interbedded with basement rocks. The whole part of the area is metamorphosed into chlorite schist and sericite schist due to regional metamorphism, which were caused by Hercynian orogeny.

The sedimentary basin of the central Jebilet had been in the extension tectonics, because





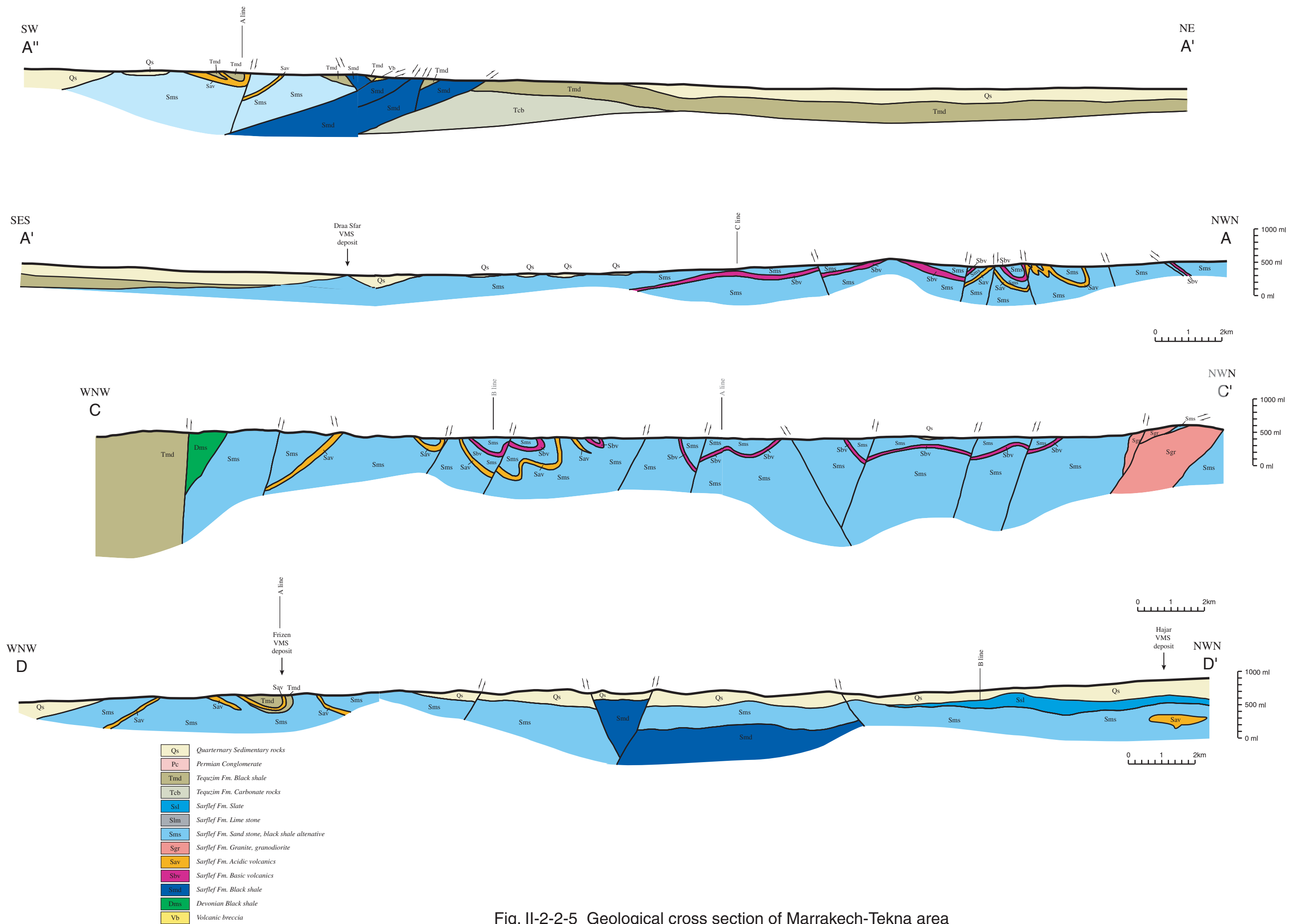


Fig. II-2-2-5 Geological cross section of Marrakech-Tekna area



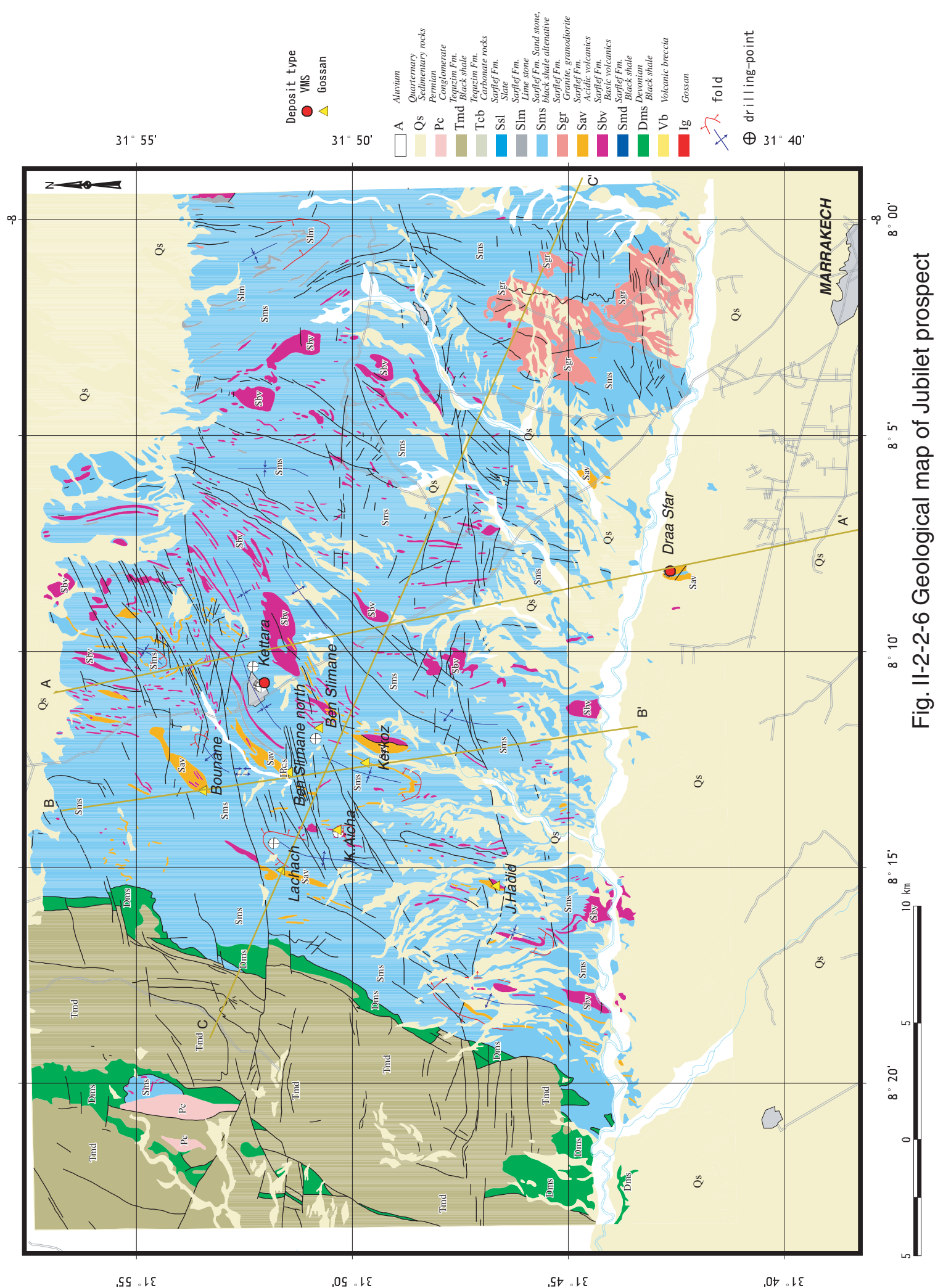


Fig. II-2-2-6 Geological map of Jubilet prospect

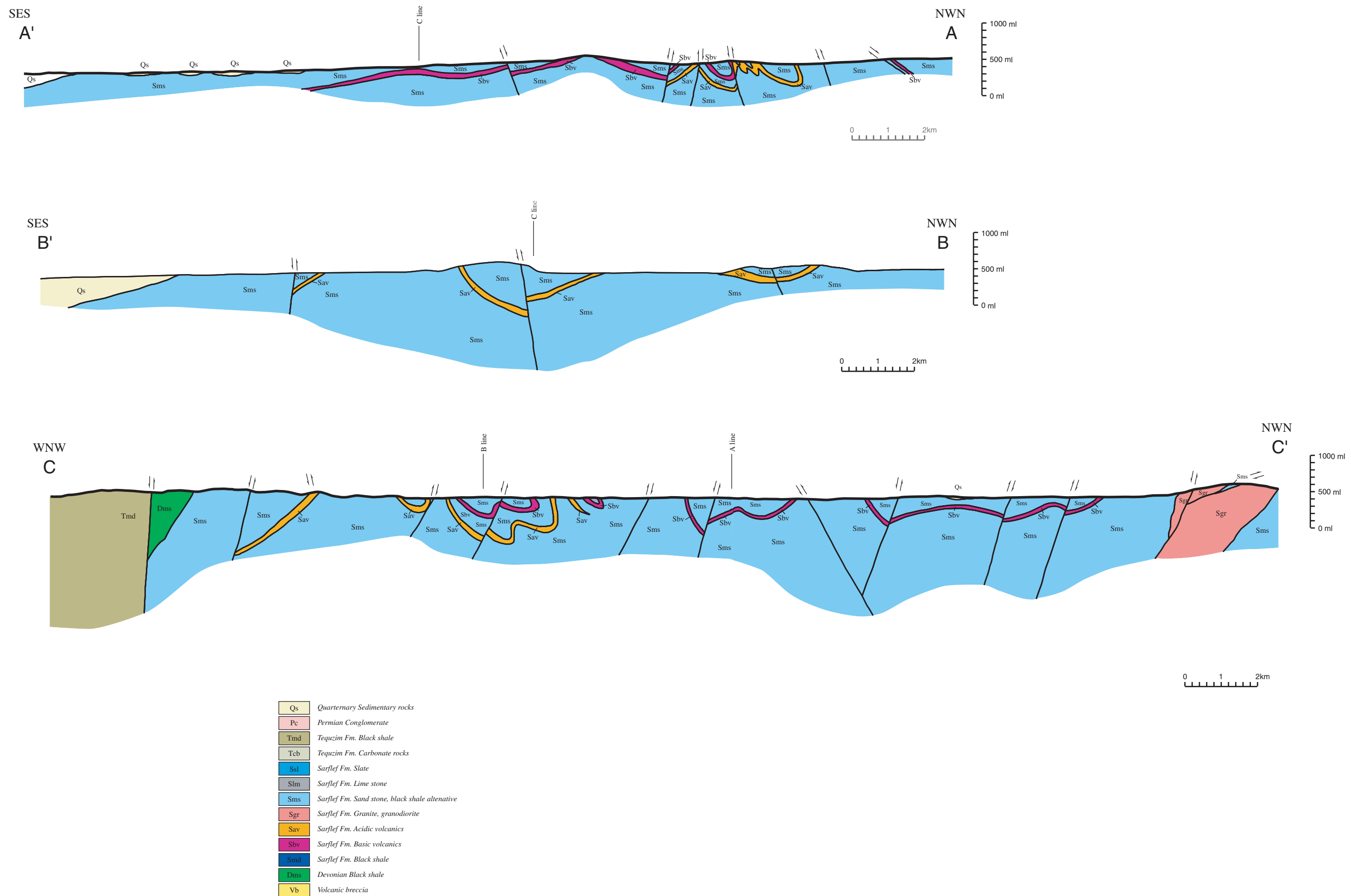


Fig. II-2-2-7 Geological cross section of Jubilet area

sedimentary concurrent normal faults in the WN-ES, EN-WS, and EW systems and slumping structures are observed (Matsutoya, 1999).

The geology of Visean in the upper Carboniferous system in the central Jebilet is divided into two groups:

-Sarhlef group: Consisting of pelite, acid volcanic rocks, basic volcanic rocks, rhythmic alteration, and phyllite, from the bottom to the top.

-Tequisim group: Consisting of lower carbonate rocks below and pelite above,

The next section describes the lithofacies of Sarhlef group and the Tequisim in the Jebilet district.

#### (1)-1 Sarhlef group

##### a) Pelite

Distribution: Benslimane, Kerkoz, etc. in the central Jebilet mountain mass

Lithofacies: Consists of alteration of black shales and sandstones. The sandstone appears light-grayed, and seems to be sorted well but no grading is observed. The blackshale appears dark-grayed and very dense. It seems to be sorted well but no grading is observed. It is metamorphosed to crystalline schist. The black shale or sandstone has lenticular sandwiches of bio-limestone layer and volcanic breccia.

##### b) Acid Volcanic Rocks

Distribution: Benslimane, Kekoz, K. Aicha, and Benslimane-north, etc. in the central Jebilet.

Lithofacies: Consists of massive dacite lava and dacitic tuff. Massive lava indicates white to milky-white colors, and some of the silicified black lava indicates light-green. Cracks in parts of the massive lava are filled with pelite. Tuff, indicating light-gray, is sorted well. No graded structure is observed.

Thin section observation: Indicates the phenocryst of quartz, sericite, and plagioclase. The phenocryst of quartz and plagioclase appears automorphic. In many cases, the phenocryst of plagioclase has been deformed into sericite. Parts of sericite is transformed into amebiform and fibrous forms. The ground mass is generally equigranular, and the long axis of particles tends to direct the same direction, and a minute region is regarded to be in imbricate structure. Since the ground mass of tuff is dominant of pebble to sub-pebble, the benthic region is regarded to have a sedimentary environment that underwent rapid dislocation and fragmentation in the bottom of water.

##### c) Basic Volcanic Rocks

Distribution: K. Aicha, J. Hadid, etc. in the central Jebilet.



Lithofacies: Consists of massive lava, tuff, and tuff breccia. Massive lava, indicating dark-gray to white colors, is dense and hyaloclastite in its formation. Tuff and tuff breccia, indicating white color, are sorted well and a graded structure is observed. The tuff interbedded with thin-layered limestone.

Thin section observation: Indicates the phenocryst of sericite and plagioclase. In many cases, the phenocryst of plagioclase is displaced with sericite. The sericite is in amebiform and fibrous forms. The ground mass is fine-grained to grained sericite and quartz in equigranular state. The long-axis particles direct the same direction.

#### d) Rhythmic Alternation

Distribution: Benslimane, Kerkoz, K. Aicha, Benslimane-north, LaChach, Bouname, J. Hadid in the central Jubilet.

Lithofacies: Consists of sandstone and pelite in alternation of strata in the lower part and pelite and quartzite in alternation of strata in the upper part. The alternation of strata is in repetitions of several centimeter intervals, and, in some cases, several millimeter to several meter thick repetition intervals. Sandstone, indicating light-gray, is sorted well, and a graded structure or de-graded structure is observed. Pelite appears dark-gray, dense, is sorted well, and no graded structure is observed. Part of the pelite sandwiches a fine-gravel conglomerate layer. The upper part of rhythmic alteration consists of a gray-colored pelitic schist layers and quartzite layers in alternation of strata. The quartzite is dense, indicating white color. The ratio of the quartzite layer increases in the upper part.

A massive sulfide ore deposit is embedded in rhythmic alteration. Turbidite is formed in the vicinity of the deposit. Accordingly, the benthic region is regarded to have had a sedimentary environment that underwent rapid turbidity. Turbidity of the mode of occurrence is also observed in the boundary area of sulfide and black shale.

#### e) Phyllite

Distribution: Benslimane, Kerkoz, etc. in the central Jebilet

Lithofacies: Consists of black shale in marked schistose formation. The lithofacies transforms from the sandstone and black shale in the lower part, in alternation of strata, to phyllite. The phyllite is dense and sorted well, indicating milky-white, light-gray, and to black colors. In general, the phyllite has cubic pyrite disseminated.

#### f) Granodiorite

Distribution: Vicinities of Kerkoz, Campu au Rumrum, etc. in the central Jebilet.

Lithofacies: Massive and spotty, indicating black to dark-gray colors

Thin section observation: Indicates the phenocryst of quartz and augite in anhedral. Pyroxene is displaced with sericite. The phenocryst of quartz contains many several- $\mu$  m fine fluid inclusions.

(1)-2 Tequaim Group

g) Carbonate Rock

Distribution: Benslimane, Kerkoz, J. Hadid, etc. in the central Jebilet mountain mass

Lithofacies: Alteration of calcareous sandstone and clastic limestone. The calcareous sandstone, indicating dark-gray color, is bad at sorting and no graded structure is observed. The sandstone also locally interbedded with breccia clast.

The clastic limestone, indicating dark-gray to dirty-white colors, is fine-grained and dense, and part of which contains common pyrite dissemination. Sandstone and clastic limestone are spumous to hydrochloric acid.

Thin section observation: The clastic limestone indicates non-porphyrific and consists of equigranular groundmass.

h) Pelite

Distribution: Benslimane, Kerkoz, K. Aicha, etc. in the central Jebilet mountain mass

Lithofacies: Consists of black quartzite and sandy quartzite in alteration of strata.

(1)-3 Geologic Section in Individual district

Fig.II-2-2-8 indicates the geologic sections of individual districts in the Jebilet district. Geological characteristics of each area are as follows;

(A) Benslimane - Kerkoz district

-Sarhlef group pelite: Consists of black shale. No bio-fossil is observed.

-Sarhlef group volcanic rocks: Consists of massive lava. No phenocryst of quartz is seen. They present networked quartz veins.

-Sarhlef group rhythmic alternation: Consists of alternation of black shale and sandstone. 10-odd meter wide gossan, mainly consisting of magnetite are intercalated in several meter above the acid volcanic rocks on the surface. The extension of the gossan coincides with the stratification of sandstone. Siliceous part in the black shale is hard and outcrops in belt in the surface of the ground.

-Sarhlef group phyllite: Consists of black quartzite in the thickness of 20 meters or longer.

-Tequsim group carbonate Rock: Mainly consists of clastic limestone.

-Tequsim group pelite: Consists of black quartzite and sandstone in alteration of strata, in

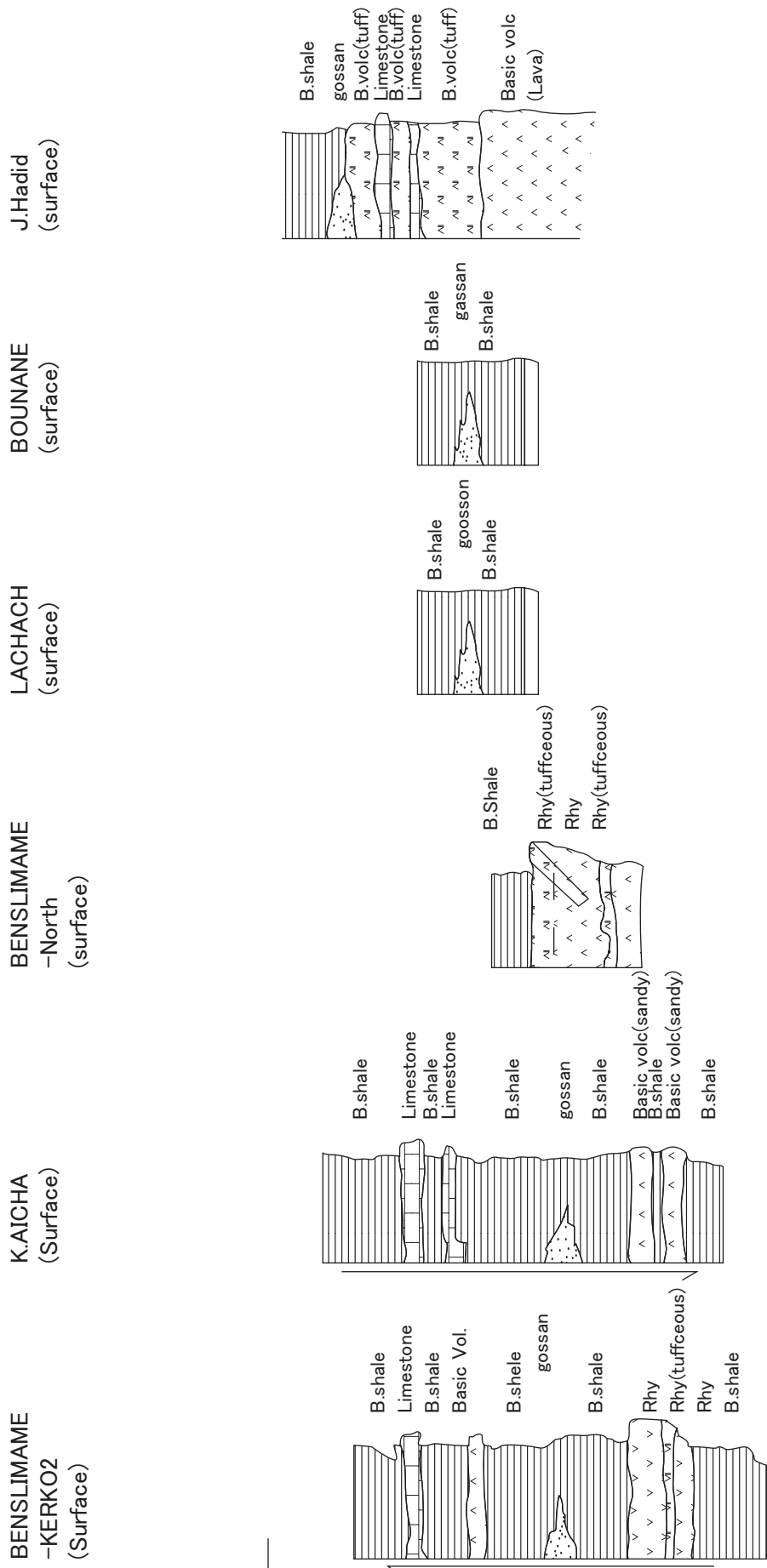


Fig. II-2-2-8 Geological column of Jubilet prospect

transformation to be schistose.

(B) K. Aicha district

-Sarhlef group pelite: Consists of an alternating bed of black shales and sandstones, and is schistized.

-Sarhlef group basic volcanic rocks: Consists of massive rhyolitic lava and rhyolitic tuff. The massive lava, 1 to 5 meters in width, consists of the upper and lower parts and is interbedded with tuff. The massive lava is siliceous and hard. It appears in two parallel belts on the ground surface.

-Sarhlef group rhythmic alternation: Consists of an alternating bed of sandstones and black shales. Gossan contains magnetite and hematite on the ground surface.

-Sarhlef group phyllite: Consists of black shales. The thickness of the bed is 10 meters or more.

-Tequsim group carbonate rock: Mainly consists of clastic limestones, which is coarse and vesicular.

-Tequsim group pelite: Consists of an alternating bed of black shales and sandstones, and is schistized.

(C) Ben slimane-north district

-Sarhlef group acid volcanic rocks: Consists of massive rhyolitic lava and rhyolitic tuff. The boundary intergrades. Cracks of massive lava is filled with pelite. The upper tuff, indicating white color due to silicification, forms networked smaller veins of quartz.

-Sarhlef group phyllite: Grades from the boundary of rhyolitic tuff, grading into black shales.

(D) LaChach-Bounane district

-Sarhlef group rhythmic alternation: Consists of alternation of black shales and sandstones, and black shales and quartzites. Marked folds and kink folds are observed. The alternating bed of black shales and quartzites contains lenticular sulfide gossan, accompanied by white alteration. This district observes no carbonate rock, such as limestone, in the neighborhood of the gossan.

(E) J. Hadid district

-Sarhlef group basic rocks: Consists of massive lava and tuffaceous rock. The bed of the massive lava is thick. The upper part of the massive lava grades into tuff to tuff breccia.

-Sarhlef group rhythmic alternation: Consists of a alternating bed of black shales and sandstones, and an alternating bed black shales and quartzites. In the ground surface, a sulfide gossan is embedded in the boundary of basic rock tuff and black shale. The gossan is good at

continuity in the same horizon. The surrounding area accompanies a several meter long alteration zone of kaolinite.

-Tequsim group carbonate rock: Consists of clastic limestone.

## (2) Geological Stratigraphy in the Guemassa Area

The geological structure in the Guemassa almost strikes NNW-SSE or NE-SW, and is piled up with eastern dip. The geological stratigraphy in the Guemassa district shows the similar stratigraphy as indicated in the Jebilet district, consisting of basement rocks formed in the Devonian period, Carboniferous period, and through Permian period in the Palaeozoic Era. The baserocks in Visean in the Carboniferous period in the Guemassa district are also divided into the Sarhlef group and the Tequsim group.

-Sarhlef group: Consists of pelite, acid volcanic rocks, rhythmic alternation, and phyllite, from the lower part to the upper part.

-Tequsim group: Consists of carbonate rock in the lower part, and pelite bed in the upper part. Geological map and geological section of the Guemassa are shown as Fig.II-2-2-9 and Fig.II-2-210.

### (2)-1 Sarhlef group

#### i) Pelite

Distribution: Frizen, Amzough, Hajar, etc. in the Guemasa district

Lithofacies: Consists of an alternation of black shales and sandstones. The black shales, indicating dark-gray color, is compact and is sorted well, but no grading is observed. The sandstones, indicating light-gray color, is sorted well but no grading is observed.

#### j) Acid volcanic rocks

Distribution: Frizen, Amzough, Hajar, etc. in the Guemassa district

Lithofacies: Consists of massive rhyolitic lava and tuff. The massive lava, indicating light-gray to milky-white color, shows a flow structure. The rock that underwent silicification indicates light-green color. The tuff, which is banded in graded structure and de-graded structure, is sorted well of particles. In Frizen, rhyolitic lava and rhyolitic tuff are located just under a massive sulfide ore deposit.

Thin section observation: For the phenocryst of the massive rhyolitic lava, the quartz phenocryst is idiomorphic. Some of the samples of granite porphyry indicate a megacryst, which is formed when several pieces of quartz phenocryst came together. Plagioclase appears idiomorphic, and some of which is resplaced with sericite, and near the ground surface, with kaolinite or alunite. The groundmass of rhyolitic lava is dominant of sericite and quartz. The

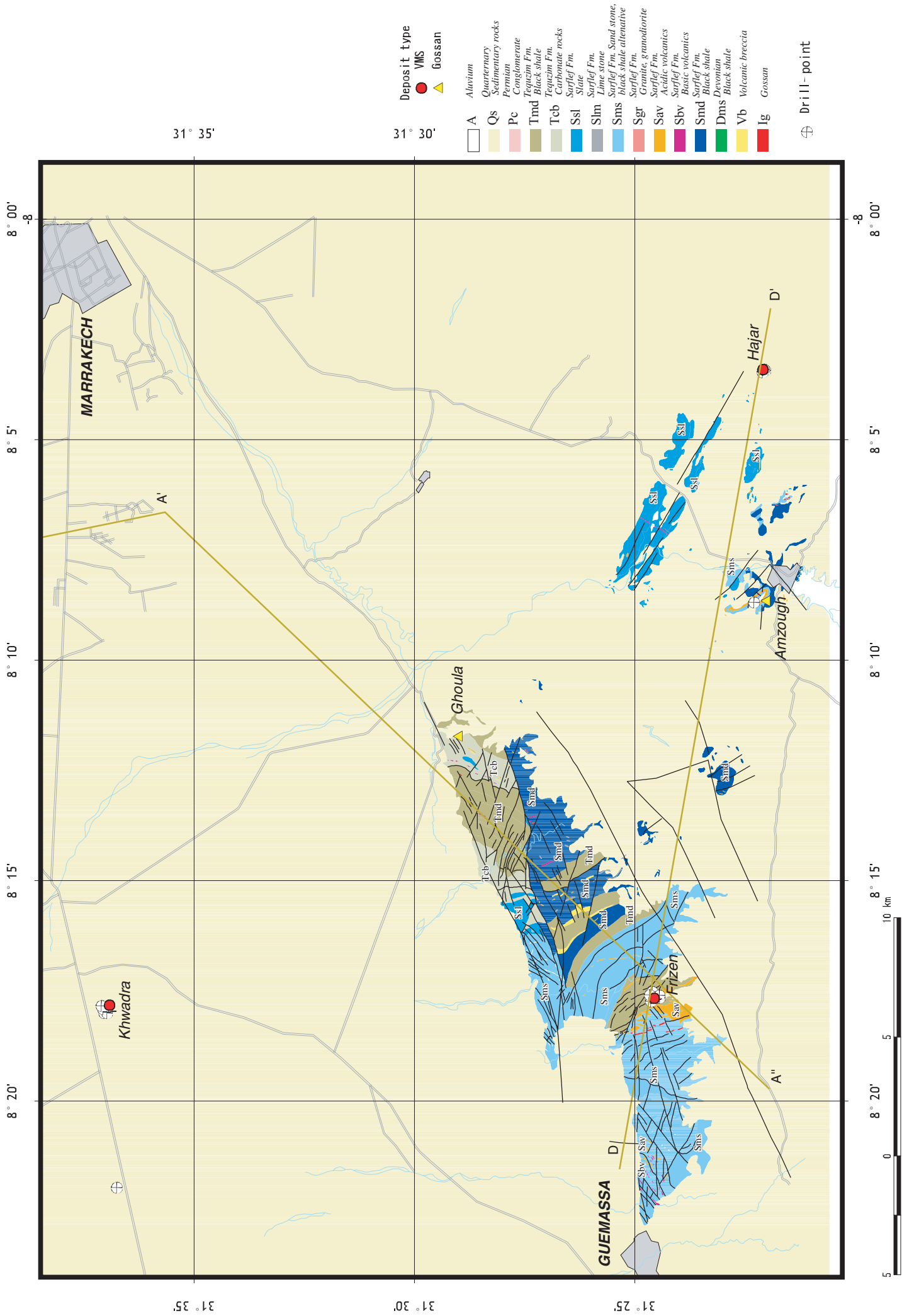


Fig. II-2-2-9 Geological map of Guemassa prospect

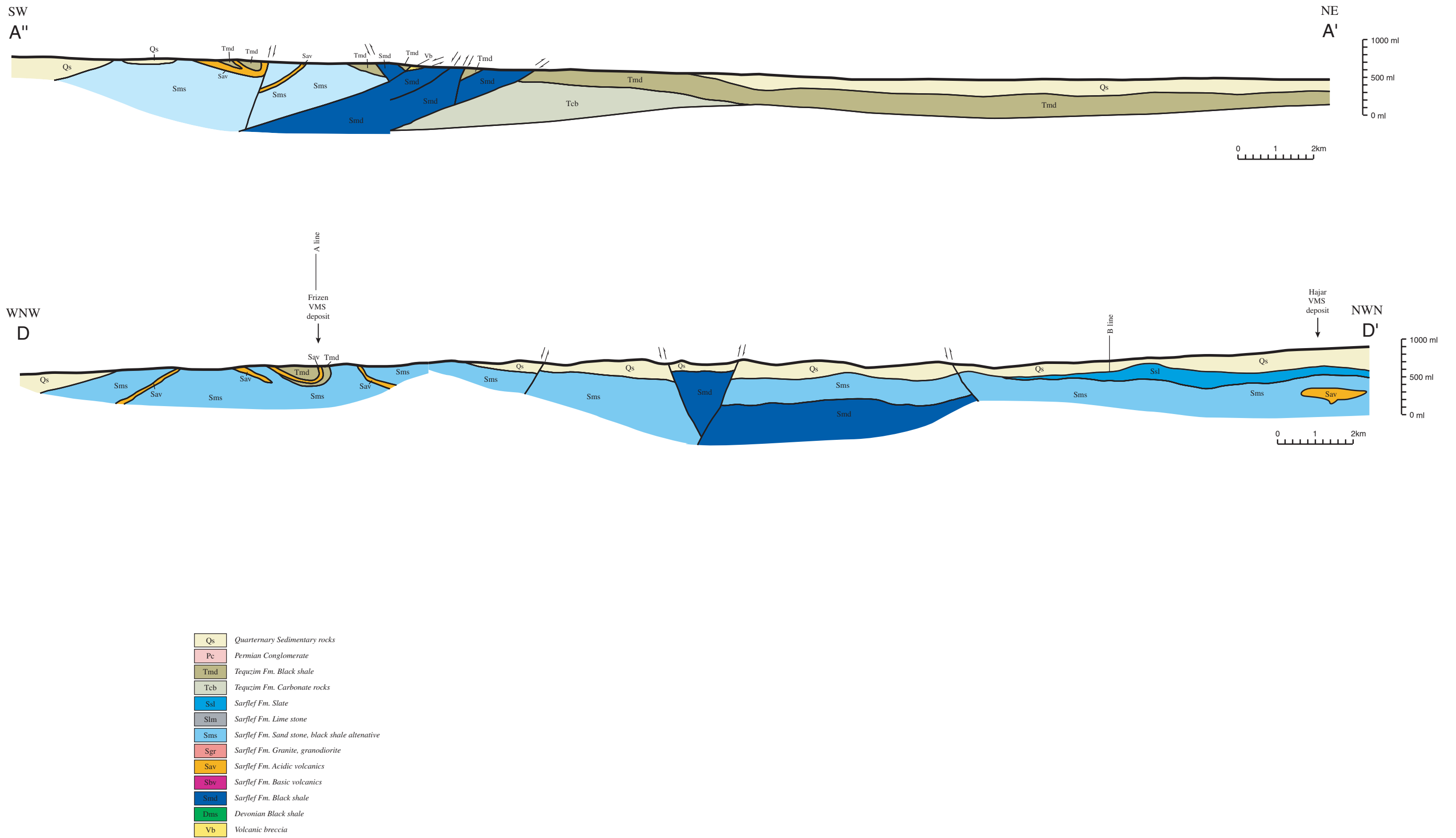


Fig. II-2-2-10 Geological cross section of Guemassa area

long axis of particles directs the same direction. Rhyolitic tuff consists of equigranular fine-grains to grains .

#### k) Rhythmic Alternation

Distribution: Frizen, Bal-Azzouz, Amzouz, Hajar, etc. in the Guemassa.

Lithofacies: Consists of a rhythmic alternating bed of black shales and quartzites. The alternation is repeated in several millimeter to several centimeter intervals. The black shale, indicating dark-gray to black, is very compact and sorted well. A graded structure and a de-graded structure are observed. Part of the black shales interbedded with a tuff bed in homogenous fine gravel of sub-pebble to sub-rubble. Rhythmic alteration is the source of the massive sulfide ore deposit, and neighbors of the deposit shows a marked turbidite, indicating a sedimentary environment that underwent rapid move in the benthic region.

Thin section observation: The boundaries of pelite and sulfides show a fracture zone in many cases. The form that sulfides intrude into pelite of the host rock is observed.

#### (2)-2 Tequaim group

##### l) Carbonate Rock

Distribution: Tawida (northwest to Hajar) in the Guemassa district

Lithofacies: Consists of bio-limestone, which indicates black to dark-gray-brown. It is compact and very fine-grained. Part of which contains common pyrite disseminated.

Thin section observation: The matrix of bio-limestone is equigranular and oblong.

#### (2)-3 Geological columnar section of individual district

Fig.II-2-2-11 indicates the geological columnar section of individual district in the Guemassa area. Described below are their geological characteristics.

#### (F) Frizen district

-Sarhlef group pelite: Consists of an alternating bed of black mudstones and sandstones in alteration of strata.

-Sarhlef group acid volcanic rocks: Massive rhyolitic lava, indicating a flow structure, has some silicification. The phenocryst of quartz is rich in the groundmass. Rhyolitic tuff, having some sericite alteration, forms networked quartz veins. Networked quartz veins are embedded.

-Sarhlef group rhythmic alternation: Consists of an alternation of black mudstones and sandstones. It is the base rock of a massive sulfide ore deposit. The contact with rhyolite observes a chilled margin.



-Intrusive rock (granite porphyry): Granite porphyry intrudes or injects the rhythmic alternation as sill. The contact with pelite has some clinkers, filled with hematite. The granite porphyry observes alunite and alterations of kaolinite.

(G) Bal Azzouz district

-Sarhlef group rhythmic alternation: Consists of an alternation of black mudstone and sandstone. Pelite is fine to coarse-grained, and limestony. Although it was deformed markedly, metamorphism is relatively weak.

(H) Amzough district

-Sarhlef group pelite: Consists of black mudstone. The lithofacies of the mudstone is compact, fine-grained, and hard. The boundary with the upper acid tuff is intergradational.

-Sarhlef group acid volcanic rocks: Consists of rhyolitic tuff and tuff breccia. The rhyolitic tuff indicates idiomorphic quartz.

-Sarhlef group rhythmic alternation: Consists of black mudstones and sandstones. The black mudstones in the lower part is interbedded with a thin bed of rhyolitic tuff and rock fragments. A thin bed of calcareous rock is interbedded in the black mudstones.

(I) Tawida (northwest of Hajar) district

-Tequsim district carbonate rock: Consists of bio-limestone. It is black, massive, fine-grained, and compact. Part of the limestone indicates common pyrite disseminated.

(J) Hajar District

-Sarhlef group pelite: Consists of fine-grained black mudstone. It is sorted well. A stockwork of quartz veins is embedded in the mudstones.

-Sarhlef group acid volcanic rocks: Consists of rhyolitic lava (massive, hyaloclastite), which is located just under the massive sulfide ore body. The hyaloclastite underwent sericite alteration. The phenocryst of plagioclase also underwent sericite alteration under microscope.

-Intrusive rock (granite porphyry): Granite porphyry is massive and compact, and is characterized by megacryst of quartz phenocryst by being. For an aggregate of quartz phenocryst, the central part is idiomorphic and has larger particles in diameter while the marginal part is fine-grained, xenomorphic, and circular.

-Sarhlef group rhythmic alternation: Consists of black mudstones and quartzites, and marked turbidite is observed. The black mudstone sandwiches several to tens of dozens of thin sulfide beds. The mode of occurrence is similar to mineralization in sedimentary spiracle deposits.

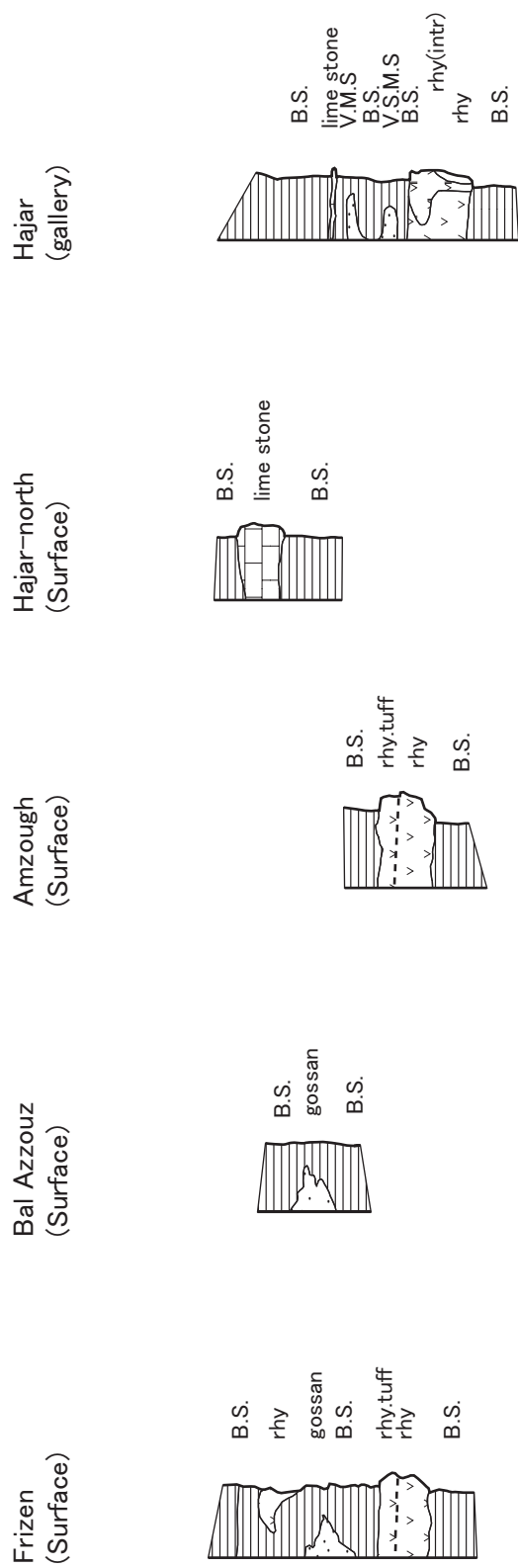


Fig. II-2-2-11 Geological column of Guemassa prospect

## 5) Characteristics of massive sulfide ore deposits

Location of the major deposits and mineral occurrences are plotted on Fig.II-2-2-12.

### <Jebilet Area>

#### (1) Kettara Deposit

The Kettara Deposit is located approximately 32km NNW from Marrakech. The mine had extracting from 1945 through 1961 for a reduced zone. From 196 through 1963, the mine extracted common pyrite and copper. It extracted pyrrhotite from 1965 through 1980. The bed thickness of the deposit stands at above 11 meters, the maximum is 70 meters. The deposit is estimated to extend some 1,500 meters into N30° E directions and to extend continuously some 500 meters into the underground. The deposit consists of an oxidized zone under 50 meters from the ground surface, a 5- to 10-meter long reduced zone under the oxidized zone, and an primary deposit under the reduced zone.

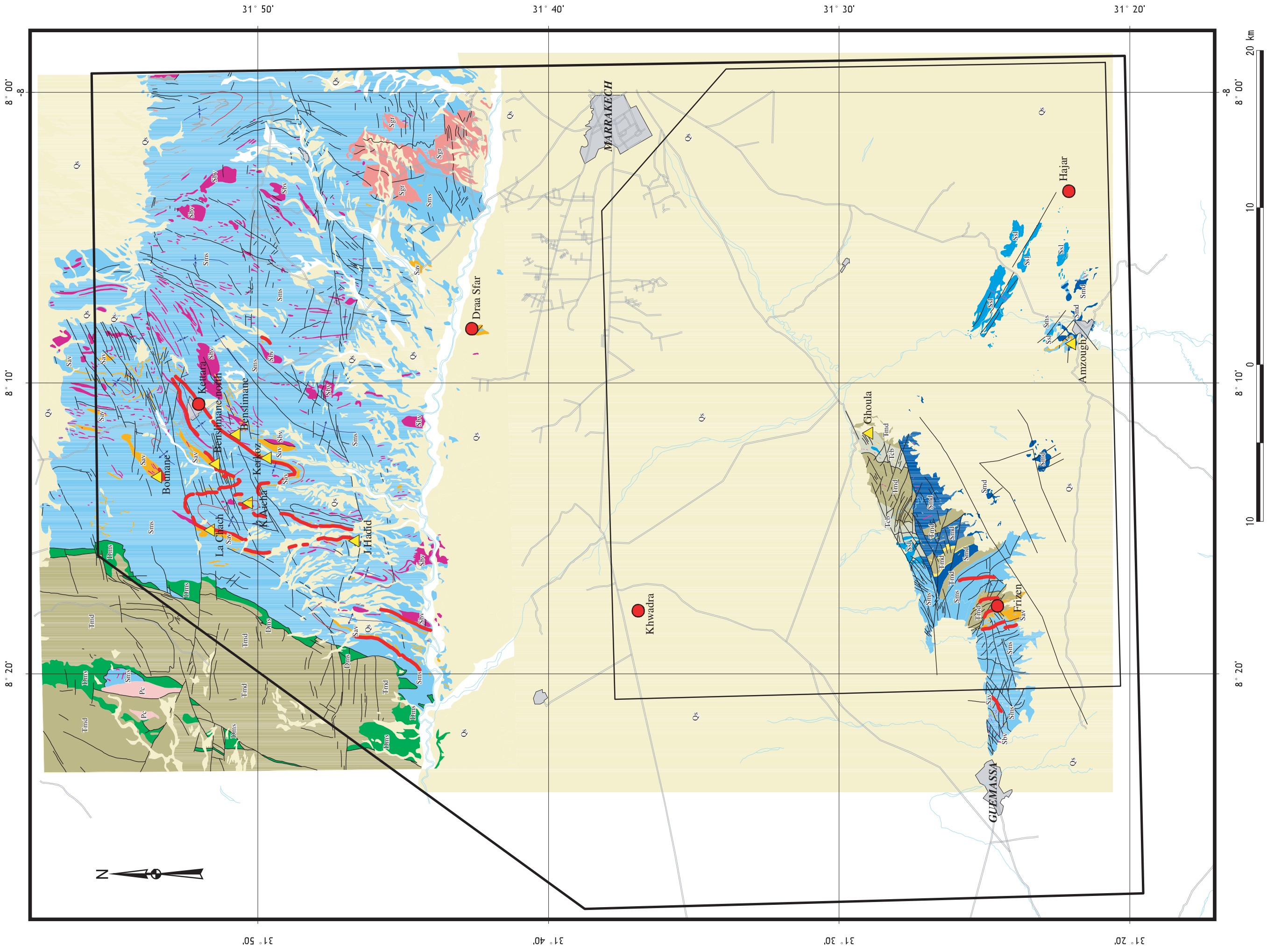
-Oxidized zone: Supergene brought about secondary alternation of the primary deposit and formed an oxidized zone into the deep underground. The major sulfides include limonite, hematite, and goethite. Silicate minerals include quartz, geoso, sodium, alumite, and jarosite. Accompanying minerals include brimstone, perlite, malachite, etc.

-Reduced zone: It begin with an underground water surface at average 50 meter deep from the surface. This lasts some 5 to 10 meters long. Combinations of minerals include pyrite, chalcopyrite, covellite, native copper, and pyrrhotite. This reduced zone has a high grade of copper at an average of 8% and 20% at maximum.

-Primary deposit: Ore bodies are massive, zonal, or banded. Ore bodies and ores were affected by alteration that brought about schistosity in the base rock. Combinations of minerals include pyrrhotite, pyrite, marcasite, chalcopyrite, arsenopyrite, sphalerite, magnetite, red hematite, chalybite, quartz, isinglass, and chlorite.

The footwall of the deposit consists of an alternating bed of black shales and sandstones, and part of which contains basic volcanic rocks. The sulfide ore body is massive or zonal or banded. The upper part of the sulfide ore body contains rust-colored siliceous rock, and a siliceous rock bed similar to ferruginous quartz that contains thin layers of bedded clay. The hanging wall is dominant of alternating beds of black mudstones and quartzites. The hanging wall and footwall of the ore body indicate alteration, and formation to sericite and chlorite is dominant, beside silicification.

The ore reserve base of pyrrhotite in the Kettara Deposit stands at some 21 million tons. The average grades are 55% for Fe, 20% for S, and 20% for Cu, and the deposit is massive sulfide ore bodies which is poor in base metal and rich in pyrrhotite.



**Geology**

- A Alluvium
- Qs Quaternary
- Pc Sedimentary rocks
- Tmd Permian
- Tcb Conglomerate

**Deposit type**

- VMS (Red circle)
- Gossan (Yellow triangle)

**Drilling point**

- ⊕

**Estimated Ore horizon**

- Red wavy line

**fold**

- Blue line with 'X'

**Geological units and their descriptions:**

- Ssl Sarfajef Fm.
- Ssl Devonian Black shale
- Ssl Black shale breccia
- Ssl Gossan
- Slim Slate
- Slim Lime stone
- Slim Sarfajef Fm.
- Slim Sand stone, black shale alternative
- Sms Sarfajef Fm.
- Sms Granite, granodiorite
- Sms Acidic volcanics
- Sms Sarfajef Fm.
- Sms Basic volcanics
- Sms Sarfajef Fm.
- Sms Black shale
- Sgr Sand stone
- Sav Granite
- Sby Granite
- Smd Black shale
- Dms Devonian Black shale
- Vb Black shale breccia
- IG Gossan

Fig. II-2-2-12 Distribution of deposits at Marrakech-Tekna area

## (2) Ben Slimane Prospect

The Ben Slimane Prospect is located to a southwestern extension from the Kettara Deposit. The copper grade stands at 1%, and ore reserves are estimated to reach 1 million ton. The geological stratigraphy is similar to that of the Kettara Deposit. Mineralization is located in rhythmical alteration beds of pelites and sandstones or quartzites, in the Sarhlef group. The upper part contains carbonate rock in the Tequsim district represented by limestone. The Ben Slimane Prospect is an extension along the synclinal axis in the Kettara Deposit. The prospect is located in a hinge in large synclinal axis structure which was formed at the early schistosity and deformation. The Ben Slimane Prospect appeared as a series of lenticular gossan; its thickness varies, ranging 1 to 10 meter small lenticular deposits whose continual extension lasts about 600 to 700 meters.

Composition of ore minerals in the Ben Slimane Deposit is similar to that of Kettara Deposit. Pyrrhotite is predominant in the deposit, accompanied by small quantities of chalcopyrite, pyrite, and arsenopyrite. The forms of the deposit include massive deposits and disseminated deposits. Although the base metal grades are relatively low, the copper grade stands at 1% or so, a relatively high percentage.

## (3) Kerkoz Prospect

This prospect is located approximately 1 km to the southwestern of Ben Slimane. The Kerkoz Prospect located in the same base rock as Ben Slimane that extends along the Kerchenet structure axis, which is accompanied by dislocation to the west due to the right-lateral fault of the Kerkoz fault.

The prospect strikes N10° and crosses with the bedding, stands at vertical gossan. The gossan in the ground surface accompanies alterations to sericite, kaolinite, and silicification.

## (4) Lachach Prospepct

The Lachach Prospect is 0.5 to 2 m in thickness and extends 5 km in length. The prospect, with a NNE-SSW strike, appears to have gossan altered in red color along a shear zone. Mineralization indicates gossan, stockwork and vein. Red to white altered schist contains hematite and goethite, which are distributed in veining and zonal. According to past surveys conducted by BRPM, a low geochemical anomaly was observed in the entire gossan. Although several drillings were conducted in the past, no remarkable result was brought about as expected.

## (5) Bouhane Prospect

This prospect is located in an extended zone in the NNW direction from the Lachach

Prospect. The prospect is 0.5 to 2 m in thickness and extends some 2 km in length, pinching and swelling. The geology, geological structural, and prospecting of the Bouhane Prospect are similar to those of the Lachach Prospect. Although several Drillings were conducted to target for deposit extensions in deep underground, no ore bodies were captured.

<Guemassa Area>

#### (6) Draa Sfar Deposit-north

The Draa Sfarb deposit-north is found at a location, 15 km northwestern from Marrakech, along Tensift River. The deposit is at the southern edge of the Visean series baserock which sediments under the covering zone. The Draa Sfar Deposit-north is a mineralization zone found in greenish arenaceous and schistose matter. The district is a small outcrop (350 x 60m) of gossan that protected from erosion. The mineralization zone is subdivided into two zones, i.e. the north and south mineralization zones.

- Northern Draa Sfar Mineralization Zone-north: The gossan is in almost vertical banding, locally indicating a brecciated form??.

- Northern Draa Sfar Mineralization Zone-south: The gossan consists of schist, which is hardened due to silicification and iron enrichment.

Composition of ore minerals of the gossan include pyrrhotite, pyrite, marcasite, chalcocite, arsenopyrite, galena, sphalerite, magnetite, hematite, chalybite, cobalt glance, electrum, bismuth, bismuthinite, cassiterite, and other ore minerals. Gangue minerals include quartz, sericites, and chlorite. Hydrothermal alteration at the Draa Sfar Deposit-north is observed as whitish clay minerals on the margin of the mineralization zone.

#### (7) Draa Sfar Deposit-south

The Draa Sfar Deposit-south has a concealed massive sulfide ore deposit, which was found by drilling and underground prospecting. The bedded sulfide deposit extends some 1 km in the NNE-SSW directions. The stratiform sulfide ore deposit is vertical or inclined in the western direction (80°). The ore body ranges in thickness from 1 to 28m with pitch and well structure. The center of the ore body encompasses sulfide in the border between basic volcanic rocks and pelite. The northern edge and the southern edge of the ore body has sulfide in a rhythmic alternation of pelites and sandstones.

The ore minerals consist of pyrrhotite, arsenopyrite, pyrite, galena, sphalerite, chalcopyrite, and magnetite. The gangue minerals consist of quartz, carbonate minerals, and chlorite. The mineralization indicates a marked zonal distribution. About 300 m in the center of the distribution is poor at base metals but dominant of pyrrhotite. A 200 m zone in the northern deposit is rich in zinc and contains pyrrhotite. A 400 m zone in the southern deposit

encompasses lead and zinc in zonal distribution. In other words, the center of the deposit is massive (partly zonal), and the sides and extensions of the mineralization zone indicate banding, banded, and/or disseminated conditions.

#### (8) Khwadra Deposit

The Khwadra Deposit was a new deposit found in June 2000. Explorations by Drilling from the ground surface have been conducted from time to time. These drillings have identified a deposit of 500 m x 300 m in scale with 5 to 6 m of average deposit thickness. According to ore intersections from these Drillings, the proven ore reserve is estimated to reach about 4 million tons.

The sulfide ore body is embedded in the Khwadra Deposit in massive or banded state in an alternating bed of black mudstones and sandstones or quartzites. The vicinities of the deposit has acid volcanic rocks and basic volcanic rocks. Some 170m thickness from the ground surface is covered with sedimentary rocks formed in Tertiary and onward.

The ore minerals include pyrrhotite, which is pre dominant, pyrite, chalcopyrite, galena, and sphalerite. The ore assay of a drilling core were obtained Cu 0.35%, Pb 0.71%, Zn 2.6%, Au 0.27g/t and Ag 15g/t.

#### (9) Hajar Deposit

The Hajar Deposit is a lead-zinc-sulfide deposit located 150 to 400 m deep from the ground surface. The ground surface is covered with the Quaternary in the thickness of about 120m. The sulfide ore body is embedded in an alternating bed of pelite and sandstone, right above acid volcanic rocks. The ore body extends 300 m in the horizontal direction, 400 m in the vertical direction, and 100m of maximum dimension.

The major ore minerals include chalcopyrite, galena, sphalerite, and pyrrhotite. Alterations of the base rock include silicification, argillation, and to being chloritic.

According to the Basic Survey Summary Report of Haouz Plain Region Resource Development of the Kingdom of Morocco (1990), a total of 21 borehalls in a polygonal block system were conducted in 70 m intervals, covering a total extension of 8,500 m. The estimated ore reserve and grades are as follows:

Ore reserve: 1.6 million tons

Grade: Ag 74g/t; Cu 0.86%; Pb 2.78%; Zn 9.45%; S 30.3%

#### (10) Amzourh Prospect

The Amzouth Prospect is located in the Imarine district, 1 km north from the Lalla Tekerkoust Dam. The prospect has gossan accompanied by pyrrhotite and quartz, in continual

distribution that accompanies acid volcanic activities. Slate and siltstone in alteration of strata under this rock have a small-scale gossan along a fault crush zone. The highest grades of the 1-meter wide gossan were Cu 0.5%, Pb 1.0%, and Zn 1.4%.

The major geological structure is characterized as having a synclin dipping southwest. The gossan in the Amzourh district is arranged in the NNE-SSW directions, in the width of the meter. Specifically, it is distributed in units of 10 to 100 meters in straight line. The mineralization includes goethite and brown hematite, with signs of copper and manganese. As a Whole, the gossan consists of massive and lenticular iron oxide. The chemical analysis of the gossan indicated high ore grades, namely Pb 15%, Mn 24%, Cu 3.5%, and Zn 2.6% (JICA/MMAJ, 1990).

#### (11) Frizen Deposit

The Frizen Deposit is a gossan distributed in a several hundred km extension in the south-north directions. Two important ore showings, 1 km separated with each other, were identified. The sulfide ore body is embedded in an alternating bed of pelites and sandstones or quartzites, in rhythmical alteration of strata, just over acid volcanic rocks. The rhyolite in the acid volcanic rock indicates a fluidal structure, part of which is porphyritic.

##### Frizen I:

Is a lenticular gossan, embedded in two beds of rhyolite lava, with 80 cm of width and 600 m of length. The gossan consists of goethite, hematite, and beige carbonate minerals. Alterations, which cover silicification, carbonatization, sericitization, and chloritization, are observed in vicinities of the mineralization zone and acid lava.

Drillings targeting concealed ore bodies identified mineralization of massive and banded sulfide ore bodies and stock-work veins. Combinations of the massive and banded sulfide ore bodies cover sphalerite, galena, common pyrite, chalcopyrite, and small quantities of pyrrhotite. In addition, The sequencer of mineral crystallization in veins in stock-work is sphalerite + galena -> pyrite + chalcopyrite -> quartz. The margin of the veins have alteration of chloritization.

Since 1986, BRPM have conducted 9 Drillings targeting the lower zone of this gossan, in total 2,500m in length. These identified low-grade copper, lead, and zinc dissemination. The dissemination is 4 to 22 m in width. Ore assay are as follows: Ag 10 to 20 g/t, Cu 1% or less, Pb 1% or less, and Zn 1 to 3%.

##### Frizen II:

Three gossan zone, running in parallel with the western rim of western rhyolite, consist of



in several hundred meters in length in the almost NS directions. The three gossan strings were dislocated with each other by a cross fault in the N70° E direction. The characteristic of the mineralizations the same as that of the Frizen I Prospect in terms of structure, minerals, ore composition, etc.

#### 6) Anomalies in Existing data of Geophysical survey

This section describes the relation between the results of past geophysical prospecting conducted in this survey area and prospects.

##### <Kettara Deposit>

In the Kettara Deposit, an airborne geophysical prospecting (Geotrex) conducted in 1968 captured about 100nT of bi-polar magnetic anomaly just above the deposit. This anomaly was also identified with the surface geophysical prospecting at 400nT of maximum anomaly. The SP survey identified -300mV order of strong anomaly, indicating a complete overlap of gossans in the ground surface.

##### <Draa Sfar Deposit-north>

The mineralization zone in the Draa Sfar Deposit-north was found by SEGM (deposit survey section) in 1953. The magnetic anomaly in the ground surface was identified by CPGNA (North American Geophysical Exploration company). Afterwards, based on magnetic anomalies identified by Geotrex through airborne prospectings, a joint survey was conducted in cooperation with CMM (metallurgy and mining company) for explorations in the southern area. A subsequent Drilling led to the finding of the Draa Sfar Deposit in 1966.

##### <Draa Sfar Deposit-south>

For the Draa Sfar Deposit-south, SAPA and GEOTERREX each conducted airborne geophysical survey in 1964 and in 1968 including a magnetic and electromagnetic survey (INPUT). Although INPUT anomalies acquired did not match with existing prospects, two 50 to 60nT of magnetic anomalies were confirmed in the NNE-SSW axis directions. Although the anomaly in the southern part was along deposit outlines under the ground, the anomaly in the northern area slightly dislocated from the prospect of gossan (Sidi M' barek) on the surface.

Afterwards, a surface magnetic survey was conducted. It indicated very strong magnetism (maximum: 1000nT) in southern Tazakourt as in northern Sidi M' barek.

Our self-potential method conducted in Sidi M' barek acquired -150mV of anomaly, which was completely the same with the value acquired in gossan. The gravity method (Shanane, 1982) conducted by BRPM in 1982 indicated anomaly just over the known mineralization zone, and read an axis indicating load in the southern part. Although the electromagnetic method mainly

conducted on the surface (Truman) by Badissy (1970) acquired conductor in the southern ore body in Tazakourt, it did not lead to ore intersection.

#### <Amzourh Prospect>

For the Amzourh Prospect, the airborne geophysical survey conducted by Geotrex in 1968 identified 50nT of airborne magnetic anomaly and a magnetic input anomaly recorded at the INPUT 3rd channel. Result of tracing these anomalies on the surface identified 300nT of strong magnetic anomaly, which overlaps with -60mV of SP anomaly.

#### <Frizen Deposit>

The geophysical survey and the 1968 airborne prospecting captured about 75nT of magnetic anomaly and 5 channels of magnetic input anomaly just covering prospects in the Frizen Deposit. In 1984, a surface geophysical prospecting identified following results: a gossan zone which is characterized as an overlap of a strong magnetic anomaly (400nT) that accompanies SP anomaly (-80mV) and a clear electromagnetic anomaly, and rhyolite rock body in the northern area that corresponds to an overlap of a weak magnetic anomaly (60nT), an electrical anomaly (SP: -100mV), and an electromagnetic anomaly (MAX-MIN and VLF).

## Chapter 3 Existing Drilling Core Survey

### 3-1 Method of the survey

In our existing drilling core surveys, we worked on a total of 3638.15m of drilling cores and extracted mine samples. Specifically, we surveyed the drilling cores that BRPM holds in Rabat City and Kettara Village, and the major drilling cores of the Draa Sfar Mine that REMINEX explores and holds in Jebilet area, and the major drilling cores that CGM holds through exploration and operation in the Hajar Mine.

### 3-2 Results of the survey

Location of previous drilling sites are listed on Table II-3-1 and indicated on Fig.II-3-1, and geological column are shown in the end of this report.

The geological conditions we confirmed include pelite, acid volcanic rocks, basic volcanic rocks, rhythmic alternation, and phyllite in the Sarhlef group, and carbonate rock and pelite in the Tequsim group. Described below are the geological conditions and mineralization of individual Drilling cores from the bottom upwards by zone.

#### (1) Kettara district

The geology of the Kettara district consists of pelite, basic volcanic rocks, acid volcanic rocks, and rhythmic alternation in the Sarhlef group; and pelite in the Tequsim group, from the bottom upward. The KT2BS core suggests that the stratum was upside down because siliceous rock, supposed to be in the hanging wall, is located in the lower part. Sulfide ore body, generally existing in a rhythmical alternating bed of black shales and sandstones, is massive or banded. The sulfide ore body of the KT3BS core is massive in the boundary between basic tuff and black mudstone (Fig II-3-2-(1)).

#### - KT104 (180-40m)

180.0-164.5m: pelite (black shale, massive); 164.5-160.6m: massive sulfide (banded, pelite bed interbedded); 160.6-149.0m: rhythmic alternation (a rhythmical alternating bed of black shales and sandstones); 149.0-120.7m: pelite (black shale, fracture zone, schistose); 120.7-115.0m: massive sulfide (compact); 115.0-100.1m: rhythmic alternation (a rhythmical alternation of black shales and quartzites, minor alternation); 100.1-40.0m: pelite (black shale, massive, fracture zone)

#### - KT2BS (120-10m)

Table II-3-1 List of the Observating Drilling Cores

District	Drilling Name	East	North	Observating Department (m)	Length
Kettara	KT104	8.172276	31.871876	180 - 40	663.30 m
	KT2BS	8.179408	31.869356	120 - 10	
	KT4BS	8.179730	31.869356	310 - 36	
	KT3BS	8.179998	31.868927	70 - 0.7	
	KT1BS	8.180105	31.868712	70 - 0	
Ben Slimane	BA15	8.200176	31.847683	337.6 - 269.8	67.80 m
K. Aicha	KA25	8.236318	31.839026	561 - 42.95	518.05 m
La Chach	A9	8.240556	31.863769	250 - 157	93.00 m
Draa Sfar	DSF15	8.135795	31.711108	270 - 10	410.00 m
	DSF2	8.135662	31.710796	150 - 0	
Khwadra	KH4A	8.298496	31.617863	565.6 - 533.6	297.95 m
	KWS4C	8.298496	31.617863	570.7 - 514.7	
	KWS5C	8.297201	31.618472	716.05 - 621.8	
	KWS3C	8.299937	31.616413	404.5 - 303.2	
	KH1A	8.300020	31.617379	420.6 - 406.2	
Saf Safa	S2	8.365991	31.612731	472.9 - 197.4	275.50 m
Hajar	CD27	8.056880	31.368376	340.6 - 0	640.90 m
	GHC1	8.057797	31.368447	64 - 0	
	HS13	8.057162	31.367389	400.8 - 200	
	HS25	8.056668	31.367882	332 - 296.5	
Amzough	AZG480	8.144736	31.371748	410 - 144.8	265.20 m
Frizen	FZ13	8.293200	31.411156	150 - 30.25	406.45 m
	FZ12	8.294233	31.407297	80 - 7.1	
	FZ10	8.295500	31.410695	100 - 29.9	
	FZ03	8.291961	31.410238	170 - 90	
	FZ02	8.295215	31.410025	111.7 - 98	
	FZ14	8.293342	31.407409	50 - 0	
(Total)	27 site				(total) 3638.15 m

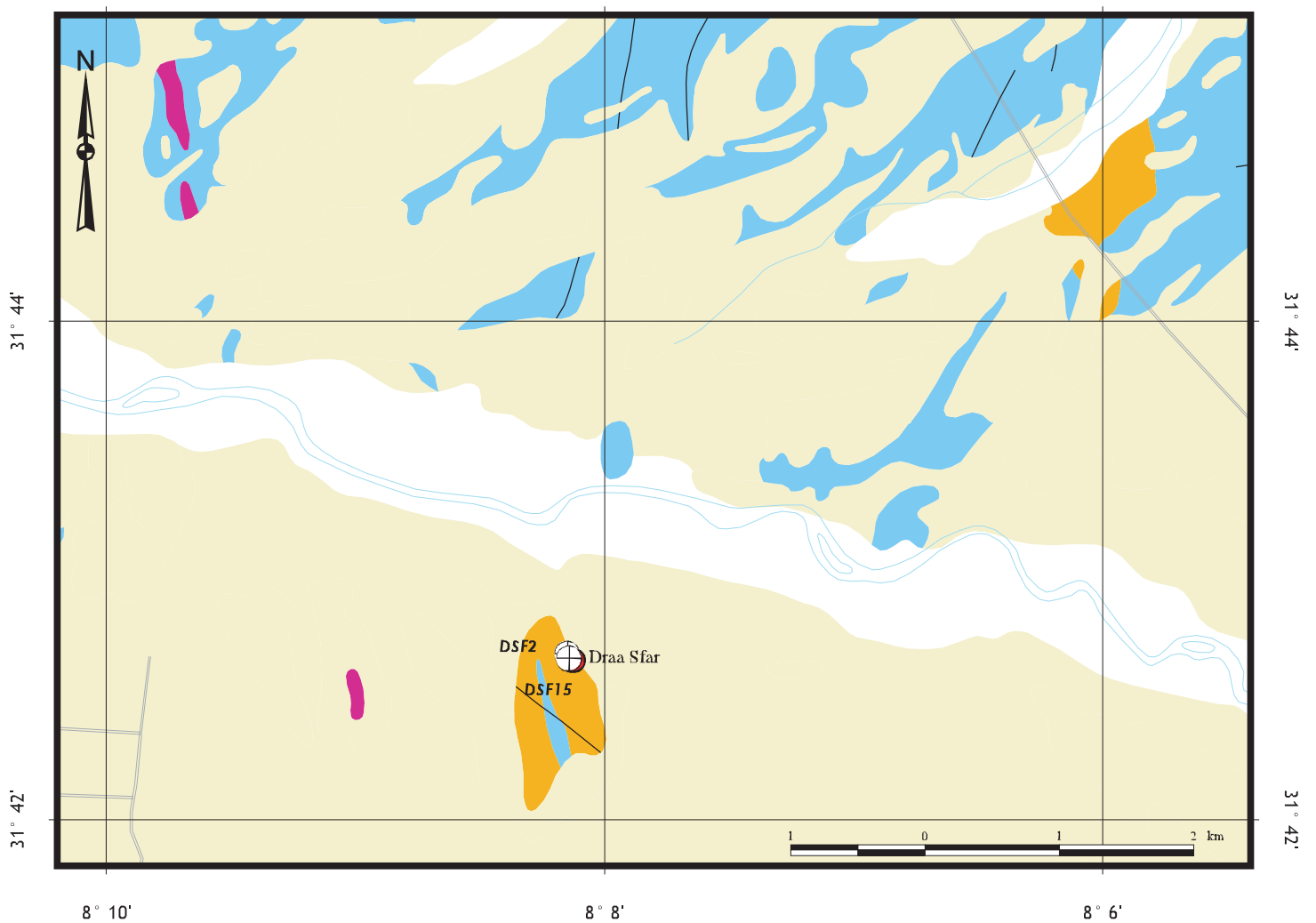
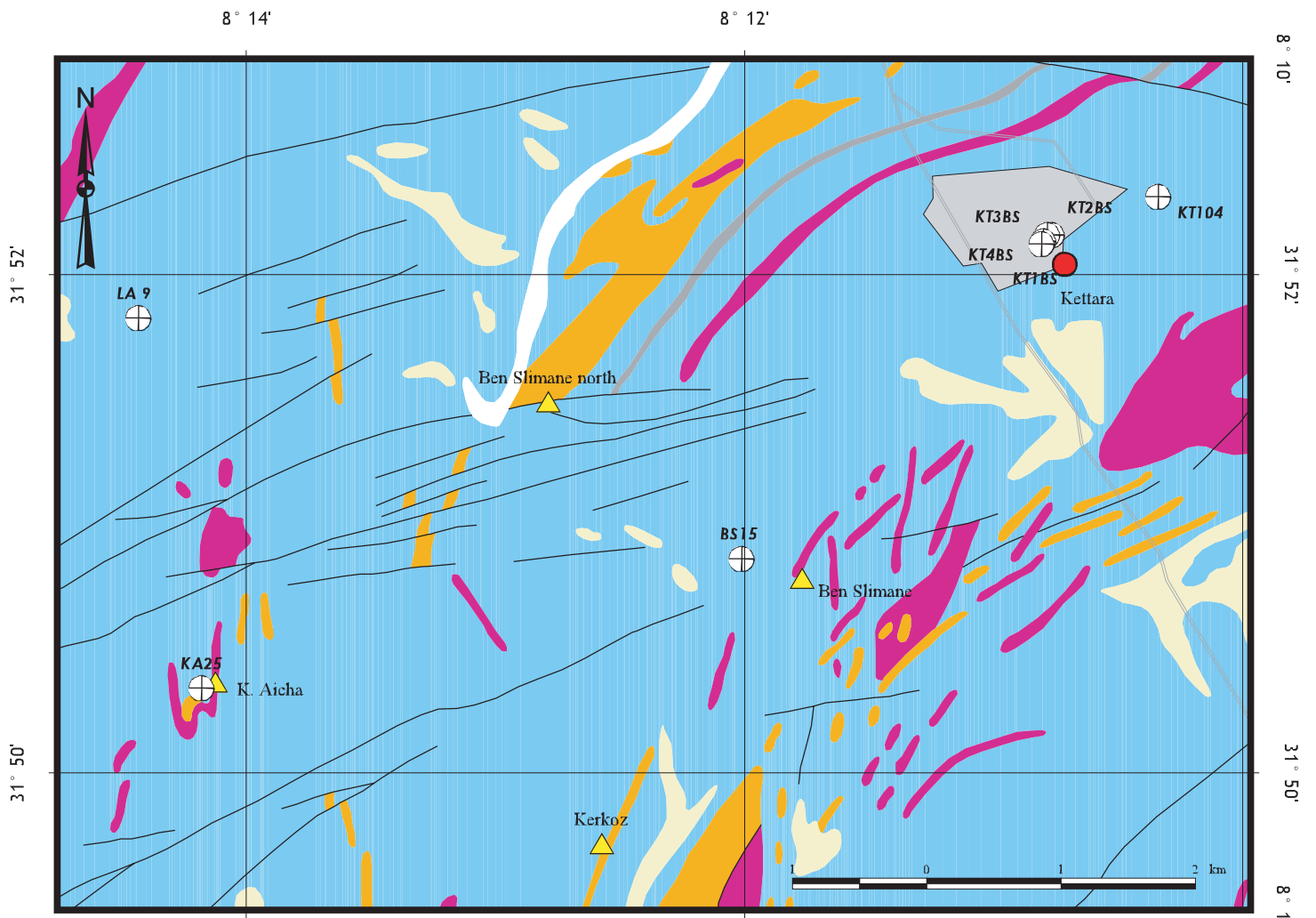


Fig .II-3-1-(1) The location of drilling posit (Kettara, Draa Sfar)  
 - 109 -

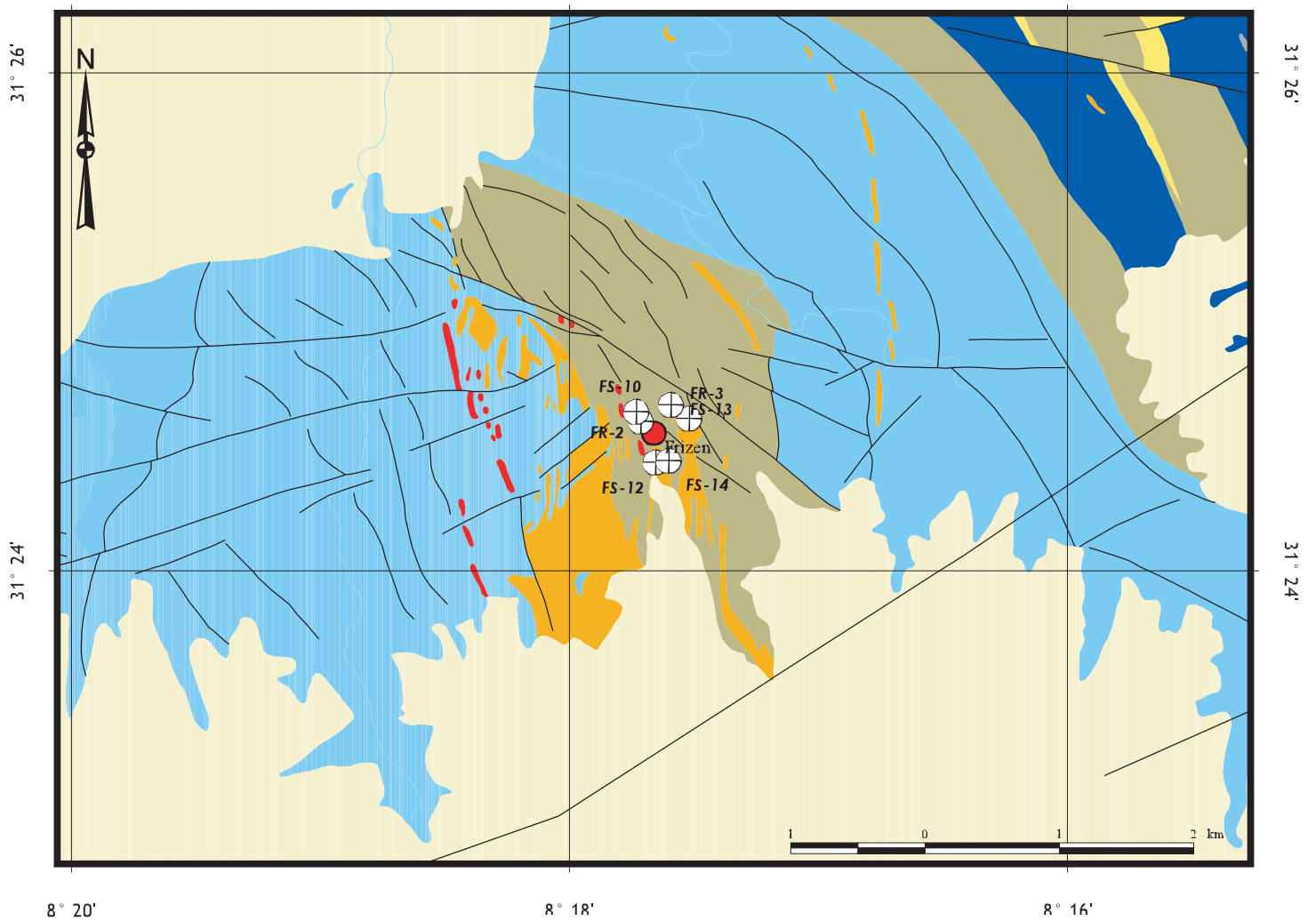
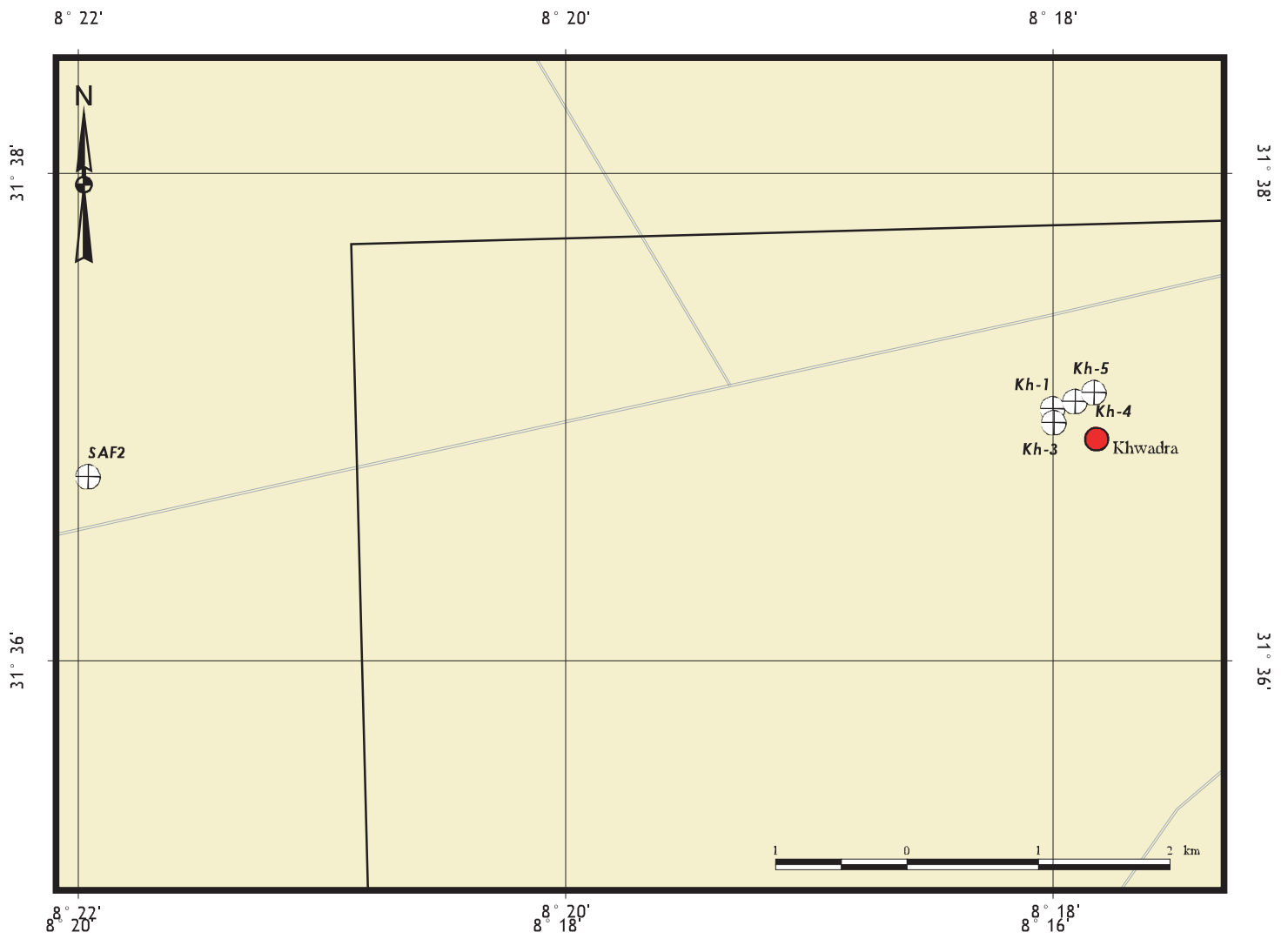


Fig . II-3-1-(2) The location of drilling posit (Khwadra, Frizen)

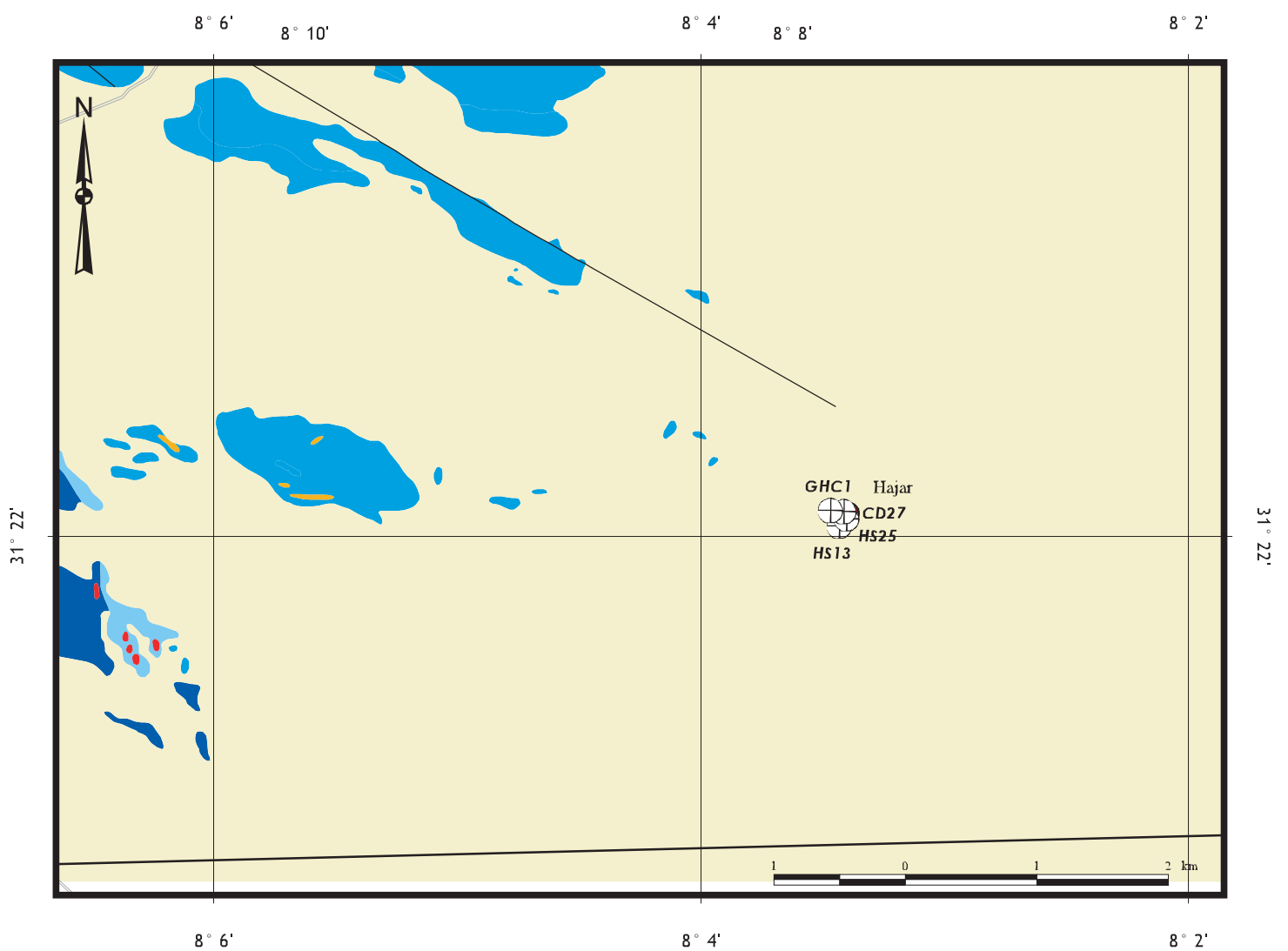
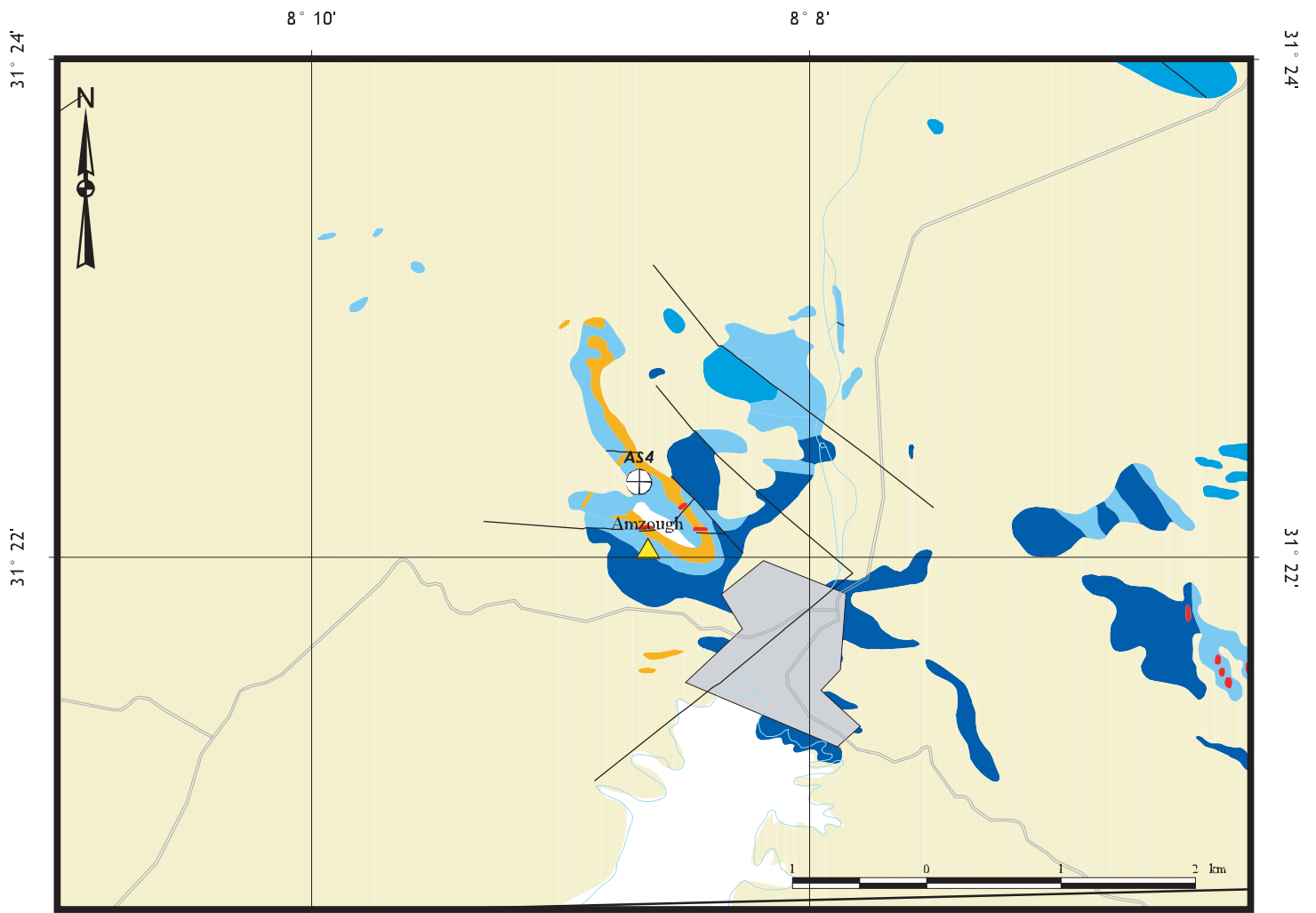


Fig .II-3-1-(3) The location of drilling posit (Amzough, Hajar)



120.0-110.35m: rhythmic alternation (a rhythmical alternating bed of black shales and quartzites, lamina dominant); 110.35-96.7m: massive sulfides (compact, quartz vein between 110.35-110.0m); 96.7-88.5m: pelite (black shale, schistosity developed, weak silicification); 88.5-83.4m: massive sulfides (compact, sandy); 83.4-42.55m: rhythmic alteration (a rhythmical alternating bed of black shales and sandstones, thin bed of hematite contained); 42.55-10.0m: pelite (black shale, massive).

#### KT4BS (310-36m)

310.0-301.3m: pelite (black shale, massive); 301.3-276.0m: massive sulfide (compact); 276.0-274.0m: pelite (black shale, lamina developed); 274.0-272.0m: massive sulfide (compact); 272.0-270.0m: pelite (black shale, massive); 270.0-267.0m: massive sulfide (compact); 267.0-263.0m: pelite (black shale, massive); 263.0-256.0m: massive sulfide (compact); 256.0-249.0m: rhythmic alteration (a rhythmical alternating bed of sandstone and black shale, lamina developed); 249.0-246.6m: massive sulfide (compact, mudstone thin bed interbedded); 246.6-234.0m: rhythmic alternation (a rhythmical alternating bed of sandstone and black shale); 234.0-231.0m: massive sulfide (mudstone thin bed interbedded); 231.0-224.0m: rhythmic alternation (an alternating bed of black shales and quartzites included); 224.0-218.0m: basic pyroclastic rock (tuffaceous); 228.0-100.0m: pelite (black shale, massive); 100.0-78.0m: limestone (black, massive); 78-59m: no core; 59.0-36.0m: rhythmic alternation (a rhythmical alternating bed of black shales and sandstones)

#### - KT3BS (70-0.7m)

70.0-58.0m: basic pyroclastic rock (tuffaceous); 58.0-55.5m: basic pyroclastic rock (pyroclastite); 55.5-54.6m: massive sulfide (compact, pyroclastic); 54.6-32.0m: rhythmic alternation (a rhythmical alternation of black shales and sandstones, marked folding); 32.0-29.0m: pelite (black shale, massive); 29.0-0.7m: rhythmic alternation (a rhythmical alternating bed of black shales and sandstones)

#### - KT1BS 70-0m)

70.0-46.4m: pelite (black shale, massive, sulfide thin bed included); 46.4-43.4m: massive sulfide (compact, mudstone and rock fragments included); 43.4-33.0m: pelite (black shale, schistose, massive, strong argillation); 33.0-10.0m: rhythmic alternation (a rhythmical alternating bed of black shales and sandstones); 10.0-0m: pelite (black shale, massive, schistose)

#### (2) Ben Slimane District

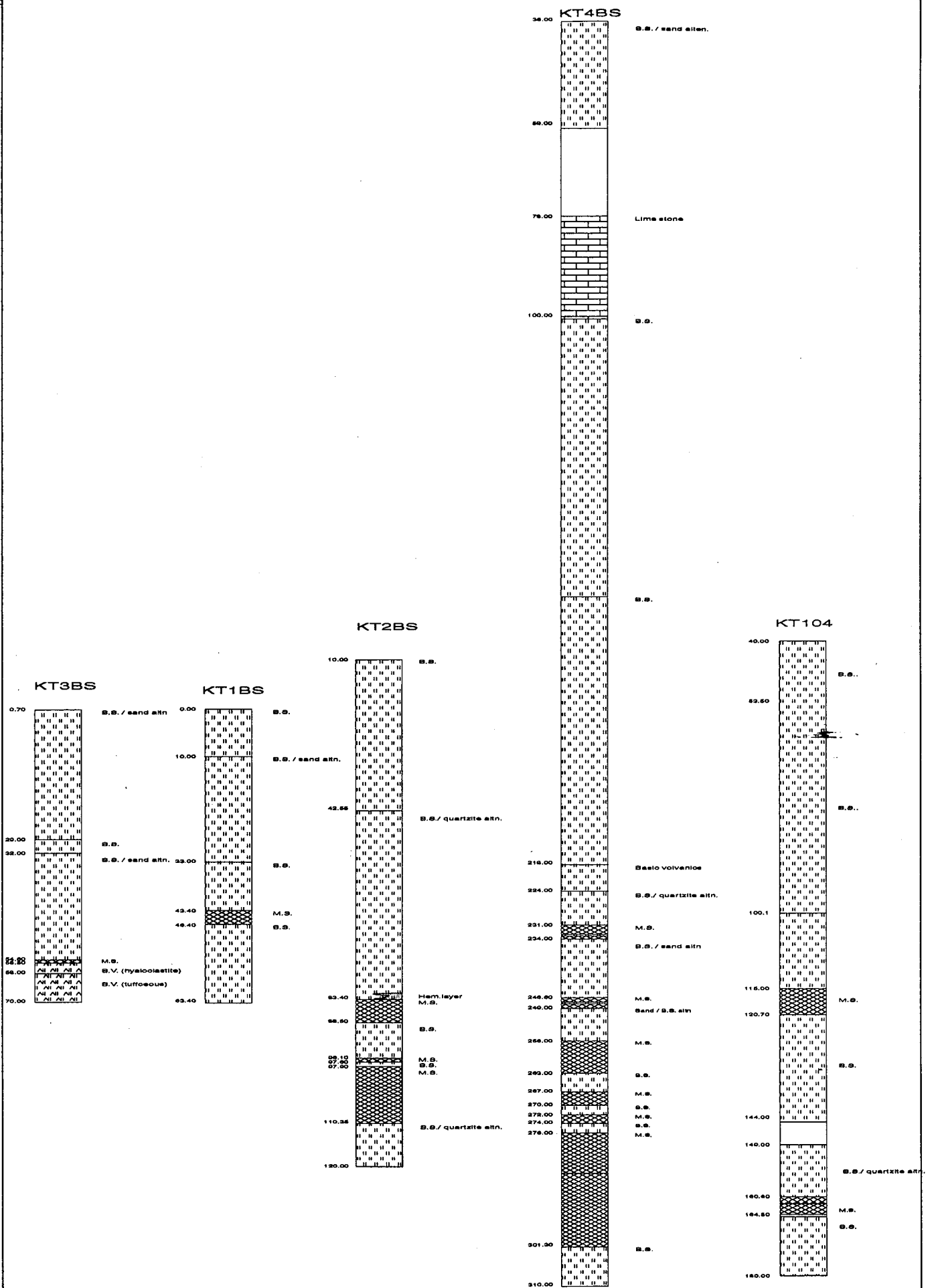


Fig II-3-2-(1) The geological column at Kettara district

The Ben Slimane district consists of an alternating bed of quartzites and pelites in the Sarhlef group, and the granularity of the quartzite becomes smaller in the lower part. In addition, the sulfide ore body is compact and coarse in the upper part and banded and fine-grained in the lower part. Since the Kettara Deposit in the vicinity indicates a graded structure, it is estimated that the stratum of the Ben Slimane is also upside down (Fig.II-3-2-(2)).

- BA15 (337.6-269.8m)

337.6-305.2m: rhythmic alteration (a rhythmical alternating bed of quartzites and pelites, quartzite dominant); 305.2-289.3m: massive sulfide (fracture zone, compact zone, stratose zone, banded, hematite chert included); 289.3-269.8m: pelite (an alternating bed of pelites and sandstones)

(3) K. Aicha District

The geological condition of the K. Aicha area consists of basic volcanic rocks and pelite in the Sarhlef group. The upper pelite indicates the mode of occurrence of turbidite rather than the lower basic volcanic rocks. Re-sedimentary sulfide bed is embedded in pelite (Fig.II-3-2-(3)).

- KA25 (561.0-42.95m)

561.0-528.0m: basic pyroclastic rocks (massive); 528.0-472.0m: basic volcanic rocks (tuffs); 472.0-402.0m: pelite (an alternating bed of pelites and sandstones, sandy sulfide bed interbedded); 402.0-320.0m: pelite (border with pelite in the lower part is a fracture zone, massive, turbidite); 320.0-283.0m: pelite (tuffaceous, fine-grained, chlorite + sericite altered); 283.0-42.95m: basic volcanic rocks (massive, characteristic phenocryst of plagioclase, schistose)

(4) La Chach District

The geological condition of the La Chach district consists of an alternating bed of basic volcanic rocks, and mudstones and sandstones, in the Sarhlef group. In addition, the upper of the sulfide ore body has a siliceous rock group accompanied by thin bedded clay similar to ferruginous quartz (Fig.II-3-2-(4)).

-A9(250-157m)

242.5-221.4m: basic volcanic rocks (massive); 221.9-217.1m: massive sulfide (rubby, marked turbidite); 217.1-191.1m: tuff (strong alternation, pyrite megacryst, moyamoya?? tuffaceous);

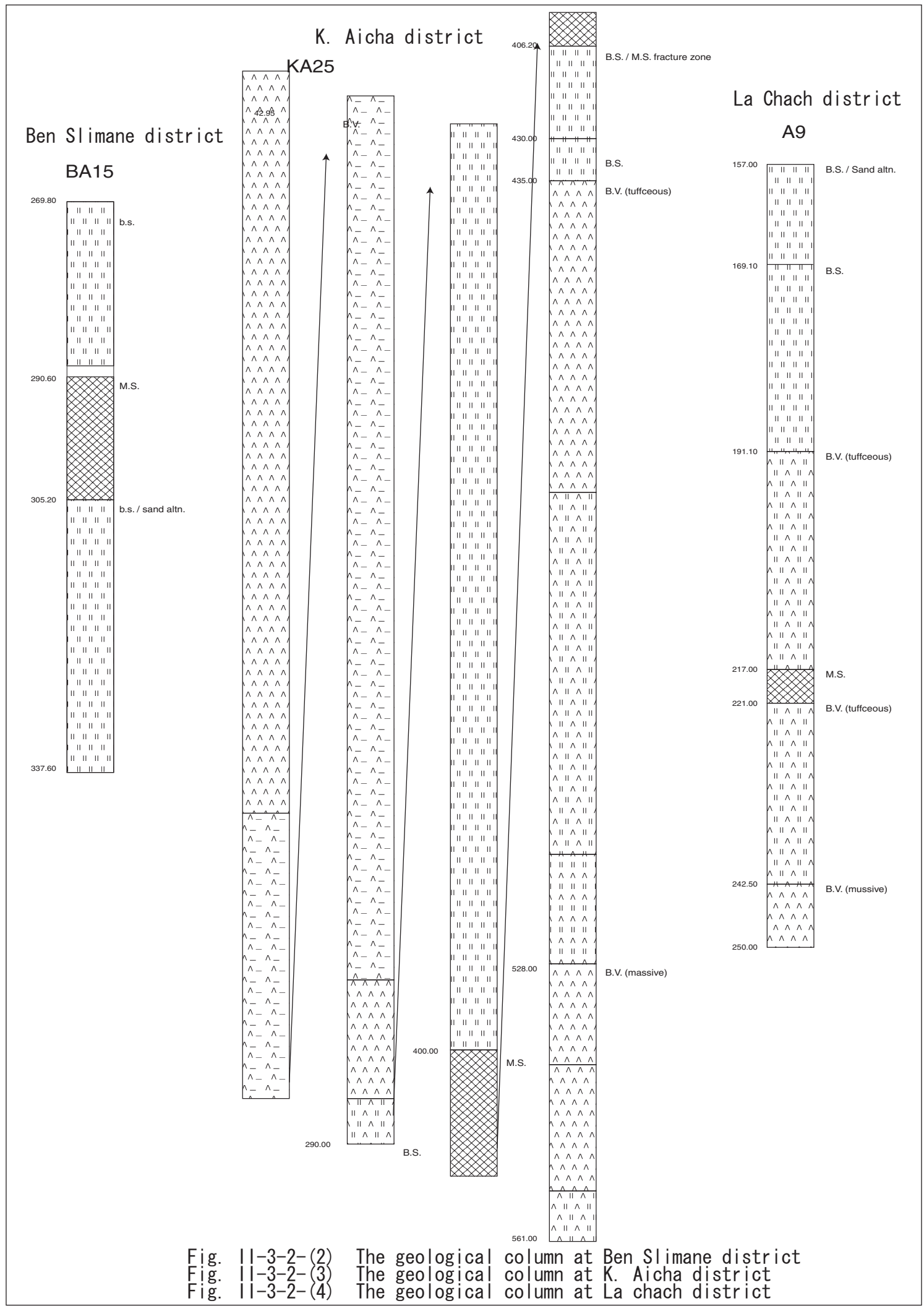


Fig. II-3-2-(2) The geological column at Ben Slimane district  
 Fig. II-3-2-(3) The geological column at K. Aicha district  
 Fig. II-3-2-(4) The geological column at La chach district

191.1-169.1m: pelite (black shale, massive); 196.1-157.1m: rhythmic alteration (an alternating bed of black quartzites and sandstones)

#### (5) Draa Sfar District

The geological condition of the Draa Sfar district consists of basic volcanic rocks, acid volcanic rocks, and rhythmic alteration, in the Sarhlef group. Massive sulfide is embedded in the boundary between basic volcanic rocks and pelite, or in the rhythmic alternating bed of black shales and quartzites) (Fig.II-3-2-(5)).

##### - DSF15 (270-10m)

270.0-253.0m: Basic volcanic rocks (tuffaceous); 253.0-246.0m: massive sulfide (compact); 246.0-244.2m: pelite (black shale, strong alternation); 244.2-241.9m: massive sulfide (compact); 241.9-236.0m: basic volcanic rocks (block lava, non-porphyrific; 240.8-241.9m: hyaloclastite); 236.0-156.15m: rhythmic alteration (an alternating bed of black shales and quartzites); 156.15-108.85m: rhythmic alteration (a rhythmical alternating bed of black shales and quartzites); 108.85-80.0m: pelite (black shale, massive, schistose); 80.0-61.9m: rhythmic alteration (a rhythmical alternating bed of black shales and sandstones); 61.9-54.7m: fracture zone (many tuff fragments); 54.7-10.8m: rhythmic alteration

##### - DSF2 (150-0m)

125.3-122.0m: rhythmic alteration (an alternating bed of fine-grained black shales and quartzites); 122.0-115.1m: massive sulfide (compact, wedge form fragments of pelite (agglomeration), markedly turbiditic); 115.1-98.7m: rhythmic alteration (a rhythmical alternating bed of black shales and quartzites, tuffaceous); 98.7-97.7m: acid volcanic rocks (tuff breccia, homogenous, argillation); 97.7-94.0m: acid volcanic rocks (dacite lava, clinker developed); 94.0-92.4m: acid volcanic rocks (dacite lava, chlorite + sericite altered); 94.2-30.0m: rhythmic alteration (a rhythmical alternating bed of black shales and quartzites, tuffaceous); 30.0-0.0m: basic volcanic rocks (massive, tuffaceous, flat phenocryst of plagioclase)

#### (6) Khwadra District

The geological condition of the Khwadra district consists of pelite, basic volcanic rocks, and rhythmic alteration, in the Sarhlef group. Sulfide ore body is formed in massive or banded state in a rhythmical alternating bed of black shales and sandstones. The upper part of the sulfide ore body has a siliceous rock group accompanied by thin bedded clay similar to ferruginous quartz (Fig.II-3-2-(6)).

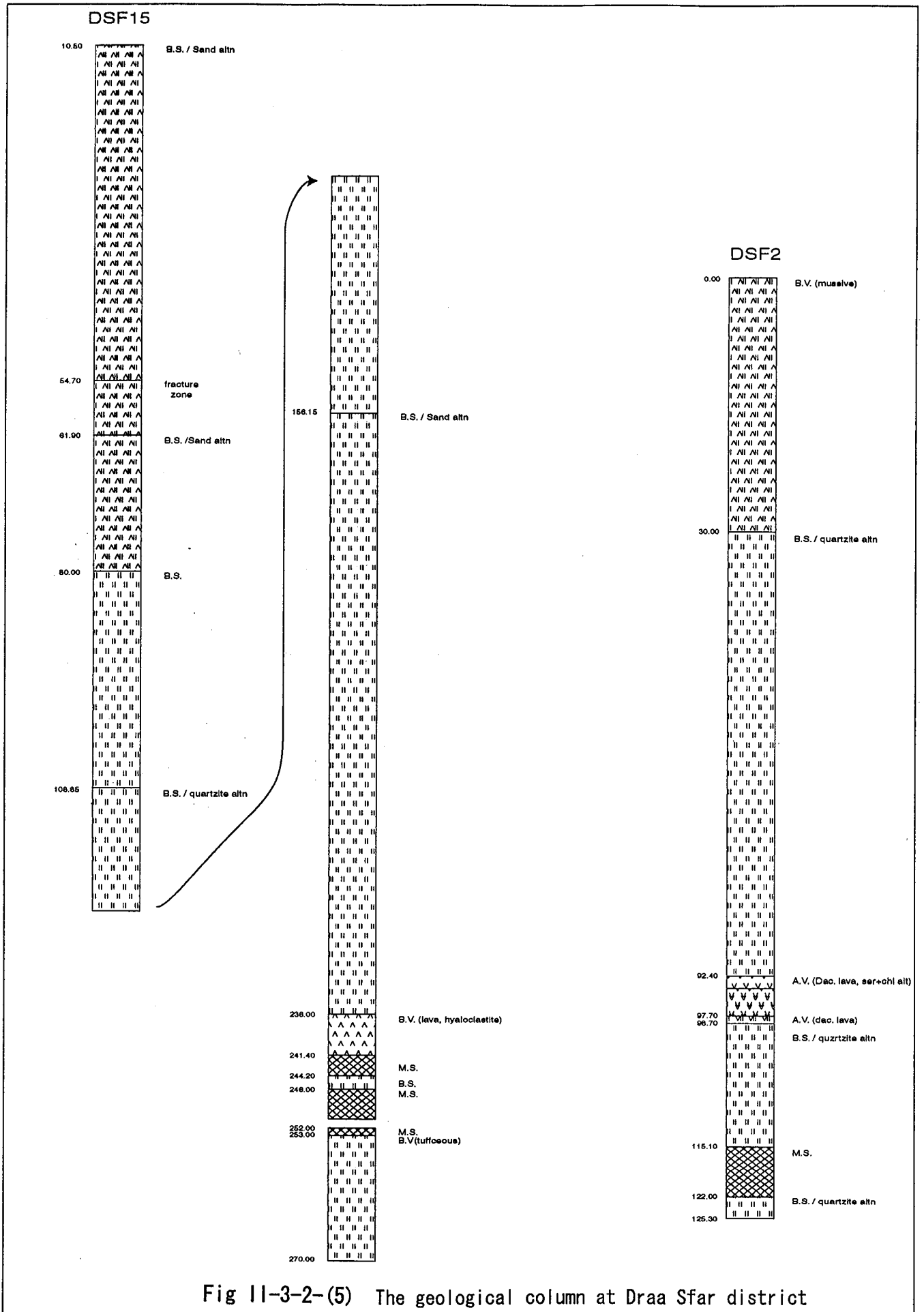


Fig 11-3-2-(5) The geological column at Draa Sfar district

- KH4A (565.6-533.6m)

565.0-563.4m: pelite (black shale, schistose); 563.4-561.3m: massive sulfide (eluviation oxidized zone, hematite dominant); 561.3-542.3m: massive sulfide (compact, fine-grained to coarse); 542.3-541.5m: pelite (black shale, massive, tuffaceous); 541.5-538.4m: massive sulfide (compact, fine-grained to coarse); 538.4-533.6m: pelite (black shale, massive, tuffaceous)

- KWS4C (570.7-514.7m)

570.7-566.35m: basic volcanic rocks (lower part: massive; upper part: massive, sericite alternation); 566.35-563.9m: massive sulfide (compact); 563.9-552.5m: rhythmic alternation (a rhythmical alternating bed of sandstones and black shales); 552.2-529.9m: massive sulfide (compact, fine-grained to coarse, graded structure and de-graded structure); 529.9-518.7m: massive sulfide (thin bedded pelite interbedded); 518.7-514.7m: rhythmic alteration (a rhythmical alternating bed of black shales and sandstones, fluidal structure)

- KWS5C (716.05-621.8m)

716.05-671.7m: rhythmic alternation (a rhythmical alternating bed of sandstones and black shales); 671.7-663.2m: acid volcanic rocks (porphyritic, plagioclase dominant); 663.2-663.0m: thin sulfide bed (hematite zone); 663.0-660.0m: sulfide vein (network, rubbly); 666.0-647.4m: massive sulfide (compact, fluidal structure); 647.4-644.6m: rhythmic alternation (a rhythmical alternating bed of sandstones and black shales); 644.6-642.8m: massive sulfide (compact); 642.8-620.0m: rhythmic alternation (a rhythmical alternating bed of sandstones and black shales)

- KWS3C (404.5-303.2m)

404.5-400.2m: pelite (black shale, massive, sericite alternation); 400.2-381.0m: acid volcanic rocks (block lava); 381.0-373.5m: acid volcanic rocks (fluidal structure, "moyamoya"?-tuffaceous); 373.5-329.9m: acid volcanic rocks (massive lava to hyaloclastite); 329.9-327.5m: massive sulfide (compact, the boundary on acid volcanic rocks in the lower part is a fracture zone or fault); 327.5-303.2m: rhythmic alternation (a rhythmical alternating bed of sandstones and black shales)

- KH1A (420.6-406.2m)

420.6-415.6m: acid volcanic rocks (massive lava to hyaloclastite); 415.6-412.1m: massive sulfide (compact, fluidal structure); 412.1-406.2m: rhythmic alternation (a rhythmical



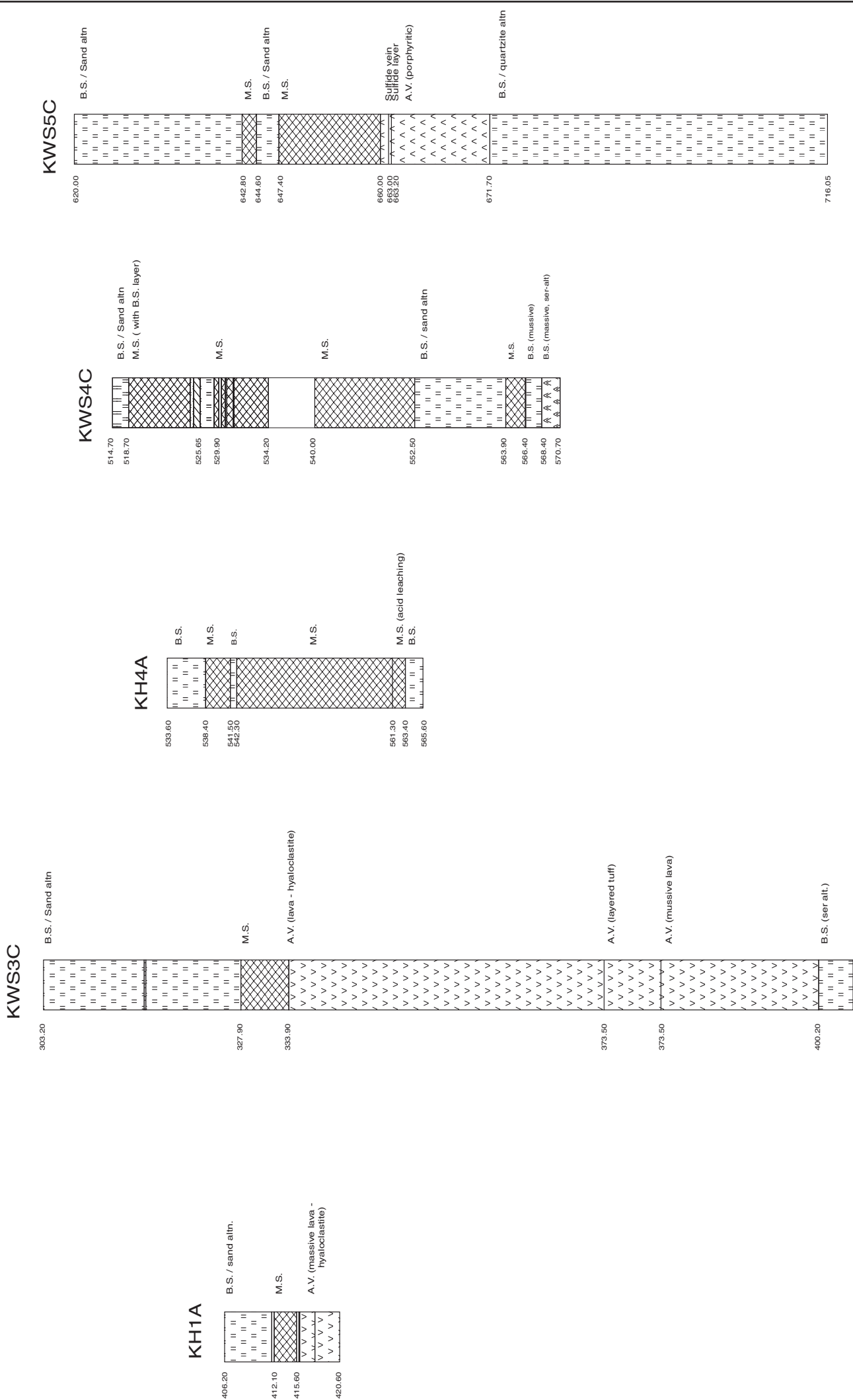


Fig. 11-3-2-(6) The geological column at Khwadra district

alternating bed of black shales and sandstones, coarse to fine-grained)

(7) Saf Safa District

The geological condition of the Saf Safa district consists of basic volcanic rocks, acid volcanic rocks, and pelite, in the Sarhlef district. No mineralization of massive sulfide is observed (Fig.II-3-2-(7)).

-S2 (472.9-197.4m)

472.9-409.7m: basic volcanic rocks (porphyritic, quartz phenocryst); 407.8-388.8m: pelite (black shale, fine-grained); 388.8-366.5m: acid volcanic rocks (dacite lava, quartz phenocryst); 366.5-413.5m: pelite (black shale, massive, sericite alternation); 314.5-197.4m: acid volcanic rocks (porphyritic block lava and non-porphyritic tuff in repetition)

(8) Hajar Area

The geological condition of the Hajar district consists of pelite in the Sarhlef group, basic volcanic rocks, acid volcanic rocks, rhythmic alternation, carbonate rock, and pelite. Sulfide ore body is formed in a rhythmical alternating bed of mudstones and sandstones or quartzites right above the acid volcanic rocks (Fig.II-3-2-(8)).

- CD27 (340.6-0m)

340.6-333.3m: basic volcanic rocks (pelitic); 333.3-296.0m: basic volcanic rocks (tuffaceous); 296.0-161.0m: basic volcanic rocks (massive lava in the base, fluidal structure); 161.0-113.4m: pelite (black shale, fine-grained); 113.4-110.8m: carbonate tuff (limestony, pumice); 110.8-70.4m: acid volcanic rocks (fine-grained tuff -> coarse tuff -> tuff breccia ); 70.4-69.6m: acid volcanic rocks (rhyolite, non-porphyritic); 69.6-67.5m: pelite (black shale, fine-grained); 67.5-60.35m: massive sulfide (disseminated); 60.35-60.3m: pelite (black shale); 60.3-59.1m: massive sulfide (fluidal structure); 59.1-1.0m: pelite (black shale, several thin sulfide bed interbedded); 0.5-0.0m: 10.0-0.0m pelite (black shale)

- GHC1 (64-0m)

65.0-49.0m: acid volcanic rocks (rhyolite, massive, quartz, plagioclase phenocryst); 49.0-39.0m: pelite (sericite alternation); 9.0-32.0m: pelite (silicified); 32.0-22.3m: basic volcanic rocks (block lava to hyaloclastite, fluidal structure); 22.3-19.9m: basic volcanic rocks (tuffaceous); 19.9-13.0m: basic volcanic rocks (block lava (porphyritic) to hyaloclastite); 13.0-10.0m: basic volcanic rocks (tuffaceous); 10.0-0.0m pelite (black shale)

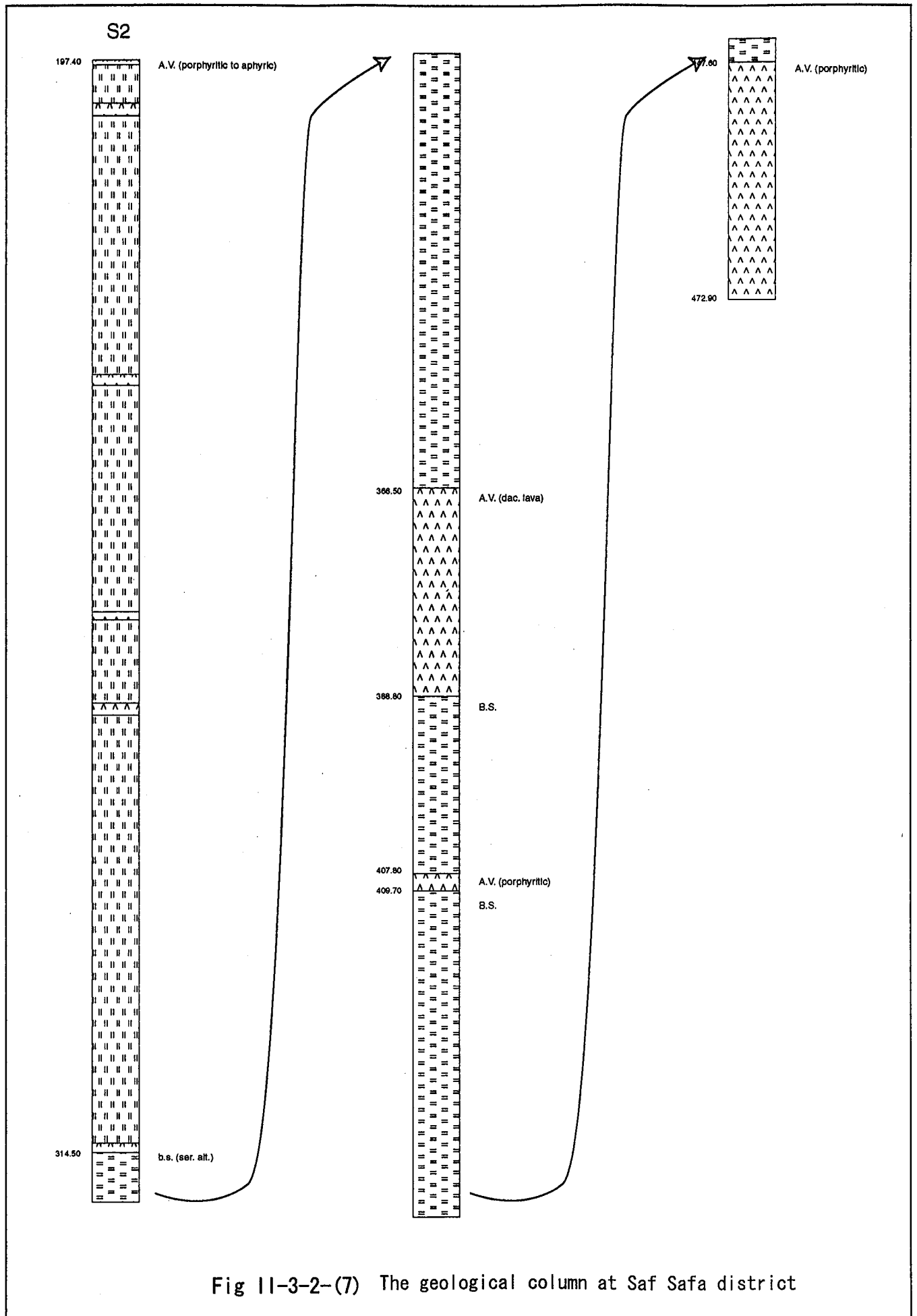


Fig II-3-2-(7) The geological column at Saf Safa district

- HS13 (400.8-200m)

400.8-303.0m: acid volcanic rocks (dacite, massive, porphyritic); 303.0-302.0m: pelite (black shale); 302.0-301.0m: massive sulfide (compact); 301.0-296.0m: pelite (black shale, massive, bedded sulfide); 296.0-250.0m: pelite (black shale); 250.0-207.0: pelite (bedded sulfide layer interbedded); 247.0-226.0m: rhythmic alternation (a rhythmical alternating bed of black shales and quartzites); 226.0-221.0m: basic volcanic rocks (porphyritic); 221.0-200.0m: acid tuffs (rhyolite)

- HS25 (332.0-296.5m)

332.0-327.0m: rhythmic alternation (a rhythmical alternating bed of black shales and quartzites); 327.0-321.6m: acid volcanic rocks (non-porphyritic massive dacite lava, networked quartz vein (1-10cm)); 321.6-321.5m: acid volcanic rocks (tuffaceous); 321.5-321.45m: rhythmic alteration (a rhythmical alternating bed of black shales and quartzites, the border on acid volcanic rocks in the lower part is a fracture district); 321.45-315.0m: massive sulfide (compact, fluidal structure, wedge forme fragments of mudstone included); 315.0-314.4m: pelite (black shale, strong alternation); 314.4-308.0m: massive sulfide (fluidal structure, different sedimentation direction in some parts) 308.0-306.0m: massive sulfide (rubbly); 306.0-304.0m: massive sulfide (sandy, fluidal structure); 304.0-303.5m: acid volcanic rocks (rock fragment due to secondary sedimentation) 303.5-303.4m: massive sulfide (rhyolite, massive); 303.1-301.1m: massive sulfide (fine-grained, tuffaceous); 301.1-290.5m: massive sulfide (sandy, structure where the accumulation of common pyrite is extended)

#### (9) Amzough Area

The geological condition of the Amzough district consists of thick rhythmic alternation sedimented in the Sarhlef group (Fig.II-3-2-(9)).

- AZG480 (410-144.8m)

405.0-401.4m: rhythmic alternation (a rhythmical alternating bed of black shales and quartzites, a sulfide zone is interbedded in quartzite zone); 286.0-281.5m: rhythmic alternation (black shales and quartzites, marked turbidite, quartz veins contain fragments of mudstone); 147.0-144.8m: rhythmic alternation (a rhythmical alternating bed of black shales and quartzites, marked turbidite, accumulation of pyrite is found in parallel with the stratification of quartzite)

#### (10) Frizen Area

The geological condition of the Frizen area consists of pelite in the Sarhlef group, acid volcanic rocks, rhythmic alternation, and pelite. Sulfide ore body is embedded in a rhythmical

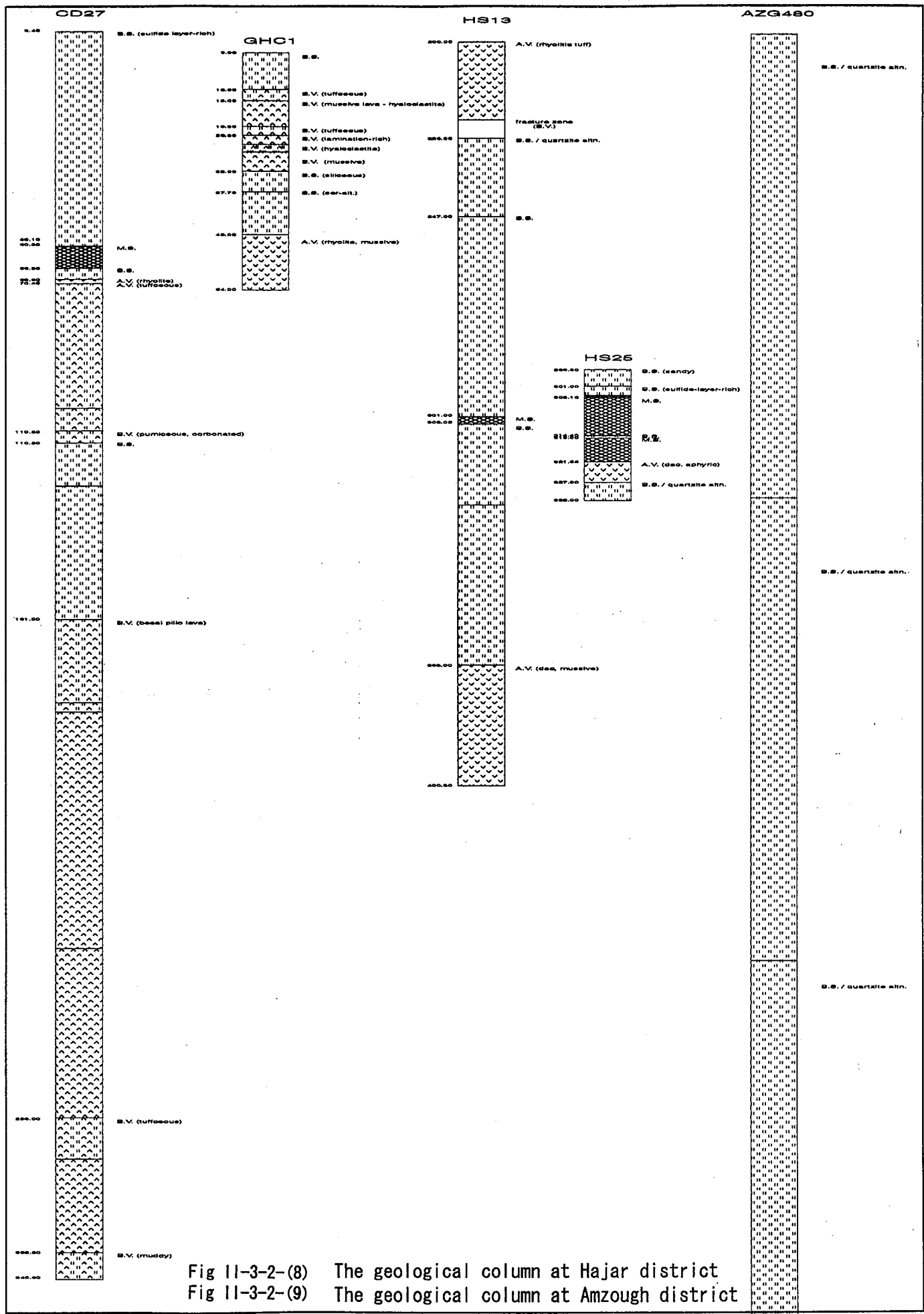


Fig II-3-2-(8) The geological column at Hajar district  
 Fig II-3-2-(9) The geological column at Amzough district

alternating bed of pelites and sandstones or quartzites just above acid volcanic rocks. The geological condition of the FZ13 core, FZ12 core, FZ10 core, FZ03 core, FZ02 core, and FZ14 core is estimated to be upside down because the acid volcanic rocks are distributed in the upper part (Fig.II-3-2-(10)).

- FZ13 (150-30.25m)

150.0-140.55m: pelite (black shale, massive); 144.55-135.0m: massive sulfide (fluidal structure -> compact); 135.6-126.0m: rhythmic alteration (a rhythmical alternating bed of black shales and quartzites); 126-90m: no core; 90.0-85.7m: acid volcanic rocks (tuffaceous); 85.7-84.0m: acid volcanic rocks (dacite, quartz phenocryst); 84.0-64.2m: acid volcanic rocks (dacitic tuffs, massive, quartz veins); 64.2-60.0m: acid volcanic rocks (block dacite lava, large quartz phenocryst, grading into tuffs in the lower part, quartz veins); 60.0-53.2m: acid volcanic rocks (dacitic tuffs, rare quartz phenocryst, quartz veins); 53.2-44.4m: acid volcanic rocks (block dacite lava, flat quartz phenocryst, quartz veins); 44.4-41.25m: acid volcanic rocks (dacite lava, fluidal structure, rubbly, sulfide veins (sphalerite + galena -> pyrite + chalcopyrite)); 41.25-30.25m: acid volcanic rocks (massive dacite lava, non-porphyrific, heavily silicified, sulfide veins (chlorite -> galena -> chalcopyrite -> quartz))

- FZ12 (80-7.1m)

80.0-70.8m: rhythmic alteration (a rhythmical alternating bed of black shales and quartzites); 70.8-65.3m: massive sulfide (compact, fragments of pelite contained); 65.3-65.0m: pelite (black shale, heavy argillation); 65.0-60.0m: massive sulfide (sandy); 60.0-57.0m: pelite (black shale, massive); 57.0-52.0m: massive sulfide (porous, sericite altered, secondary accumulation of megacryst of chalcopyrite and pyrite, the upper part contacts with dacite); 52.0-7.1m: acid volcanic rocks (dacitic tuff to tuff breccia (homogeneous fragments of rocks dominant))

- FZ10 (100-29.9m)

100.0-84.0m: rhythmic alteration (a rhythmical alternating bed of black shales and quartzites, thin pyrite bed); 84.0-73.0m: rhythmic alteration (a rhythmical alternating bed of black shales and sandstones); 73.0-63.8m: pelite (black shale, massive); 63.8-46.0m: rhythmic alteration (a rhythmical alternating bed of black shales and quartzites, quartz veins); 46.0-36.8m: rhythmic alteration (a rhythmical alternating bed of black shales and quartzites, thin pyrite bed dominant); 36.8-29.9m: pelite (black shale, massive, lamina)

- FZ03 (170-90m)

170.0-87.0m: rhythmic alteration (upper part: a rhythmical alternating bed of black shales and

sandstones; lower part: a rhythmical alternating bed of black shales and quartzites)

- FZ02 (111.7-98m)

111.7-98.0m: rhythmic alteration (upper: a rhythmical alternating bed of black shales and sandstones; lower : a rhythmical alternating bed of black shales and quartzites)

- FZ14 (50-0m)

50.0-29.5m: pelite (black shale); 29.5-24.8m: acid volcanic rocks (tuffaceous); 24.8-0.0m: acid volcanic rocks (rhyolite)

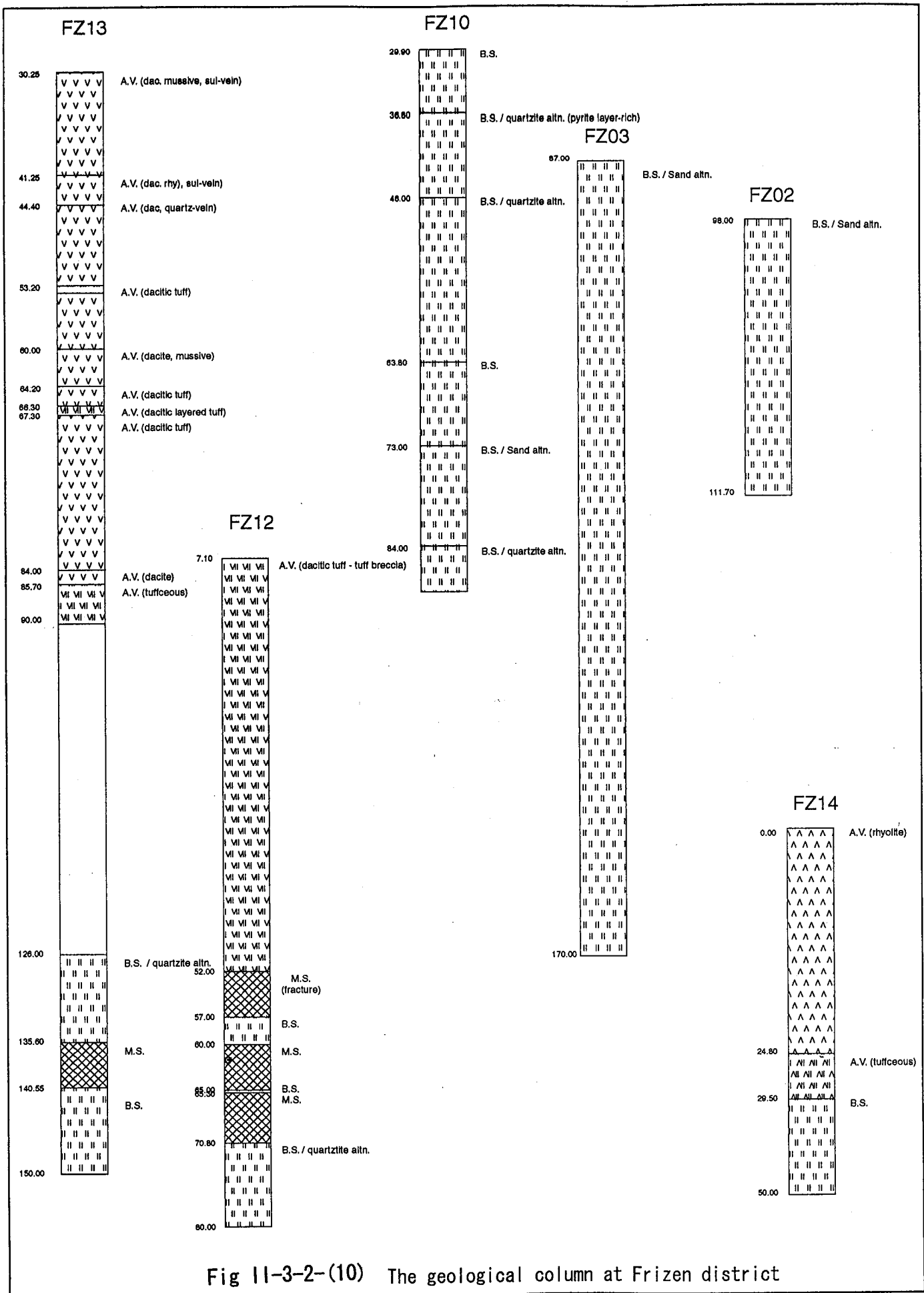


Fig II-3-2-(10) The geological column at Frizen district



## Chapter 4 Laboratory Works

### 4-1 Sulfides ore minerals

#### 4-1-1 Method

Observation of thin section and polished thin section were conducted by Metal Mining Agency of Japan (MMAJ). MMAJ asked Ohdate Analysis Technology Center to make the measurements of fluid inclusions homogenization temperatures and saline concentrations, X-ray diffraction measurements and identifications of ore minerals, Oxygen/hydrogen isotope ratio measurements, Sulfur isotope ratio measurements, were conducted by Ohdate Technology Center. Laboratory work items, samples and their quantity are given in the table below.

Table II-4-1 List of Laboratory works (Sulfide ores)

Test item	Samples	QTY
Thin section	Sulfide ores, volcanic rocks, sedimentary rocks	53
Polished thin section	Sulfide ores, stockwork quartz	130
Fluid inclusion	Stockwork quartz veins	22
X-ray diffraction (metallic minerals)	Sulfide ores, volcanic rocks, sedimentary rocks	154
Oxygen/hydrogen isotope ratio determination	Sulfide ores,	7
Sulfur isotope ratio determination	Sulfide ores	88

#### 4-1-2 Results

##### 4-1-2-1 Results of of the obserbation of thin section and polished thin section

Polished rock thin section appraisals were carried out with volcanic rocks and sedimentary rocks of the drilling core samples and the surface samples in the neiborhood of massive sulfide deposits distributing in this area. The results of the thin section appraisal of representative samples are shown below. All results are shown in the end of this report.

Polished thin section appraisals were conducted on the samples from 5 major massive sulfide deposits (Kettara, Draa Sfar, Khwadra, Hajar and Frizen deposits) distributing in this area. The results of ore mineral appraisals of representative samples from each deposit are shown below. All results are shown in the end of this report.

##### (1) Kettara deposit

Point 87.20m-87.20m of KTBS2 core (02MRN166): Ores at this point are porous. The point is

composed of small quantities of chalcopyrite, magnetite, quartz and clay mineral, and a large quantity of pyrrhotite. Paragenesis of pyrrhotite, magnetite and chalcopyrite is observed. Magnetite shows its own grain state. Chalcopyrite is crystallized solely in quartz.

Point 232.50m-232.60m of KT03 core (02MRN171): This point is composed of a medium quantity of sphalerite, a small quantity of chalcopyrite and a large quantity of pyrrhotite. Pyrrhotite is deformed by a minor fold. There is scattered and spotted distributions of sphalerite and chalcopyrite in the pyrrhotite.

Point 233.25m-233.30m of KT03 core (02MRN174): This point is composed of small quantities of sphalerite and chalcopyrite, medium quantities of pyrite and quartz, a large quantity of pyrrhotite, and minute quantities of marcasite and magnetite. Pyrrhotite is in intergrowth with marcasite. There is a porphyritic morbid state of chalcopyrite spotted in sphalerite. Pyrite has a hexahedral automorphic shape. No zonal structure is found in sphalerite. Quartz has an allotriomorphic shape.

Point 300.00m-300.10m of KT03 core (02MRN178): This point is composed of a medium quantity of chalcopyrite, small quantities of pyrite, marcasite and clay mineral, large quantities of pyrrhotite and quartz and a minute quantity of magnetite. Paragenesis of marcasite and pyrrhotite is observed. Magnetite is fibrously aggregated and crystallized. There is pyrrhotite acicularly drawn out in the host rock's groundmass. Quartz has an allotriomorphic shape and it is slightly folded.

## (2) Draa Sfar deposit

Point 112.50m-112.60m of DSF2 core (02MRN143-2): This point is composed of small quantities of sphalerite and chalcopyrite, marcasite and quartz, a minute quantity of galenite, and a large quantity of pyrrhotite. Paragenesis of marcasite and pyrrhotite is observed. There are banded distributions of the dominant parts of pyrrhotite and sphalerite. The marcasite's twinning is remarkable. Quartz is crushed wedgelike and lenticularly. No zonal structure is found in the sphalerite. Secondary alteration of marcasite is found along the pyrrhotite's fissure and cleavage.

Point 118.50m-118.60m of DSF2 core (02MRN145): This point is composed of the respective medium quantities of sphalerite and galenite, a minute quantity of chalcopyrite, a large quantity of pyrrhotite, and small quantities of marcasite and quartz. Paragenesis of pyrrhotite, galenite, marcasite and sphalerite is observed. Most of these ore minerals, including quartz, are

remarkably crushed and have a wedgelike shape. There is a minor fold structure of quartz grains found at the point. Quartz shows allotriomorphic shape. No zonal structure is found in the sphalerite.

Point 243.60m-243.65m of DSF15 core (02MRN147): This point is composed of small quantities of sphalerite, galenite and pyrite, minute quantities of chalcopyrite and quartz, and a large quantity of pyrrhotite. Paragenesis of pyrrhotite, chalcopyrite, sphalerite, and galenite is observed. Quartz is anhedral and it is crushed wedgelike or aciculately. Pyrite has a hexahedral automorphic shape. No zonal structure is found in the sphalerite.

Point 400mL of Draa Sfar underground (02MRN150): Ores at this point are porous. This point is composed of a medium quantities of sphalerite, small quantities of galenite and quartz, a minute quantity of chalcopyrite, and a large quantity of pyrrhotite. There are the dominant parts of pyrrhotite and sphalerite. There are the row distributions of sphalerite and allotriomorphic quartz at the pyrrhotite's and sphalerite's dominant parts respectively. This seems to show resedimentary environment. No zonal structure is found in the sphalerite.

### (3) Khwadra ore deposit

Point 559.60m-559.65m of KH4A core (02MRN015): Ores at this point are porous. It is composed of small quantities of sphalerite, chalcopyrite and quartz and a large quantity of automorphic pyrite. No zonal structure is found in the sphalerite. Parageneses of sphalerite and galenite, and chalcopyrite and pyrite are observed. Some of the chalcopyrite are crystallized solely in the quartz. The pyrites have the hexahedral automorphic aggregate, but a part of them are crushed, showing brecciated and wedgelike shapes.

Point 558.90m-559.00m of KH4A core (02MRN016): This point is composed of a small quantity of sphalerite, minute quantities of galenite and quartz, a medium quantity of chalcopyrite, and large quantities of pyrite and pyrrhotite. The pyrite shows its own hexahedral automorphic shape. Parageneses of chalcopyrite and pyrrhotite, and sphalerite and galenite are observed. The cleavage face of pyrrhotite shows its fixed direction. Quartz, which is crushed wedgelike, fills up among the ore minerals. The pyrite is crushed along its cleavage and indicates states of brecciation to irregularity. No zonal structure is found in the sphalerite. Ores' banded structure differently seen in color by the naked eye is due to the difference of the pyrite's quantity ratios.

Point 642.90m-643.00m of KHS5C core (02MRN043): This point is composed of minute

quantities of sphalerite, galenite, marcasite and clay mineral, small quantities of chalcopyrite and quartz, and a large quantity of pyrrhotite. Parageneses of marcasite and pyrrhotite, chalcopyrite and pyrrhotite, and sphalerite and galenite are observed. The pyrrhotite is crystallized solely in the quartz. Some of the pyrrhotite shows the pyrite's skeleton crystal. Quartz is packed lenticularly among ore minerals.

Point 334.70m-334.80m of KHS3 core(02MRN060): This point is composed of small quantities of chalcopyrite and clay mineral, and medium quantities of pyrrhotite and quartz. The chalcopyrite is crystallized solely in the quartz. The fine veins of chalcopyrite are found in the pyrrhotite. Quartz is allotriomorphic and has a sutural structure. The point is accompanied with clay minerals.

Point 332.30m-332.40m of KHS3 core (02MRN065): This point is composed of small quantities of sphalerite, chalcopyrite and clay mineral, a medium quantity of pyrrhotite, and a large quantity of quartz. Paragenesis of chalcopyrite, pyrite and pyrrhotite is observed. Chalcopyrite and pyrrhotite are predominant at the central and marginal part, respectively. A linear alteration sign of chalcopyrite is found in the sphalerite, but there is no zonal structure in it. The pyrrhotite is compact. Quartz is automorphic with a sutural structure. Anorthosite has altered to sericite through argillation.

Point 561.90m-561.95m of KH4A core (02MRN014): This point is composed small quantities of sphalerite, chalcopyrite, pyrite, carbonate mineral and lamella marcasite, a large quantity of pyrrhotite, and a minute quantity of quartz. The pyrite's hexahedral automorphic shape in its fine-grained state is crushed and showed rhombohedral and irregular shape. Paragenesis of pyrrhotite is observed around the sphalerite. No zonal structure is found in the sphalerite. The marcasite makes exfoliating composite lamella on both sides along the quartz-carbonate mineral vein crossing, the pyrrhotite's crack, mineral grains' interfaces and the pyrrhotite. The fine-grained marcasite sometimes forms a bird's-eye or agate-like tissue. In marcasication marcasite-like minerals' fine foliated small grains develop in parallel with pyrrhotites' crystallographic orientation. Also, there are many cases that an infinite number of fine crystals exist between the marcasite's exfoliation lamella and the pyrrhotite.

Point 644.30m-644.40m of KHS5C core (02MRN047) : This point is composed of the respective medium quantities of sphalerite and quartz, small quantities of galenite, chalcopyrite, automorphic marcasite and lamella marcasite, and large quantities of pyrite and pyrrhotite. Paragenesis of pyrrhotite, sphalerite and galenite is observed. There is a slight alteration sign

of the chalcopyrite in the sphalerite. Pyrite is hexahedral and automorphic and is brecciated. Automorphic marcasite is found. Quartz has an allotriomorphic shape. The marcasite makes its own exfoliating composite lamella on both sides along the pyrrhotite's crack, mineral grains' interfaces and the quartz-carbonate mineral fine vein crossing the pyrrhotite. The fine-grained marcasite sometimes forms a bird's-eye or agate-like tissue. In marcasication marcasite-like minerals' fine foliated small grains develop in parallel with pyrrhotites' crystallographic orientation. Also, there are many cases that a great many fine crystals exist between the marcasite's exfoliation lamella and the pyrrhotite.

#### (4) Hajar deposit

Point 218.15m-218.20m of A9 core (02MRN087): This point is composed of small quantities of sphalerite and chalcopyrite, a large quantity of pyrite, and minute quantities of marcasite and quartz. Parageneses of marcasite and pyrrhotite, and chalcopyrite and pyrrhotite are observed. The pyrite has a hexahedral, automorphic shape, and it is remarkably crushed in various shapes of breccia to subbreccia along its cleavage. There is a slight alteration sign of the chalcopyrite in the sphalerite.

Point 59.80m-59.85m of CD27 core (02MRN095): Ores at this point are porous. The point is composed of medium quantities of sphalerite, galenite and pyrrhotite and a minute quantity of chalcopyrite. Parageneses of chalcopyrite and pyrrhotite, and chalcopyrite and galenite are observed. Quartz is allotriomorphic. No zonal structure is found in the sphalerite.

Point 314.30m-314.40m of HS25 core (02MRN106): This point is composed of large quantities of sphalerite and pyrrhotite and small quantities of galenite, chalcopyrite, pyrite, quartz and lamella marcasite. The pyrite has a hexahedral, automorphic shape and it is crushed irregularly. The galenite is allotriomorphic. There is no class resistance increase found in the sphalerite. The marcasite makes its own exfoliating composite lamella on both sides along the pyrrhotite's crack, mineral grains' interfaces and the quartz-carbonate mineral fine vein crossing the pyrrhotite. The fine-grained marcasite sometimes forms its bird's-eye or agate-like tissue. In marcasication marcasite-like minerals' fine foliated small grains develop in parallel with pyrrhotites' crystallographic orientation. Also, there are many cases that a great many fine crystals exist between the marcasite's exfoliation lamella and the pyrrhotite.

Point 317.00m-317.10m of HS25 core (02MRN107): This point is composed of large quantities of sphalerite and pyrrhotite, medium quantities of galenite and pyrite, and a small quantity of chalcopyrite. Paragenesis of allotriomorphic sphalerite is observed in the

pyrrhotite. The extremely fine-grained, circular marcasite exists in paragenesis with the pyrrhotite. There is a possibility of the marcasite's secondary alteration along its cleavage because there are many parageneses inside the cleavage. No zonal structure is found in the sphalerite.

Point 530mL of Hajar underground (02MRN098): This point is composed of a minute quantity of sphalerite, small quantities of chalcopyrite and pyrite, a medium quantity of pyrrhotite and a large quantity of quartz. Quartz is predominant in its host rock's groundmass. The pyrite and pyrrhotite are drawn out acicularly in the host rock's pelite. Paragenesis of chalcopyrite, pyrrhotite and pyrite is observed. The pyrite has a automorphic hexahedral or colofrom shape.

Point 380mL of Hajar underground (02MRN099): This point is composed of a little quantity of chalcopyrite and large quantities of pyrite, pyrrhotite and quartz. The chalcopyrite is crystallized solely in the quartz. Paragenesis of pyrite and chalcopyrite is observed. Quartz has a xenophormic shape.

#### (5) Frizen ore deposit

Point 43.40m-43.50m of FZ13 core (02MRN124): Ores at this point are veinlike. The point is composed of large quantities of sphalerite and chalcopyrite, small quantities of galenite, pyrite, pyrrhotite and marcasite and a medium quantity of quartz. Parageneses of pyrite, pyrrhotite and chalcopyrite, pyrrhotite and sphalerite, and marcasite in the chalcopyrite are observed. The allotriomorphic chalcopyrite is crushed. No zonal structure is found in the sphalerite. Quartz is automorphic and it is equally grained.

Point 50.00m-50.10m of FZ13 core (02MRN127): Ores at this point are veinlike. The point is composed of the respective medium quantities of sphalerite, pyrrhotite and quartz, minute quantities of galenite and chalcopyrite and a large quantity of pyrite. The pyrite, which is automorphic and hexahedral, is crushed along its cleavage and the quartz is packed in it. Paragenesis of chalcopyrite and pyrrhotite is observed. There is the banded and rowlike distributions of sulfide ores in the quartz vein. No zonal structure is found in the sphalerite. Quartz has a allotriomorphic shape.

Point 64.80m-64.90m of FR12 core (02MRN133): This point is composed of large quantities of sphalerite and pyrite, a minute quantity of galenite, a small quantity of chalcopyrite, and a medium quantity of quartz. Parageneses of chalcopyrite and pyrite, and pyrite in sphalerite are observed. Pyrite has a hexahedral and automorphic shape, and parts of it are fine-grained.

Quartz has a allotriomorphic shape. There is the spotted and linear morbid parts of chalcopyrite found in sphalerite. No zonal structure is found in the sphalerite.

Point 70.00m-70.20m of FR12 core (02MRN135): This point is composed of a small quantity of sphalerite, minute quantities of galenite and chalcopyrite, a large quantity of pyrite and a medium quantity of quartz. Paragenesis of galenite, chalcopyrite, sphalerite and pyrite is observed. Many fine-grained, automorphic hexahedrons of the pyrite aggregate in the quartz. Quartz is allotriomorphic and has a phenocrystic aggregate sutural structure. No zonal structure is found in the sphalerite.

Point 70.00m-70.20m of FZ13 core (02MRN138): This point is composed of minute quantities of sphalerite, galenite, and chalcopyrite, a small quantity of pyrite, a medium quantity of pyrrhotite, and a large quantity of quartz. Paragenesis of chalcopyrite and pyrrhotite is observed. Not only pyrrhotite but also pyrite are aciculately drawn out in quartz. Quartz shows its own allotriomorphic shape, but it is crushed and deformed aciculately and wedgelike. Quartz which is the host rock's groundmass is composed of an aggregate of cristobarite and is slightly folded.

#### 4-1-2-2 Fluid inclusions

In order to infer the temperature of ore deposit formation, we made measurements of the homogenization temperatures and NaCl equivalent saline concentrations of fluid intrusions in the quartz, using its veins sampled from their drilling core and surfaces. As for their temperatures and concentrations 21 samples were used to measure the homogenization temperatures and NaCl equivalent saline concentrations. The histogram of the measurements results is shown in Table II-4-1-1 and Fig. II-4-1-1.

##### <Hajar ore deposit>

As for the homogenization temperatures of fluid intrusions, there is no tendency of systematic variations between the temperatures and their distribution. There are generally three types; the first type has a homogenization temperature of 150-200°C, 200-250 °C, and 250-300 °C. There is no tendency in their NaCL equivalent concentrations corresponding to temperature ranges, but the concentrations are generally high and most of them show approximately 8%-13%.

##### <Frizen deposit>

As for the homogenization temperatures of fluid intrusions, there is no tendency of systematic variations between the temperatures and their distribution. There are generally two types; the

Table II-4-1-1 List of key statistics of homogenization temperature and salinity of quartz

Number	Sample	Mineral	Homogenization Temperature					NaCl wt. % eq.				
			Pieces	Maximum	Minimum	Average	Standard deviation	Pieces	Maximum	Minimum	Average	Standard deviation
1	02MRN 096	Quartz	20	253	184	224.7	17.5	17	13.4	9.0	10.57	0.29
2	02MRN 097	Quartz	20	303	213	263.4	24.8	13	10.9	6.6	9.36	0.34
3	02MRN 099	Quartz	13	267	216	243.0	12.6	8	10.7	7.3	9.48	0.41
4	02MRN 103	Quartz	20	172	123	143.2	12.6	15	8.7	6.9	7.81	0.13
5	02MRN 108	Quartz	20	275	202	238.3	17.1	15	6.9	2.4	5.66	0.33
6	02MRN 110	Quartz	20	247	181	213.8	20.2	17	19.1	17.3	17.90	0.10
7	02MRN 111	Quartz	20	293	216	255.0	18.9	17	10.5	7.3	8.54	0.23
8	02MRN 112	Quartz	20	188	138	157.3	13.6	15	19.6	17.7	18.97	0.13
9	02MRN 113	Quartz	20	231	185	201.3	12.8	17	6.0	3.4	4.94	0.23
10	02MRN 123	Quartz	20	281	214	253.1	20.9	15	6.7	4.0	5.75	0.21
11	02MRN 124	Quartz	20	295	232	260.2	14.4	16	8.7	5.9	6.90	0.19
12	02MRN 130	Quartz	20	283	237	261.5	13.6	16	9.5	5.9	7.33	0.25
13	02MRN 139	Quartz	20	246	193	216.1	12.5	17	13.5	11.1	12.19	0.16
14	02MRN 142-2	Quartz	20	212	143	181.7	19.2	18	14.7	11.9	13.26	0.18
15	02MRN 148	Quartz	20	214	134	177.9	20.7	15	15.1	11.5	13.19	0.27
16	02MRN 149	Quartz	20	311	259	283.6	13.6	16	13.2	7.6	9.28	0.35
17	02MRN 151	Quartz	20	263	199	234.6	18.2	17	11.1	9.0	10.22	0.16
18	02MRN 157	Quartz	20	313	263	290.9	15.3	12	11.9	7.7	9.54	0.38
19	02MRN 158	Quartz	20	262	183	225.9	20.9	14	6.7	1.2	2.47	0.45
20	02MRN 170	Quartz	20	279	213	249.1	16.8	14	10.9	0.2	3.57	0.98
21	02MRN 175	Quartz	20	253	195	229.2	14.4	16	14.5	11.5	13.46	0.19



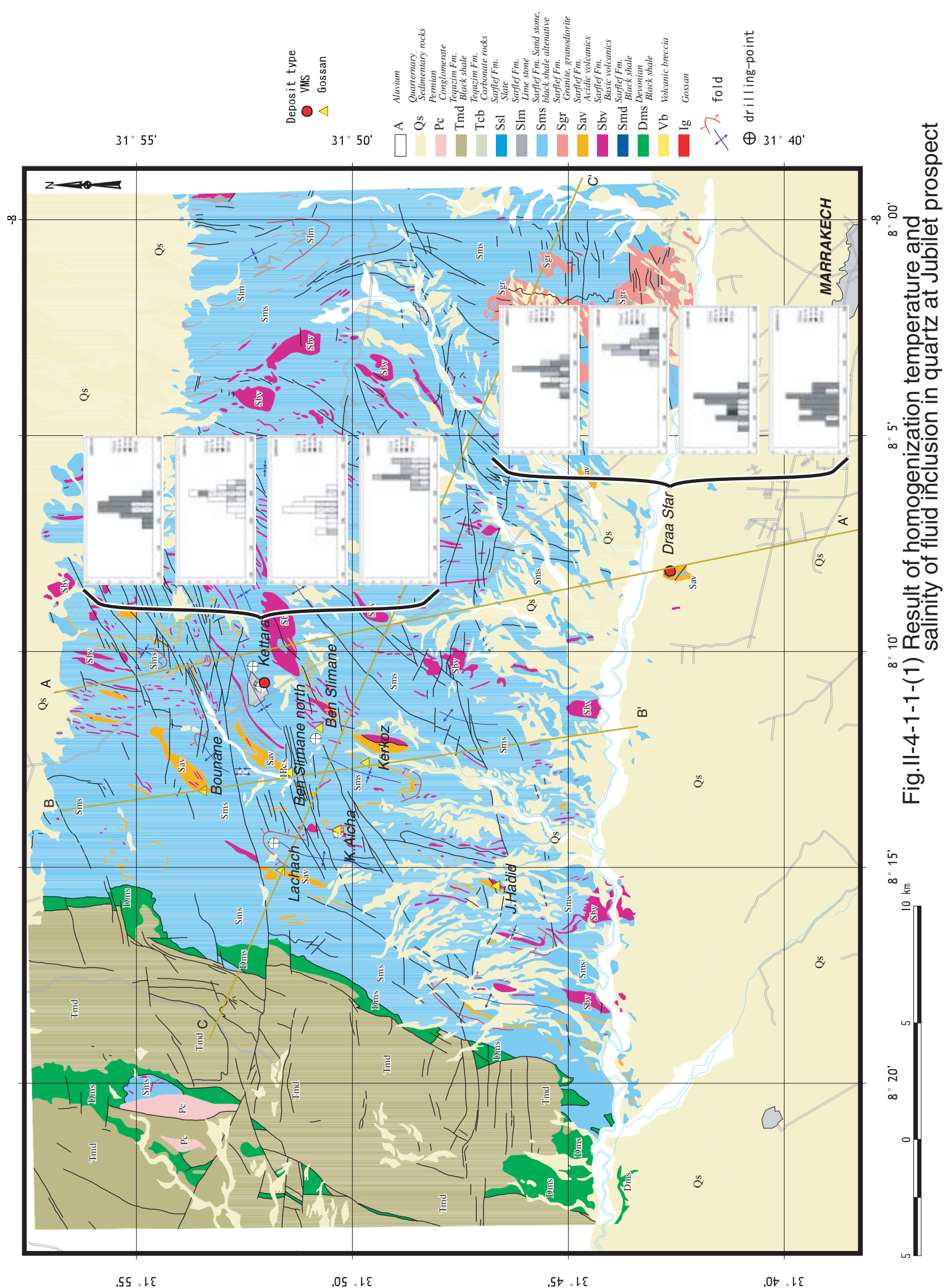


Fig.II-4-1-1-(1) Result of homogenization temperature and salinity of fluid inclusion in quartz at Jubilet prospect

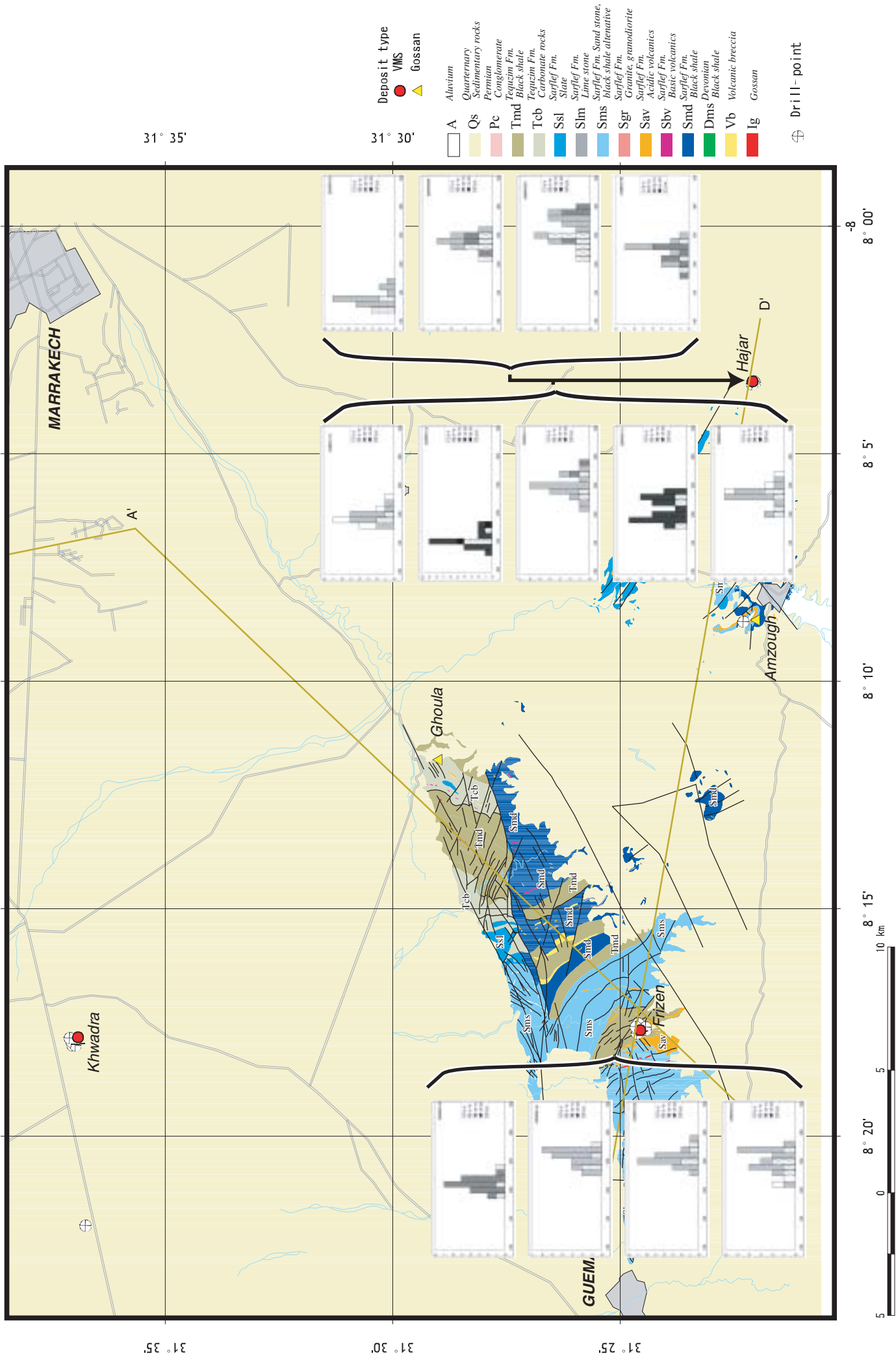


Fig. 11-4-1-1-(2) Result of homogenization temperature and salinity of fluid inclusion in quartz at Guemassa prospect

first type has a homogenization temperature of 190-240°C, and 230-280°C. Also, there is no tendency in their NaCl equivalent concentrations corresponding to temperature ranges, but the concentrations are generally high and most of them show approximately 4%-9%.

<Draa Sfar deposit>

As for the homogenization temperatures of fluid intrusions, there is no tendency of systematic variations between the temperatures and their distribution. There are generally three types; the first type has a homogenization temperature of 140-200°C, the second one 200-250°C, and the third one 250-310°C. Also, there is no tendency in their NaCl equivalent concentrations corresponding to temperature ranges, but the concentrations are generally high and most of them show approximately 7%-13%.

<Kettara deposit>

As for the homogenization temperatures of fluid intrusions, there is no tendency of systematic variations between the temperatures and their distribution. There are generally two types; the first type has a homogenization temperature of 200-250°C, and the second one 250-300°C. Also, there is no tendency in their NaCl equivalent concentrations corresponding to temperature ranges, but the concentrations are in a wide range of their low and high values, and most of them show approximately 0%-13%.

#### 4-1-2-3 Sulfur isotope ratio measurements

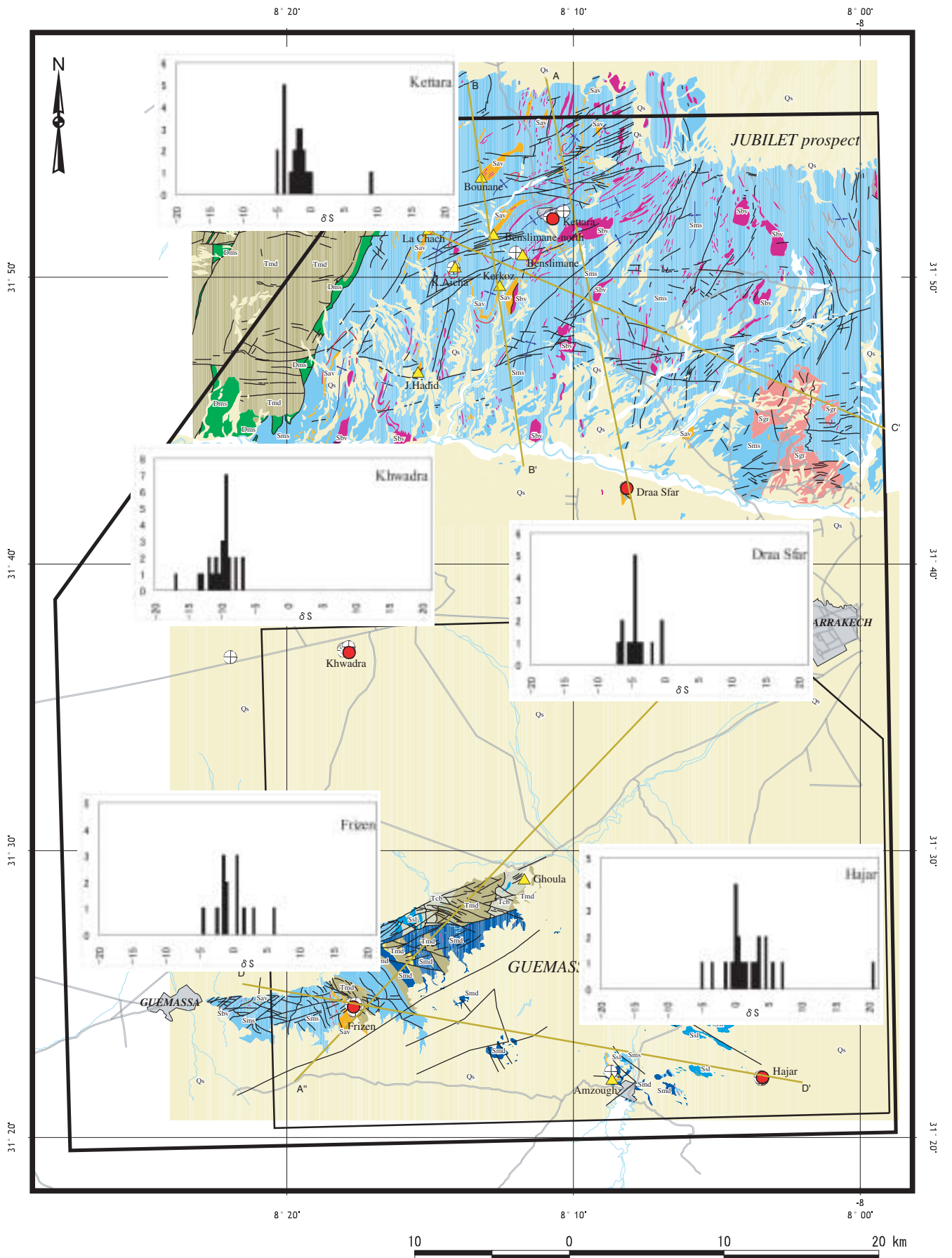
In order to infer the environment of ore deposit formations, we carried out sulfur isotope ratio measurements using sulfide ores sampled from the drilling cores and the surfaces. 88 samples were used for the measurements. The histogram of their results is shown in Fig..II-4-1-2.

<Khwadra deposit>

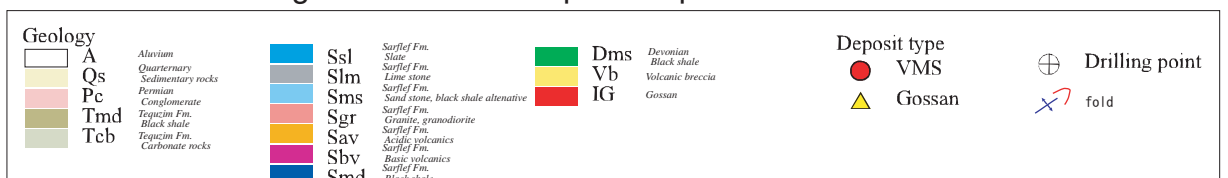
As for the sulfur isotope ratios, there is no tendency of systematic variations between the ratios and the distribution. It showed generally the normal distribution. And the ratios indicate the average of -9.9‰, mode of -9.3‰, standard deviation of 2.16, variance of 4.67 and the minimum value of -16.8‰, as their basic statistics.

<Draa Sfar deposit>

As for the sulfur isotope ratios, there is no tendency of systematic variations between the ratios and the distribution. It showed generally the normal distribution. And the ratios indicate the average of -4.0‰, mode of -4.1‰, standard deviation of 1.96 and variance of 3.83, as their



Fi. II-4-1-2 Histogram of sulfur isotope of deposits at Marrakech-Tekna area



basic statistics

<Kettara deposit>

As for the sulfur isotope ratios, there is no tendency of systematic variations between the ratios and the distribution. It showed generally the normal distribution in case of which the ratios are biased toward lighter values. The ratios indicate the average of -1.7‰, mode of -3.8‰, standard deviation of 2.92, and variance of 8.53, as their basic statistics.

<Hajar deposit>

As for the sulfur isotope ratios, there is no tendency of systematic variations between the ratios and the distribution. It showed generally the normal, but slightly wide, distribution. The ratios indicate the average of +2.5‰, mode of +0.3‰, standard deviation of 5.08, variance of 25.8, and the max. value of +20.8‰, as their basic statistics.

<Frizen deposit>

As for the sulfur isotope ratios, there is no tendency of systematic variations between the ratios and the distribution. It showed generally the wide, normal distribution. The ratios indicate the average of +0.2‰, mode of -0.5‰, standard deviation of 2.63, and variance of 6.95, as their basic statistics.

Making a comparison of these ore deposits from a broad view, the sulfur isotope ratios become lighter in the order of Khwadra, Draa Sfar, Kettara, Hajar and Frizen deposits.

#### 4-1-2-4 X-ray diffraction (metallic minerals)

In order to infer the environment of ore deposit formations, metallic minerals' x-ray diffraction analysis, using sulfide ores sampled from the drilling cores and the surfaces was carried out. 15 samples were used for the x-ray diffraction analysis.

As the lattice constants of hexahedral pyrrhotite vary successively according to its chemical composition, the composition can be found by calculation, using the diagram of a correlation between its chemical composition (102) and a lattice face distance given by Arnord (in 1962) or its empirical formulas. The crystal system of pyrrhotite can be discerned by a powder method. In the hexahedral pyrrhotite, the crystal system can be distinguished as one line which is sharp in its peak on the powder diffraction image (102), on the other hand, in the monoclinic pyrrhotite it can be displayed as two peaks which are equal in intensity. In case the intensity of a peak on the low angle side is stronger than the other, that means the latter pyrrhotite is mixed with the former pyrrhotite (Bystrom, 1945), so if the diffractometer's

scanning rate and slit system and how to rub or apply samples are adjusted properly, the mixture's weight ratio can be calculated through a relative strength of two peaks separated (Arnold, 1966 and 1969; Graham, 1969). However, you must be careful as to judging the pyrrhotite to be mixed simply because the peaks are splitted on the image, because even a specimen in which troilite and hexahedral pyrrhotite are mixed indicates the same image as the above one in appearance.

## 4-2 Igneous Rocks

### 4-2-1 Method

We collected 42 surface and existing drilling core samples at Jebilet, Haouz and Guemassa and made their petrologic laboratory works. The list of the samples collected is shown in the table in the end of this report. Of the samples, we made the thin section production and appraisal of 35 samples, the X-ray analysis and ore appraisal of 24 samples, the Whole rock chemical composition analysis of 17 samples and the K-Ar radioactive dating of 13 samples. We sent all the samples to Ohdate Analysis Center, Inc. and made their arrangement. Their thin section production, observation, X-ray analysis and ore determination were made at the Center, their whole rock chemical composition analysis at Chemex Laboratory (Canada), using the XRF, ICP and ICP-MS method, and their K-Ar radioactive dating at Secoscience Co., Ltd.

Table II-4-2 List of Laboratory works (Igneous rocks)

Test item	Sample	Quantity
Thin section	Volcanic rocks	35
X-ray analysis	Volcanic rocks	24
Analysis of Trace component	Volcanic rocks	17
Analysis of Main component	Volcanic rocks	17
K-Ar age determination	Volcanic rocks	13

### 4-2-2 Results

In the sample collections we tried as much as possible to collect samples which are not affected by hydrothermal alteration and regional metamorphism, but because all the samples were affected by some alteration or metamorphism, we could not collect samples without any alteration. The alteration indexes of the sample collected were 10 to 70. The results of the thin section observation of the samples, X-ray ore diffraction, whole rock chemical composition analysis and K-Ar radioactive dating are listed in the tables in the end of this report.

#### 4-2-2-1 Whole rock chemical composition

##### (1) Major components

In the examination of the main components of the samples collected we used their recalculated values so that they could reach a 100 percentage point in all except for their ignition loss (LOI) (Table 2). The content of those to SiO<sub>2</sub> are shown in Fig. 1. Moreover, the sample 02MRS21 was judged to be rhyolite through the microscope, but its analysis results showed that it was very poor in SiO<sub>2</sub> (35.98 percent) but rich in iron (38.49 percent). So, we

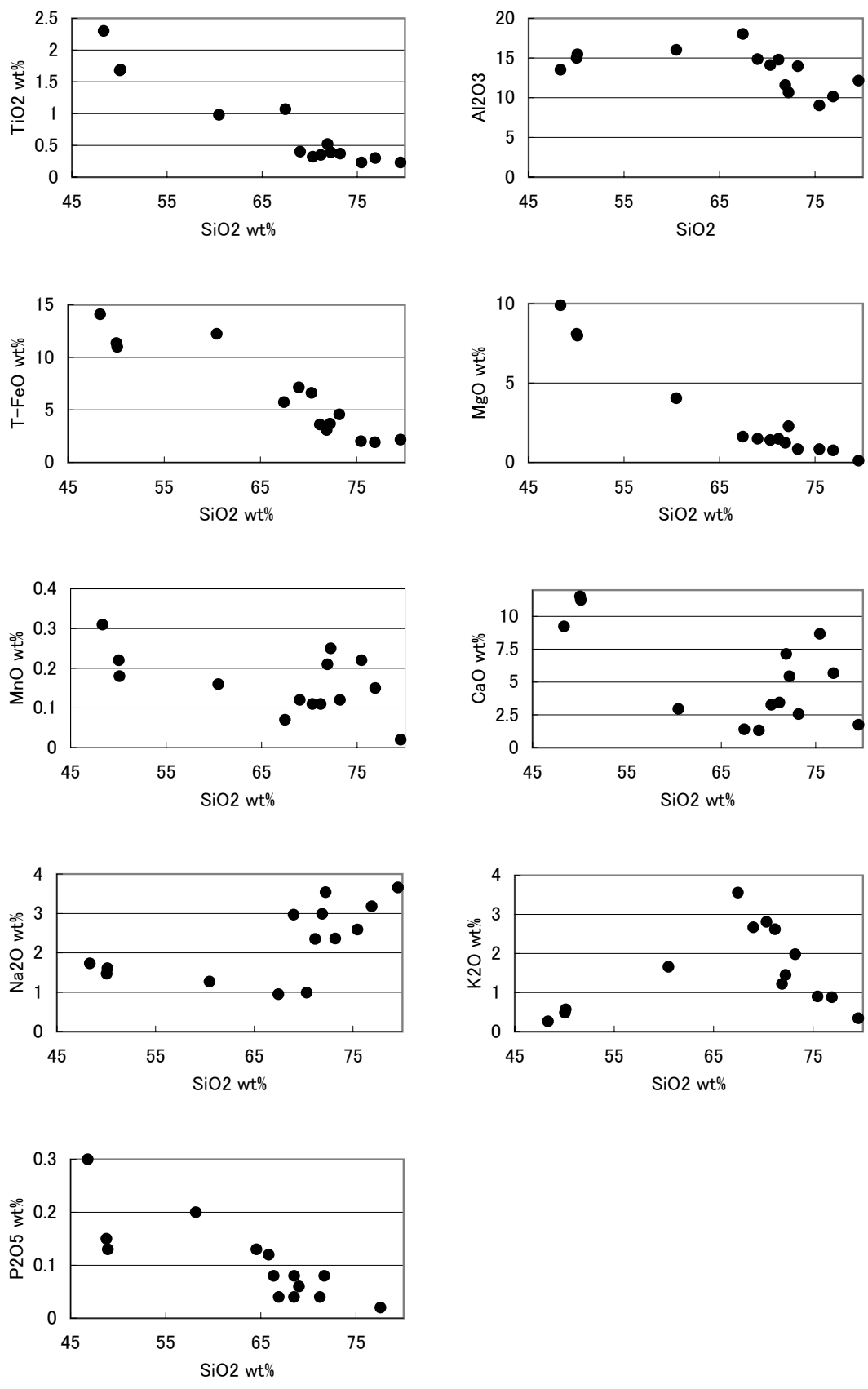


Fig.II-4-2 Plots of major elements against SiO<sub>2</sub> of igneous rocks of Tekna-Marakech area



excluded it from the examination because it did not seemingly reflect its proper composition.

Three basic rock samples (metadolerite) have the respective contents similar to one another in their main components. The content of the main component of the sample 02MRS17 which was an only intermediate composition of the samples analysed recorded a mean value between the values of the basic and acidic rock samples. The sample 02MRS17 could be described as rhyolite through the microscope, but its chemical analysis results showed that it was dacitic andesite.

In 10 igneous rock samples with their acid composition their six elements of  $\text{TiO}_2$ ,  $\text{Al}_2\text{O}_3$ ,  $\text{T-Fe}_2\text{O}_3$ ,  $\text{MgO}$ ,  $\text{K}_2\text{O}$ , and  $\text{P}_2\text{O}_5$  have a correlation with their content of  $\text{SiO}_2$ , but their content of three elements of  $\text{MnO}$ ,  $\text{CaO}$  and  $\text{Na}_2\text{O}$  vary widely and the latter contents have no correlation with their  $\text{SiO}_2$  content. As for the sample igneous rocks, including basic-and intermediate-composition rocks, their content of  $\text{TiO}_2$ ,  $\text{T-Fe}_2\text{O}_3$ ,  $\text{MgO}$  and  $\text{P}_2\text{O}_5$  have the same correlation as in  $\text{SiO}_2$ . In the igneous rocks, including basic-and intermediate-composition rocks, their content of  $\text{K}_2\text{O}$  has a positive correlation with that of  $\text{SiO}_2$  up to 66 percent and a negative correlation with it after the value.

All of the rocks analysed this time can be plotted in the range of low K series (Gill 1981).

Basic-and intermediate-composition igneous rocks can be plotted in the Tertiary range and acid-composition igneous rocks can be plotted in the Calc-Alkaline range in the AFM diagram.

## (2) Trace elements

### 1) Rare earth element (REE)

We drew up a normalization diagram using values obtained through normalizing the REE content of the sample rocks by a primitive mantle's REE content. We used the Hofmann's values (1988) as the mantle's. The values normalized is shown in diagram in Fig.II-4-3.

The REE pattern of the basic rock of the samples is flat, and the 02MRS15, among others, is richer in the REE than two other samples and shows its little Eu anomaly. The REE content of the samples 02MRS13 and 02MRS16 are around ten times that of the primitive mantle composition and similar to their content of N-MORB (Hofmann 1988).

The intermediate-composition rock samples are rich in the light REE and show their Eu anomaly. All the REE patterns of the acid-composition rock samples show patterns rich in the light REE. All the samples have a Eu anomaly. In their comparison with the REE content of the primitive mantle Safsafa's four samples (tonalitic mylonite) are low in their heavy REEs' primitive mantle normalized values, or 8 and less, on the other hand, samples (rhyolite) from Hajar, Khwadra, Drasfaa and Jebilet are high in the values, or 10 to 40. The normalization pattern of sandstone hornfels (02MRS12) is rich in the light REE and flat and has no Eu anomaly and has resemblance to Hofmann's (1988) continental crust pattern.

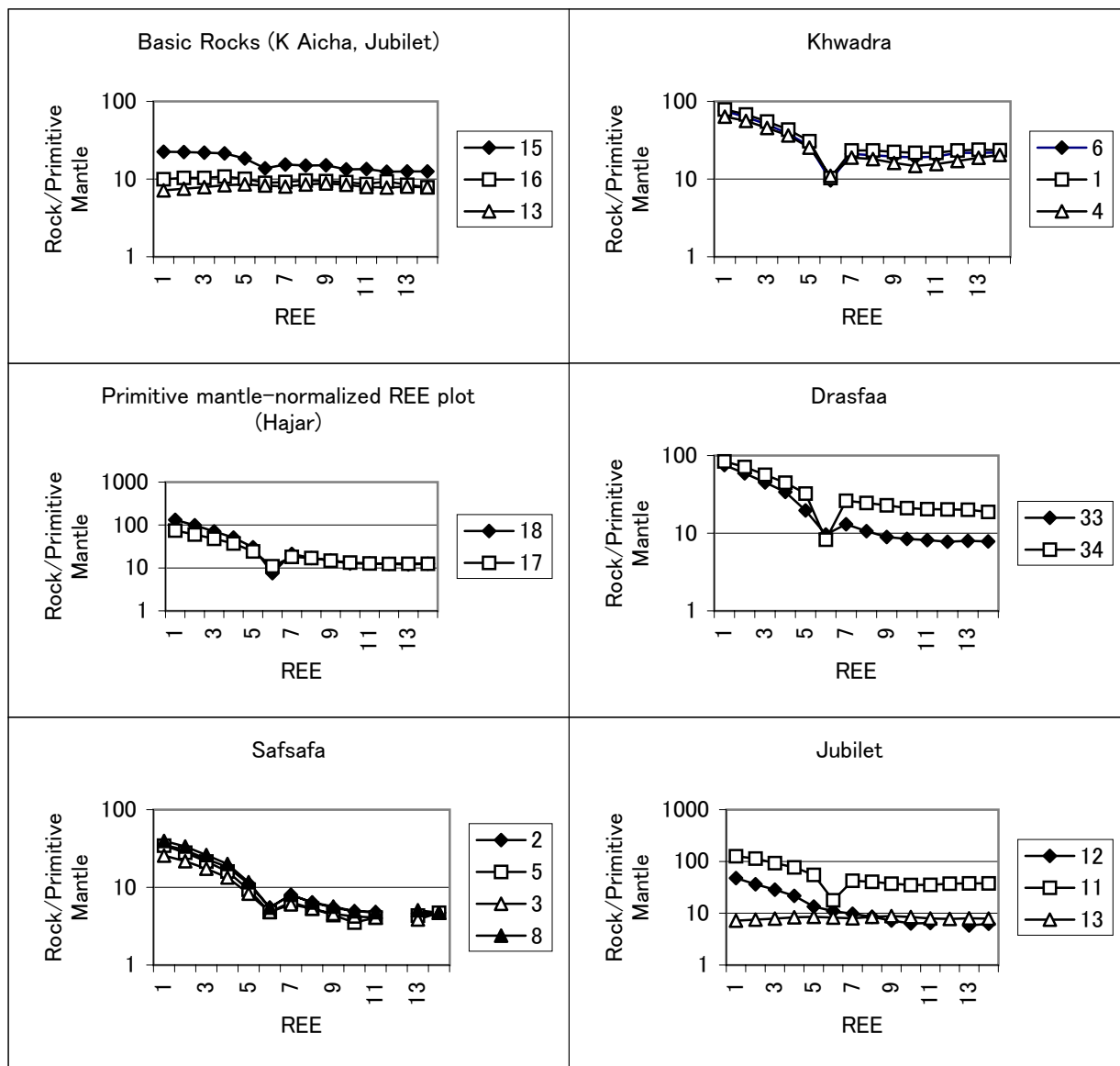


Fig. II-4-3. Primitive mantle-normalized trace element abundances

## 2) Large-ion lithophile (LIL) element and high field-strength (HFS) element

There are Rb, Ba and Cs (Fig.II-4-4) as minor elements showing the same tendency as  $K_2O$  to  $SiO_2$ . All the elements are large-ion lithophile elements (LIL), but Sr belonging to the LIL elements does not show the same tendency as K.

The spidergram drawn up by Sudo and Osanai (2002) is shown in Fig.II-4-5. This is a diagram in which LIL and HFS elements have been normalized by an average N/MORB (published in 2002 by Sudo and Osanai). Iberian Pyrite Belt's average basic rock composition (Thieblemont et al., 1998) is also shown in the spidergram. The patterns of the basic rocks in this area and the IPB are similar to each other, the rocks are abundant with LIL elements such as K, Rb and Ba, and the content of their HFS element is about the same as that of the average MORB or a little richer than the content of that.

## (3) Considerations

### 1) Existing data

We could hardly obtain existing data on the chemical composition of igneous rocks in the area. Hibiti(2001) reported various values obtained by analysing igneous rocks in Hajar Mine's wellbore. We can judge the rocks are much mineralized because all the analysis results show that the content of Fe in them is more than that of  $SiO_2$ . The results do not show their peculiar chemical composition.

Essaifi et al. (1995) reported on the content of the main and minor elements of leucogabbro in the vicinity of Kettara and said in the report, "Leucogabbro is tcoreiitic intrusive rocks stratifiedly intruded in the lower Carboniferous metasedimentary rock unit and it was formed in the same period as the Variscan orogeny."

Bauchau and Ferrari (1999) analysed ten igneous rocks samples and they collected in the vicinity (Amzough and Imarine) of Hajar Mine and said, "The igneous rocks are relatively flat in their REE pattern, a little rich in their HREE and poor in their LREE." and "Interpreting them overall, Amzough and Imarine are now in the calc-alkaline volcanism, continental marginal arc islands and probably have a subduction." But they did not show the samples' analysis values.

### 2) Correlation of $K_2O$ and $SiO_2$

The  $K_2O$  of acid rocks has a negative correlation with their  $SiO_2$ , and their Rb, Ba and Cs also have the same relation. Two reasons can be cited for the above explanation: Components (minerals) including K, Rb, Ba and Cs were removed from the rocks' system or components without the latter elements were added to the rocks.

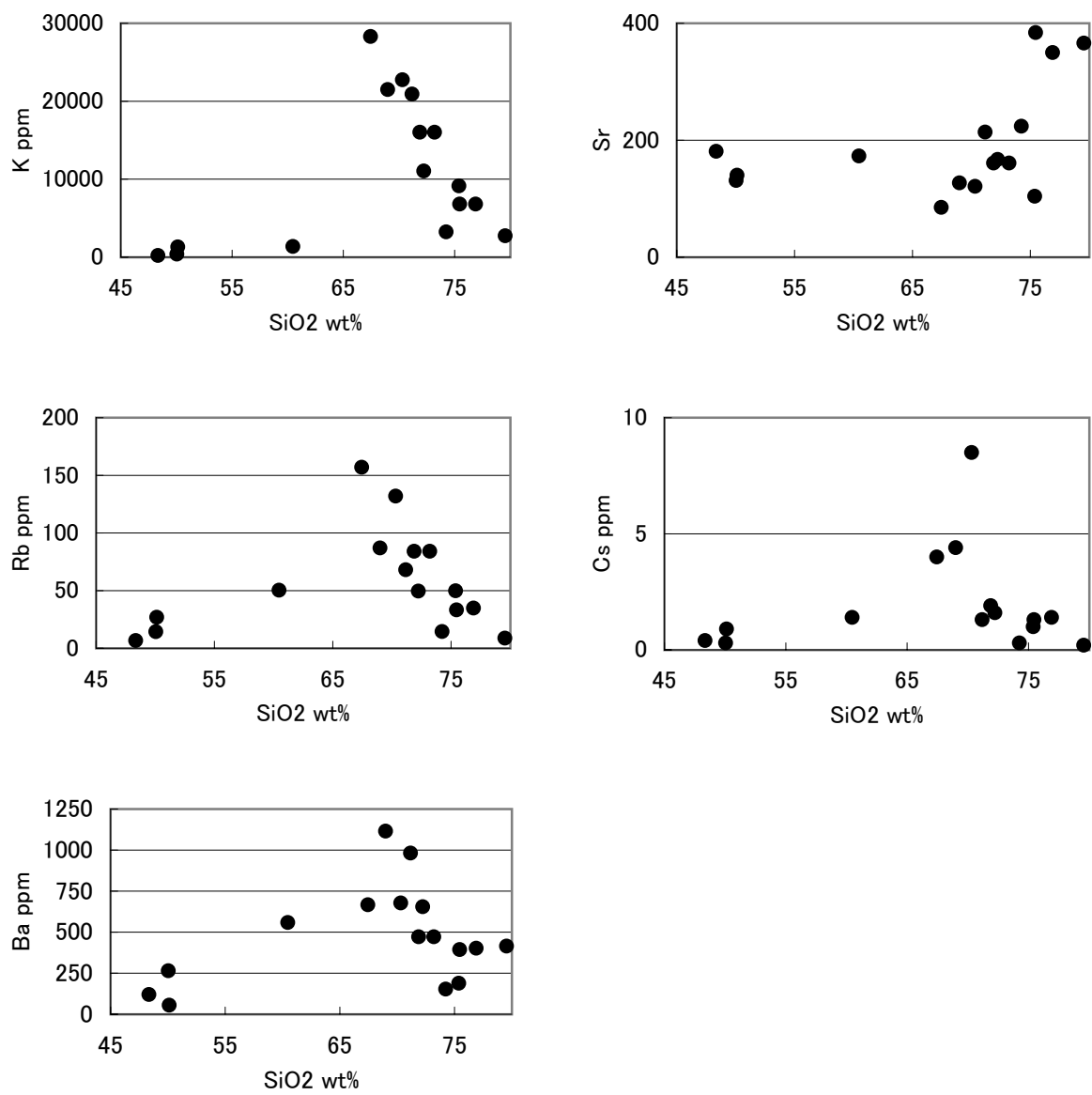


Fig. II-4-4 LIL - HFS (Igneous rocks)

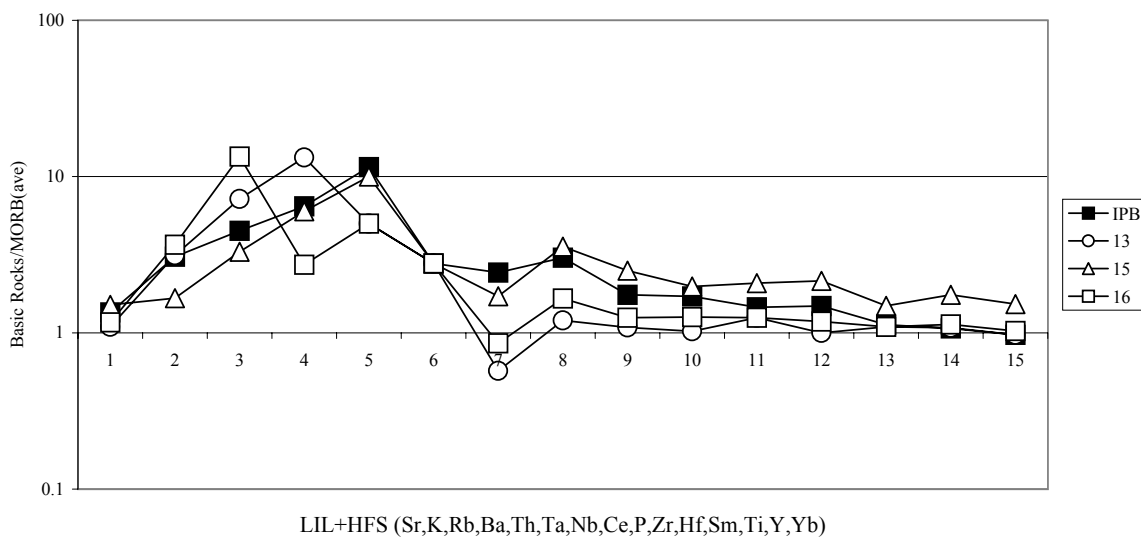
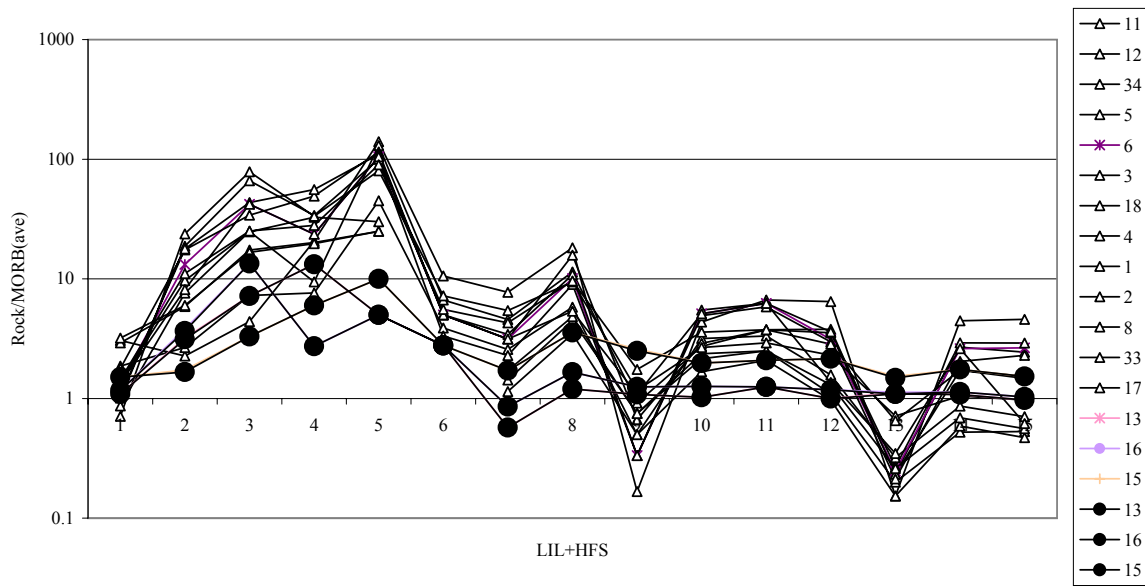


Fig. II-4-5 LIL-HFS Spider diagram (Ignious rocks)

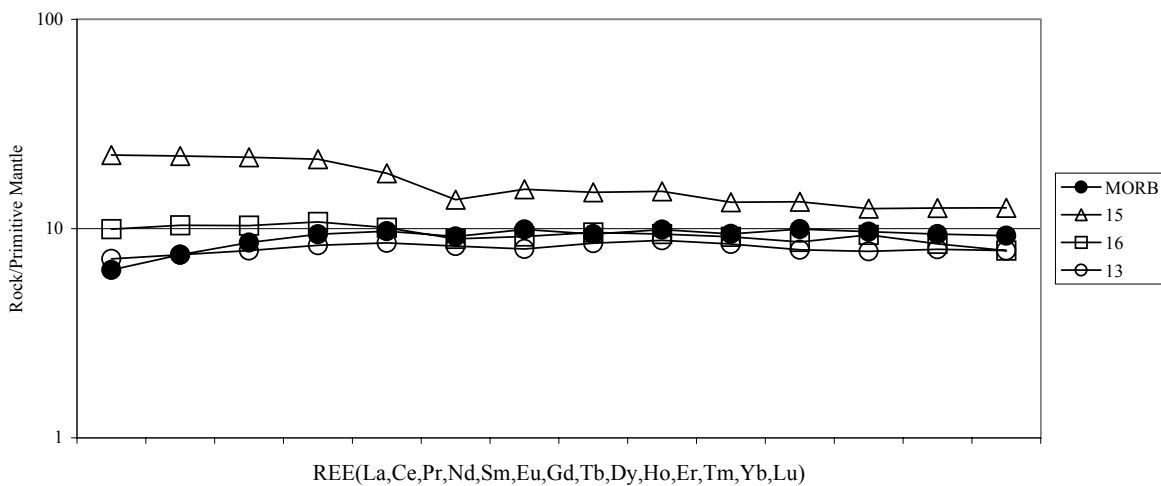


Fig. II-4-6 REE Spider diagram (Ignious rocks)

Alkali feldspar is considered to be components (minerals) including the elements. Alkali feldspar includes  $KAlSi_3O_8$ ,  $NaAlSi_3O_8$  and  $CaAlSi_3O_8$  as its end member and Ba, Ti, Fe, Mg, Sr, Rb and Li as its minor element (Deer et al., 1992). But in the igneous rock samples of this time, Sr has a positive correlation with  $SiO_2$ , which is different from K, and the correlation is not in harmony with a hypothesis that it is due to Alkali feldspar's fractional crystallization. Also, there is no data on the content of Li in the feldspar.

Quartz is considered to be components (minerals) without K, Rb, Ba and Cs. Almost the whole quartz is usually composed of  $SiO_2$  and it includes the respective scant quantities of Li, Na, K, Al, Fe, Mn and Ti (Deer et al. 1992) except for an existence of intrusions into it. So, as far as Sr does not exist as an intrusion, it does not include Sr and harmonize with Sr's tendency.

### 3) Comparison on chemical composition between rhyolites and tonalitic mylonites

The primitive mantle normalized REE pattern of an acid igneous rock is shown in the Figure. The REE pattern of tonalitic mylonite from Safsafa can be plotted in the range of lower values than values in that of rhyolite. In the comparison on the content of main elements between them there is a tendency that tonalitic mylonite is higher in CaO and it is a little lower in T-FeO. Judging from the REE patterns and the CaO and T-FeO content, an igneous rock of tonalitic mylonite can be said to have geochemical features different from those of rhyolite.

The REE patterns of rhyolites from Hajar, Khwadra and Drasfar are about the same, and the content of their main elements can be also plotted on the same trend. So, rhyolites of Hajar, Khwadra and Drasfar can be said to have similar geochemical features.

### 4) Comparison between basic rock and MORB

We compared the chemical components of three basic samples (dolerite) with those of basic rock (basalt) from other areas.

Judging the LIL and HFS elements of the samples and the rocks from the spidergram, dolerite in this area are rich in the LIL element, similar to the features of an island arc basalt, and different from the N-MORB (Sudo and Osanai 2002) which is less in both the LIL and HFS elements.

The primitive mantle normalized REE patterns of the samples are flat, and the 02MRS13 and 02MRS16, among others, are almost the same as Hofmann's N-MORB (1988) (Fig.II-4-6).

#### 4-2-2-2 Radioactive dating

We made the K-Ar radioactive dating of the 13 igneous rock samples to grasp the mineralization and igneous activity ages in this area.

## (1) Results

### 1) Mineralization ages

As for the mineralization age of the Hajar deposit were reported by Watanabe (2002). We sampled sericitized rhyolites in the under ground of Hajar mine and made the mineral separation of sericite from the sericitized rhyolite as to the 02MRS026 and the K- Ar analysis of the Whole rhyolite as to the 02MRS022 as same as Watanabe (2002). As a result, the 02MRS026's value and the 02MRS022's value recorded  $300 \pm 8\text{Ma}$  and  $312 \pm 8\text{Ma}$ , respectively, and they were almost the same as that of Watanabe (2002).

Two samples (02MRS035 and 02MRS042) were collected to consider the mineralization ages of Drasfa and Kettara deposits and submitted them to Secoscience Co., Ltd. for analyzation. The sample 02MRS035 was collected from the point 124.5m of the former deposit's DSF2 bore. It was a host rock contacting a massive sulphide where the sulphide and the rock appear one after another, and it was chloritized. The sample 02MRS042 was collected from the point 110.25m to 110.40m of the latter deposit's 2BS drilling core. It was a host rock contacting a massive sulphide and it was silicified and chloritized. Because the host rocks were judged to be not contacted to the sulphides at the fault and the degrees of the rocks' chloritization appeared to become stronger as they approached the sulphides, according to the samples, we judged their chloritization might have a close association with their mineralization and made the K-Ar radioactive dating of the samples. But the K content of both the samples was low and no reliable dating results of them could be obtained.

### 2) Igneous activity age

As for the radioactive ages of igneous activities in the Jebilet. Haouz and Guemassa area the dating results of acid volcanic rock at Amzourh, Oukhribane and Frizem in the Guemassa area were carried in the JICA/MMAJ (1990). As for the acid plutonic rock in the Jebilet area Pique and Michard summarized their past results (1989). We sampled acid igneous rock and basic intrusive rock in these areas this time and submitted them to the laboratory.

#### (a) Jebilet

Four samples were collected in the Jebilet area and whole rocks were analysed. The samples 02MRS015 and 02MRS016 from the Koudiat Aicha deposit's KA25 bore. The latter sample was collected from the point 46.0m to 46.2m of the bore and the former sample from the bore's point of 271.50m to 271.80m. Both samples are metadolerites and have tremolite and chlorite formed by metamorphism. As for the sample 02MRS016 its sericitation due to hydrothermal alteration was found. The results were  $303 \pm 8\text{Ma}$  and  $279 \pm 7\text{Ma}$ , respectively. The 02MRS016 hydrothermally altered showed its newer age. The dating of 02MRS015 was the

same period as that of the mineralization of Hajar ore deposit.

The sample 02MRS011 is rhyolitic welded tuff sampled at the south-west end of the hill between Bourana and Ben Suriname. It was altered hydrothermally and alteration ores such as biotite, chlorite and sericite were found in it. Its dating result value was  $267 \pm 7$ Ma and the value was the same as that of the Kudiat Aicha sample (02MRS016) hydrothermally altered.

The 02MRS012 is a sandstone hornfels sampled in the vicinity of Salah Gossan west of Kechnet. The hornfels has tremolite formed by metamorphism. Its dating result was  $248 \pm 8$ Ma, and it showed the newest age of the samples submitted for dating.

#### (b) Hauz

In the Hauz district, we collected four samples from the deilling core of Khwadra, Draa Sfar and Safsafa and submitted the samples for analyzation.

The samples 02MRS001 and 02MRS004 are rhyolites in Khwadra. The former sample was collected from the point 365.7m to 366.00m of the KHS3 bore and the latter from the point 350.60m to 350.70m of the Khwadra deposit's KHS1 bore. Both the samples were hydrothermally altered and contains biotite, chlorite and sericite. In the sample 02MRS001 we made the radioactive dating of the Whole rock of it, and in the sample 02MRS004 we separated sericite from it and then made its radioactive dating. Their dating results were  $326 \pm 8$ Ma and  $270 \pm 7$ Ma, respectively.

The 02MRS034 is a tuffaceous slate sampled from the point 16.20m to 16.35m of the Drasfar Deposit's DSF15 drilling core. Most of its broken waste grains are originated from rhyolite and its consolidation deformation and recrystallization were found. Its matrix is mainly clay minerals of sericite and illite. The dating of the Whole rock of it was made. The dating result value was  $350 \pm 9$ Ma.

The sample 02MRS005 is tonalitic myronite sampled from the point 279.00m to 279.30m of the S2 bore in the Safsafa area. It had sericite formed by a slight hydrothermal alteration. The dating of the Whole rock of it was made. The dating result was  $362 \pm 9$ Ma and it showed the oldest age of all the samples analysed.

#### (2) Considerations

The dating result of samples after ore mineral separation shows its minerals forming age and its whole rock analysis result seems to show an intermediate value between its primary and alteration ages. It seems that the stronger the degree of its alteration is, the nearer it is to its alteration age and that the weaker the degree is, the nearer it is to its primary age.

Based on this premise, we divided the dating results into groups of plutonic igneous



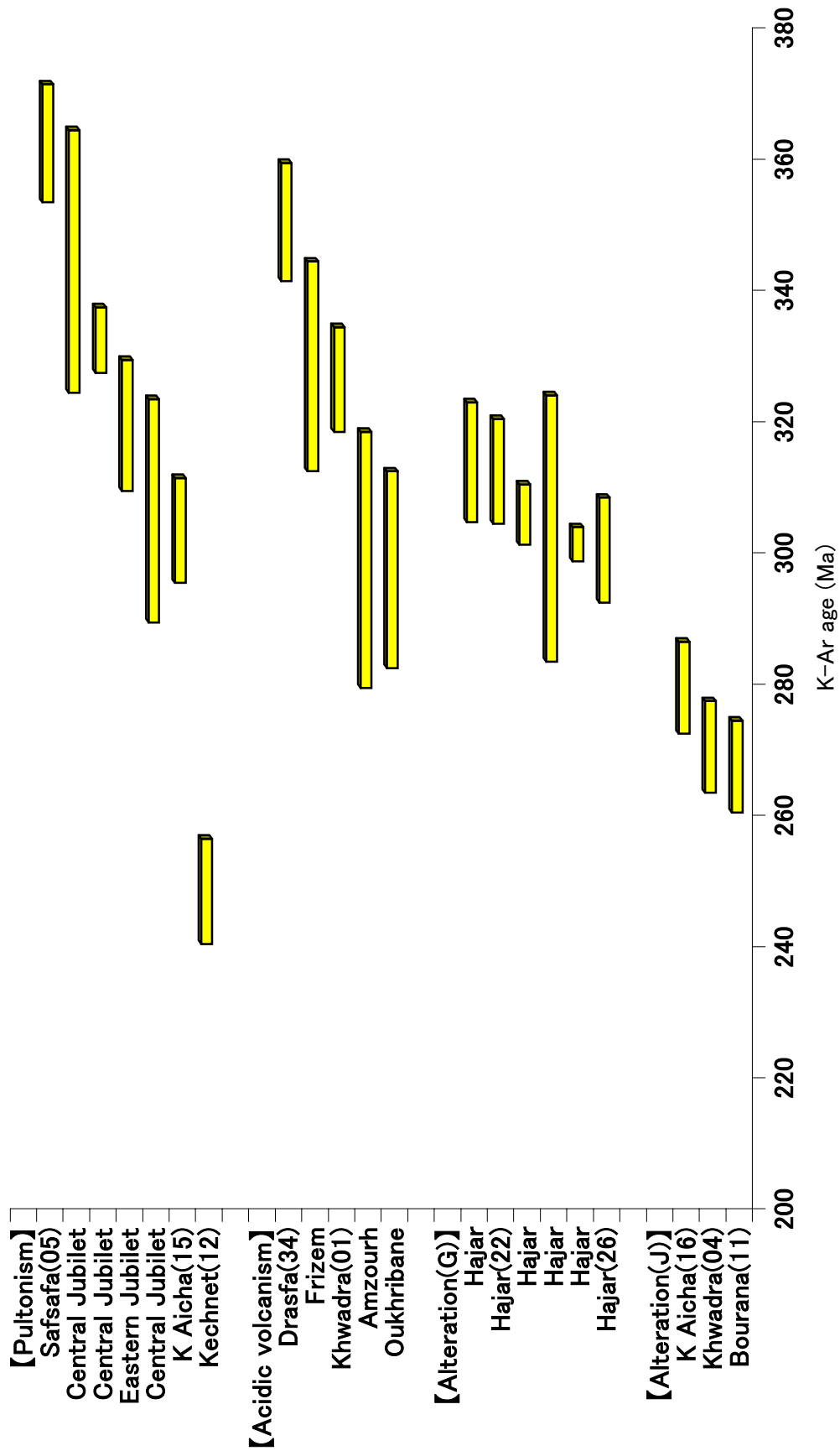


Fig.II-4-7 K-Ar age of rocks of Tekna-Marakech area

activities, acid volcanic activities and the respective mineral alterations of Guemassa and Jebilet. And they are shown in Fig.II-4-7.

The plutonic igneous activity group includes Jebilet's granites mentioned in a treatise by Pique and Michard (1989), Safsafa's tonalitic myronite (02MRS005), Koudiat Aicha (02MRS015) and Kechnet (02MRS012). The 02MRS015 was contact-metamorphied. And although the 02MRS016 sampled at Koudiat Aicha was hydrothermally altered, the degree of the former sample's hydrothermal alteration was weak. So, we interpreted that it showed a value in the proximity of an age of volcanic activity in the earlier period and included it into this group. The 2MRS012 is a sandstone hornfels sampled near Salah Gossan. It is not an igneous rock, but there is the distribution of basic intrusion (dolerite) near there and the K-Ar age of this sample was likely to show an intrusion age of dolerite. So, we included it into this group.

The acid volcanic activity group included the samples of Frizem, Amzourh, Oukhribane according to JICA/MMAJ (1990), and the sample Khwadra (02MRS001) and the sample Drasfar (02MRS034). The Khwadra (02MRS001) was hydrothermally altered, but it showed an older value than that obtained by making the dating of the sample 02MRS004 collected from there after the mineral separation of sericite from it. So, we could think it showed an age of more primary igneous activity and included it into this group. The sample Draa Sfar (02MRS034) is a tafacious slate, not an igneous rock. But it has many broken waste grains originated from rhyolite, so we included it into this group.

As to mineral alteration we divided its samples into the Guemassa area group and the Jebilet area group. The mineral alteration group in the former area was composed of the samples Hajar (02MSR022 and 02MRS026) and data of Watanabe(2002). The mineral alteration group in the latter group was composed of the sample Koudiat Aicha (02MRS016), the sample Khwadra (02MRS001), the sample Bourane (02MRS011) and the sample Kechnet (02MRS012). Khwadra is located on the Haouz plain, but we included it into the Jebilet group for convenience.

Fig.II-4-7 shows that the ages of plutonic igneous activities and acid volcanism are both 290 to 360Ma, except for Kechnet's sandstone hornfels. Guemassa's mineral alteration period is 290 to 320Ma, which falls on the end of the period of plutonic rock and igneous rock activities. Jebilet's mineralization period is 260 to 290Ma, which falls on a period after those activities. Data on igneous activities in about the same period as the mineralization period of Jebilet could not be obtained in our research field this time. There is a possibility that the mineralization did not involve the igneous activities in the same period, and we need to further collect and examine data on their ages, together with those in the younger period Kechnet's sandstone hornfels shows.

### 4-3 Sedimentary rocks

#### 4-3-1 Method

A whole rock chemical analysis (X-ray diffraction, major component analysis, main element analysis, trace element analysis such as rare earths, etc.) (102 samples, which were not overlapped), a sulfur isotope analysis (100 samples), thin-section appraisal including a fossil reconnaissance survey (47 samples), and a polished thin section appraisal (21 samples) were made on pelites such as schist, shale, and slate.

Several samples were collected from the upper and lower parts in a drilling core between which a massive sulfide ores in order to study geochemical characteristics of the hanging wall and footwall. The whole rock chemical analysis (the major component analysis, the major element analysis, and the trace element analysis such as rare earths) was conducted by Als Chemex (Canada). As for the sulfur isotope analysis, after the samples were pulverized and prepared by the Ohdate Analysis Technical Center, they were measured by Activation Laboratory (Canada). As for the fossil reconnaissance survey, boron treatment, hydrogen fluoride treatment, and thin-section observation were conducted by Parino Survey.

Table 4-1-3 List of Laboratory works (Sedimentary rocks)

Laboratory test items	Samples	Quantity
Thin-section (including a fossil survey)	Sedimentary rocks	47
Rock and ore polished thin sections	Sedimentary rocks, sulfide ores	21
X-ray diffraction	Sedimentary rocks	102
Trace element analysis	Sedimentary rocks	102
Major component analysis	Sedimentary rocks	102
Sulfur isotopic ratio determination	Sedimentary rocks	100

#### 4-3-2 Results

##### 4-3-2-1 Major components, main elements, and trace elements

###### (1) Results

The X-ray diffraction and microscopic observation revealed that the samples contain a lot of altered minerals such as sericite and chlorite. The samples may have been influenced by mineralization and alteration, and regional metamorphism. The results of the major component analysis are in the tables in the end of this report.

The samples have an alkaline alteration intensity  $(K_2O+MgO)/(K_2O+MgO+CaO+Na_2O)$  of 0.22 to 0.90 and averages at 0.67, indicating a high level of alteration and metamorphism. The alkaline alteration intensity by depth, on the Hajar Mine (HS25, CD27), Draa Sfar deposit (DFS2, DFS15) Khwadra deposit (S4), and Jebilet Central Gossan (LA9, KA25), changes to a

higher value toward the foot wall side or toward the hanging wall side if a massive sulfide ore is intercalated. On the other hand, the alkaline alteration index changes to a higher value toward the hanging wall side on the Khwadra deposit (S3, S5). Also, the samples substantially agree with a change in copper, lead, and zinc (Cu+Pb+Zn) related to the alkaline alteration intensity and mineralization (Fig.II-4-8).

As for the relation between the major components and each element,  $\text{TiO}_2$ , V,  $\text{K}_2\text{O}$ , and  $\text{P}_2\text{O}_5$  show a relatively good positive correlation with  $\text{Al}_2\text{O}_3$  and  $\text{SiO}_2$ ,  $\text{CaO}$ , and  $\text{FeO}_3$  show a negative correlation with  $\text{Al}_2\text{O}_3$ . As for horizon mainly on the hanging wall,  $\text{CaO}$ ,  $\text{FeO}_3$ , and  $\text{K}_2\text{O}$  tends to indicate a high value that deviates from a positive correlation with  $\text{Al}_2\text{O}_3$ , while  $\text{N}_2\text{O}$  tends to show a low value that deviates from a positive correlation with  $\text{Al}_2\text{O}_3$  on the foot wall. As for ore deposits, the correlation between  $\text{Al}_2\text{O}_3$  and  $\text{SiO}_2$  tends to be low on the Hajar deposit, Draa Sfar deposit, and Kettara deposit if the  $\text{Al}_2\text{O}_3$  content is relatively high. The relation between  $\text{CaO}$  and  $\text{Al}_2\text{O}_3$  shows that the Khwadra ore deposit tends to have a higher  $\text{CaO}$  content than other ore deposits (Fig.II-4-9, Fig.II-4-10).

The result of the principal component analysis and the contribution rate of elements to each principal component are shown in the table of the end of this report. Cs, La, Nb, Rb, Ta, and Th showed a relatively high contribution rate to the first principal component, Al, Co, Cu, Fe, Ga, Mg, and Th to the second principal component, Cr, Na, and K to the third principal component, HF, Zr, and Na to the fourth principal component, and Pb, Zn, and Cd to the fifth major component. The first, second, third, fourth, and fifth principal components might represent trace elements that are highly concentrated near the hydrothermal activity area, copper and iron mineralization, mineralization and alteration, clastic material such as zirconium, and lead and zinc mineralization, respectively.

## (2) Considerations

The elements of pelite may have three types of origins: clastic rock, organism, and water source (Seibold et al 1982). The clastic rock origin means that country rock was crushed, transferred by a river, wind, etc., and accumulated again by waves or sea currents. Elements insoluble in water such as Al, Ti, Nb, and Zr are known (a positive correlation with  $\text{Al}_2\text{O}_3$ ). The living body origin means that elements consist of the dead bodies of organisms. Si that composes radiolaria and diatom, Ca that composes calcareous foraminifer, and Sr are known (a negative correlation with  $\text{Al}_2\text{O}_3$ ). The water origin means that elements are formed from sea water or interstitial water by means of sedimentation and diagenesis. It is said that Mn of wolframite nodule is said to be formed in this way. The sedimentary rock in this area tends to have the same elements of a seabed sediment as the above-mentioned.  $\text{CaO}$  tends to vary toward a higher  $\text{CaO}$  concentration in the correlation between  $\text{CaO}$  and  $\text{Al}_2\text{O}_3$ . This tendency

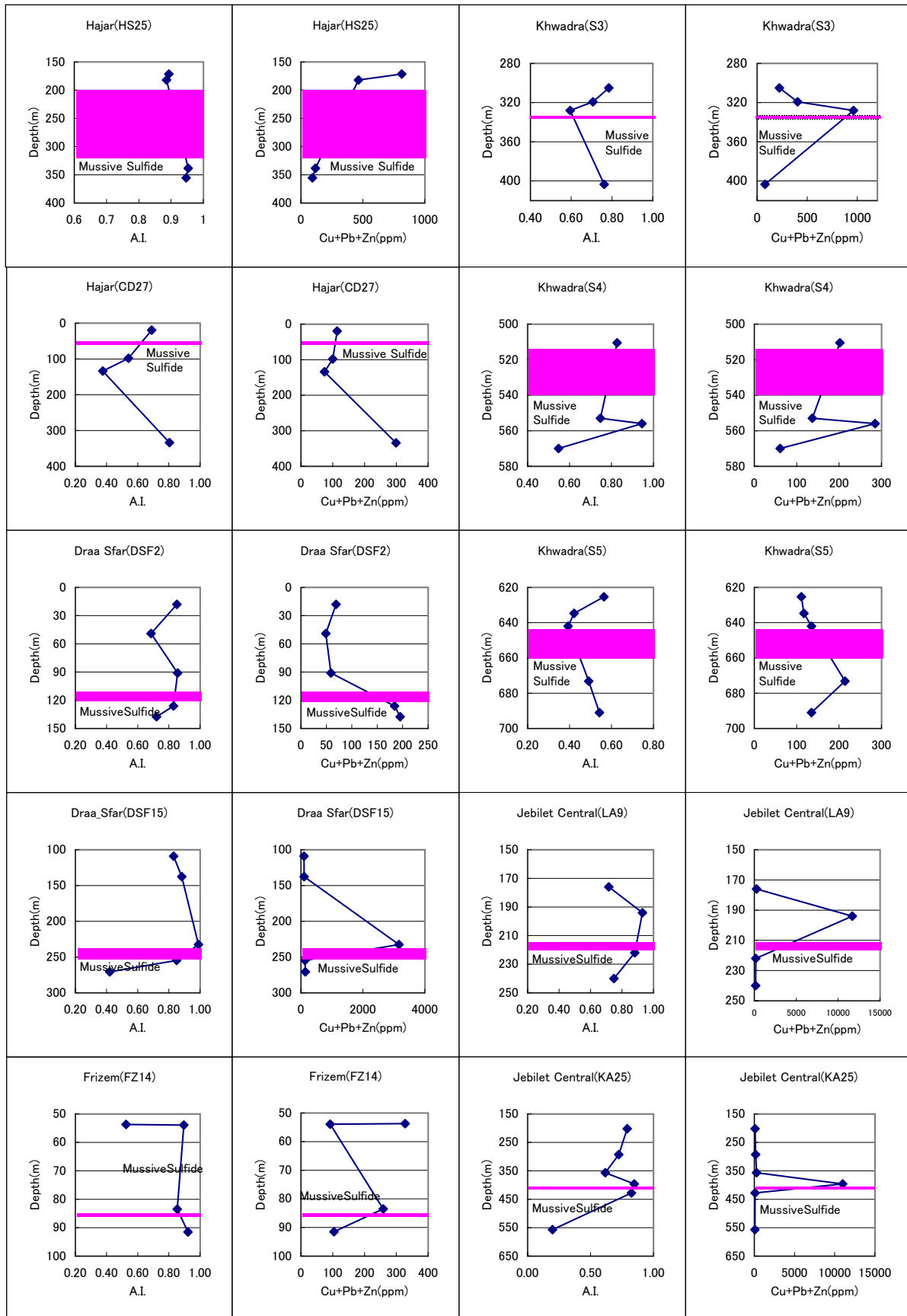


Fig. II-4-8 Variation of Alkali Index and Metal contents (Cu+Pb+Zn) by Depth of Drilling

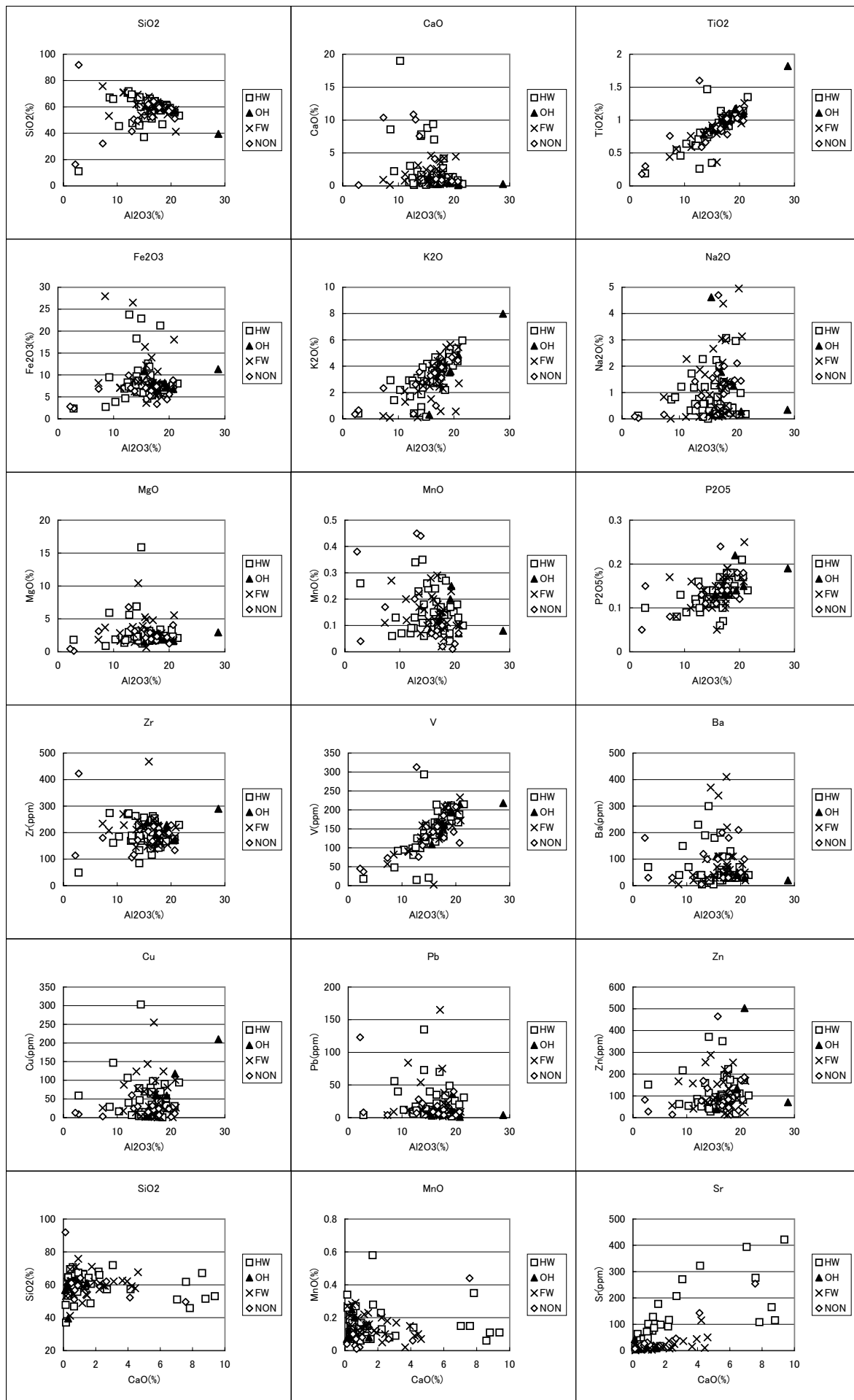


Fig. II-4-9 Relationship between Al<sub>2</sub>O<sub>3</sub> contents and various constituents of Sedimentary Rocks (1)

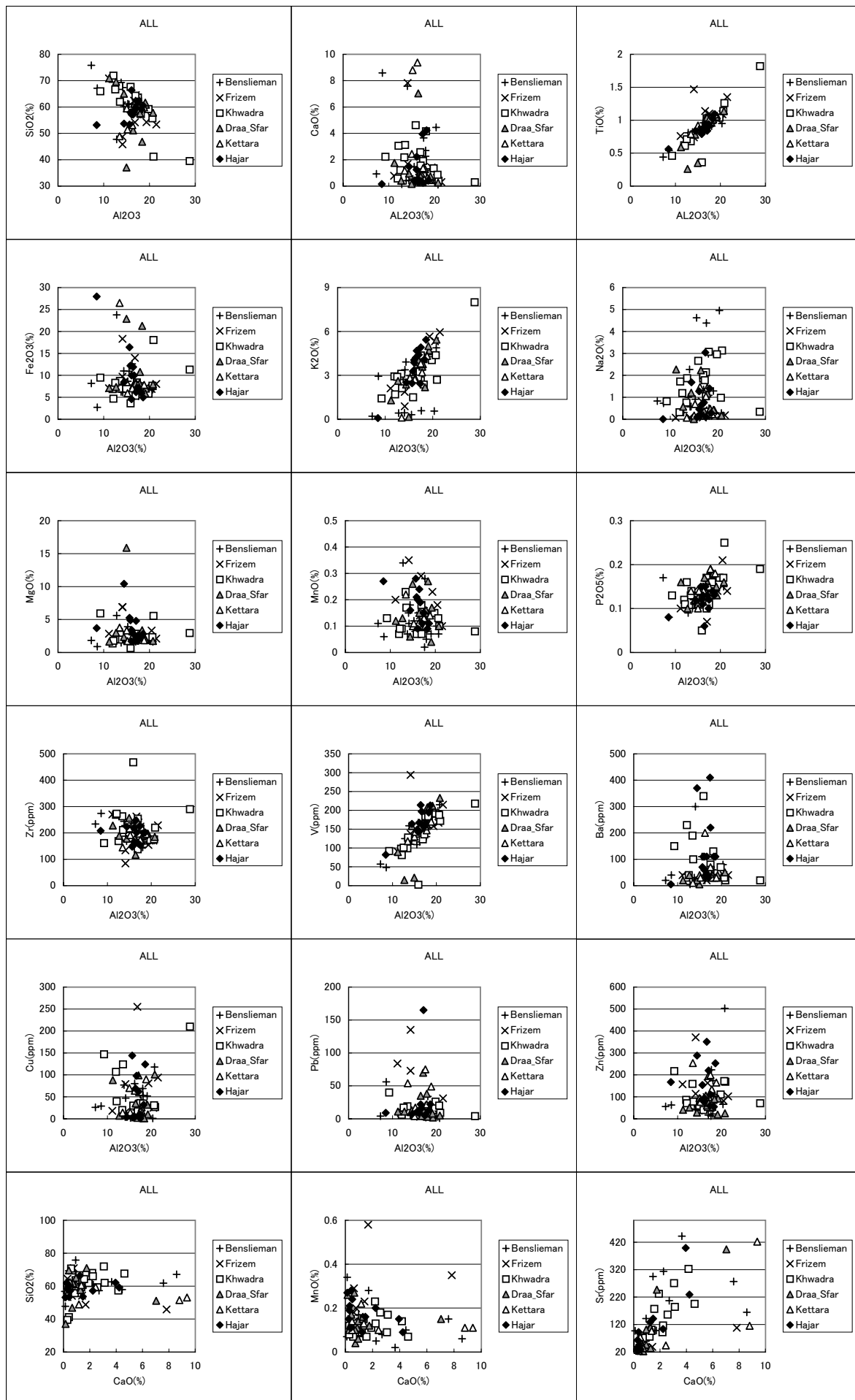


Fig. II-4-10 Relationship between Al<sub>2</sub>O<sub>3</sub> contents and various constituents of Sedimentary Rocks(2)

matches the fact that the hanging wall consists of carbonate rich mudstone, which is characteristic of this area. The variation of  $K_2O$  and  $N_2O$  may have reflected the mineralization and alteration. The variation of  $SiO_2$  on the Hajar, Draa Sfar, and Kettara deposits and a tendency of a higher CaO content on the Khwadra deposit mean that more material derived from clastic rock caused by acid volcanic activities was supplied to the three ore deposits than to the Khwadra deposit and that a relatively large amount of material derived from living bodies was supplied to the Khwadra deposit.

#### 4-3-2-2 Trace elements

##### (1) Results

REE that are standardized with chondrite pattern shows in spider diagrams. All the diagrams show a gradual rise toward the left on the light rare earth side and a europium anomaly is conspicuous. The mode of occurrence of pelite observed in the drilling cores, together with the mode of occurrence which grade into pyroclastic rock, reveals that material that composes the pelite contains rock derived from an island arc crust (an island arc volcano and others) (Fig II-4-11).

Comparing the total rare earth elements (TREE) divided into two groups: pelite on the hanging wall and that on the foot wall, based on the spider graphs, both pelite on the hanging wall and the foot wall tend to have a higher TREE content near massive sulfide. A similar tendency can also be seen on KUROKO deposit. Plotting the relation between light rare earth and heavy rare earth on the La-Sm and La-Yb scatter diagrams (Fig II-4-12) reveals a positive correlation and shows that the distribution area is different on the upper and foot walls. In other words, high La-high Sm concentration and high La-high Yb concentration areas tend to be distributed on the hanging wall, and high to medium La-medium to low Sm and high to medium La-medium to low Yb concentration areas tend to be distributed on the foot wall on the Hajar and Frizem deposits. Also, from the drilling cores of the Khwadra deposit, it is known that the distribution area is moving to high La-high Sm concentration and high La-high Yb concentration areas toward the horizon above the hanging wall and footwalls.

Europium anomaly ( $Eu/Eu^*$ ), cerium anomaly ( $Ce/Ce^*$ ), and total rare-earth elements (TREE) of the drilling core samples were plotted by depth. The  $Eu/Eu^*$  value tends to be low near a massive sulfide deposit on both upper and foot walls on the Hajar deposit (HS25, CD27) and Draa Sfar deposit (DSF2, DSF15) and it tends to be high on the Khwadra deposit (S3, S4, and S5). The total rare-earth elements (TREE) tends to be high near a massive sulfide deposit on the Hajar deposit (HS25, CD27) and Draa Sfar deposit (DSF15) and it tends to be low on the Khwadra deposit (S3, S4, and S5). On the other hand, the  $Ce/Ce^*$  value does not show any noticeable change by depth (Fig II-4-13).



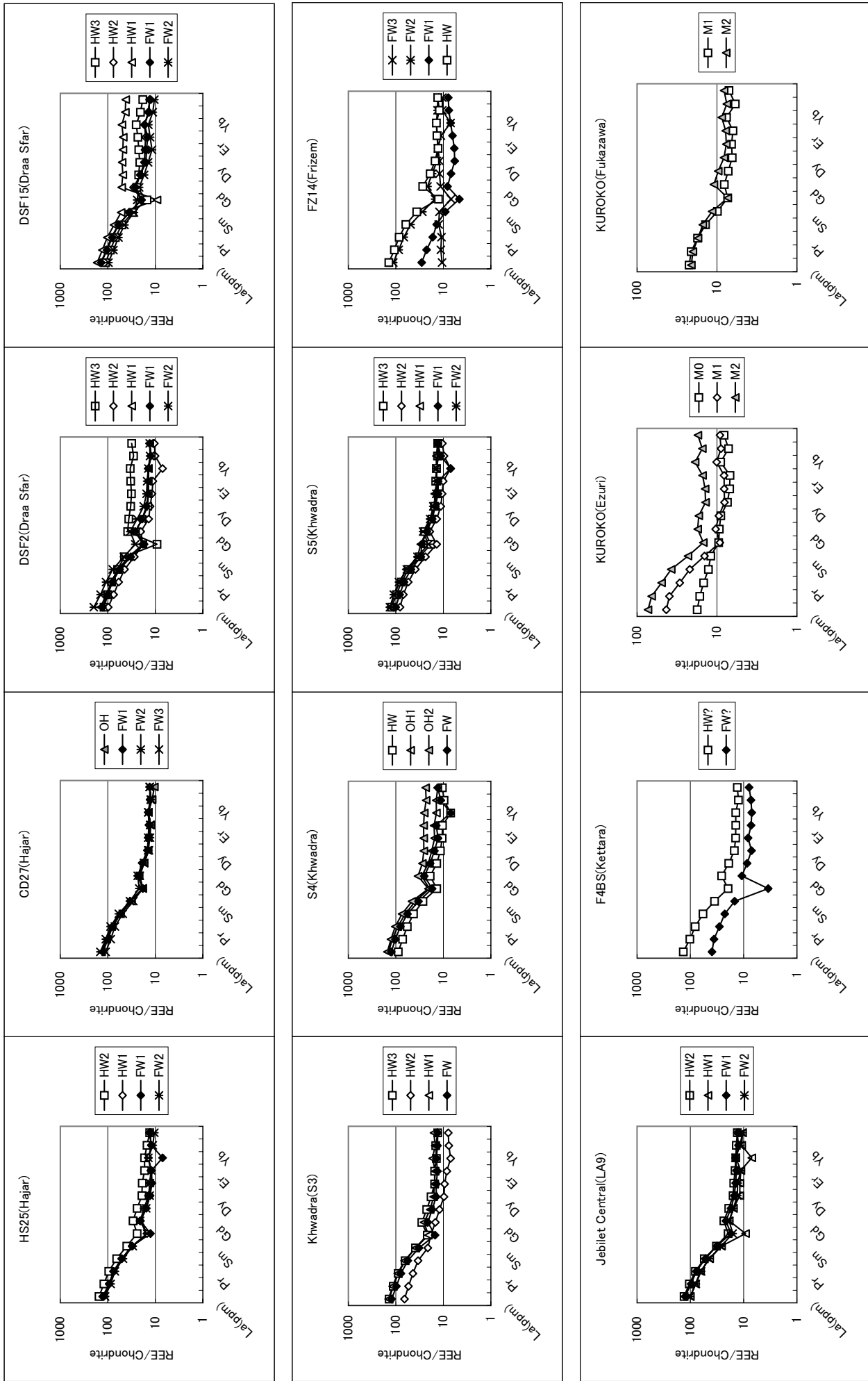


Fig. II-4-11 Spider Graph of REE (normalized Chondrite)

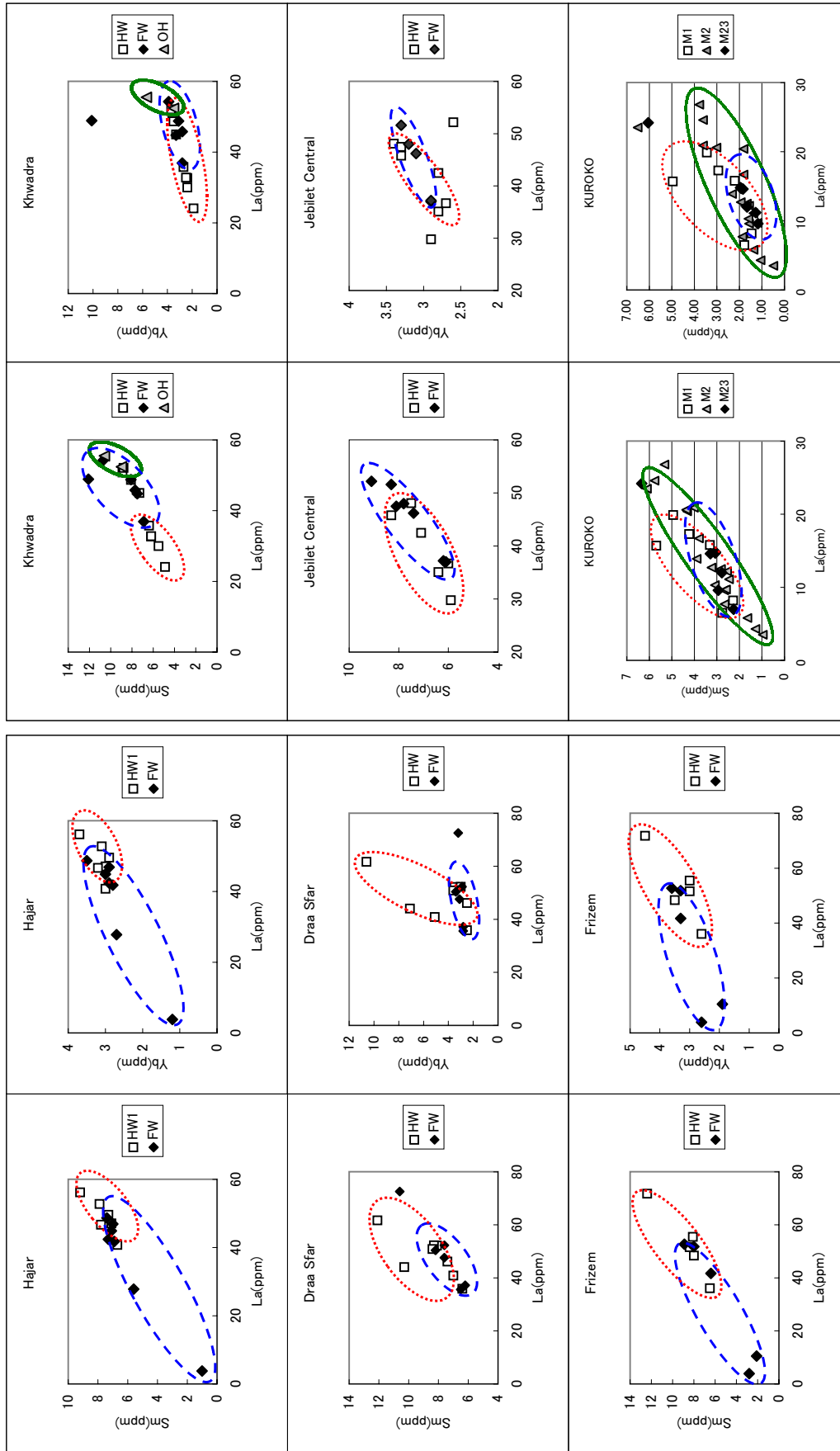


Fig.II-4-12 La-Sm diagram and La-Yb diagram

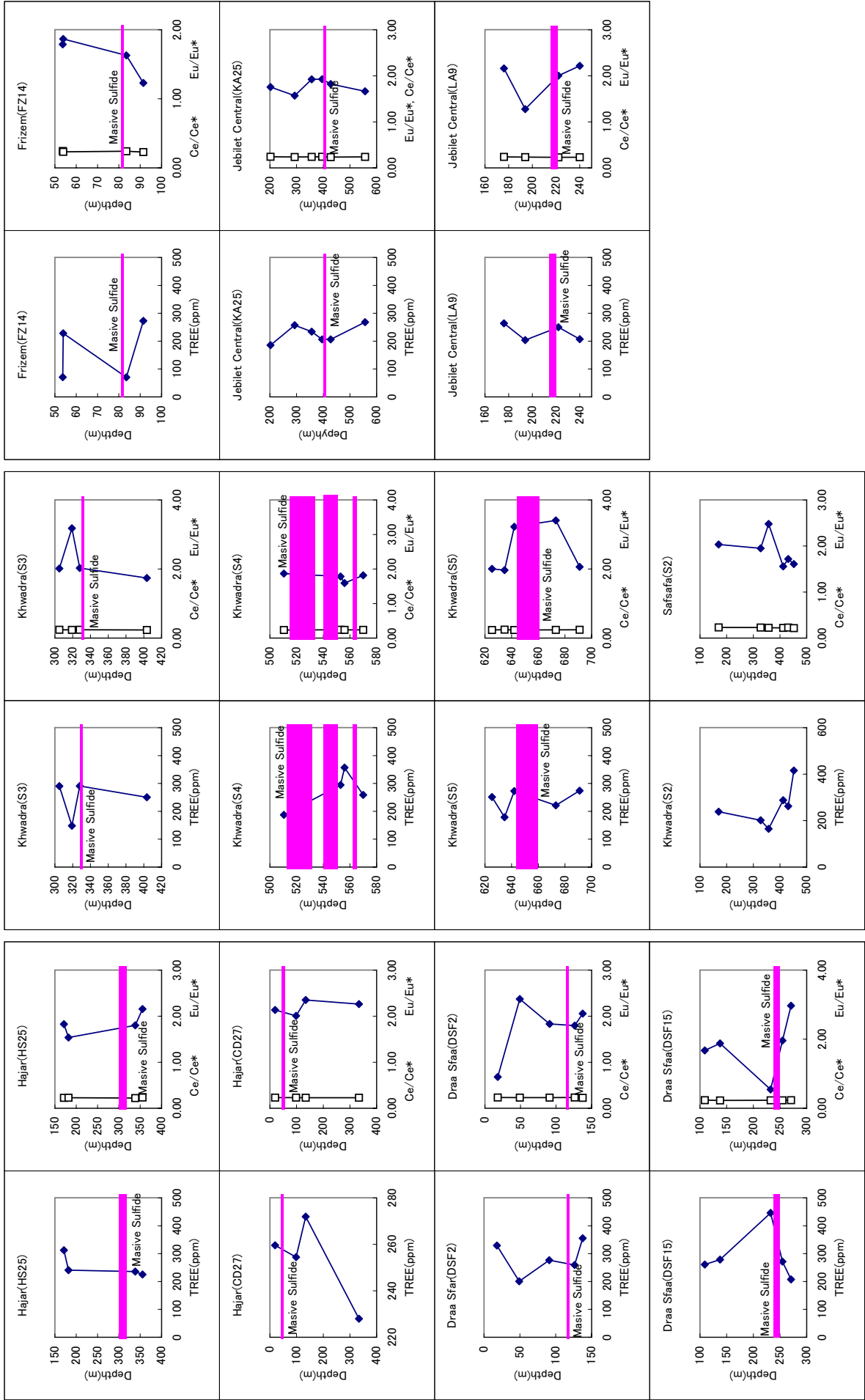


Fig. II-4-13 TREE, Ce/Ce\* and Eu/Eu\* of Mudstone (Depth)

## (2) Considerations

Shikazono (1999) believes that altered minerals and sulfate minerals in volcanic rock on the KUROKO deposit show a positive Eu/Eu\* anomaly because the altered minerals and sulfate minerals were deposited from reductive and evolved hot water derived from seawater and that the rare-earth element concentration in manganese and iron oxide silica rock is high because rare-earth elements in seawater were replaced removed by manganese and iron oxide. A decrease in the Eu/Eu\* value and an increase in total rare-earth elements (TREE) from the foot wall to the hanging wall with a massive sulfide deposit intercalated between the plates may be attributable to sedimentation of rare earth elements caused by sedimentation of ore on the hot water side. On the other hand, an increase in the Eu/Eu\* value and a decrease in total rare-earth elements (TREE) may be attributable to removal of the rare-earth elements on the hot water side from pelite, which is country rock, because hydrothermal activities continued after sedimentation of ore. The above conjecture is corroborated by the fact that the alkali alteration index changes to a high value on the foot wall side or toward the hanging wall side with a massive sulfide intercalated between the plates on the Hajar deposit (HS25, CD27) and Draa Sfar deposit (DFS2, DFS15), which show the former pattern, while the alkali alteration index changes to a high value on the hanging wall side on the Khwadra deposit (S3, S5).

### 4-3-2-3 Sulfur isotope

#### (1) Results

The microscopic observation and X-ray diffraction of pelite show that sulfate mineral hardly exists. In view of the fact, it was conceived that a major part of the sulfur contained in the pelite might be sulfide such as pyrite. Sulfur isotope of Whole pelite was measured (when elemental sulfur was contained in a large quantity, it was removed by solvent extraction). In order to measure sulfur isotope, 1 to 5 mg of sulfide was reacted with 40 ml of chromium chloride (Cd (II) Cl<sub>2</sub>, 1M) in a 100 °C container, with nitrogen gas used as a carrier gas. After it was deposited as CdS, it was reacted with silver nitrate and recovered as Ag<sub>2</sub>S, which was measured by EA-IRMS.

The result of measurements of the sulfur isotope is in the table in the end of this report. The measurements have the mode near 1 to 0 ‰ on the Whole and generally vary between -35 ‰ and +25‰. The stratigraphic horizon almost always shows positive measurements. The measurements on the foot wall have the mode at 5 ‰ and vary between -15 ‰ and +10 ‰ and those on the hanging wall have the mode at 1 ‰ and vary between -35 ‰ and +3 ‰. The measurements of sulfur isotope of the pelite (which may be older than the ore-bearing layer) collected in the non-mineralization area have the mode at 13 ‰ and vary between -3 ‰ and

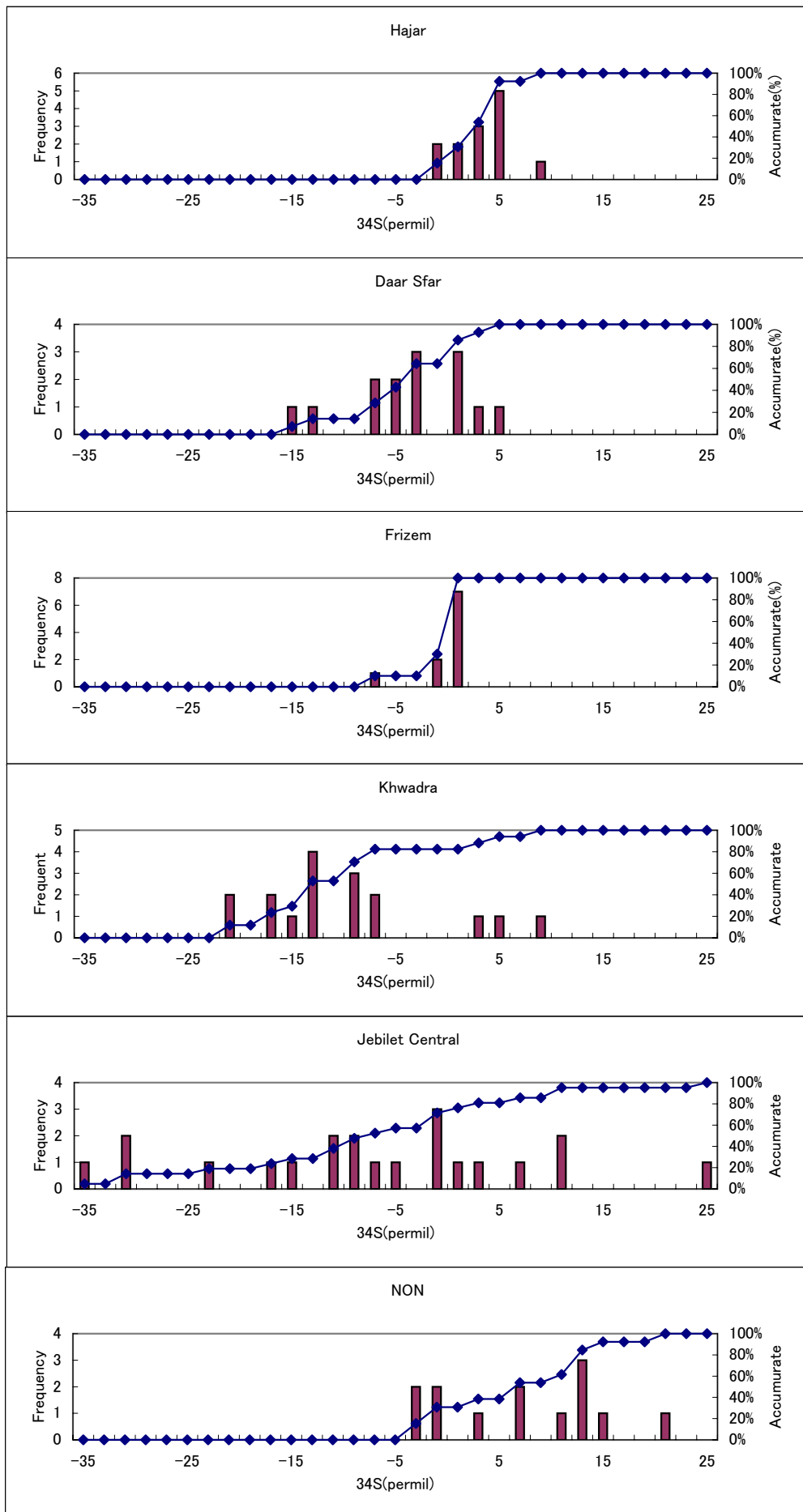


Fig.II-4-14 Histogram of Sulfide Isotope of sulfide in Mudstone (1)

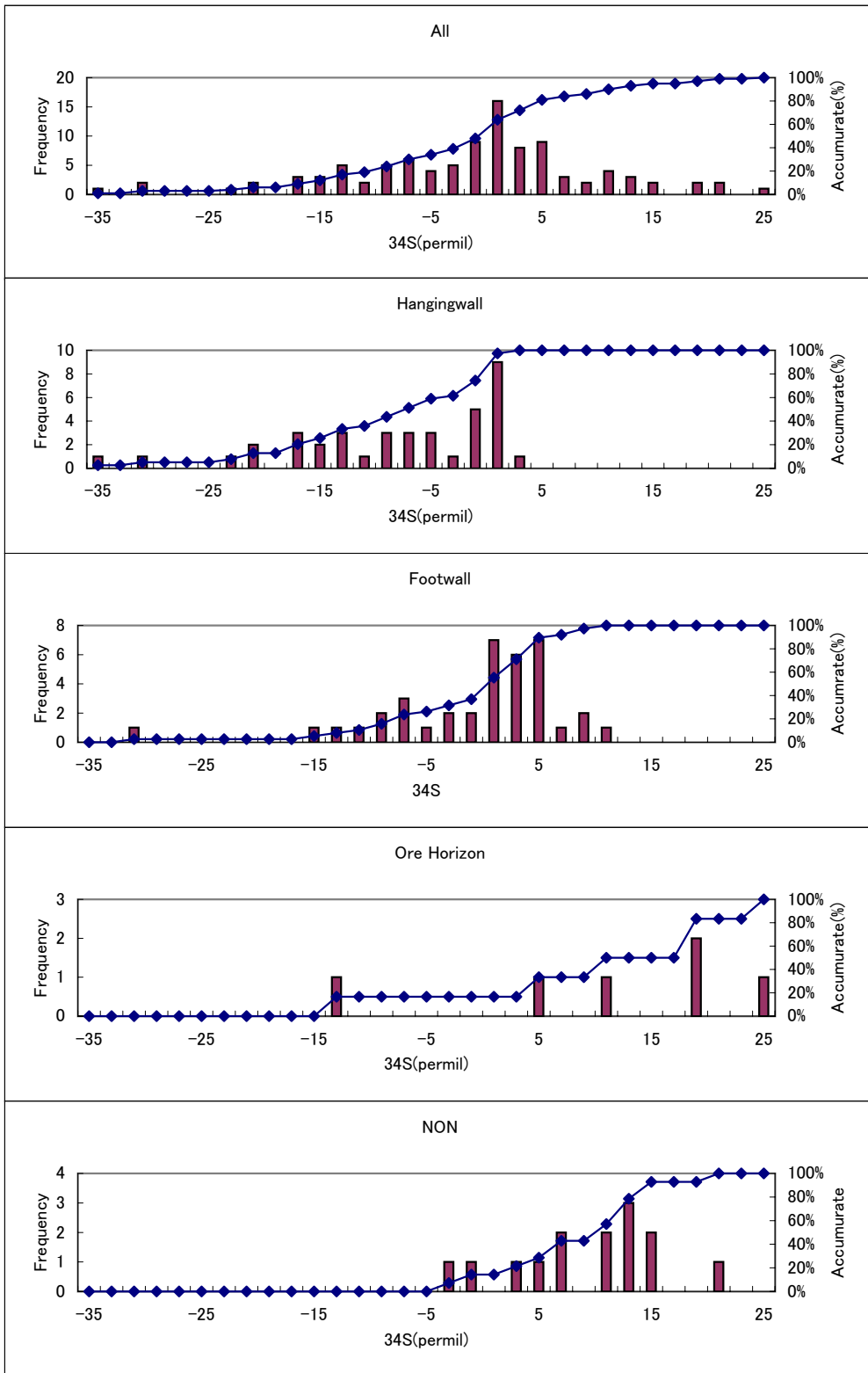


Fig.II-4-15 Histogram of Sulfide Isotope of sulfide in Mudstone (2)

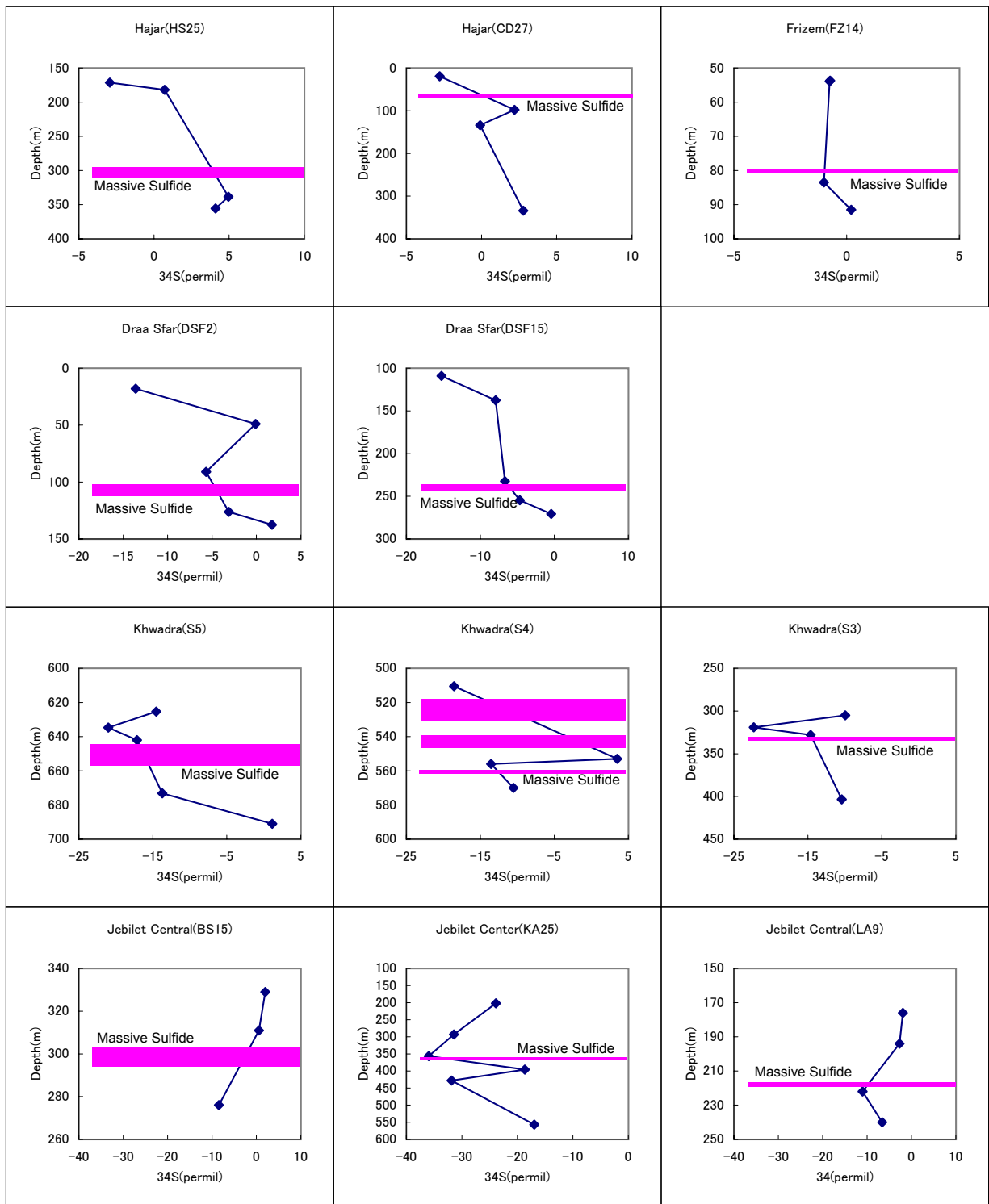


Fig. II-4-16 Variation of Sulfur Isotope of sedimentary rocks by depth of drilling

+21 ‰) (Fig.II-4-14).

For the sulfur isotope composition of the pelite on each ore deposit, the measurements have the mode around +5 ‰ and vary between -1 ‰ and +10 ‰ on the Hajar deposit, the mode from -3 ‰ to +1 ‰ and vary between -15 ‰ and +5 ‰ on the Draa Sfar deposit, and the mode around -11 ‰ and vary between -20 ‰ and +10 ‰ on the Khwadra deposit. The measurement results show that the distribution of the measurements differ in each ore deposits(Fig.II-4-15).

Also, there is a change in measurements of sulfur isotope composition of the pelite by depth. The measurements vary between +5 ‰ and -5 ‰ from the foot wall to the hanging wall, with a massive sulfide mineralization area intercalated, on the Hajar deposit (HS25, CD27), from +0 ‰ to -15 ‰ on the Draa Sfar deposit (DSF2, DSF15), and from +0 ‰ to -20 ‰ on the Khwadra deposit (S5) (Fig.II-4-16).

## (2) Considerations

It is known that bacterial interference will enrich light sulfur. From this fact, the above-mentioned tendency of the sulfur isotope composition to shift to negative values from the Hajar deposit (-1 ‰ to +10 ‰) to the Draa Sfar deposit (-15 ‰ to +5 ‰) and to the Khwadra deposit (0 ‰ to +10 ‰) suggests a strong bacterial influence from the Hajar deposit to the Khwadra deposit (-20 ‰ to +10 ‰) and a strong element of indirect sulfide sedimentation from hydrothermal activities.

On the other hand, Kaiwara (1989) and Kajiwara and Kaiho (1992) maintained that whether the formation atmosphere of marine sediment is oxidative or reductive can be estimated, on the basis of the sulfur isotope composition of the marine sediment.

Also, Komuro (1999) created a sulfur isotope separation model in oxidation - reduction atmosphere. Komuro maintained that oxidation and reduction would be repeatedly caused by oxidation and reduction bacteria on sediment formed in oxidative atmosphere while only reduction would be caused by reduction bacteria on sediment formed in reduction atmosphere, and as a result, if the sulfur of the marine sediment was as light as about 25 ‰ of the seawater sulfur in reduction atmosphere, the marine sediment had been formed in reduction atmosphere and if it was lighter than 25 ‰ in reduction atmosphere, the marine sediment had been formed in oxidation atmosphere. From the present sulfur isotope measurement of the pelite, the fact that the sulfur isotope composition changes to light values from the foot wall to the hanging wall with a massive sulfur deposit intercalated in the Whole areas and on each ore deposit suggests that the seabed changed from reduction atmosphere to oxidation atmosphere, passing through a period of massive sulfide deposit formation.



#### 4-3-2-4 Fossil survey and others

##### (1) Results

In this survey area, sedimentary rocks with a relatively low level of metamorphism such as shale, sandy shale, slate, and sandy slate and those with a relatively high level of metamorphism such as muscovite schist, garnet biotite muscovite schist, and crystalline limestone are distributed in this area. An existing document (BHP-UTAH 1987) describes that conodont fossils were furnished near Tameslouht in the Guemassa mountain mass, in Ghoula, Mjed North, Haloudi West, Amzourh, Douar Akhlij, to the east of Hajar, and in other places, but details are unknown.

In the fossil survey, the following three types of treatment were conducted and thin sections of rock were observed with a microscope.

- 1) Hydrogen fluoride treatment (A rock was crushed, leached in 2% hydrogen fluoride for a day, etched, and then observed with a stereomicroscope in order to extract fossils of pelite origin.)
- 2) Boron treatment (A rock was crushed, chemically treated with boron, and then observed with a stereomicroscope in order to extract fossils of limestone and pelite origins.)
- 3) Acid - alkali treatment (A rock was treated with acid, alkali, and heavy fluid (specific gravity 2.2) to separate organic microfossils) and a microscopic observation with rock thin section were carried out.

In the present fossil survey, a fossil assumed to be a foraminifer with a diameter of 2.3 mm or less and the other assumed to be coral with a diameter of 5.5 mm or less were discovered from a specimen of calcareous sandstone (02MR-K049) that cropped out near Tameslouht in the Guemassa mountain mass, as pseudomorphs replaced by carbonate minerals. The observation results of the rock thin sections, the observation results of the rock and polished sections, and the results of the fossil survey are shown in the table and photograph in the end of this report.

##### (2) Considerations

In the fossil survey, the existence of fossils was not recognized in almost all samples because diagenesis or metamorphism may have decomposed and destroyed fossils in the treated samples.

## Chapter 5 Airborne Geophysical Survey

### 5-1 Outline of the survey

Airborne electromagnetic survey and airborne magnetic survey were carried out as the airborne geographical survey in Marrakech-Tekna area. The obtained data was analysed together with the one obtained from the existing airborne geophysical survey and surface geological survey. The purpose was to extract prospective area of massive sulfide ore deposit and to examine the prospective areas as the target area for the second year survey.

The survey area (Tekna area) was an area of about 1,100km<sup>2</sup> between the Jebilet mountain massif and the Guemassa mountain massif, which lies southwest of Marrakech (Fig.II-5-1, Table II-5-2). The northern half of the area is a flat ground of 400m-500m above sea level, almost the entire part of which is covered with the Quaternary system Alluvium. The southern half of the area is a hill of 600m-800m above sea level, in the western part of which there are pelites, shales, limestones, and tuffs as the bedrock formed in the Paleozoic Carboniferous Period exposed. The area includes 3 known ore deposits, namely, Hajar deposit (being extracted as Hajar Mine) in the southeast of the area, Frizen deposit (unextracted) in the southwest, and Khwadra deposit in the northwest.

We carried out the airborne electromagnetic/magnetic prospecting as an airborne geophysical prospecting method. Marrakech Airport was used as the working base for the site survey. Period for the data acquisition was from January 11, 2002 to February 5, 2003. Total traverse line was 6,835.5 line km (Table II-5-1).

Table II-5-1 Schedule of the Airborne Geophysical Survey

Function	From	To	NOV	DEC	JAN	FEB	MAR
Aviation Permitting	Nov. 26	Dec. 31		██████████			
Move Aircraft	Jan. 4	Jan. 8			██		
Mobilisation	Jan. 4	Jan. 10			██		
Data Acquisition	Jan. 11	Feb. 5			██████████		
Preliminary processing	Jan. 11	Feb. 20			██████████		
Final Processing	Feb. 21	Feb. 28				██	
Preliminary Report	Mar. 28	Mar. 3					██
Final report	Mar. 3	Mar. 10					██

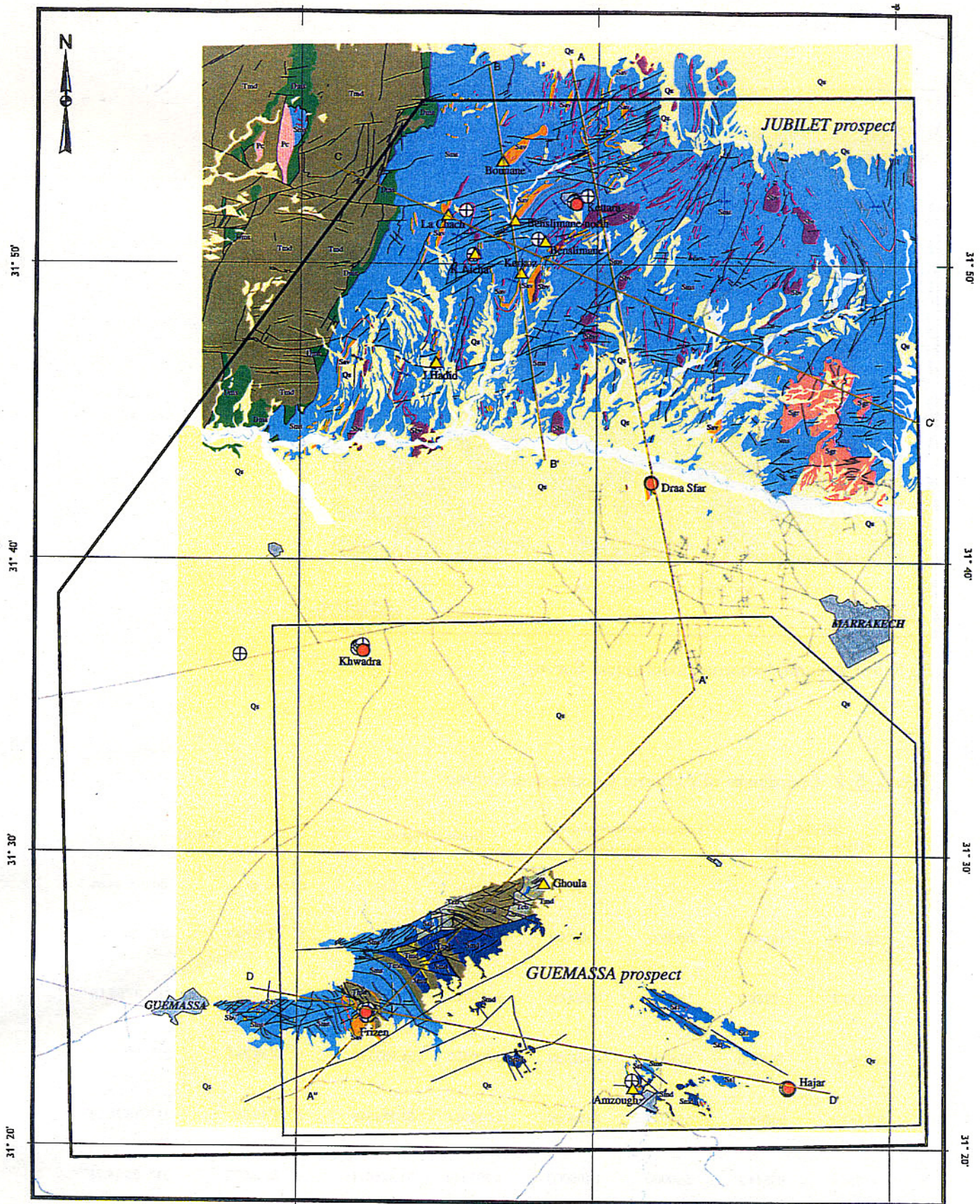


Fig.II-5-1 Area of Airborne Geophysical Survey

TableII-5-2 Coordinate of Airborne Geophysical Survey

#	WGS84, UTM Zone 29N		Lambert conformal conic Morocco Zone1		Decimal Degree		Degree	
	x	y	E	N	Lon	Lat	dd mm ss.ss	dd mm ss.ss
1	218377.6	119540.9	560000	3500000	-8.367288	31.633619	8 ° 22'2.24"	31 ° 38'1.03"
2	240373.3	118788.9	582000	3500000	-8.135313	31.632258	8 ° 08'7.13"	31 ° 37'56.13"
3	252098.0	110381.3	594000	3492000	-8.009553	31.559170	8 ° 0'34.39"	31 ° 33'33.01"
4	251213.2	84384.8	594000	3466000	-8.012017	31.324618	8 ° 0'43.26"	31 ° 19'28.62"
5	217214.4	85544.2	560000	3466000	-8.369349	31.326871	8 ° 22'9.66"	31 ° 36'36.73"





Geology		Deposit type	
A	Albium	● VMS	⊕ Drilling point
Qs	Quaternary	▲ Gossan	✕ fold
Pc	Sedimentary rocks		
Tmd	Permian		
Teb	Conglomerate		
	Toguin Fm.		
	Black shale		
	Toguin Fm.		
	Carbonate rocks		
Ssl	Sarraf Fm.	Dms	Devonian
Ssm	Sarraf Fm.	Vb	Black shale
Sms	Sarraf Fm.	IG	Volcanic breccia
Sgr	Sarraf Fm.		Gossan
Sav	Sarraf Fm.		
Sbv	Sarraf Fm.		
Smd	Sarraf Fm.		
	Black shale		

Fig.II-5-2 Geological map of Marrakech-Tekna area



## 5-2. Airborne electromagnetic/magnetic survey system

Airborne electromagnetic survey systems being available for ore deposits survey at present is specified in Table II-5-3 by its time ranges and frequency ranges. The system used for this survey is Fugro's GEOTEM system. This system was an airborne electromagnetic survey system for time ranges which Geotrex, Inc. in Canada developed and commercialized in the first half of the 1990s. But Fugro owns the system now as a result that Geotrex merged with Dighem and then Fugro bought out the merged company. The specifications and the measurement concept of this system are shown in Table II-5-4 and Fig.II-5-2.

Table II-5-3 Airborne Electromagnetic system

AEM system	Aircraft	Time/Frequency	Developer	Organization	Status
GEOTEM	Fixed wing	Time	Fugro	Contractor	Operating
SPECTREM TEM	Fixed wing	Time	Angro American	Mining Company	Operating
TEMPEST	Fixed wing	Time	Fugro	Contractor	Operating
MAGTEM	Fixed wing	Time	Fugro/Noranda	Contractor / Mining Company	Operating
Heli TEM	Helicopter	Time	MIM/Aerodat	Mining Company /Contractor	Operating
EXPLORHEM	Helicopter	Time	Angro American	Mining Company	Commercialization?
Aero TEM	Helicopter	Time	Aeroquest	Contractor	Operating
T.H.E.M	Helicopter	Time	T.H.E.M. Geophysics	Contractor	Operating
HoistEM	Helicopter	Time	Normandy	Mining Company	Operating
Newmont Airborne EMP	Helicopter	Time	Newmont	Mining Company	Operating
MIDAS	Fixed wing	Frequency	Fugro	Contractor	Operating
GTK AEM	Fixed wing	Frequency	Geological Survey of Finland	Laboratory	Operating
DIGHEM	Helicopter	Frequency	Fugro	Contractor	Operating
GEM 2A	Helicopter	Frequency	Geophex-UTS	Contractor	Operating
Humming bird	Helicopter	Frequency	Geotech	Contractor	Operating

(Nabighan and Asten(2002), Geophysics vol.67, no.3)

The GEOTEM system is a system which has a current transmission loop stretched on fixed wings of an airplane, where a current of 1-25Hz with its wave shape shown in Fig.II-5-3 is transmitted and two components (x component: the airplane's flying direction, z component: its vertical direction) of electromagnetic response of the earth, which is induced by the current, are measured by an induction coil installed on an electromagnetic sensor bird in tow. The

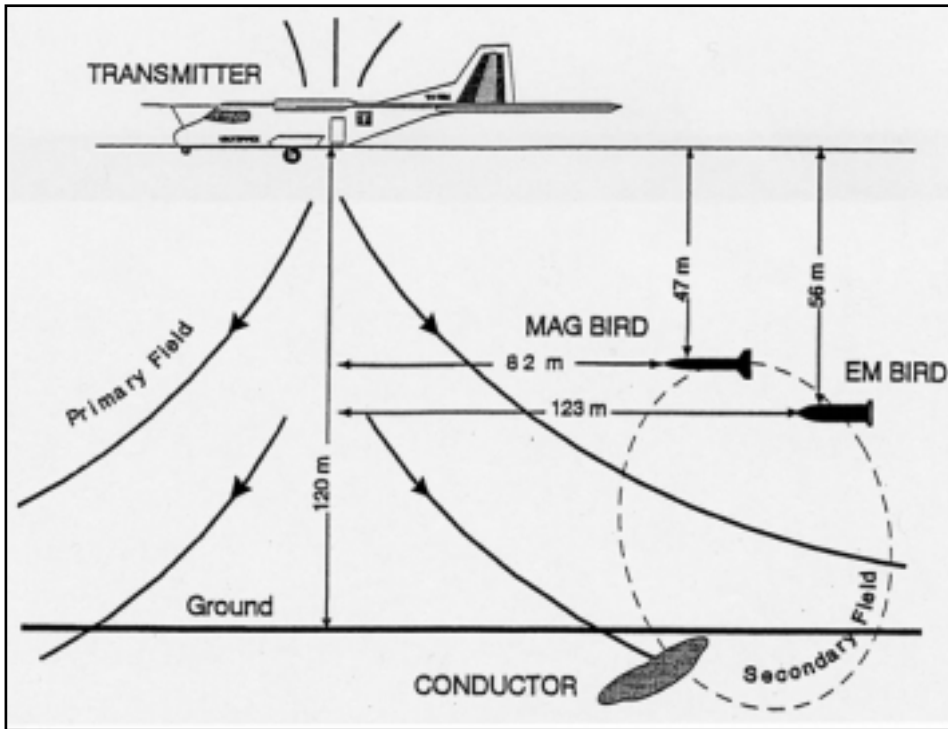


Fig.II-5-3 GEOTEM electromagnetic and magnetic System

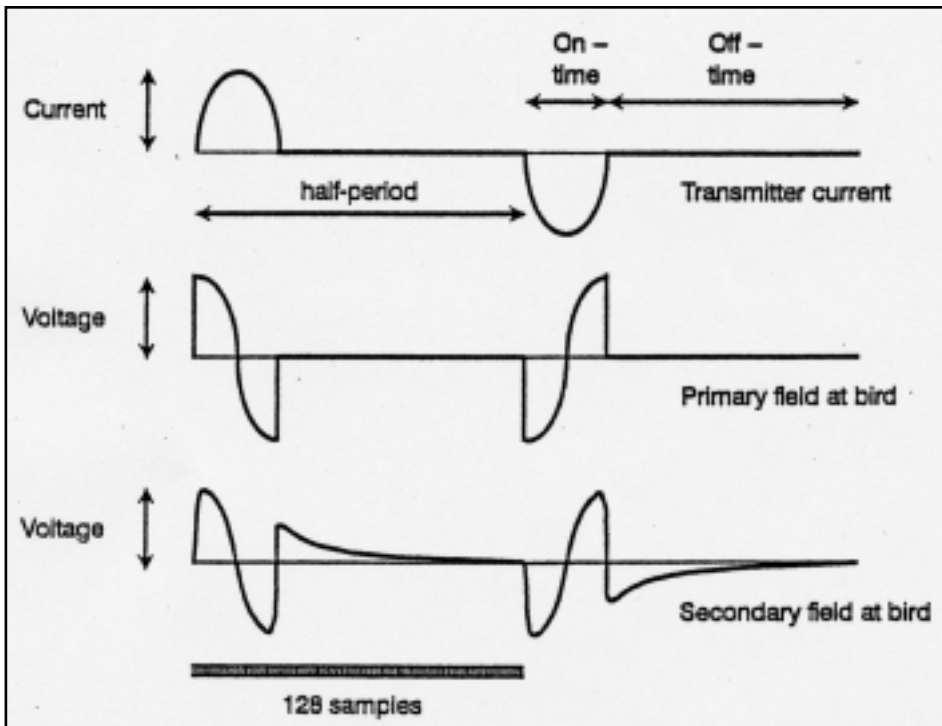


Fig.II-5-4 The half-sinoidal bipolar current wave form showing the on time and off time

flying altitude to the ground of the airplane is 120m and that of the sensor bird is 60m. The sampling cycle of the response is 0.1 seconds, and it can be measured through 20-channel windows from an early time to a late time (Table II-5-5).

The magnetic data was obtained through the measurements of geomagnetic field intensity by a Cs magnetometer installed in another magnetic sensor bird in tow. The former sensor bird's height to the ground was 70m, and the sampling frequency of the geomagnetic field was 0.1 seconds.

Table II-5-4 GEOTEM system (on the aircraft)

Manufacturer	FUGRO AIRBORNE SURVEYS			
Model	GEOTEM <sup>®</sup>			
Base frequency	15 or 12.5 Hz	30 or 25 Hz	90 or 75 Hz	150 or 125 Hz
Pulse width	4 ms	4 ms	2 ms	1 ms
Loop	6 turns	6 turns	5 turns	3 turns
Loop area	231 m <sup>2</sup>	231 m <sup>2</sup>	231 m <sup>2</sup>	231 m <sup>2</sup>
Dipole moment (approx.)	0.69x10 <sup>6</sup> Am <sup>2</sup>	0.69x10 <sup>6</sup> Am <sup>2</sup>	0.62x10 <sup>6</sup> Am <sup>2</sup>	0.40x10 <sup>6</sup> Am <sup>2</sup>
Peak transmitter current	500 AMP	500 AMP	540 AMP	585 AMP
½ Waveform sampling rate	384 per pulse	384 per pulse	128 per pulse	128 per pulse
Windowed data sampling rate	4 Hz	4 Hz	4 Hz	4 Hz
Pre-stack ("stream") data sampling rate	192 per pulse	192 per pulse	64 per pulse	192 per pulse
Receiver	3-component induction coil sensor			
Measured response	voltage (dB/dt) and B-field			
Noise levels	< +/-3500 pT/s as measured on raw, late off time dB/dt data			
Bandwidth	Base frequency to 10 kHz			
Stacking rate	4 per second			
Digital recording	all raw data channels			
Analog chart	12 channels of real-time filtered dB/dt EM data ( X component), 4 channels of raw EM data (2 X and 2 Z component), X and Y primary EM field strength monitor			

Table II-5-4 GEOTEM system (on the base station)

<b>Equipment</b>	<b>Specification</b>	<b>Equipment</b>
<b>Magnetometer</b>	Manufacturer	Scintrex
	Type	Cesium vapour optically pumped, split beam
	Model	CS-2
	Sampling rate	2 Hz
	Sensitivity	0.01 nT
	Noise envelope	< 0.5 nT
<b>GPS Receiver</b>	Manufacturer	Sercel
	Type	10 channel C/A code & carrier phase
	Model	NR 109, NR 106 or NR103
	Sampling rate	1.66 Hz
	Differential position accuracy	Better than 5 m
	Autonomous position accuracy	Better than 20 m if SA disabled
	Autonomous position accuracy	Better than 100 m if SA enabled
<b>PC and Printer</b>	Laptop Pentium PC	1 Ghz CPU, 512 mB RAM, 30 GB HDrive
	Colour inkjet plotter	HP 750C
	Colour inkjet printer	HP 350c



Table II-5-5 Electromagnetic Sampling data

Channel	Start (p)	End (p)	Width (p)	Start (ms)	End (ms)	Mid (ms)
1	3	9	7	0.104	0.469	0.286
2	10	31	22	0.469	1.615	1.042
3	32	55	24	1.615	2.865	2.24
4	56	77	22	2.865	4.01	3.438
5	78	83	6	4.01	4.323	4.167
6	84	86	3	4.323	4.479	4.401
7	87	89	3	4.479	4.635	4.557
8	90	93	4	4.635	4.844	4.74
9	94	99	6	4.844	5.156	5
10	100	107	8	5.156	5.573	5.365
11	108	117	10	5.573	6.094	5.833
12	118	129	12	6.094	6.719	6.406
13	130	143	14	6.719	7.448	7.083
14	144	161	18	7.448	8.385	7.917
15	162	183	22	8.385	9.531	8.958
16	184	211	28	9.531	10.99	10.26
17	212	245	34	10.99	12.76	11.875
18	246	285	40	12.76	14.844	13.802
19	286	331	46	14.844	17.24	16.042
20	332	384	53	17.24	20	18.62

## 5-3 Results of the Airborne Gyophysical Survey

### 5-3-1 Outline

The airborne electromagnetic/magnetic survey data was obtained with the survey line in E-W direction and the spacing lines of 200m and with the tie line in NS direction and the spacing lines of 1000m. The length of the flight was total 6,853.5 line-km (survey line (200 survey lines: Line No. 10,000-15,000), and that of the tie line (20 survey lines: Line No. T10,000-T15,000)) (Fig.II-5-5). The final data was produced as 39-channel digital data composed of positional (latitude, longitude, etc.), topographical (height above the sea level), magnetic and electromagnetic data by flight survey lines (survey line and tie line )(Table II-5-6).

The final grid data which Fugro submitted includes one kind of magnetic data (residual magnetic intensity) and four kinds of electromagnetic data (apparent conductivity, total energy envelope, decay constant, and moment).

(a) Residual magnetic intensity (RMI): This is a value obtained by deducting the value of the international geomagnetic reference field (IGRF) from the value of the total magnetic intensity (TMI).

(b) Apparent conductivity: This can be obtained, calculating the  $B_x$  and  $B_z$  obtained by time-integrating the  $x$  and  $z$  components ( $(dB/dt)_x$  and  $(dB/dt)_z$ ) of each channel's electromagnetic response.

(c) Total energy envelope: The value can be obtained, using the  $x$  and  $z$  components ( $(dB/dt)_x$  and  $(dB/dt)_z$ ) of each channel's electromagnetic response and values obtained by Hilbert-converting them. It can be defined as the following formula (Smith & Keating, 1996). It is similar to the "Analytic Signal," which is one of the magnetic data processing methods.

(d) Decay constant: In case a signal transmission electromagnetic field intensity attenuates on an exponential function basis under the ground, it can be found by calculating time up to its value of  $1/e$ . The decay constant will be larger in the conductive (low resistivity) ground than in the nonconductive (high resistivity) ground.

(e) Moment: This can be obtained by time-integrating the product of an impulse response and an  $n$  power of time, defined as the following formula and described as an  $n$ -degree moment (Smith & Lee, 2002). The response in the deeper parts can be emphasized on by increasing its graveness in late time rather than in early time.

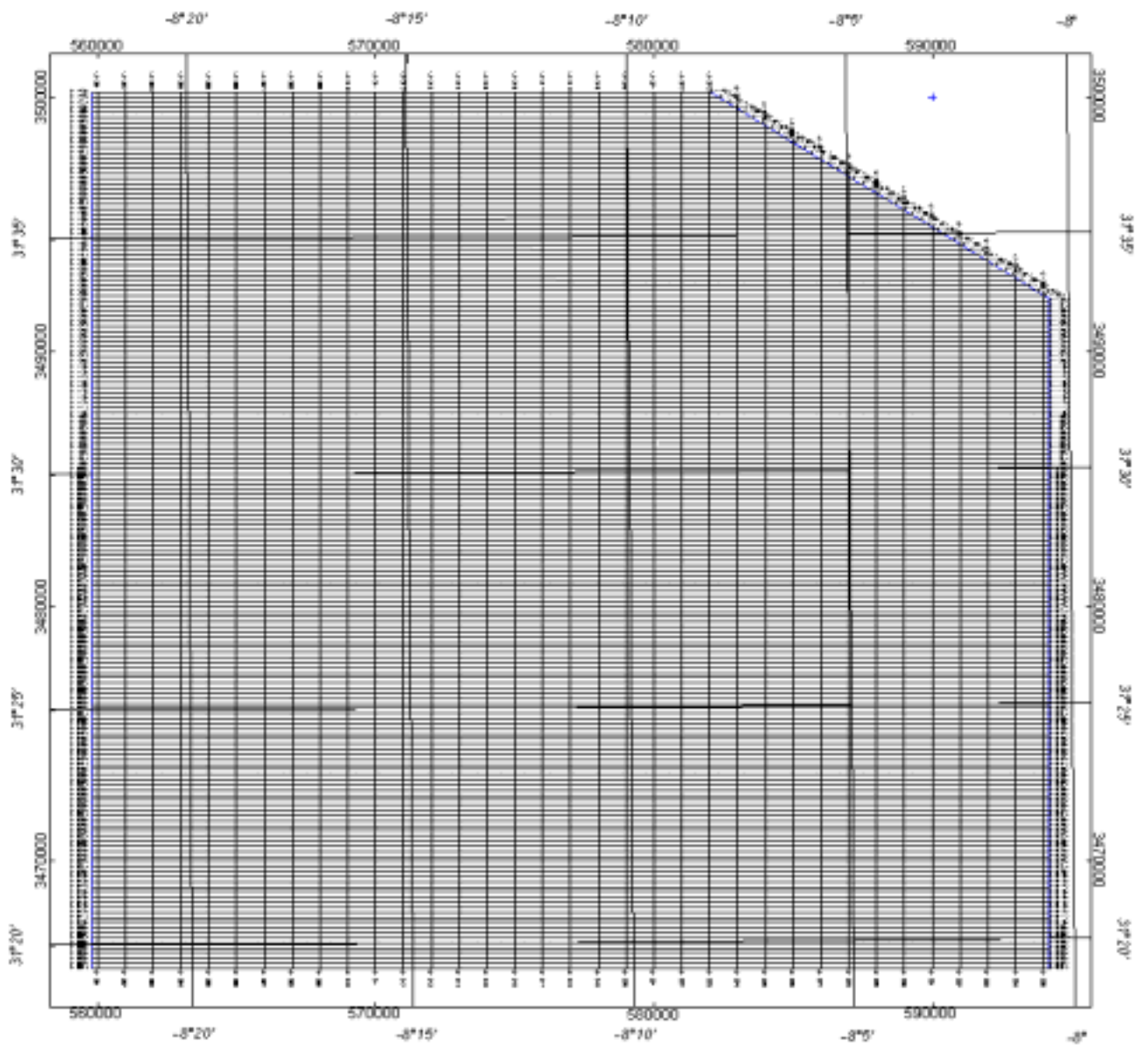


Fig.II-5-5 Flight Pass

Table II-5-6 List of data acquired in the survey

FIELD	VARIABLE	UNITS
LINE	Line	line *100 + part
FID	Fiducials	seconds
FLT	Flight Number	flight Number
DATE	Date	ddmmyy
LAT_WGS84	Latitude in WGS 84	degrees
LONG_WGS84	Longitude in WGS 84	degrees
X_LAMBERT	Easting (X) in Lambert	metres
Y_LAMBERT	Northing (Y) in Lambert	metres
X_WGS84	Easting (X) in WGS 84	metres
Y_WGS84	Northing (Y) in WGS 84	metres
ELEVATION	GPS Elevation	metres
RADAR	Radar Altimeter	metres
BARO	Barometric Altimeter	metres
TERRAIN	Terrain	metres
DIURNAL	Ground Magnetic Intensity (Diurnal)	nT
LFC_DIURNAL	Low Frequency Component of the Diurnal	nT
TMI	Airborne Total Magnetic Intensity (TMI)	nT
IGRF	Regional Magnetic Field	nT
RMI	Final Airborne Residual Magnetic Intensity	nT
TX_CURRENT	Transmitter Current	amps
EMPF	Electromagnetic Primary Field	$\mu$ V
HZ_MONITOR	Powerline Monitor (50Hz)	$\mu$ V
dBdtx_raw	Raw dB/dt X-coil Channels 1-20	pT/s
dBdty_raw	Raw dB/dt Y-coil Channels 1-20	pT/s
dBdzt_raw	Raw dB/dt Z-coil Channels 1-20	pT/s
dBdtx_fin	Final dB/dt X-coil Channels 1-20	pT/s
dbdty_fin	Final dB/dt Y-coil Channels 1-20	pT/s
dBdzt_fin	Final dB/dt Z-coil Channels 1-20	pT/s
Bfieldx_raw	Raw B-Field X-coil Channels 1-20	fT
Bfieldy_raw	Raw B-Field Y-coil Channels 1-20	fT
Bfieldz_raw	Raw B-Field Z-coil Channels 1-20	fT
Bfieldx_fin	Final B-Field X-coil Channels 1-20	fT
Bfieldy_fin	Final B-Field Y-coil Channels 1-20	fT
Bfieldz_fin	Final B-Field Z-coil Channels 1-20	fT
VG_1	Vertical Gradient	nT/km
MOMENT	5 <sup>th</sup> Order Moment (B-field X and Z)	ppm
COND	Apparent Conductivity (B-field X and Z)	mS/m
TAU	Decay Constant (dB/dt Z 12-20)	$\mu$ s
TEE	Total Energy Envelope (dB/dt X and Z 08)	pT/s

### 5-3-2 Digital topographical data

The survey area gradually heightens from its low-level ground with less than 400m of altitude above sea level in the northern part of this area toward the SSW direction. The flat shape changes to the hilly shape at the height of 550m-600m in the central part of the area and has a height above the sea level is over 800m at the southern end of the area. A national highway runs toward Marrakech along the boundary between the flat ground and the hill. There is a river flowing from its NNW-SSE direction to NNW in the center of the survey area. Water systems on the hill on its southern side runs between the northwestern and north-northwestern directions (Fig.II-5-6).

### 5-3-3 Airborne magnetic data

#### (1) Residual Magnetic Intensity (RMI) or Total Magnetic Intensity (TMI)

The southern part of the area is a low magnetic zone and its northern part a high magnetic zone. The boundary between these two zones almost corresponds to that between the flat ground and the hill. Judging from this, the boundaries seemingly originate from its geological structure such as a fault (ENE-WSW).

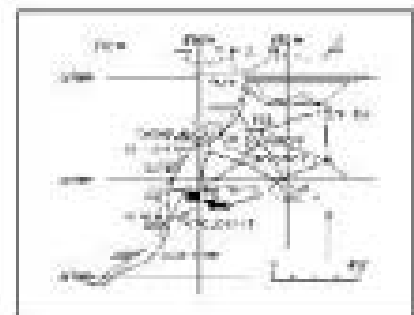
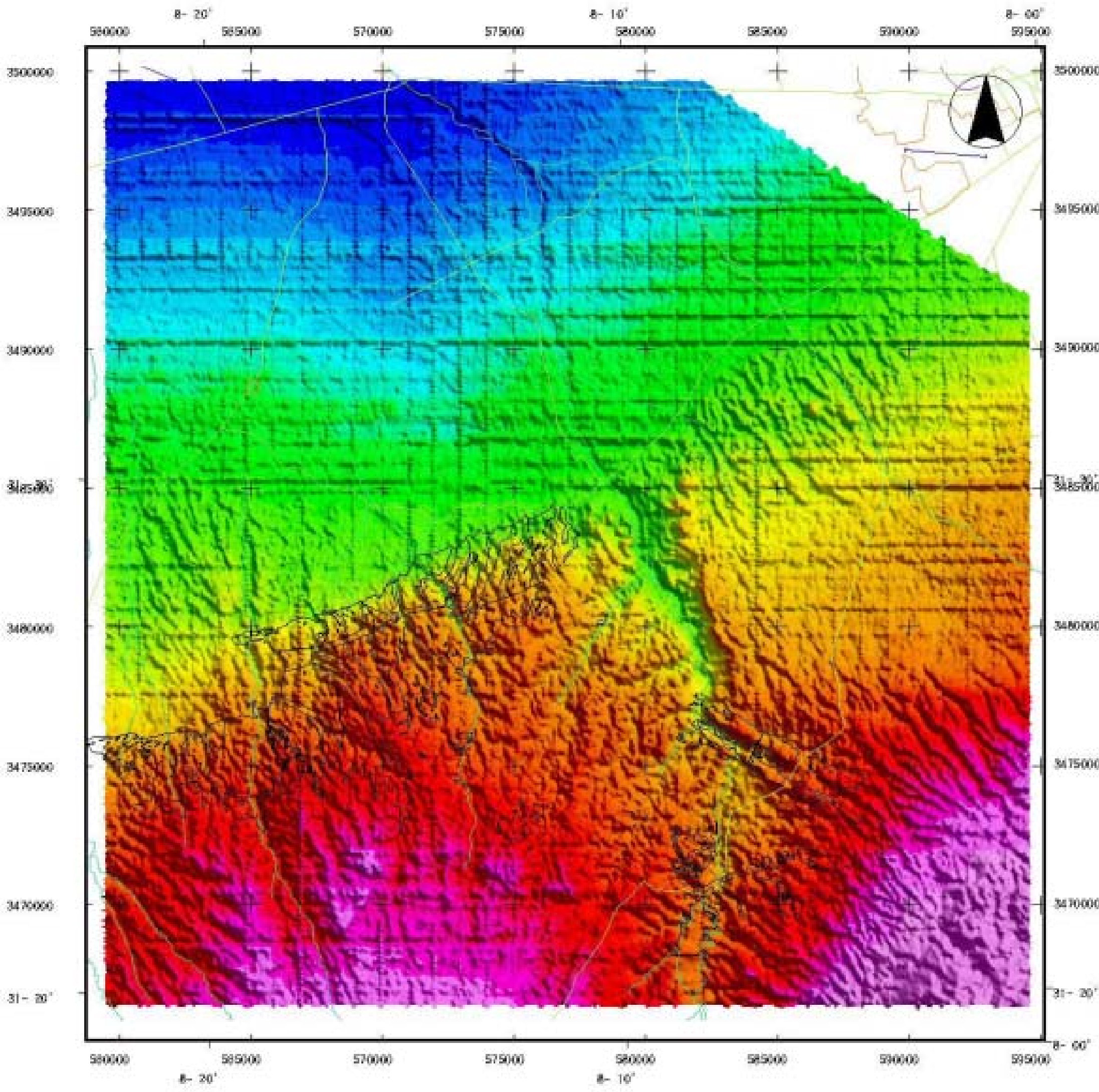
A high magnetic anomaly zone in the northern magnetic zone is relatively large with its diameter of 2-4km. There is a high magnetic anomaly with its diameter of about 8km at the northeastern end of the area, which seems to be a stock of granites.

There is a NW-SE magnetic arrangement confirmed in the western part of the northern part's high magnetic zone, and it extends over to the southern part's low magnetic zone. Also, there is a NNE-SSW magnetic arrangement confirmed at the western end of the abnormality which seems to be their stock mentioned above on the northern side's eastern part, and the arrangement's continuity can be traced to the southern side's low magnetic zone.

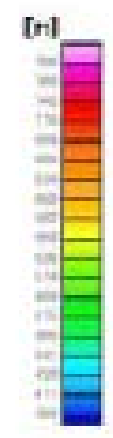
There are dotted slight magnetic anomalies with their diameter of 200m from the center of the high magnetic zone in the northern part of the area. On the eastern part, there is a repetition of minor magnetic rolls extending in the NW-SW direction. Judging from their appearances, they may be related to the stratification or schistosity.

The low magnetic zone on the southern side has a NW-SE trend as a Whole, and there is a wide low magnetic anomaly zone with the same trend extending especially on its central part. There are a high magnetic anomaly (almost corresponding to the Hajar deposit) at the eastern end of the zone and a high magnetic anomaly (a part of it almost corresponding to the Frizen ore deposit) at the western margin of the zone. The zone has a structure looking as if it has been cut in several sections by NE-SW faults.

There is a high magnetic anomaly with its diameter of 1-3 km confirmed in the western and eastern directions outside of the wide low magnetic anomaly zone (Fig.II-5-7, Fig.II-5-8).



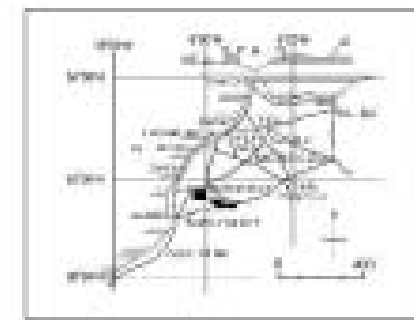
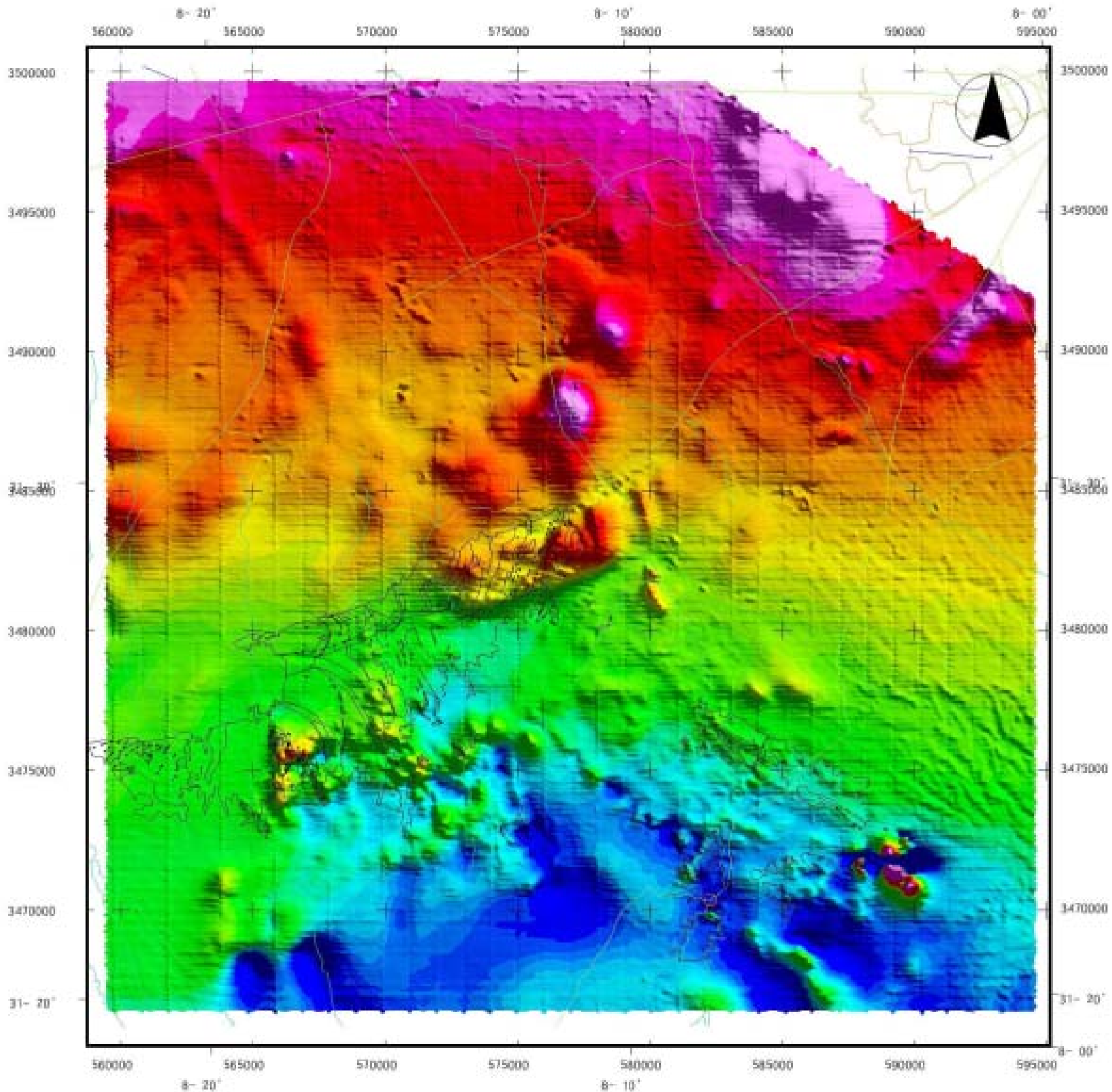
Digital Terrain Model



- Town
- Road
- River
- Railway



Fig.II-5-6 Digital terrain Model

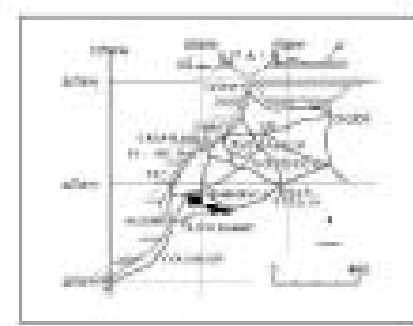
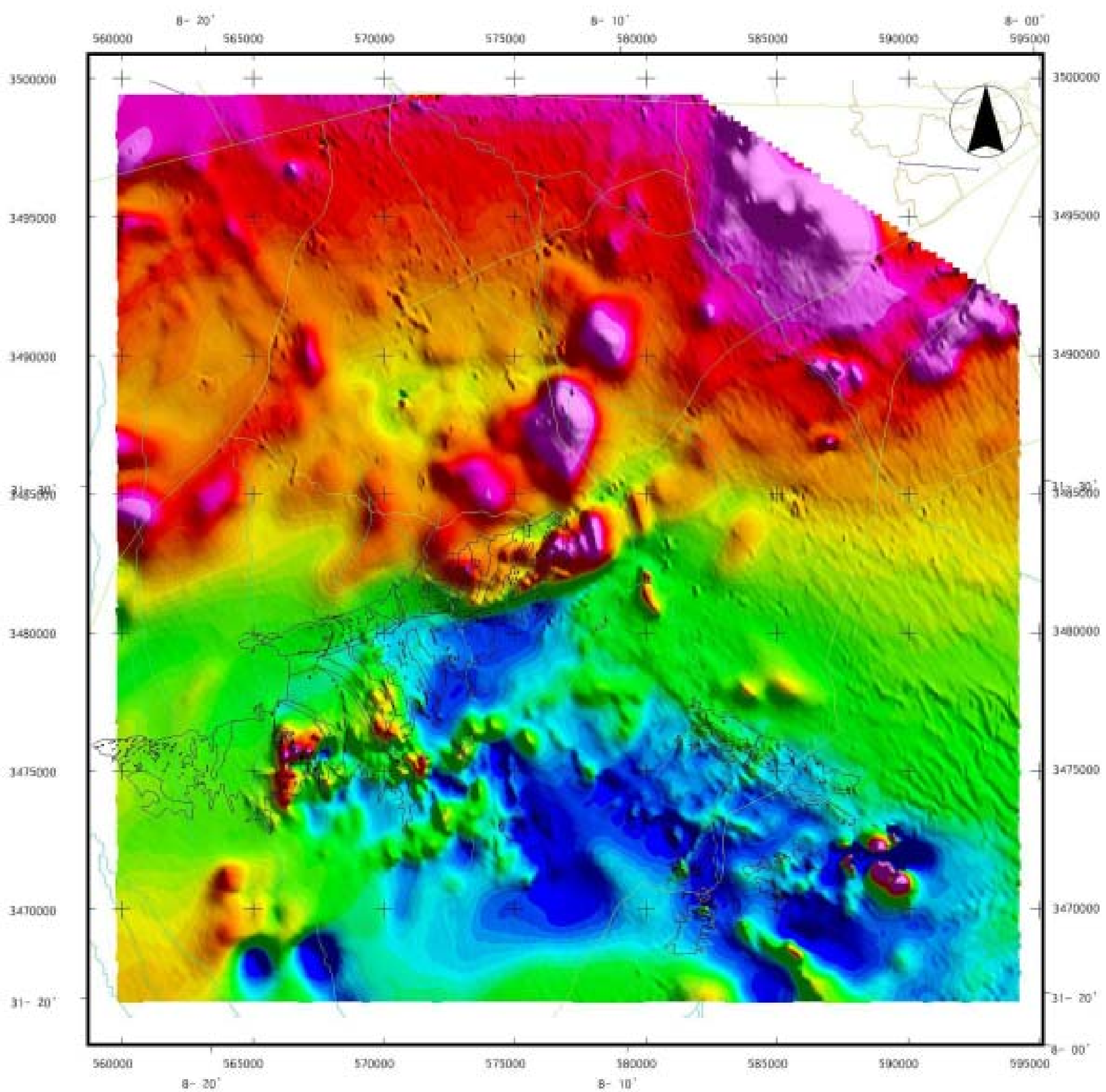


Total Magnetic Intensity

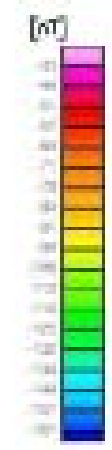


Fig.11-5-7 Total Magnetic Intensity





Residual Magnetic Intensity



- Town
- Road
- River
- Railway



Fig. 11-5-8 Residual Magnetic Intensity  
- 185 ~ 186 -



#### 5-3-4 Airborne electromagnetic data

Overviewing a drawing obtained from four kinds of electromagnetic data (apparent conductivity, total energy envelope, decay constant, and moment), all data indicate the same tendency in general, but there are differences in details. Culture noises due to power-transmission wires, etc. are almost removed in the total energy envelope, but remains remarkable in the moment and the decay constant. In the apparent conductivity, they are almost removed on the western side of the area and remains on its eastern side.

Resistivity structures on the northern and southern sides of a national highway running NE-SW in the middle of the area are different from each other, and the highway boundary seemingly corresponds to the boundary between its geological structures.

##### (1) Apparent conductivity

On the southern side of the resistivity boundary dividing the area into two parts, a high resistivity zone with its large distribution area on the western part and some high resistivity zones on the eastern part almost correspond to the exposed part of bedrocks (Paleozoic carboniferous-series sedimentary rocks and pyroclastic rocks) on the existing geological map.

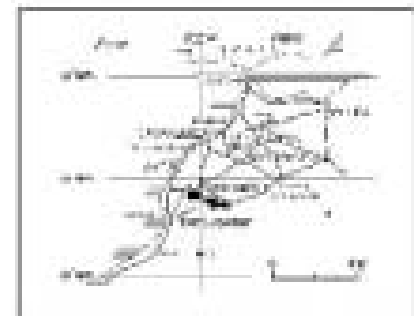
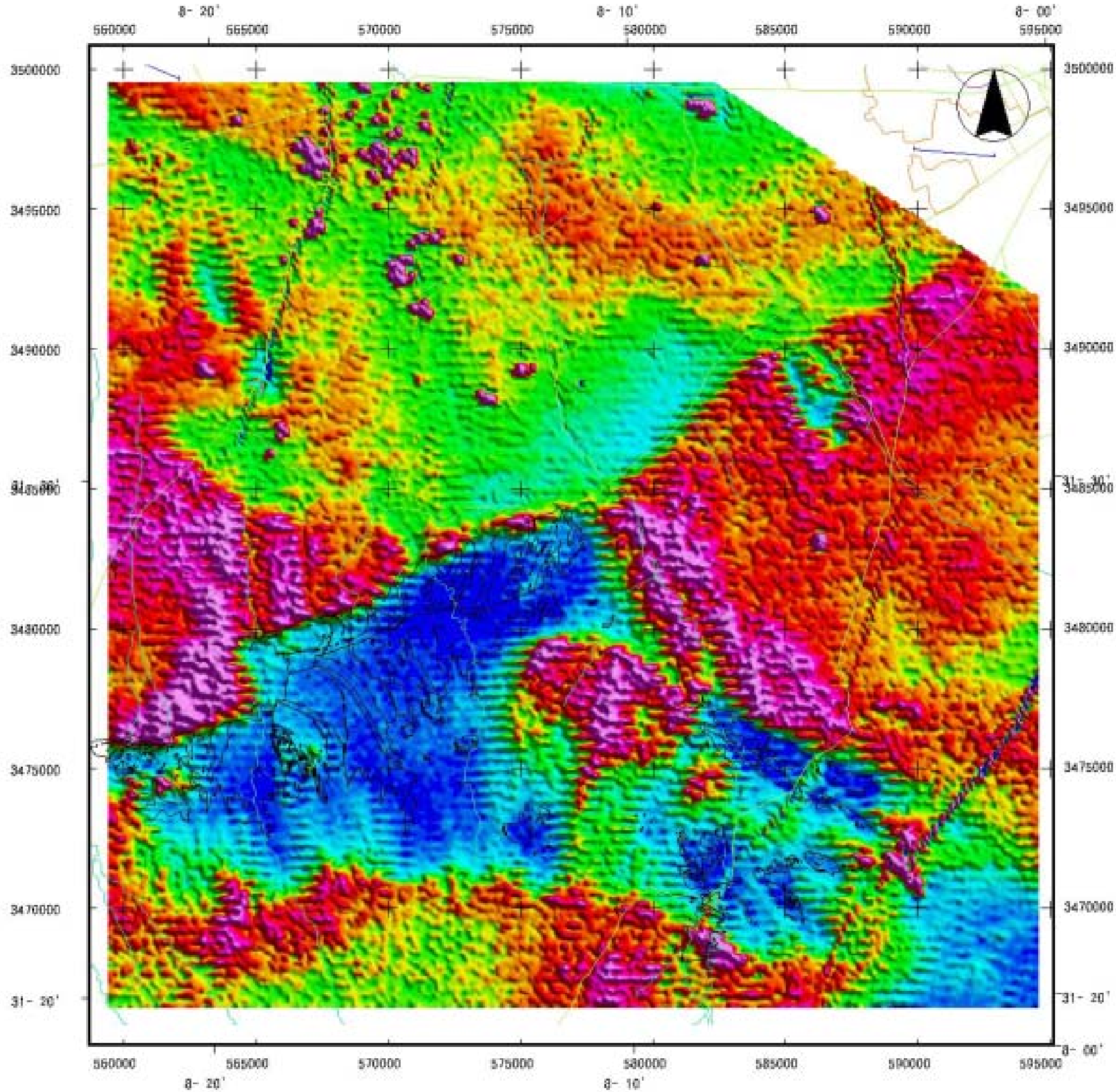
And it is obvious that the bedrocks generally show a high resistivity. On the other hand, almost the entire part other than the bedrocks exposed is an area where the Neogene's sediments (mp) distribute and the area has a low resistivity. Also, most of the distribution area (q) of the Quaternary sediments on the eastern part shows its low resistivity. It seems that there is a clear boundary between the high resistivity part which seems to be bedrocks and the low resistivity part around the former part and that the outcrop of a stratum boundary with its sharp inclination is covered.

The northern side generally has low-to-mid resistivity, but there is an area nearing the resistivity boundary in the middle, in a part of which a high resistivity distributes. There is a remarkable low resistivity zone confirmed on the western part. Comparing the part with the existing geological map, the zone corresponds to the distribution area (mp, pV2) of the Neogene's sediments.

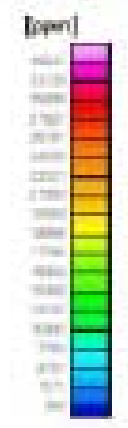
Besides, in the regional low-to-middle resistivity zones, a large number of marked local low resistivity areas of 200 – 2000 m are seen. No particular regularity is observed in the distribution or arrangement (Fig.II-5-13, Fig.II-5-9 – Fig. II-5-10).

##### (2) Total Energy Envelope

As a Whole, electromagnetic response (resistivity structure) shows the same tendency as in the apparent conductivity. The shadow extending in the E-W direction is stronger than that observed in apparent conductivity. This is considered to be attributable to the orientation of flight survey line. Following differences can be seen between the apparent conductivity data and total energy envelope data:



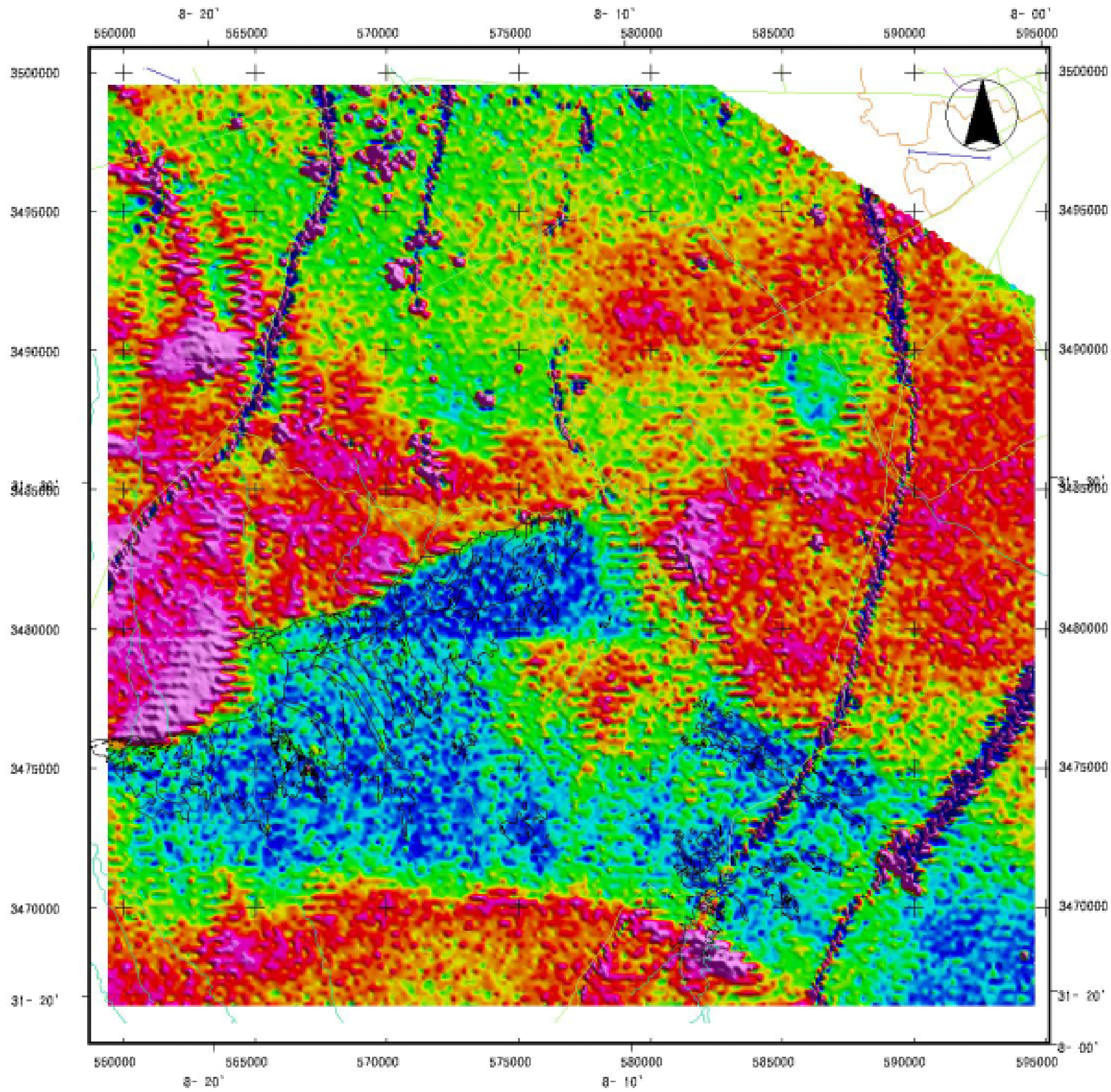
(dB/dt) x early time



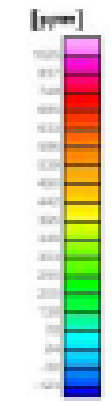
- Town
- Road
- River
- Railway



Fig.11-5-9 (dB/dt) x early time



(dB/dt)x late time



-  Town
-  Road
-  River
-  Railway



Fig.11-5-10 (dB/dt)x late time

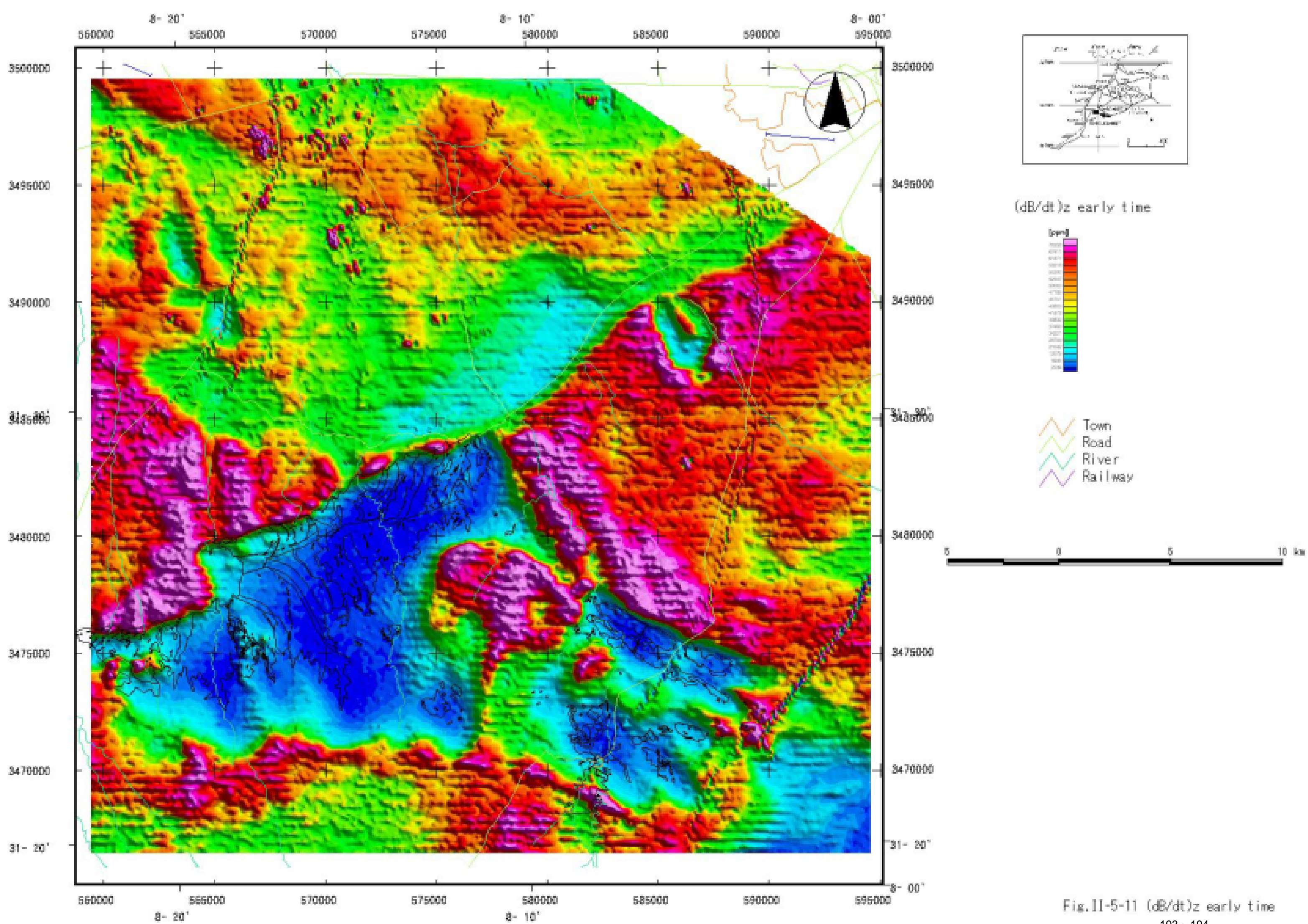


Fig.11-5-11 (dB/dt)z early time



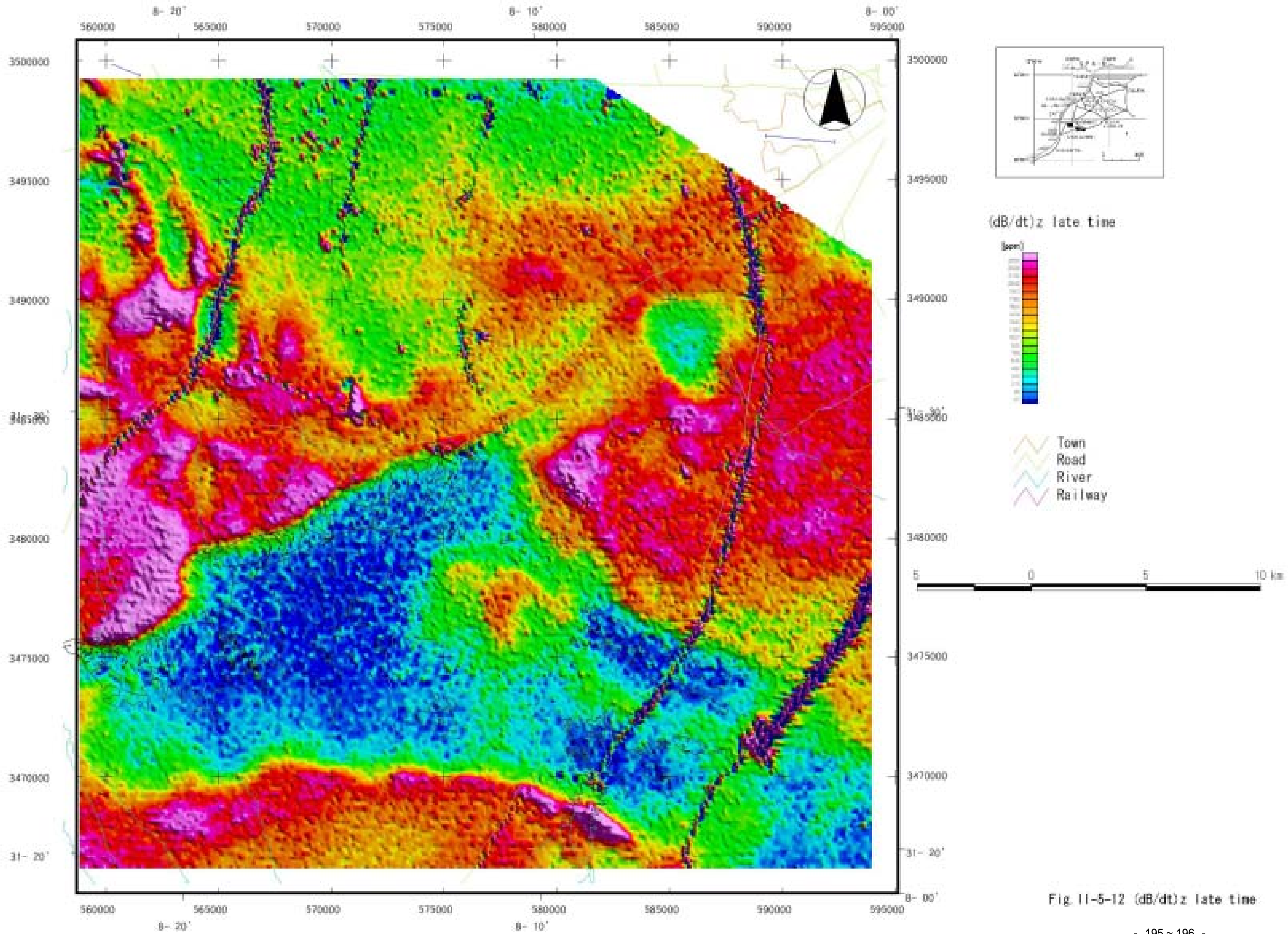


Fig II-5-12 (dB/dt)<sub>z</sub> late time

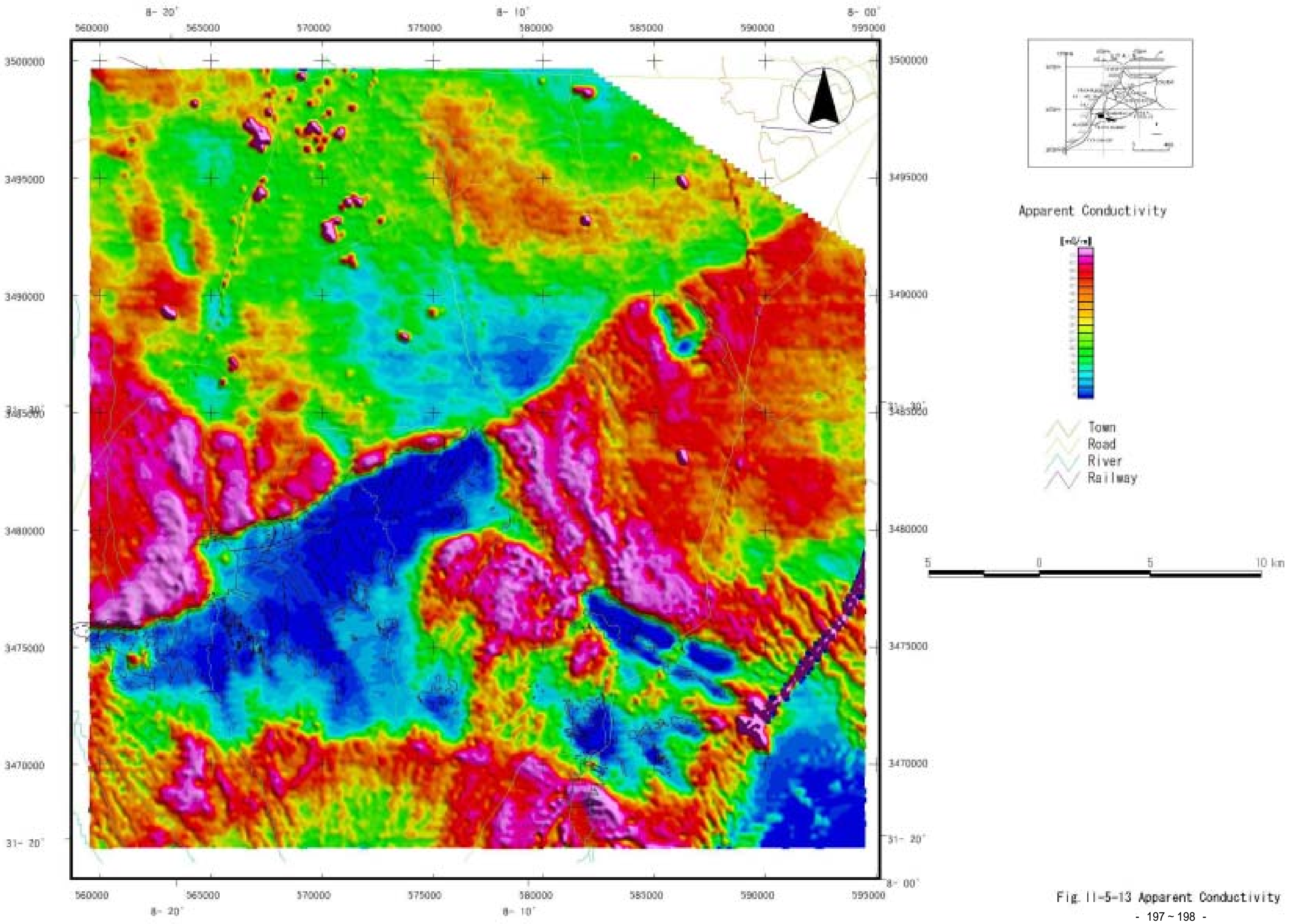


Fig. 11-5-13 Apparent Conductivity

1) South of the resistivity boundary at the center of the survey area (NE-SW system)

Both data show almost same results. In the north of the east end, however, the resistivity in the total energy envelope was a little higher than that in apparent conductivity.

2) North of the resistivity boundary at the center of the survey area (NE-SW system)

In total energy envelope, a low resistivity zone extends in the E-W direction at the north end. A part of the east and west sides occurring as a low resistivity zone in apparent conductivity indicates middle resistivity in the total energy envelope. The marked local low resistivity seen in apparent conductivity has partly remained in the total energy envelope and partly disappeared.

(3) Decay Constant and Moment

Both of these data show a similar resistivity structure except that fine dot-shaped signals are emphasized in moment whereas these signals seem to be averaged in decay constant. Comparing them with the apparent conductivity, following differences are found:

1) South of the resistivity boundary at the center of the survey area (NE-SW system)

All of the apparent conductivity data and these two data indicate that the base rock distribution area has a high resistivity except an area covered with sediments of the Neo-Tertiary where a considerable difference is observed. According to the data obtained by the apparent conductivity, the area around the base rock distribution area has a high – middle resistivity, while the same area appears as a low resistivity zone in the total energy envelope. In decay constant, the outside of this high-to-middle resistivity zone, i.e. to the east, south and west sides of the survey area, is a low resistivity zone, presenting a clear boundary with the middle resistivity zone.

2) North of the resistivity boundary at the center of the survey area (NE-SW system)

Except for the low resistivity zone at the west end, the apparent conductivity presents a resistivity structure contrary to the total energy envelope. That is, the low resistivity zone in the E-W direction at the north end observed in the total energy envelope presents a middle resistivity in the decay constant. A high-to-middle resistivity area extending to the east and west sides from the center in the total energy envelope appear as a low resistivity zone in the apparent conductivity.

However, the remarked local low resistivity extracted in the apparent conductivity is almost left as a low resistivity, except some parts. This also applies to moment.

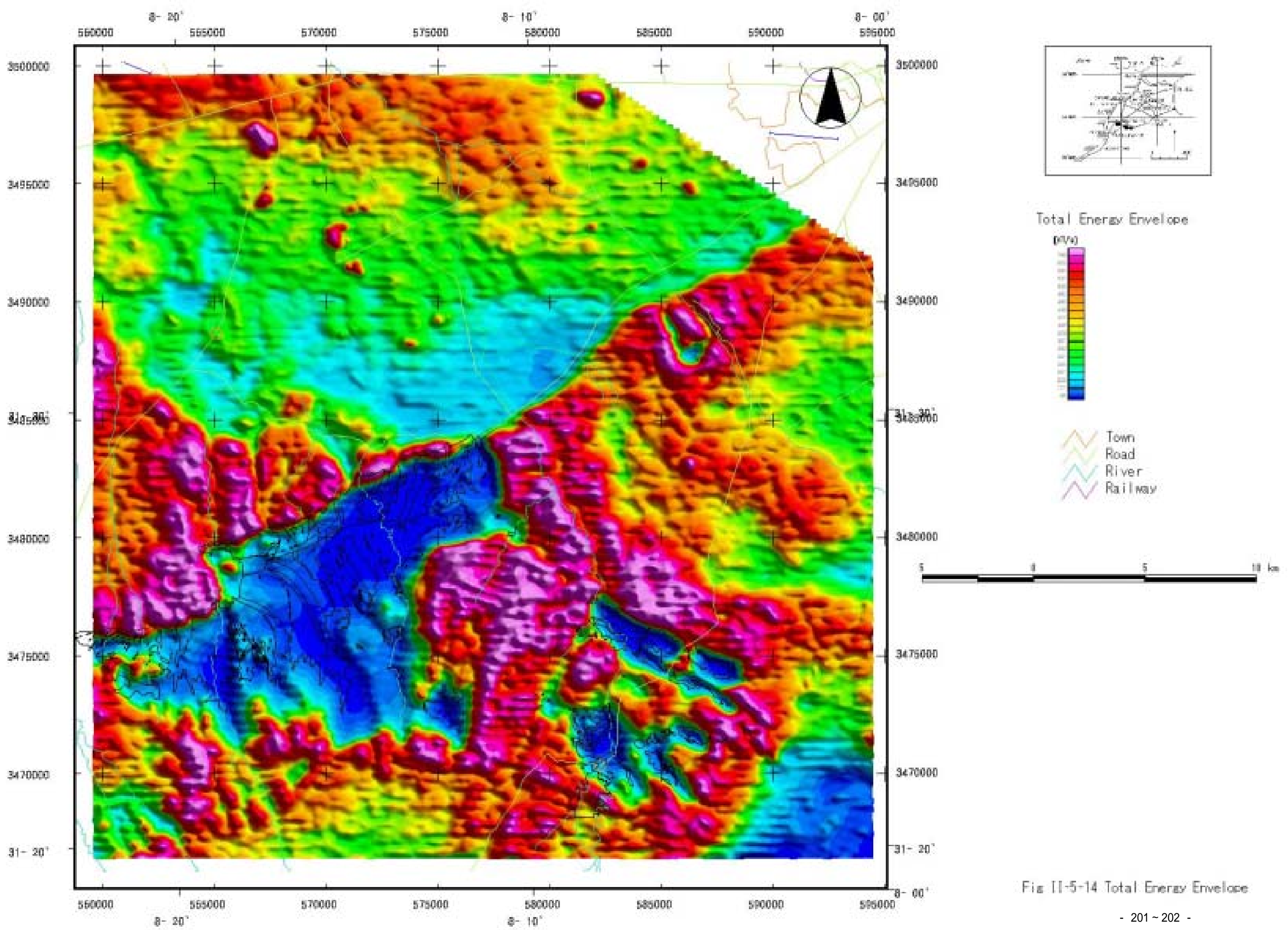
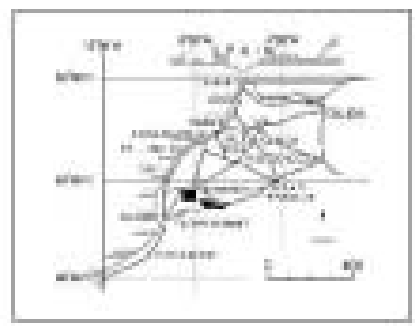
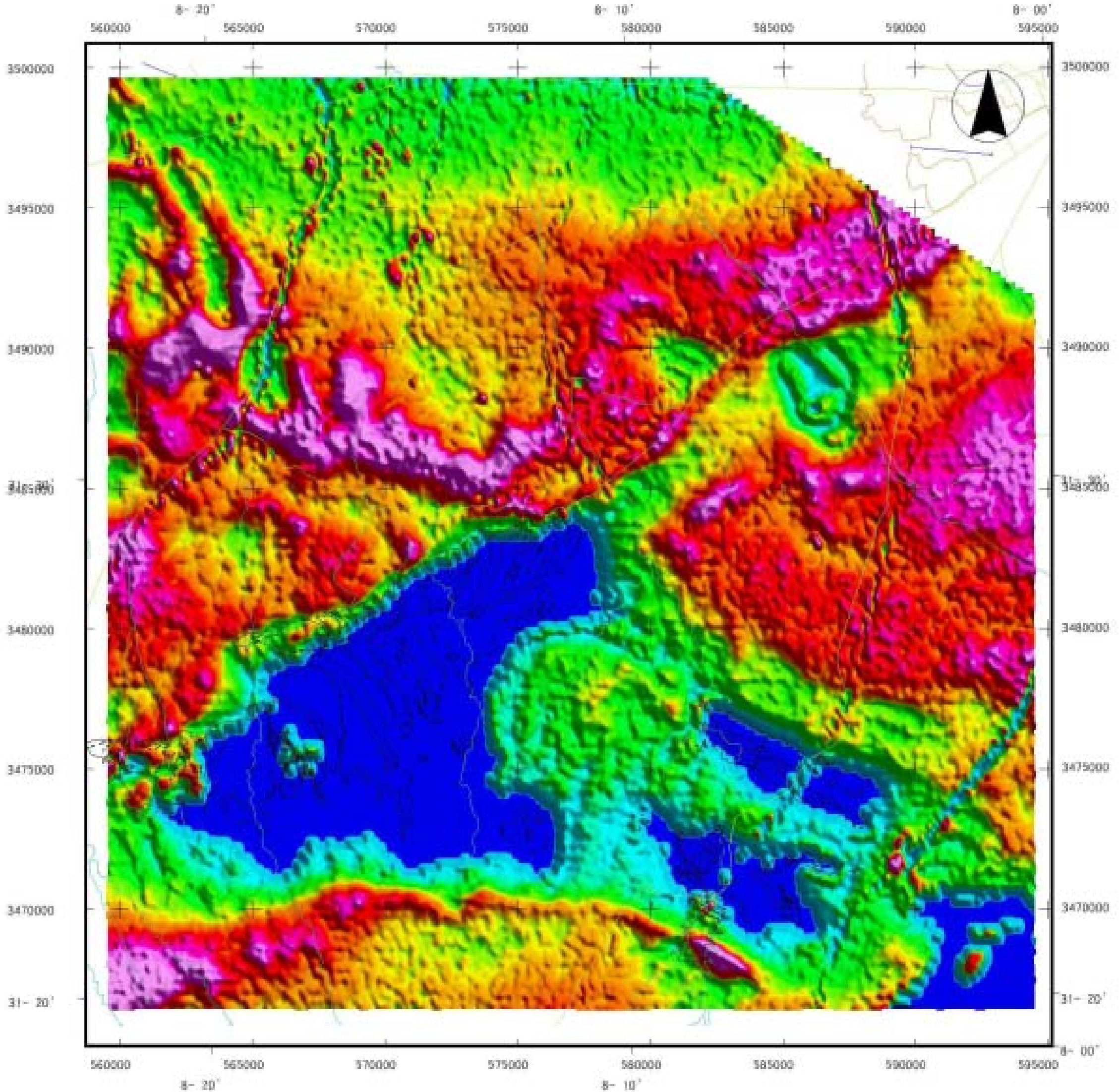
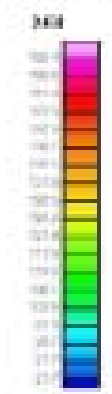


Fig II-5-14 Total Energy Envelope





Decay Constant



- Town
- Road
- River
- Railway



Fig. II-5-15 Decay Constant

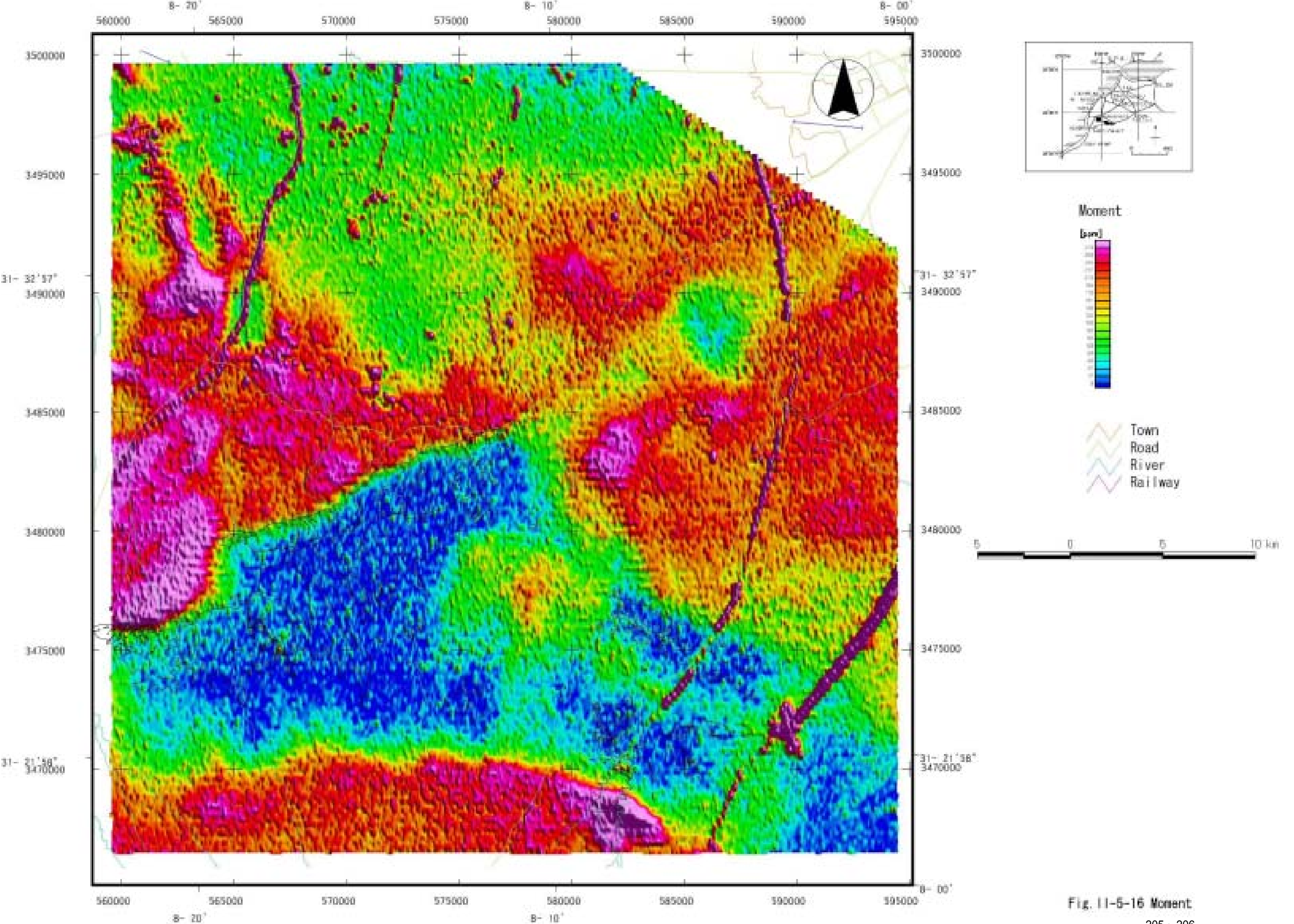


Fig. 11-5-16 Moment

#### 5-4. Interpretation and extraction of potential area

Interpreting the geology of the survey area by combining airborne magnetic survey data with airborne electromagnetic survey data gives following results:

##### (1) South of the boundary of resistivity at the center of the survey area (NE-SW system)

The distribution area of basement rock (exposed and concealed outcrop) is a part extracted as a low magnetic zone by RMI and low resistivity zone by the decay constant. It is thought that the resistivity is high with a shallow outcrop of basement rock and middle with a deep one. All from igneous rocks through volcanic clastic rocks occur at 3 points: southeast (Hajar deposit), west (Frizen deposit) and north. In addition, magnetic indications suggestive of the occurrence of the said rocks in other area can be observed.

Given as promising sites are those where there is concurrence of local low resistivity and high magnetic anomaly or where these two are adjacent.

##### (2) North of the boundary of resistivity at the center of the survey area (NE-SW system)

As a result of studying the airborne magnetic survey data, it is estimated that physical properties (resistivity) of the basement rocks in this area is largely different from that of the south side. A comparison between the total energy envelope (resistivity structure at shallow part) and the decay constant (resistivity structure at a deep zone) make it possible to extract the following 3 areas:

- (a) Area at the west end: low resistivity from shallow through deep part
- (b) Central area extending from east to west: middle/high resistivity at shallow part - low resistivity at deep part
- (c) Northern area extending from east to west: low resistivity at shallow part-middle resistivity at deep part

If in the areas (b) and (c) there is a basement rock with concealed outcrop, the location containing igneous rock to volcanic clastic rock shows a high magnetic anomaly with a diameter of 2 to 4 km as verified by RMI.

If in the areas (b) and (c) there is a base rock with concealed outcrop, the location containing igneous rock to volcanoclastic rock shows a high magnetic anomaly with a diameter of 2 to 4 km as verified by RMI.

Given as promising sites are the zones of overlapping local low resistivity and high magnetic anomaly locally or where these two are adjacent. Such a zone are obtained in the northwest area and around high magnetic anomalies that is considered granite stock in the northeast area.

Many low resistivity zones exist in the following areas.

- (a) From Khwadra deposit to Guemassa mountain massif Choule in the northwest part

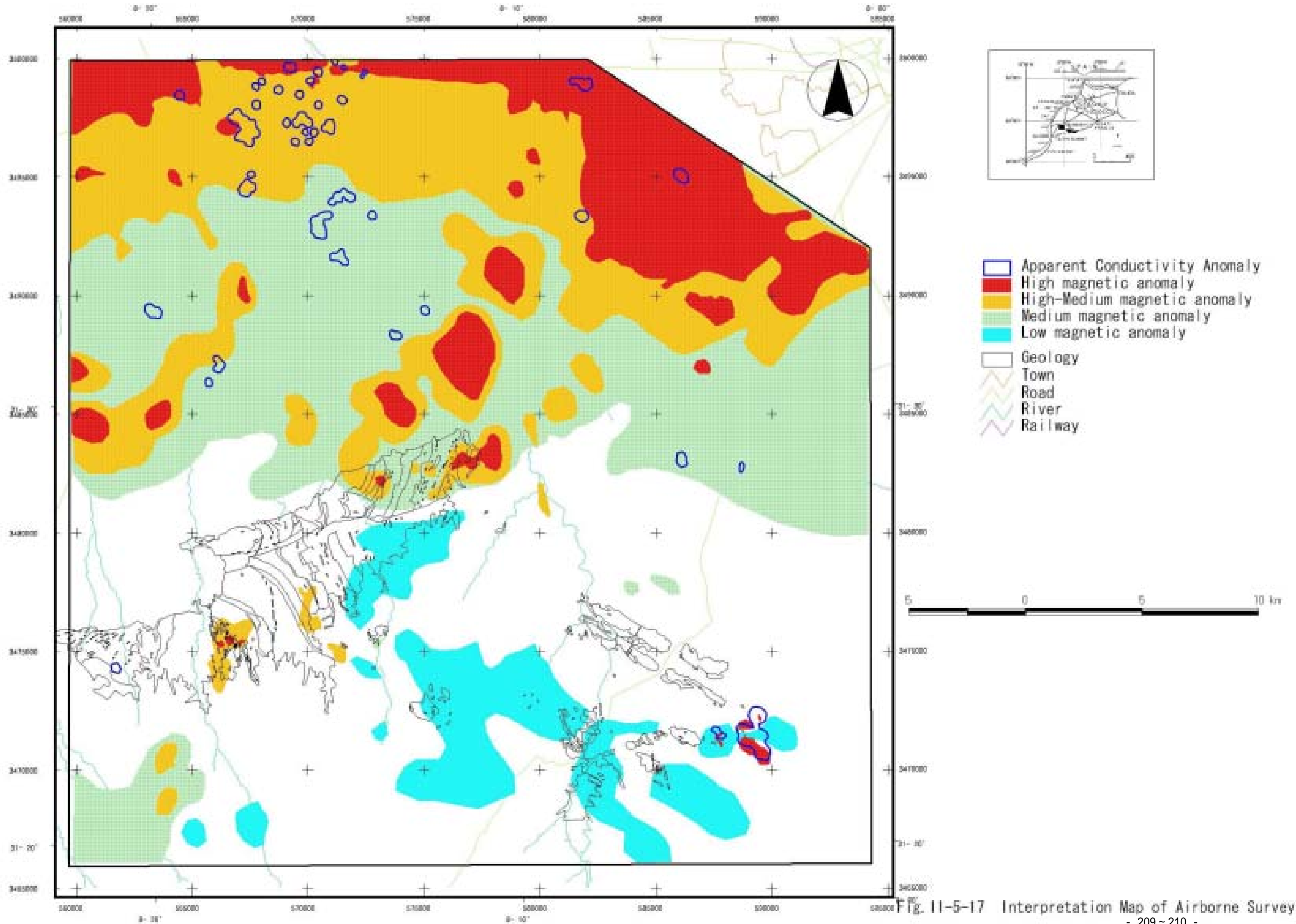


Fig. 11-5-17 Interpretation Map of Airborne Survey

of the airborne geophysical prospecting area.

- (b) Marginal part of magnetic anomaly zone of Nasfer at southwest part of Khwadra deposit.
- (c) Northeast part, west of Marrakech airport.
- (d) Marginal part of Tamslot in the east part of Guemassa mountain massif.

Also as for magnetic anomaly zone, relatively small scale, marked magnetic anomaly as shown in the known ore deposits of Khwadra deposit and Hajar deposit was not observed. Relatively large scale and high anomalies were recognized in the following areas. These anomalies are considered to be due to geological element such as volcanic rocks or plutonic rocks

- (a) Northern part of Guemassa mountain massif Choula.
- (b) Southwest part of Khwadra deposit Nasfer and its western part.
- (c) Northeast part, west of Marrakech airport.

From the results of airborne geophysical prospecting as mentioned above and the existence of medium to low magnetism ore deposit obtained by geological survey, areas indicating following anomaly at airborne geophysical prospecting are selected as prospecting areas.

- 1) Low resistivity zone + high to medium magnetic anomaly: possibility of the existence of high magnetic massive sulfide ore deposit.
- 2) High magnetic anomaly zone: Possibility of the existence of high magnetic massive sulfide ore deposit.
- 3) Low resistivity zone: possibility of the existence of medium to low magnetic massive sulfide ore deposit.

Specifically they are following areas.

- 1) Low resistivity zone + high to medium magnetic anomaly
  - (a) The area where low resistivity zone overlaps medium magnetic anomaly which exist numerously from Khwadra deposit at northwest part of the airborne geophysical prospecting area to Guemassa mountain massif Choula though marked high magnetic anomaly was not obtained by the survey at this time.
  - (b) Low resistivity area existing in relatively large scale high magnetic anomaly in the northeast part, western part of Marrakech airport.
- 2) High magnetic anomaly part
  - (a) Small scale medium to high magnetic anomaly zone dotted in relatively large scale

- high magnetic anomaly in the north east part, western part of Marrakech airport.
- (b) Small scale medium to high magnetic anomaly zone dotted in relatively large scale high magnetic anomaly at south west part of Khwadra ore deposit, Nasfar.
- 3) Low resistivity part
- (a) Low resistivity zone near Tamasloht, eastern direction of Ghoula. Magnetic anomaly is not seen.

## Chapter 6 Integrated Discussion

### 6-1 Characteristics of Sulfide ore deposits

The purpose of this survey is to find the exploration potential area by surveying the geology and deposits and ore mineral occurrences in Jubilet and Guemassa districts, referring to the characteristics of the concealed massive sulfide ore deposit in the Marrakech district, For this purpose, the characteristics of the massive sulfide ore deposit that were obtained by the geological survey, study of past drilling cores and the laboratory tests are listed for the index to extract the prospective ore-bearing places.

#### 1) Geology and Ore Showing in Jubilet District and Guemassa District

As mentioned above, the center of the Jubilet in the north of the area consists of the basement rocks that were deposited with the strike of the direction approximate NS or NNE – SSW and the dip to the east. On the other hand, the geological structure of Guemassa in the south of the area consists of the sediments with the strike of the direction NNW – SSE or NE – SW and the dip to the east. The basement rocks are mainly composed of pelite rocks of Devonian - Carboniferous - Permian that are interbedded with limestone, tuff and psammytic rock layers. Besides them, the basement rocks are interbedded with many acid or basic sill-like rock bodies.

The geology of Visean, upper Carboniferous, in the central Jubilet mountain massif and Guemassa district, is composed of pelite rocks, acid volcanic rocks, basic volcanic rocks, rhythmic alternation, phyllite of the Sarhlef Formation, and carbonate rocks and pelite rocks of the Tequsim Formation that is the upper of the Sarhlef Formation.

The ore deposits in Jubilet and Guemassa districts are the Cu-Pb-Zn-Fe massive sulfide ore deposits that were embedded in sedimentary rocks of Visean and volcanoclastic rocks.

Kettara deposit in the center of the Jubilet mountain massif, Draa Sfar and Khwadra deposits in the southern end of the Jubilet mountain massif forming the boundary area of the basement and Tertiary layer, Hajar deposit in the western end of the Guemassa, and Frizen deposit in the east are the main massive sulfide ore deposits in this area.

The shapes of these ore deposits are layered, massive, lenticular, and banded. The major combination of minerals is pyrrhotite, pyrite, galena, and chalcopyrite. Acid and/or basic volcanic rocks are distributed in the vicinity of the ore deposit. The volcanic rocks relates to the mineralization.

#### 2) Classification of Mineralization and the Mode of Occurrence of Pyrrhotite

Khwadra, Draa Sfar, Kettara, Hajar, and Frizen deposits are classified as the massive

sulfide ore deposits by the deposit shape, the combination of minerals and related igneous rocks. It becomes obvious that these ore deposits were formed by repetition of mineralization in the early stage and the late stage, considering the mode of occurrence of these ore deposit, ore minerals and alteration of the host rocks.

The classification of mineralization and the combination of minerals and gangue minerals are shown in Fig.II-6-1. The characteristics of the mineralization and the combination of ore and gangue are listed in Table II-6-1.

The positions of the early stage and the late stage mineralization are generally arranged vertically. The early stage mineralization mainly occurred within the sedimentary rocks and volcanic rocks of the middle to the upper part of the Sarhlef Formation, the late stage mineralization occurred in the sedimentary rocks of the upper layer of the Sarhlef Formation. The early stage and the late stage mineralization are represented by pyrrhotite and pyrite respectively, from the view of the Fe–S minerals. The gangue minerals are different depending on the stage. The mineralization stage is clearly distinguished by the difference of secondary minerals that were altered by the repetition of mineralization.

The combination of minerals is classified by mineral identification by microscope and polymorphism analysis of minerals by X- ray diffraction in this survey. The flow chart of the mineralization by the classification of minerals is shown in Fig.II-6-2. The comment of Fig.II-6-2 is as follows; the mineralization stage of massive, layered and banded ore deposit is divided into the early stage and the late stage by the existence of pyrrhotite in sulfide minerals. Then, the early stage is divided into the early I sub-stage and the early II sub-stage. The early I sub-stage include hexagonal pyrrhotite and the secondary marcasite that is described later. In the case of the inexistence of pyrrhotite, the early stage and the late stage is divided by the existence of idiomorphic pyrite. The early stage includes idiomorphic pyrite. In case of the existence of idiomorphic quartz, the ore deposit is the stockwork ore deposit.

#### (1) The Early Stage Mineralization

The early stage mineralization occurred within the alternating beds of mudstone and sandstone, the alternating beds of mudstone and quartzite or acid volcanic rocks in Sarhlef Formation to form massive, layered or banded shape. The main part of the Khwadra, Draa Sfar, Kettara, and Hajar deposits, and the lower layer of Frizen deposit belong to the early stage. Most of the early stage mineralization occurred in the brecciated part before the late stage mineralization.

The ore minerals are composed of large quantity of pyrrhotite and sphalerite that are accompanied by medium quantities of chalcopyrite and galena. The gangue minerals are accompanied by quartz and carbonate minerals.



Mineral	MINERALISATION									
	Early-I			Early-II	Latar			Stockwork		
	1	2	3	2	1	2	3	2	3	
Ore minerals	sphalerite	█	█	█	█	█	█	█	█	█
	galena	█	█		█	█	█	█	█	
	chalcopyrite	█	█	█	█	█	█	█	█	█
	pyrite (euhedral)		█	█	█	█	█	█	█	█
	pyrrhotite	█	█	█	█					
	arsenopyrite									
	marcasite (euhedral)		█	█	█	█				█
	marcasite (exfoliating lamellae)				█					
	magnetite		█	█	█		█	█	█	█
	ilmenite									
	hematite							█		█
	covellite						█	█		
	acanthite		█							
	stannite		█							
Primary minerals	quartz		█	█	█		█	█	█	█
	plagioclase		█		█		█	█	█	█
	augite		█	█			█	█	█	█
	hornblende									
Altered minerals	clay minerals		█	█	█		█	█	█	█
	carbonate minerals				█		█	█		

Fig. II-6-1 Mineral assemblage at each stage

Table II-6-1 The list of the characteristics of the mineral assemblage

Mineralisation	Stage	Ore mineral	Gangue mineral	Description
Early mineralisation	Early-I	<u>pyrrhotite(hexagonal)</u> · sphalerite·chalcopyrite		hex.po→mono.po
	Early-II	<u>pyrrhotite(monoclinic)</u> · sphalerite·galena·(pyrite)	quartz, carbonate minerals	mono.po·marcasite
Later mineralisation	Later	<u>pyrite·sphalerite·galena</u> · chalcopyrite·marcasite	quartz, clay minerals, carbonate minerals	

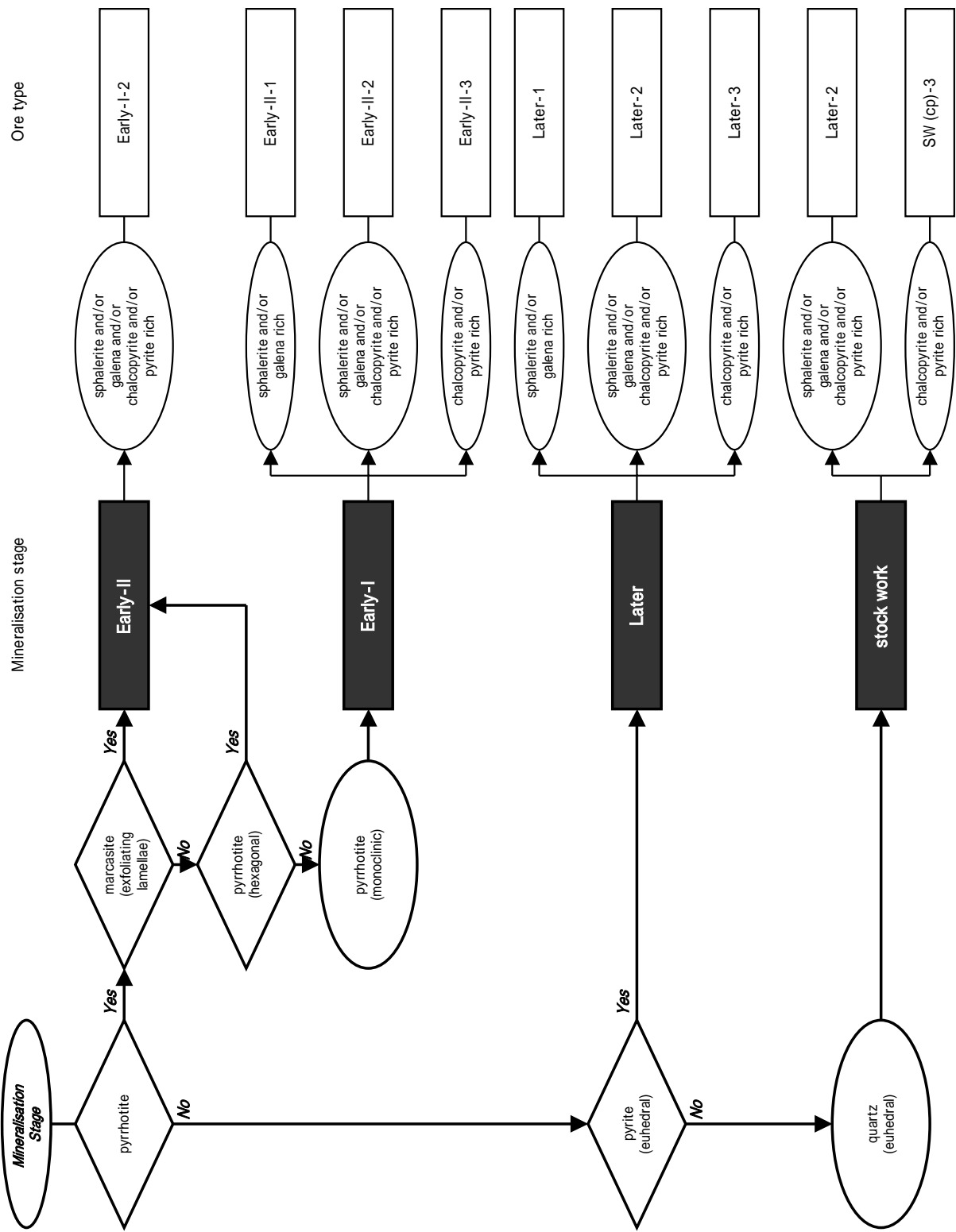


Fig. II-6-2 The flow chart of mineralisation by the mineral classification

## (2) The Late Stage Mineralization

The late stage mineralization occurred within the alternating beds of mudstone and quartzite or the calcaceous pelite rocks of the upper Sarhle Formation to form layered, massive or stockwork shape sulfide ore deposit. Kettara deposit and the upper Frizen deposit belong to this type. The mineralization generally occurred in the upper part or the remote part from the early stage mineralization. Comparing to the early stage mineralization, it was often affected by the geological structure. The mineralization partly occurred in the part of the early stage mineralization. The early stage mineralization was affected by marked alteration due to the late stage mineralization.

The ore minerals consist of large quantities of pyrite and sphalerite with medium quantities of galena, chalcopyrite and marcasite. There are markedly large quantities of pyrite in the minerals.

## (3) Polymorphism Identification of Pyrrhotite

As mentioned above, pyrrhotite only occurred in the early stage mineralization. Pyrrhotite occurs almost all the same range of sphalerite. The quantity of pyrrhotite has a tendency that relatively increases toward the lower. The early stage mineralization is further divided into the early I sub-stage and the early II sub-stage depending on the mode of occurrence of pyrrhotite, the combination of ore and gangue and the secondary alteration.

The major ore mineral in the early stage I sub-stage is fine-grained pyrrhotite. As the result of polymorphism identification by X-ray diffraction, almost all pyrrhotites are the mixture of hexagonal pyrrhotite and monoclinic pyrrhotite. The monoclinic pyrrhotite is the secondary one that changed from the hexagonal pyrrhotite during the late stage mineralization. The monoclinic pyrrhotite is explained later. Hexagonal pyrrhotite generally includes altered chalcopyrite and sphalerite. The quantity of altered chalcopyrite is markedly more than that of altered pyrrhotite in the early II sub-stage. The magnetism of this hexagonal pyrrhotite is weak.

The ore minerals of the early II sub-stage are mainly composed of pyrrhotite and sphalerite that is the main mineral of Zinc ore deposit with the ore minerals of the late stage. The gangue minerals mainly consist of quartz and carbonate minerals. All the pyrrhotites in the early II sub-stage are monoclinic. It includes altered sphalerite and altered chalcopyrite, its magnetism is markedly strong. The monoclinic pyrrhotite is considered to be juvenile by the mode of occurrence and homogenized temperature of Fluid inclusion within quartz that coexists. The description about quartz is explained later.

As mentioned above, it is found that the morphology of pyrrhotite differs from the mineralization stage.

#### (4) Alteration of Pyrrhotite

##### i) Monoclinic Pyrrhotite from Hexagonal Pyrrhotite

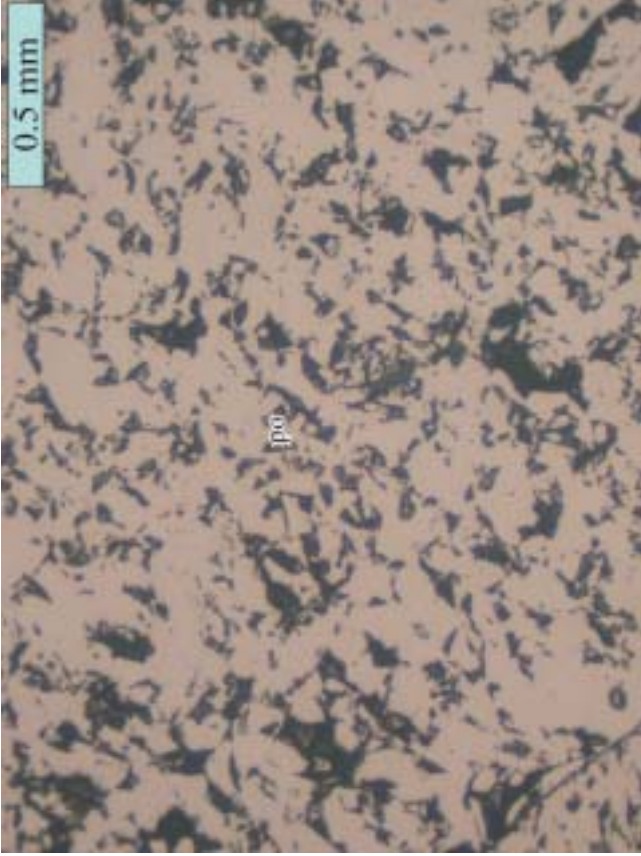
The mode of occurrence that the hexagonal pyrrhotite crystallized in the early I sub-stage mineralization of massive ore deposit was cut by the fine veins of pyrite – quartz – carbonate minerals is observed in Frizen deposit (Fig.II-6-3). The magnetism of the contact part of the fine vein is strong. The magnetism becomes weaker as the distance from the vein increases. The phenomenon is confirmed by a compass. The above phenomena seems to show that the hexagonal pyrrhotite was deformed to the monoclinic pyrrhotite in the contact part along pyrite – quartz – carbonate minerals fine vein. The monoclinic pyrrhotite exists separately like islands in the part, which is far from the vein. The deformation of pyrrhotite from hexagonal to monoclinic progressed along the cracks, the margins and the cleavages of hexagonal pyrrhotite. The massive pyrrhotite ore is confirmed to be the mixture of hexagonal pyrrhotite and monoclinic pyrrhotite by X-ray diffraction of powder samples in this survey. The massive pyrrhotite ores are sampled in Khwadra, Draa Sfar, Kettara, and Frizen deposits, and all the samples were crystallized by the early stage mineralization. By the microscope observation and magnetic survey, hexagonal pyrrhotite was deformed to monoclinic pyrrhotite along the mineral boundary and cracks itself, the central part of hexagonal pyrrhotite remains with irregular outline. The above texture is similar to the texture that is obtained as the heating experiment result of synthetic pyrrhotite by Arnord (1969). These phenomena are considered to generate as a series of the alteration. Therefore, since the mineralization that occurred in different time repeated in Khwadra, Draa Sfar, Kettara, Hajar, and Frizen deposits, the sulfide minerals including pyrrhotite that had been mineralized in the early II sub-stage were markedly altered by the late stage the mineralization.

##### ii) Marcasite from Monoclinic Pyrrhotite

Marcasite yields in the upper part to the lowest part in Khwadra deposit and Hajar deposit. The marcasite is divided into the following two kinds by the mode of occurrence: i) marcasite obviously changed from pyrrhotite in the margins, within cracks of pyrrhotite and along the vein of quartz – carbonate minerals, ii) idiomorphic crystalline marcasite that occurs as fine fiber or scattered dots, it makes fine vein with quartz, carbonate minerals and clay minerals without relationship to pyrrhotite. The latter differs from the former as the genesis, and it is considered to directly precipitate as marcasite in the latest stage. In the following, describe only about the above i), because the marcasite relates to genetically classify the mineralization.

Marcasite occurred in the margin of pyrrhotite and within the cracks is shown in Fig.II-6-4.

Marcasite occurs as exfoliating composite lamella within the cracks, in the margins, in the

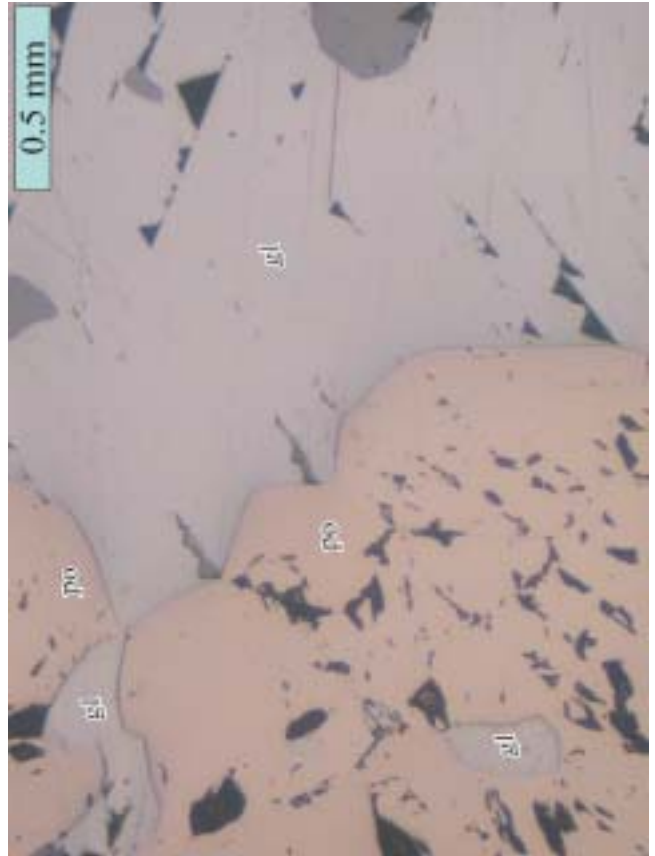


02MRN065



02MRN086

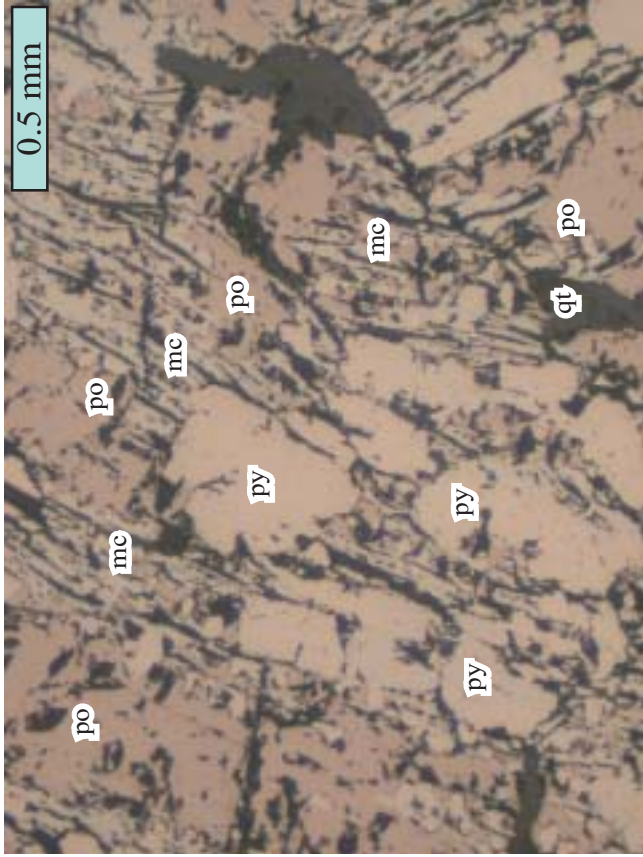
- po pyrrhotite
- py pyrite
- cp chalcopyrite
- sp sphalerite
- gl galena
- mc marcasite
- mg magnetite
- hm hematite
- cv covellite
- ac acanthite
- st stannite
- qt quartz
- cb carbonate minerals



02MRN113

Fig. 11-6-3 The characteristics of the Early I mineralization stage





- po pyrrhotite
- py pyrite
- cp chalcopyrite
- sp sphalerite
- gl galena
- mc marcasite
- mg magnetite
- hm hematite
- cv covellite
- ac acanthite
- st stannite
- qt quartz
- cb carbonate minerals

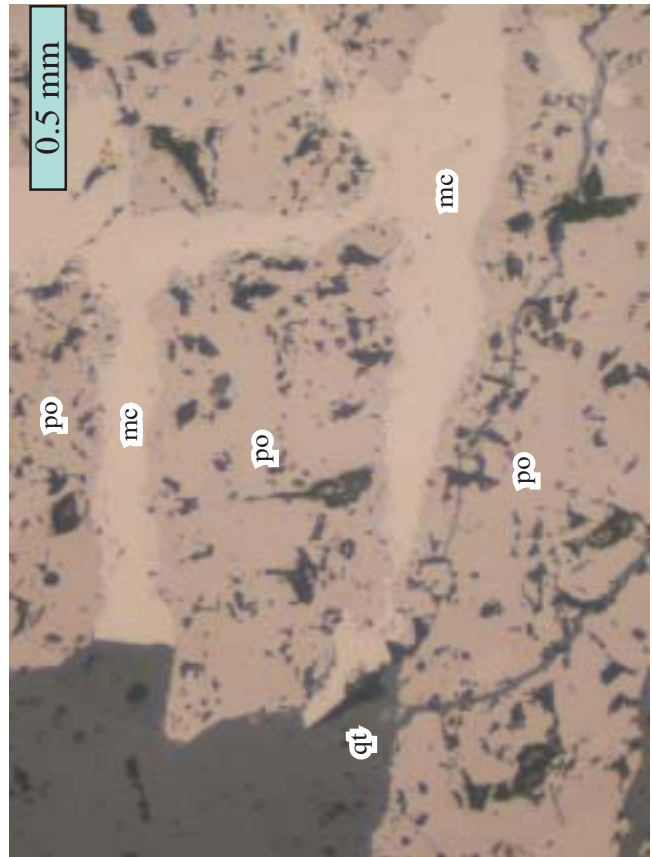


Fig. 11-6-4 The characteristics of the Early II mineralization stage

contact parts along the vein of quartz – carbonate minerals that cut the pyrrhotite. The ultra-fine marcasite sometimes shows bird eye's texture or agate like texture. Numerous micro-crystals are often observed between exfoliating composite lamella and pyrrhotite. Pyrrhotite exists like the small isolated islands in the part that the change to marcasite was markedly progressed. However, since marcasite shows characteristic pseudomorph of pyrrhotite even after the change to marcasite was completed, original existence of pyrrhotite is easily recognized. These features seem to indicate the chemical alteration of pyrrhotite. The generation of magnetite is not observed around the marcasite that changed from pyrrhotite. Only the monoclinic pyrrhotite changed to marcasite from the upper to the lowest of the ore deposit. This phenomena is in contrast to the fact that hexagonal pyrrhotite crystallized in the early I sub-stage widely changed to monoclinic pyrrhotite by hydrothermal alteration.

According to Edward(1954), "marcasite from pyrrhotite is not the common metasomatism that matasomatic mineral is generated by the contact with the original mineral but occurs by the change in acidity and temperature of residual Fluid. That is, pyrrhotite becomes unstable by the change in acidity and the temperature of residual Fluid and pyrrhotite immediately decomposes. In this condition, free Fe and S make re-precipitate stable marcasite. These changes often occurred at the same time of generation of carbonates, and marcasite closely coexist carbonate minerals and becomes complicatedly combined foliation or radiated foliation in equilibrium." The phenomena that the crevices of exfoliating lamella of marcasite were mostly filled by carbonate minerals and the coexistence of both minerals in Khwadra deposit and Hajar deposit is well consistent with his explanation.

Therefore, the characteristics of the mineralization are summarized in Table II-6-1 by the combination of ore minerals, combination of gangue minerals, morphology of pyrrhotite, and the characteristics of secondary minerals.

#### (5) Fluid Inclusion within Quartz coexists with Pyrrhotite

Pyrrhotite crystallized in each mineralization stage and quartz coexists in Hajar, Frizen, Draa Sfar, and Kettara deposits. The quartz that coexists with hexagonal pyrrhotite was collected and the homogenized temperature of the juvenile two phases fluid inclusion with quartz was measured. The accumulated histogram of the homogenized temperature is shown in Fig.II-6-5. The ore deposits are listed in the column and the measured result are listed in line according to the mineralization stage of each ore deposit. The homogenized temperature of mineralization in the early I sub-stage varies from 250°C to 320 °C, and the data concentrates between 270°C and 280 °C. This temperature corresponds to the higher temperature of the lower limit of the stable temperature of hexagonal pyrrhotite that was pointed out by Kissin and Scott (1982). The result and the mode of occurrence seem to indicate that the hexagonal



pyrrhotite of the early I sub-stage directly precipitates in the high temperature in Hajar, Frizen, Draa Sfar, and Kettara deposits.

The monoclinic pyrrhotite of the early II sub-stage also coexists with quartz in Hajar and Khwadra deposits. Particularly, hexagonal flat pyrrhotite is commonly observed with quartz and sphalerite in druse. The quartz that coexists with monoclinic pyrrhotite was selected and the homogenized temperature of the two phases fluid inclusion was measured. The result is shown in Fig.II-6-5. The homogenized temperature of mineralization in the early II sub-stage varies from 180°C to 280°C, and the data highly concentrates between 230°C and 250 °C. The Fluid inclusion in quartz with solid phase was sometimes observed. Most of the solid phase is considered to be carbonate minerals. At the measurement of the homogenized temperature, multi-phase inclusion was excluded. This temperature is lower than the upper limit of the stable temperature of monoclinic pyrrhotite stable temperature that was pointed out by Kissin and Scott (1982). The result and the mode of occurrence seem to indicate that the monoclinic pyrrhotite did not generate in the early II sub-stage by the conversion during high temperature type hexagonal pyrrhotite cooled down, but directly precipitate as monoclinic pyrrhotite in the Hajar deposit.

On the other hand, the homogenized temperature of the fluid inclusion in quartz, which is accompanied by pyrite and sphalerite in the late stage, ranges from 200°C to 250 °C. The above temperature is lower than the homogenized temperature of quartz that coexists with pyrrhotite in the early II sub-stage.

The homogenized temperature of fluid inclusion within pyrite - quartz vein that cut the massive hexagonal pyrrhotite and make change the hexagonal pyrrhotite in the both side of the vein to monoclinic is 180 – 250 °C in Frizen, Draa Sfar, and Kettara deposits.

#### (6) Generation Mechanism of Monoclinic Pyrrhotite

There are some ideas for the generation mechanism of monoclinic pyrrhotite including metamorphism. The following two mechanisms seem to be possible as the result of this survey: i) hydrothermal alteration of hexagonal pyrrhotite, and ii) direct crystallization of monoclinic pyrrhotite.

##### i) Hydrothermal Alteration of Hexagonal Pyrrhotite,

Yund and Hall (1969) synthesized monoclinic pyrrhotite by adding pyrite to hexagonal pyrrhotite (48.15at.%Fe) at the temperature of 150 °C, using the dry method. Meanwhile, Kissin and Scott (1982) synthesized hexagonal pyrrhotite and pyrite from monoclinic pyrrhotite at the temperature of 254 °C. These synthetic experiment show that hexagonal pyrrhotite is altered in sulfur rich circumstance in the low temperature (less than 254 °C) to generate monoclinic pyrrhotite.

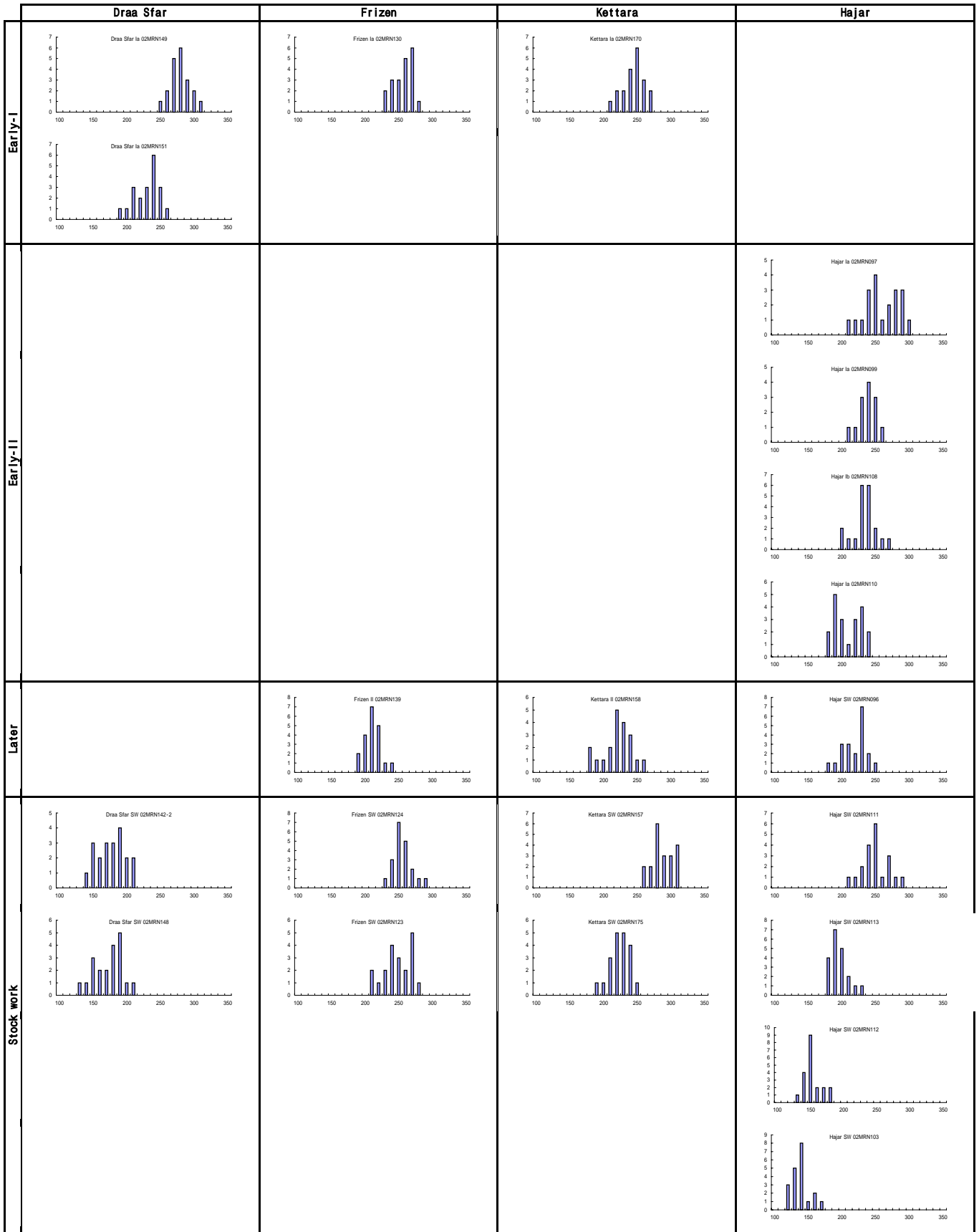


Fig. II-6-5 Histogram of Homogenization Temperature about Mineralization Stage

As mentioned above, in case that hexagonal pyrrhotite generated in the early stage was cut by pyrite – quartz – carbonate minerals of the late stage, the contact part of hexagonal pyrrhotite changed to monoclinic pyrrhotite in Kettara and Frizen deposits. Therefore, this change is obviously due to the hydrothermal alteration of the late stage. Moreover, the homogenized temperature of Fluid inclusion within quartz that coexists with pyrite during the late mineralization is 200 – 250 °C. This temperature well corresponds to the temperature of the above laboratory synthesise experiment results. Therefore, monoclinic pyrrhotite that coexists with hexagonal pyrrhotite in the early I sub-stage is the product by hydrothermal alternation of hexagonal pyrrhotite.

#### ii) Direct Crystallize of Monoclinic Pyrrhotite

The laboratory experiment of direct synthesis of monoclinic pyrrhotite was carried out by Sawkins et al. (1964) and Nakai (1969). Sawkins et al. (1964) reported that monoclinic pyrrhotite was generated in the temperature between 140 °C and 230 °C judging from the study of the homogenized temperature of Fluid inclusion within quartz and fluorite that are accompanied with monoclinic pyrrhotite.

Any mixing or reminds of hexagonal pyrrhotite are not recognized by X-ray diffusion of powder samples in the monoclinic pyrrhotite that coexists sphalerite and quartz of the early II sub-stage in Khwadra deposit and Hajar deposit. And, from the fact that the homogenized temperature of Fluid inclusion within quartz that coexists monoclinic pyrrhotite concentrated in the range from 200°C to 250 °C, monoclinic pyrrhotite is considered to be directly crystallized from the beginning of mineralization in the above temperature.

#### (7) Conclusion

The classification of minaralization and the mode of occurrence of pyrrhotite are summarized as follows:

- i) Although each ore deposit in this area was formed through complicated process, the mineralization is roughly divided into the early stage and the late stage. The mineralization of the early stage and the late stage is represented pyrrhotite and pyrite respectively, from the viewpoint of Fe–S minerals. In Khwadra deposit and Hajar deposit, the early stage mineralization is further divided into the early I sub-stage and the early II sub-stage. The former is represented by hexagonal pyrrhotite and the latter is represented by monoclinic pyrrhotite.
- ii) Hexagonal pyrrhotite coexists with quartz of the early I sub-stage. The homogenized temperature of Fluid inclusion within quartz that coexists with pyrrhotite of the early I sub-stage is 270 – 280 °C. Monoclinic pyrrhotite is divided into the following two types by the

generation mechanism; (i) the original monoclinic pyrrhotite crystallized with quartz and sphalerite as in the early II sub-stage in the temperature of less than 300 °C (230 – 250°C), (ii) monoclinic pyrrhotite changed from hexagonal pyrrhotite that was generated in the early I sub-stage by the mineralization of the late stage that was in high fs<sub>2</sub> environment. The homogenized temperature of Fluid inclusion within quartz that coexists the ore minerals generated in the late stage is 200 – 250 °C.

iii) The hexagonal pyrrhotite crystallized in the early I sub-stage was generally changed to monoclinic pyrrhotite by the late stage mineralization. On the other hand, the monoclinic pyrrhotite crystallized in the early II sub-stage was changed to marcasite.

iv) Mineralizations repeatedly occurred in the massive sulfide ore deposits in this area in different time. The pyrrhotite in such ore deposits changed its composition according to the mineralization stage and the change of fs<sub>2</sub> in each mineralization stage after crystallization.

### 3) Characteristics of Sulfur Isotope Ratio

#### (1) Characteristics of Mineralization and Sulfur Isotope Ratio

To consider the genesis of hydrothermal ore deposit, sulfur isotope ratio was studied. The characteristics of sulfur isotope ratio in each mineralization stage of each ore deposit are described below.

The comparison of the sulfur isotope ratio of various kinds of sulfide ore deposits shown in Fig.II-6-6. Shyakanai ore deposit is one of the representative black-ore deposit in Japan. The black-ore deposit is closely related to acid volcanic rocks that erupted near the sea bottom in Miocene. The isotope ratio of the sulfide shows heavy value, +5 ~ +8 ‰, and that of sulfide is +22 ~ +24 ‰, which is the same value of evaporite rocks. The isotope ratio of sulfide from the Iberian Pyrite Belt is -6 ~ +3 ‰ according to Yamamoto et al. (1993). The sulfur isotope ratio of sulfide of the survey area is lighter than that of black-ore deposit and it is almost within the same range of the Iberian Pyrite Belt. The sulfur isotope ratio of basalt and alkaline rock of Europe in Tertiary, evaporite rock in Devonian, seawater, and sedimentary rocks and volcanic rocks in this survey area is shown in Fig.II-6-6 additionally.

To study the difference of the mineralization of the early stage and the late stage, the sulfur isotope ratios of Khwadra, Draa Sfar, Kettara, Hajar, and Frizen deposits were compared. In Khwadra deposit, though the number of sulfur isotope data of the late stage is less than that of the early stage, the ratio of the late stage is higher than that of the early stage. The ratio becomes lighter as the mineralization progressed. On the other hand, in Kettara and Frizen deposits, the ratio of the late stage is almost the same as that of the early stage or a little lower. The ratios become heavier as the mineralization is progressed. Considering only the early stage mineralization, the difference among the ore deposits is distinct. For example, the sulfur

isotope ratio, from lowest to highest, is in Khwadra deposit, Draa Sfar deposit, Kettara deposit, Hajar deposit, and Frizen deposit. In case of the late stage mineralization, the ratio, from lowest to highest, is Khwadra deposit, Kettara deposit, and Frizen deposit. However, comparing to the case of the early stage, the big difference among the ore deposit is not recognized.

To study the difference of mineralization between the early I sub-stage and the early II sub-stage, the sulfur isotope ratios of Khwadra deposit and Hajar deposit were compared. Comparing to the ore deposit in only the early I sub-stage of mineralization, the ratio of the Khwadra deposit is the lowest, and the ratio, from lowest to highest, is in Draa Sfar deposit, Kettara deposit, Hajar deposit, and the Frizen deposit. Comparing to the early I sub-stage and early II sub-stage, the early II sub-stage shows the higher ratio than that of the early I sub-stage. On the other hand, the ratio of the early I sub-stage and that of the early II sub-stage are almost the same.

To study the difference between the mineralization of the massive ore deposit and the stockwork ore deposit, the comparison of the sulfur isotope ratio was carried out. In spite of the difference of the host rock (volcanic rocks and pelite rocks), the massive ore deposit in this area is accompanied by stockwork mineralization zone. Though the number of the sulfur isotope ratio data are less than that of the massive ore deposit and the layered ore deposit, the ratio of the stockwork ore deposit has almost the same or a little higher ratio compared to the massive ore deposit and the layered ore deposit.

## (2) Causes of Variation of Sulfur Isotope Ratio

The marked variation of the sulfur isotope ratio within one ore deposit or one ore-bearing area is in sharp contrast to the sulfur uniformity of black-ore deposit of Japan. The following ideas have been proposed to explain the difference; the difference of the physical and the chemical condition in ore deposit generation (Lusk, 1972; Munha and Kerrich, 1980), mixing of organic sulfur (Sangster, 1968; Rickard et al., 1979; Arnord et al., 1977). When massive sulfide precipitates in high  $f_{O_2}$  or high pH environment, Munha and Kerrich (1980) reported that the sulfur isotope ratio decreases as sulfide/sulfate ratio increases. Sangster et al. (1968) showed the variation of sulfur isotope ratio by the mixing of sulfur of bacteria origin by sulfuric acid reduction in the sea bottom.

Sangster (1968), Sasaki (1970), Sasaki and Kajiwarra (1971), and Kajiwarra (1971) proposed that the most important factor that controls the sulfur isotope ratio in volcanic origin sulfide ore deposit is sulfur within seawater. The total amount of sulfur in the seawater that participated to mineralization was less than the sulfur of the other origin in the ore deposit or the ore-bearing place with marked variation of sulfur isotope. Sato (1983) proposes following

factors of the field that the contribution of the sulfur within the lower rocks or the contribution of the sulfur of organic origin relatively increased by the restriction to supply the sulfur of seawater origin to hydrothermal mineralization system: i) forming the small scale, closed basin, ii) penetration of rainwater to the basin itself or circulated metallogenic hydrothermal water, iii) the reduction environment occurred in the basin and the activity of sulfuric acid reduction bacteria is considered.

The sulfur isotope ratios of sulfides within the massive sulfide ore deposit in this area indicated that the ratios are relatively constant in this area, but there are marked variation of the ratios between the northern ore deposits and the southern ore deposits. The contrast of the average and the standard deviation of the sulfur isotopic ratio of each ore deposit are shown in Fig.II-6-7.

Considering to the sulfur isotope ratio within the same stage as shown in Fig. II-6-6 and II-6-7, the ratio in the early stage is observed the variation of approximate 13 ‰ (the lowest average ; the Khwadra deposit: -10.7 ‰, the upper most average; the Hajar deposit: +2.5 ‰). As mentioned above, the following causes of the variation are considered; the different physical and chemical conditions of ore solution in each ore deposit, the difference of mineralization environment, for example, the difference of penetration of the sulfur of organic origin. Particularly, the contribution of magma origin was relatively bigger in the Hajar deposit and the Frizen deposit, because of the existence of acid volcanic rocks.

Comparing to the isotope ratio of the early I sub-stage and the early II sub-stage, the ratio of the early I sub-stage is lighter than that of the early II sub-stage. From this fact, the following two reasons are considered; the early I sub-stage occurred in comparatively reductive basin or was relative highly affected by the penetration of the sulfur of sulfuric acid reductive bacteria origin.

The sulfur isotopic ratios of the five ore deposits in the late stage mineralization show almost the same value. The fact indicates that there are not so much differences of the physical and chemical conditions in ore solutions and the metallogenic environments were similar each other.

The physical and the chemical conditions of the ore solutions and mineralization environment were considered to be similar at the mineralization of the foot wall of the ore deposit that brought the stockwork ore deposit, because of the sulfur isotope ratios of the stockwork ore deposits of the five ore deposits.

As mentioned above, according to the progress of the mineralization (the early I sub-stage → the early II sub-stage → the late stage), the dispersion of the sulfur isotopic ratio gradually becomes small. From this fact, the environment is considered to transfer from the different environment (more than one basin with small volume and closed) to the similar environment

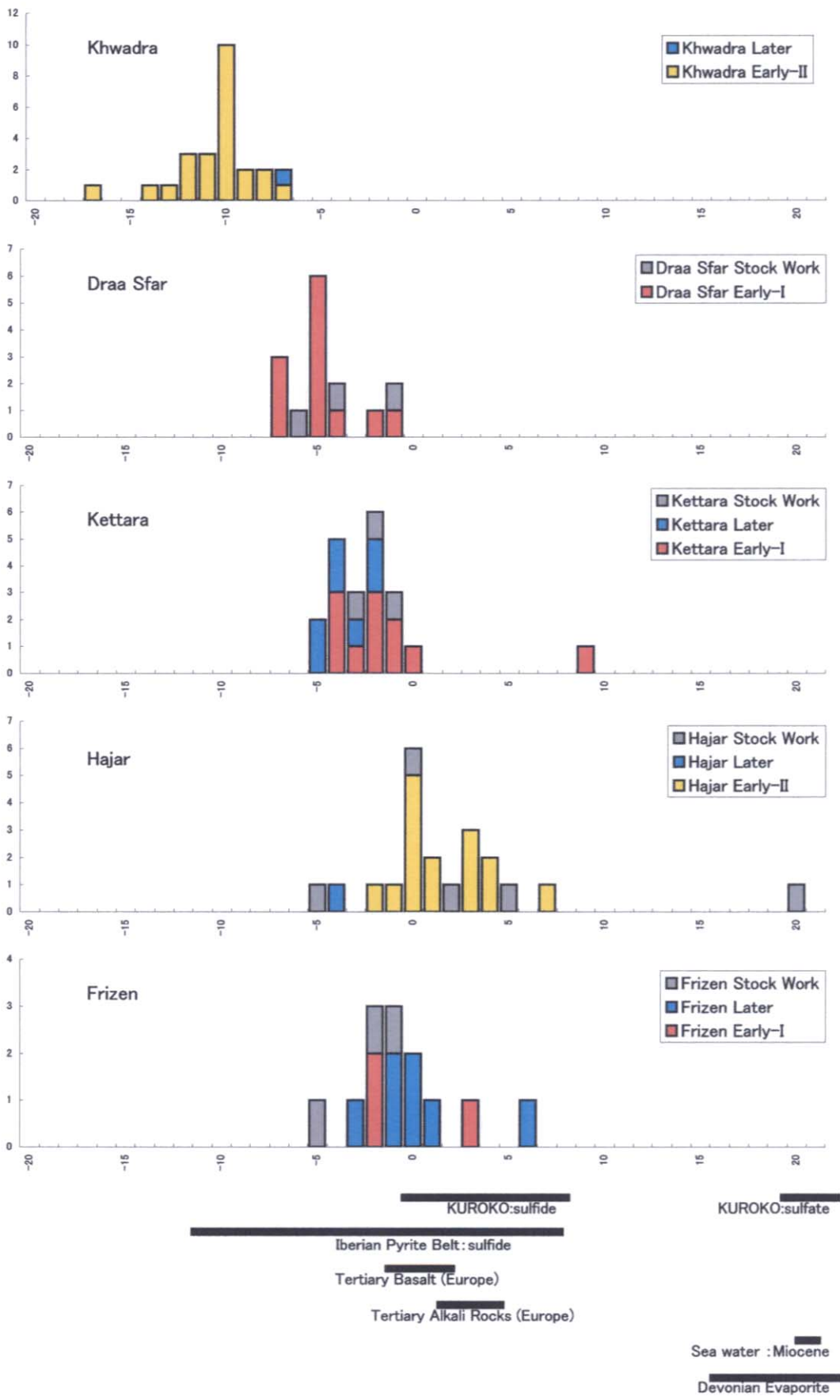


Fig . II-6-6 The histogram of sulfur isotope ratio which mineralisation in each deposit

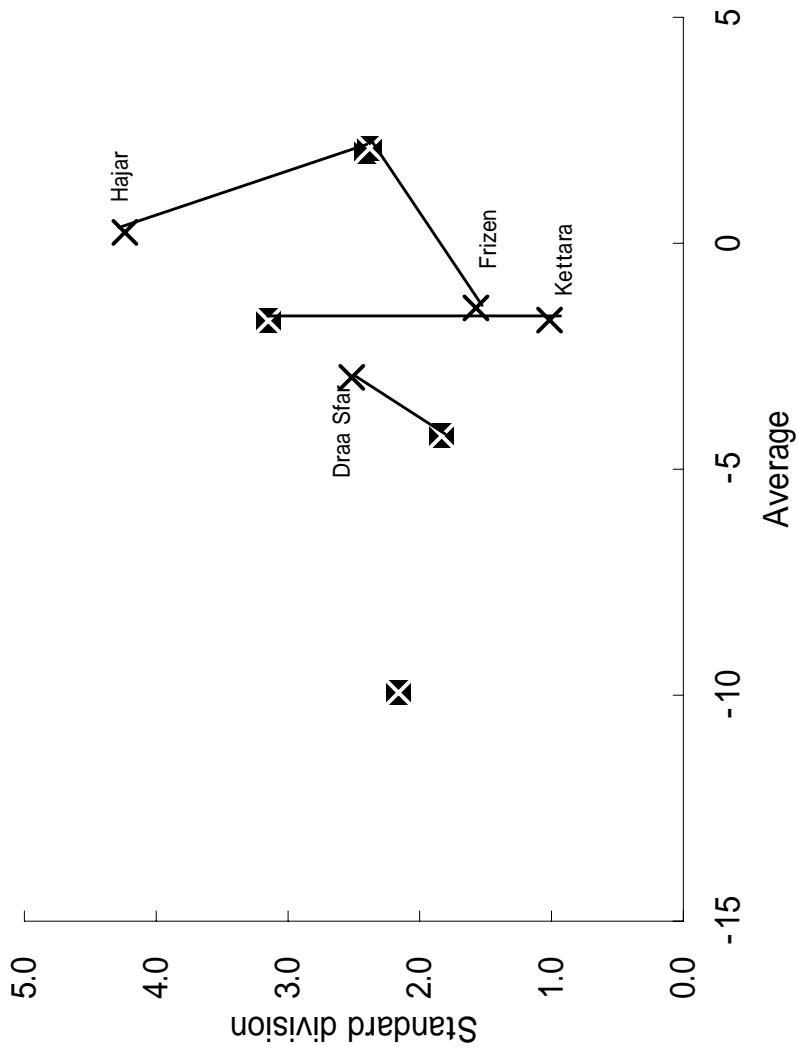


Fig. II-6-7 The average and standard deviation of sulfur isotope ratio in each deposit



(open and integrated one basin).

Therefore, the basin in the early stage was composed of several sedimentary basins with small volume due to the similarity of sulfur isotope ratio. This idea is compiled as the following; The Hajar – Frizen Basin in the south, the Draa – Kettara Basin in the north and Khwadra Basin in the center are considered to exist. Then, these closed basins were integrated as the one sedimentary basin with the same mineralization environment in the time of the late stage mineralization.

#### 4) Mineralization and Magnetism

The repetition of the mineralization of the early stage and the late stage in each ore deposit was confirmed by this survey. The mineralization of the early stage and the late stage are represented by pyrrhotite and pyrite respectively, from the viewpoint of Fe–S mineral. The early stage mineralization is further divided into the early I sub-stage and the early II sub-stage. The former is represented by hexagonal pyrrhotite and monoclinic pyrrhotite from the altered hexagonal pyrrhotite affected by the late stage mineralization. The latter is represented by monoclinic pyrrhotite that was directly crystallized from the ore solution. The magnetism of monoclinic pyrrhotite is the strongest within the above pyrrhotites. Considering to the homogenized temperature of the Fluid inclusion of coexisting quartz, minerals of the early stage was generated in 230 – 280 °C, and those of the late stage was generated in 180 – 250 °C. From the difference of the sulfur isotopic ratio among the early I and II sub-stages and the later stage, the difference of the physical and the chemical conditions in mineralization environment and the difference of the mixing of organic origin sulfur are considered.

Finally, paying attention to the magnetism of pyrrhotite, it is obvious that the magnetism of the area around each ore deposit is related to the characteristic of the polymorphism of pyrrhotite of each ore deposit. That is, the high geomagnetic anomalies are detected in Khwadra and Hajar deposits where the monoclinic pyrrhotite characteristically occurs. On the other hand, a high magnetic anomaly area and a low magnetic anomaly area are adjacent in Draa Sfar deposit where hexagonal pyrrhotite and monoclinic pyrrhotite coexist. The low geomagnetic anomalies were only detected in Kettara deposit and Frizen deposit where hexagonal pyrrhotite and pyrite coexist.

The prospecting of the massive sulfide ore deposit in Morocco has historically been carried out by the extraction of high magnetic anomaly. This survey suggests new possibilities. One possibility is that there is a massive zinc sulfide ore deposit composed of hexagonal pyrrhotite + pyrite even in the medium to low anomaly areas, and another possibility is that there is a massive zinc ore deposit composed of hexagonal pyrrhotite + monoclinic pyrrhotite in the area where the high magnetic anomaly area and the low magnetic anomaly area are

adjacent. This means it is necessary to pay attention not only to strong geomagnetic anomaly areas but also to weak geomagnetic anomaly areas to extract all massive sulfide ore deposits in this area.

## 5) Conclusion

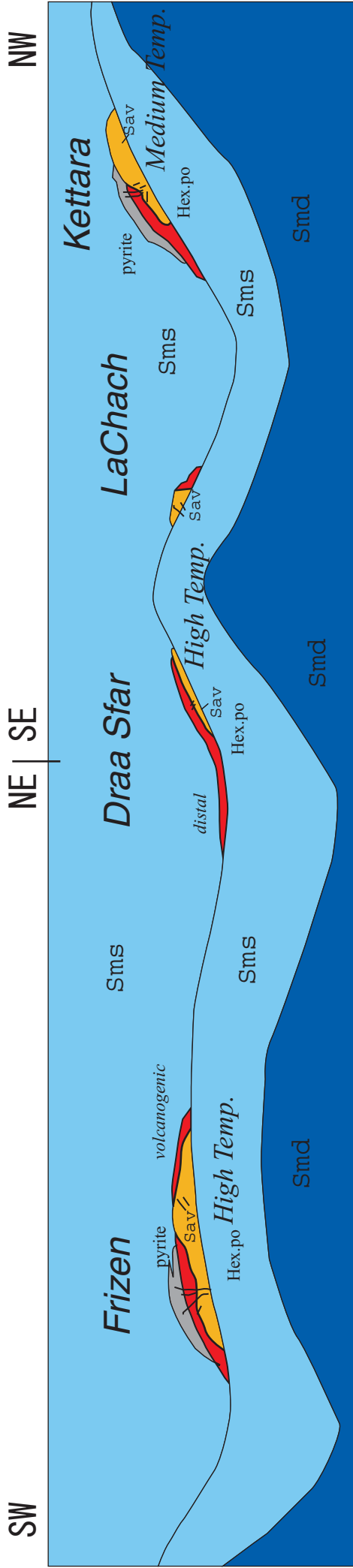
The total review of sulfide ore is summarized in Table.II-6-2. The following findings about the massive sulfide ore deposit of Morocco was obtained.

- (1) The mineralization repeatedly occurred in the massive sulfide ore deposit in the survey area. From the viewpoint of the combination of minerals, the mineralization stage is divided into the early I sub-stage, the early II sub-stage and the late stage.
- (2) - The early I sub-stage mineralization is represented by hexagonal pyrrhotite. The magnetism is comparatively weak.  
- The early II sub-stage mineralization is represented by monoclinic pyrrhotite. The magnetism is strong.  
-The late stage mineralization is represented by pyrite. The magnetism is weak.
- (3) The mineralization temperature was 270 – 280 °C in the early I sub-stage, 230 – 250 °C in the early II sub-stage and 200 – 250 °C in the late stage, judging from the homogenized temperature of fluid inclusion of quartz which coexists with sulfide ore minerals.
- (4) The marked variation of sulfur isotope ratio within the area is explained by the difference of the physical and chemical conditions, mixing of the sulfur of organic origin and limitation of providing sulfur of seawater origin to the hydrothermal water. It is considered that in Khwadra deposit, the contribution of the sulfur mixing of organic origin was effective, and in Hajar deposit and Frizen deposit, the contribution of the sulfur of magma origin was relatively effective.
- (5) According to the above fact, the classification of the ore deposit types is as shown Fig. II-6-8. Following three types of ore deposits seem to exist in this area:
  - a) Early I sub-stage dominant type  
Medium geomagnetic anomaly [Draa Sfar deposit]
  - b) Repeated type of the early I sub-stage + the late stage  
Medium + low magnetic anomaly  
[Frizen deposit, Kettara deposit]
  - c) Repeated type of the early II sub-stage + the late stage  
High + low geomagnetic anomaly  
[Khwadra deposit, Hajar deposit]

Table 11-6-2 The list of the characteristics of mineralisation

Deposit	Mineralisation type	Sulfide mineral	Homogenization Temperature	Magnetic Anomaly
Draa Sfar	Early I	<b>pyrrhotite(hex.)</b> pyrrhotite(mono) Sphalerite galena chalcopyrite	High-Temp.  270-280°C concentrate	Medium anomaly
Kettara Frizen	Early I + Later	<b>pyrrhotite(hex.)</b> pyrrhotite(euhedral) sphalerite galena chalcopyrite	High Temp. + Low Temp.  270-280°C and 180-250°C concentrate	Medium anomaly + Low anomaly
Khwadra Hajar	Early II + Later	<b>pyrrhotite(mono.)</b> marcasite (lamella) <b>pyrite(euhedral)</b> sphalerite galena chalcopyrite	Medium Temp. + Low Temp.  230-250°C and 180-250°C concentrate	High anomaly Low anomaly

### Frizen-Draa Sfar-Kettara



### Khwadra-Frizen-Hajar

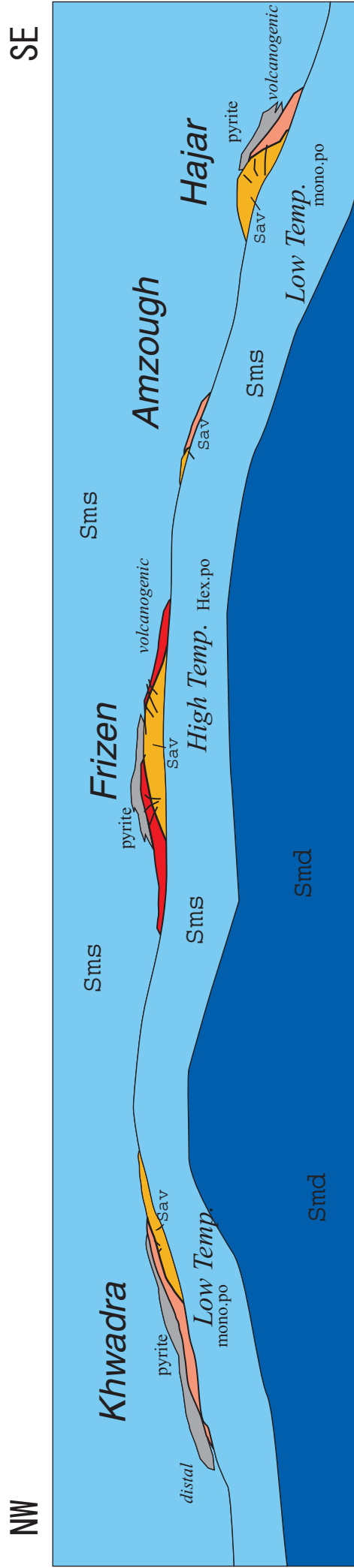


Fig. 11-6-8 Schematic geological model of Marrakech-Tekna area

## 6-2 Airborne Geophysical survey

### (Geological structure)

Interpreting the geology of the survey area by combining airborne magnetic survey data with airborne electromagnetic survey data shows that magnetic and resistivity structure is different in north and south of the boundary of resistivity at the center of the survey area (NE-SW system) in this area.

In the south distribution area of basement rock is a part extracted as a low magnetic zone by RMI and low resistivity zone by the decay constant. It is thought that the resistivity is high with a shallow outcrop of basement rock and middle with a deep one. All from igneous rocks through volcanic clastic rocks occur at 3 points: southeast (Hajar deposit), west (Frizen deposit) and north. In addition, magnetic indications suggestive of the occurrence of the said rocks in other area can be observed. Given as promising sites are those where there is concurrence of local low resistivity and high magnetic anomaly or where these two are adjacent.

In the north resistivity structure make it possible to extract the following 3 areas:

- (a) Area at the west end: low resistivity from shallow through deep part
- (b) Central area extending from east to west: middle/high resistivity at shallow part - low resistivity at deep part
- (a) Northern area extending from east to west: low resistivity at shallow part-middle resistivity at deep part

If in the areas (b) and (c) there is a basement rock with concealed outcrop, the location containing igneous rock to volcanic clastic rock shows a high magnetic anomaly with a diameter of 2 to 4 km as verified by RMI. Given as promising sites are the zones of overlapping local low resistivity and high magnetic anomaly locally or where these two are adjacent. Such a zone are obtained in the northwest area and around high magnetic anomalies that is considered granite stock in the northeast area.

### (Potential of existing massive sulfide deposits)

Areas where following airborne geophysical anomalies had been observed were selected as survey areas considering the probability of the existence of mineral deposit due to low resistivity and magnetic anomaly, and medium to low magnetic anomaly obtained by airborne geophysical survey.

#### (1) Low resistivity zone + high to medium magnetic anomaly

- (a) The area where low resistivity zone overlaps medium magnetic anomaly which exist numerously from Khwadra deposit at northwest part of the airborne geophysical survey area to Choula district in Guemassa though marked high magnetic anomaly was not

obtained by the survey at this time.

- (b) Low resistivity area existing in relatively large scale high magnetic anomaly in the northeast part, western part of Marrakech airport.
- (2) High magnetic anomaly part
- (a) Small scale medium to high magnetic anomaly zone dotted in relatively large scale high magnetic anomaly in the north east part, western part of Marrakech airport.
  - (b) Small scale medium to high magnetic anomaly zone dotted in relatively large scale high magnetic anomaly at south west part of Khwadra ore deposit, Nasfar.
- (3) Low resistivity part
- (a) Low resistivity zone near Tamasloht, eastern direction of Ghoula. Magnetic anomaly is not seen.

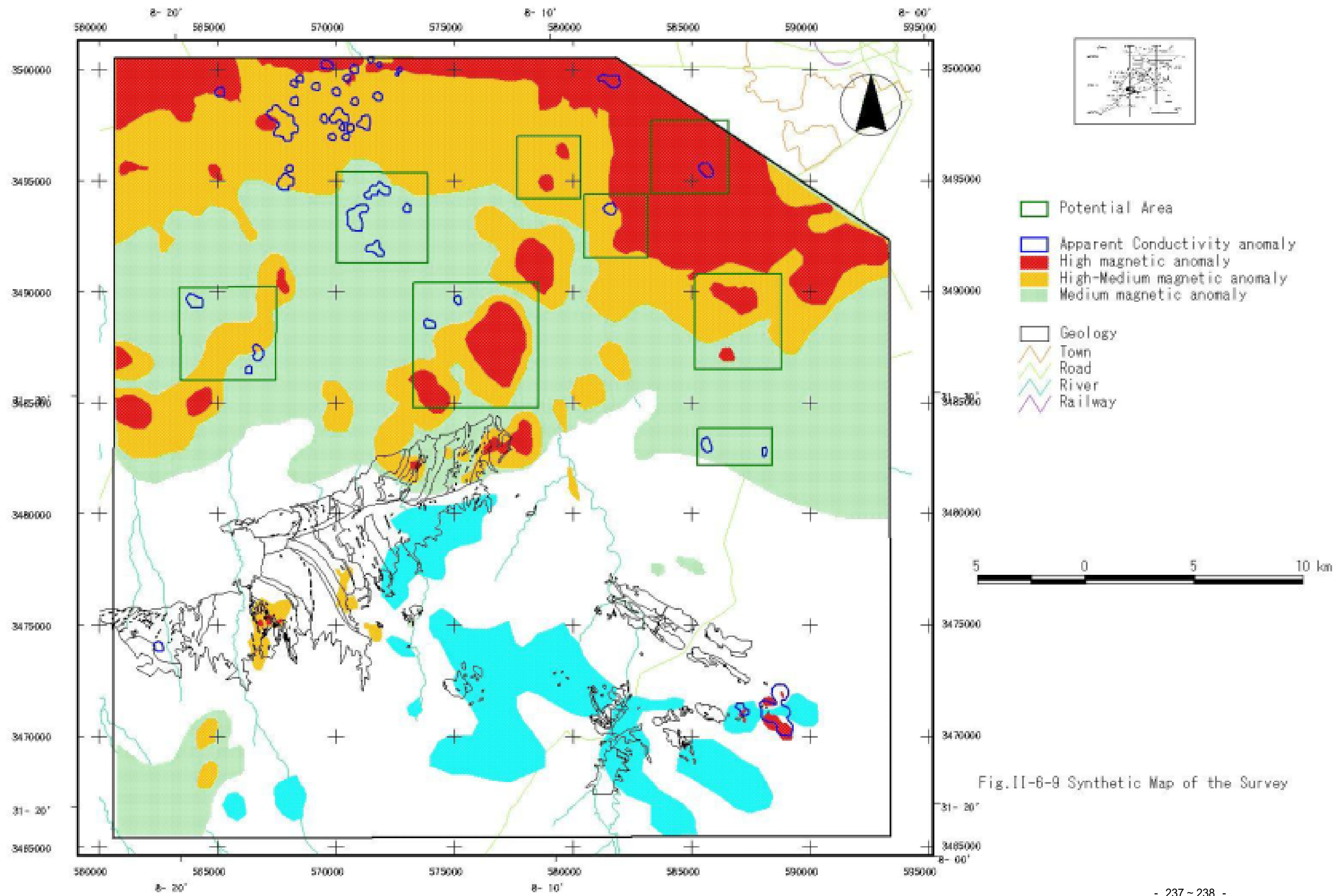


Fig.II-6-9 Synthetic Map of the Survey

## **Part III Conclusion and Recommendation**



### Part III Conclusion and Recommendation

#### Chapter 1 Conclusion

##### (General Geology and Geological Structure in the Survey Area)

The center of the Jubilet area in the north of the area consists of the basement rocks that were deposited with the strike of the direction approximate NS or NNE – SSW and the dip to the east. On the other hand, the geological structure of Guemassa district in the south of the area consists of the sediments with the strike of the direction NNW – SSE or NE – SW and the dip to the east. The basement rocks are mainly composed of pelite rocks of Devonian - Carboniferous - Permian that are interbedded with limestone, tuff and psammytic rock layers. Besides them, the basement rocks are interbedded with many acid or basic sill-like rock bodies.

The geology of Viséan, upper Carboniferous, in the central Jubilet area and Guemassa district, is composed of pelite rocks, acid volcanic rocks, basic volcanic rocks, rhythmic alternation, phyllite of the Sarhlef Formation, and carbonate rocks and pelite rocks of the Tequsim Formation that is the upper of the Sarhlef Formation.

##### (Characteristic of Mineralization in the Survey Area)

The ore deposits distributed in Jubilet and Guemassa area are Cu – Pb – Zn – Fe massive sulfide ore deposits that occurred within the alternating beds of pelites and sandstones, the alternating beds of pelites and acid volcanic rocks.

Kettara deposit in the center of the Jubilet area, Draa Sfar and Khwadra deposits in the southern end of the Jubilet area forming the boundary area of the basement and Tertiary layer, Hajar deposit in the western end of the Guemassa area, and Frizen deposit in the east are the main massive sulfide ore deposits in this area.

The shapes of these ore deposits are layered, massive, lenticular, and banded. The major combination of minerals is pyrrhotite, pyrite, galena, and chalcopyrite. Acid and/or basic volcanic rocks are distributed in the vicinity of the ore deposit. The volcanic rocks relates to the mineralization.

##### (Characteristics of Sedimentary Rocks)

Sedimentary rocks consist of shale, slate and schist and include much sericite, chlorite etc. by microscopic observation and X-ray diffraction. They are highly affected by regional metamorphism and alteration of ore mineralization. Variation of alkaline alteration strength at hanging wall and footwall of massive sulfide ore deposit was studied by boring core and the

result showed some high alteration strength at hanging wall side. This indicates the possibility that hydrothermal activity continued for some time after formation of the ore deposit or was overlapped by another hydrothermal activities. As for major elements, positive correlation with  $\text{Al}_2\text{O}_3$  and  $\text{TiO}_2$  which are said to inflect the origin of broken chips, and V,  $\text{K}_2\text{O}$  and  $\text{P}_2\text{O}_3$  and negative correlation with  $\text{SiO}_2$ ,  $\text{CaO}$  and  $\text{Fe}_2\text{O}_3$  exist and the trends of general sea floor sediments are recognized. The dispersion of  $\text{SiO}_2$  in Hajar, Draa Sfar, and Kettara deposits is due to the supply of detritus origin material by acid volcanic activity. The content of  $\text{CaO}$  has a tendency to be higher than others in Khwardra deposit because the supply of biogenic origin material is higher than others. As for rare earths pattern, LREE is rich and Eu anomaly is observed. This is due to island arc volcanic detritus origin material. The tendency that total rare earths (TREE) increases at the hanging wall side of the ore deposit is considered to be due to the move of rare earths from the hanging side to the floor side by hydrothermal solution. Sulfur isotope of sulfide in pelite varies from about -35 % to +25 % and has tendency to be lighter at hanging wall side than floor wall side. This tendency seems to indicate that the environment of sedimentation changes from Anoxic environment to oxidic environment according to Kajiwara (1989), Kajiwara and Kaiho (1992), Komuro (1999).

#### (Characteristics of igneous rocks)

Chemical composition and radioactive dating were studied on the volcanic rocks distributing in the neighborhood of each ore deposit in this area. The result of the chemical composition analysis showed the rare earths pattern of acid volcanic rocks (rhyolite) in Hajar, Khwardra, and Draa Sfar deposits has light rare earths abundantly and flat pattern having Eu anomaly. As for major components, similar tendency indicating negative correlation with  $\text{SiO}_2$ ,  $\text{K}_2\text{O}$ , Rb, Ba and Cs is seen so that these acid volcanic rocks are considered to have similar geochemical properties. However, the neighboring Safsafa deposit has different properties or the acid volcanic rocks (tonalitic mylonite) of. Also when comparing the basic volcanic rocks (dolerite) of this area with basalt, LIL element and HFS element of other area, it was found that the basic volcanic rocks of this area has features of island arc dolerite having much LIL element and differs from N-MORB which has poor LIL and HFS.

From the results of the measurement of K-Ar radioactive dating aiming at grasping mineralizing dating and igneous activity dating, volcanic rocks are classified to plutonic igneous activity, acid volcanic activity, mineralizing alteration (Guemassa) and mineralizing alteration (Jebilet). The datings of plutonic igneous activity and acid volcanic activity are 290 to 360 Ma, the dating of mineralizing alteration (Guemassa) is 260 to 320 Ma and are equivalent to the late stage of the activities of abyssal rock and volcanic rock, and the dating of mineralizing alteration (Jebilet) is equivalent to after the activities of plutonic rocks and

volcanic rocks.

#### (Characteristics of Sulfide Ore Deposit)

Khwadra, Draa Sfar, Kettara, Hajar, and Frizen deposits are classified as the massive sulfide ore deposits by the deposit shape, the combination of minerals and related igneous rocks. It becomes obvious that these ore deposits were formed by repetition of mineralization in the early stage and the late stage, considering the mode of occurrence of these ore deposit, ore minerals and alteration of the host rocks.

The mineralization of the early stage and the late stage are represented by pyrrhotite and pyrite respectively from the viewpoint of Fe-S minerals. The early stage mineralization is divided into the early I sub-stage and the early II sub-stage in Khwadra and Hajar deposits. The former is represented by hexagonal pyrrhotite and the latter is represented by monoclinic pyrrhotite. The hexagonal pyrrhotite crystallized in the early I sub-stage was generally changed to monoclinic pyrrhotite by the late stage mineralization. On the other hand, the monoclinic pyrrhotite crystallized in the early II sub-stage was changed to marcasite. Therefore, pyrrhotites crystallized in different mineralization stages was changed in their compositions by the repetition of later mineralization in the massive sulfide ore deposit in this area. The mineralization temperature of the early I sub-stage was 270 - 280 °C, that of the early II sub-stage was 200 - 230°C, and that of the late stage was 200 - 250 °C by the homogenized temperature of the liquid inclusion within quartz that coexist pyrrhotite.

The marked variation of the sulfur isotopic ratio within one ore deposit or within one ore-bearing area is in sharp contrast to the uniform sulfur ratio of the black-ore deposit in Japan. The following reasons are considered as the different sulfur isotopic ratios; the difference of the physical and the chemical conditions of mineralization environment of the ore deposit, mixing of organic origin sulfur, the restriction of supply of seawater origin sulfur. That is, the effect of the mixing of organic origin sulfur was relatively marked in Khwadra deposit, and the effect of the contribution of magma origin sulfur was relatively marked to the mineralization in Hajar deposit and Frizen deposit.

#### (Characteristics of Sulfide Ore Deposit and Magnetism)

The high geomagnetic anomalies are detected in Khwadra deposit and Hajar deposit where monoclinic pyrrhotite is characteristically occurred. On the other hand, the high and the low geomagnetic anomalies are distributed neighboring in Draa Sfar deposit where hexagonal pyrrhotite and monoclinic pyrrhotite coexist. Only the low geomagnetic anomalies are detected in Kettara deposit and Frizen deposit where hexagonal pyrrhotite and pyrite coexist. Therefore, the following possibilities are pointed out that there is a massive sulfide ore deposit composed

of hexagonal pyrrhotite and pyrite in the medium to low geomagnetic anomaly areas like Kettara and Frizen deposits, and that there is a massive Pb – Zn sulfide ore deposit composed of hexagonal pyrrhotite and monoclinic pyrrhotite in the area where a high geomagnetic anomaly area is adjacent to a low anomaly area.

The ore deposits are classified into following three types by mineralization:

a) Early I sub-stage dominant type

Medium geomagnetic anomaly [Draa Sfar deposit]

b) Repeated type of the early I sub-stage + the late stage

Medium + low magnetic anomaly [Frizen deposit, Kettara deposit]

c) Repeated type of the early II sub-stage + the late stage

High + low geomagnetic anomaly [Khwadra deposit, Hajar deposit]

(conclusion)

As results, the following prospecting policy is obtained by the total analysis of geological survey, analysis of drilling cores and laboratory tests. The chart of the total analysis is shown in Fig.III-1.

- 1) The prospective area of the existence of the rhythmic alternation of the Sarhlef Formation in deep part
- 2) The prospective area of the existence of acid volcanic rocks of the Sarhlef Formation in deep part
- 3) The prospective area of the existence of concealed sulfide ore deposit that is harmonized by the combination of the various geomagnetic anomalies by the classification of ore deposit type

(Airborne Geophysical Survey)

Interpreting the geology of the survey area by combining airborne magnetic survey data with airborne electromagnetic survey data shows that magnetic and resistivity structure is different in north and south of the boundary of resistivity at the center of the survey area (NE-SW system) in this area.

In the south distribution area of basement rock is a part extracted as a low magnetic zone by RMI and low resistivity zone by the decay constant. It is thought that the resistivity is high with a shallow outcrop of basement rock and middle with a deep one. All from igneous rocks through volcanic clastic rocks occur at 3 points: southeast (Hajar deposit), west (Frizen deposit) and north. In addition, magnetic indications suggestive of the occurrence of the said rocks in other area can be observed. Given as promising sites are those where there is concurrence of local low resistivity and high magnetic anomaly or where these two are

adjacent.

In the north resistivity structure make it possible to extract the following 3 areas:

- (a) Area at the west end: low resistivity from shallow through deep part
- (b) Central area extending from east to west: middle/high resistivity at shallow part - low resistivity at deep part
- (a) Northern area extending from east to west: low resistivity at shallow part-middle resistivity at deep part

If in the areas (b) and (c) there is a basement rock with concealed outcrop, the location containing igneous rock to volcanic clastic rock shows a high magnetic anomaly with a diameter of 2 to 4 km as verified by RMI. Given as promising sites are the zones of overlapping local low resistivity and high magnetic anomaly locally or where these two are adjacent. Such a zone are obtained in the northwest area and around high magnetic anomalies that is considered granite stock in the northeast area.

(Potential of existing massive sulfide deposits)

Areas where following airborne geophysical anomalies had been observed were selected as survey areas considering the probability of the existence of mineral deposit due to low resistivity and magnetic anomaly, and medium to low magnetic anomaly obtained by airborne geophysical survey.

- (1) Low resistivity zone + high to medium magnetic anomaly
  - (a) The area where low resistivity zone overlaps medium magnetic anomaly which exist numerously from Khwadra deposit at northwest part of the airborne geophysical survey area to Choula district in Guemassa though marked high magnetic anomaly was not obtained by the survey at this time.
  - (b) Low resistivity area existing in relatively large scale high magnetic anomaly in the northeast part, western part of Marrakech airport.
- (2) High magnetic anomaly part
  - (a) Small scale medium to high magnetic anomaly zone dotted in relatively large scale high magnetic anomaly in the north east part, western part of Marrakech airport.
  - (b) Small scale medium to high magnetic anomaly zone dotted in relatively large scale high magnetic anomaly at south west part of Khwadra ore deposit, Nasfar.
- (3) Low resistivity part
  - (a) Low resistivity zone near Tamasloht, eastern direction of Ghoula. Magnetic anomaly is not seen

## Chapter 2 Recommendation for the Second Year's Program

Khwadra, Draa Sfar, Kettara, Hajar, and Frizen deposits are classified as the massive sulfide ore deposits by the deposit shape, the combination of minerals and related igneous rocks. It becomes obvious that these ore deposits were formed by repetition of mineralization in the early stage and the late stage, considering the mode of occurrence of these ore deposit, ore minerals and alteration of the host rocks, and that each deposit has a different magnetic feature.

Areas where following airborne geophysical anomalies had been observed were selected as prospecting areas considering the probability of the existence of mineral deposit due to low resistivity and magnetic anomaly obtained by airborne geophysical prospecting, and medium to low magnetic anomaly obtained by geological survey.

- 1) Low resistivity zone + high to medium magnetic anomaly zone: possibility of the existence of high magnetic massive sulfide ore deposit.
- 2) High magnetic anomaly zone: possibility of the existence of high magnetic massive sulfide ore deposit.
- 3) Low resistivity zone: possibility of the existence of medium to low magnetic massive sulfide ore deposit.

We recommend followings as the second year survey:

- 1) Conducting gravitational survey, based on the property that the high density of massive sulfide ore deposit, as well as ground magnetic and electromagnetic survey to narrow the potential zone of existing massive sulfide ore deposit.
- 2) Conducting a drilling survey in the geophysical survey anomaly zone extracted by ground geophysical survey to confirm the underground geological structure and the condition of mineralization.

## Reffernce

- Bauchau, C.M., Ferrari, P.O., The Hajar massive sulfide deposit, Morocco, and its geological environment, *Mineral Deposits; Processes to Processing*, Stanley et al. (eds), 479-482, London, 1999.
- Deew, W. A., Howie, R. A., Zussman, J., *An introduction to the Rock Forming Minerals*, 2<sup>nd</sup> Edition, Longman, 1992.
- Essaifi, A., Capdevila, R., Lagarde, JL., Transformation de leucogabbros en chloritoschistes sous l'effet de l'alteration hydrothermale et de la deformation dans l'intrusion de Kettara (Jebilet, Maroc), *C.R. Acad. Sci. Pris. t320, serie II a*; 189-196, 1995.
- Hibti, M., Les amas sulfures des Guemassa et des Jebilet (Meseta sud-occidentale, Maroc; temoins de l'hydrothermalisme precoce dans basin mesetien, these docteur, Universite Marrakech, 2001.
- Hofmann, A., Chemical differentiation of the Earth; the relationship between mantle, continental crust, and oceanic crust, *Earth Planet. Sci. Lett*, 90, 297-314, 1988.
- Piercey, S.J., Paradis, S., Murphy, D.C., Mortensen, J.K., Geochemistry and paleotectonic setting of felsic volcanic rocks in the Finlayson Lake volcanic-hosted massive sulfide district, Yukon, Canada, *Economic Geology*, vol.96, 1877-1905, 2001.
- Thieblemont, D., Pascual, E., Stein, G., Magmatism in the Iberian pyrite belt; petrological constraints on a metallogenic model, *Mineralium Deposita*, 33, 98-110, 1998.
- JICA and MMAJ (1988), The report on the Mineral Exploration in the Haouz Central area Kingdom of Morocco Phase I
- JICA and MMAJ (1989), The report on the Mineral Exploration in the Haouz Central area Kingdom of Morocco Phase II
- JICA and MMAJ (1990), The report on the Mineral Exploration in the Haouz Central area Kingdom of Morocco Phase III
- JEMEC(2002), Report on the Mineral Exploration Project finding survey the Kingdom of Morocco
- Komuro, K and Kajiwar, Y (2003) , Paleooceanography and Heavy Metal Enrichment of Mudstones in the Green Tuff Reagion, Northeast Japan, *Resource geology* vol.53 no.1 37-49 (in printing)
- Shikazono(1999), Rare Earth Element Geochemistry of Kuroko Ores and Hydrothermally Altered Rocks: Implication for Evolution of Submarine Hydrothermal System at Back Arc Basin, *Resource geology Special Issue* no.20 23-30
- Mitsuno, C et al (1988), Geological Study of the "Iberian Pyrite Belt" – with Special Reference to its General Correlation of the Yanahara Ore deposit and Other in the Inner zone of Southwest Japan,